

STATIC AND DYNAMIC ANALYSES OF A TRANSMISSION TOWER-
LINE SYSTEM USING A SIMPLIFIED MODEL

by

Felipe Tabet

A Thesis submitted to the Faculty of Graduate Studies of
The University of Manitoba
in partial fulfilment of the requirements of the degree of

MASTER OF SCIENCE

Department of Civil Engineering
University of Manitoba
Winnipeg

Copyright © 2009 by Felipe Tabet

THE UNIVERSITY OF MANITOBA
FACULTY OF GRADUATE STUDIES

COPYRIGHT PERMISSION

**STATIC AND DYNAMIC ANALYSES OF A TRANSMISSION TOWER-
LINE SYSTEM USING A SIMPLIFIED MODEL**

By

Felipe Tabet

A Thesis/Practicum submitted to the Faculty of Graduate Studies of The University of
Manitoba in partial fulfillment of the requirement of the degree
Of

MASTER OF SCIENCE

Copyright © 2009 by Felipe Tabet

Permission has been granted to the University of Manitoba Libraries to lend a copy of this thesis/practicum, to Library and Archives Canada (LAC) to lend a copy of this thesis/practicum, and to LAC's agent (UMI/ProQuest) to microfilm, sell copies and to publish an abstract of this thesis/practicum.

This reproduction or copy of this thesis has been made available by authority of the copyright owner solely for the purpose of private study and research, and may only be reproduced and copied as permitted by copyright laws or with express written authorization from the copyright owner.

Abstract

The optimum design of a transmission line system requires a good understanding of both the static and dynamic behaviors of the system. The computational model should be capable of accurately representing the structure. In common practice, an isolated tower with loading from conductors is analyzed to represent an entire system of towers. It has been found that the behavior of the tower-cable system differs from the behavior of an isolated tower, especially for long span transmission systems. A misrepresentation of the model can lead to serious economical and social losses.

In this study, a latticed tower shaft is modeled using a tapered and a prismatic 3D beam-column element to reduce the number of degree of freedom of the structure. These simplified elements were specially formulated and verified to represent detailed tower segments. The elements are incorporated into an in-house Finite Element program called Static and Dynamic Analysis Program. The program also includes all the necessary elements required in the analysis of the transmission line system such as a cable element, truss element, spring element, insulator string element and conventional beam-column element. The 3D cable element used to model guy wires and conductors are assumed to be parabolic in shape with a modified Dischinger's modulus of elasticity. The results obtained from the model using the simplified elements and those obtained from the detailed tower model, for both static and free vibration analyses, are within 7%.

Free vibration analyses of an isolated tower and a transmission line system were conducted using the developed simplified model. The inclusion of cable spans in the model increases the number of mode shapes of vibration. The increase in the number of cable spans also increases the number of mode shapes.

Dynamic analyses of the system with different numbers of cable spans and different boundary conditions were also performed. The wind loading was modeled using a random, stationary and ergodic process. It was found that only two cable spans are required for the dynamic analysis of the system for the applied load case of wind perpendicular to the line. It was also concluded that the spring element can be used to represent the end towers.

Acknowledgement

I would like to express my deepest thanks to my supervisor, Dr. Nipon Rattanawangcharoen, P.Eng. for his assistance and guidance, Mr. Jon Kell, P.Eng. from Manitoba Hydro, who provided valuable advice, and the members of the committee, Dr. Dimos Polyzois, P.Eng. and Dr. Quan (Abraham) Wang, P.Eng.

I would like to express my appreciation to Mr. Paulo Sérgio Pinto for his time and advice as a professor, engineer and personal friend, and to Dr. Michèle Schubert Pfeil for her attention. I also would like to thank my friends Mr. Mostafa El-Mogy, Mr. Mohamed Mady, Mr. Cameron Ward and Mr. Yang Liu for their continuous support and encouragement.

Also thanks to my family for their support of my journey, without them this work could never have been accomplished. Finally, I would like to demonstrate my true gratitude to Ms. Juliana Rivera Alves for her scientific and personal attention during the development of the Finite Element program and my Master of Science thesis.

Aos meus pais, Luís Felipe e Lêda,

e aos meus irmãos, Guilherme e Bernardo.

CONTENTS

LIST OF FIGURES.....	vii
LIST OF TABLES	xi
LIST OF ABBREVIATIONS.....	xii
LIST OF SYMBOLS.....	xii
1. INTRODUCTION.....	1
1.1. GENERAL.....	1
1.2. OBJECTIVES.....	4
1.3. OUTLINE OF THE THESIS.....	5
1.4. SCOPES OF THE RESEARCH.....	5
2. LITERATURE REVIEW	7
2.1. BEAM-COLUMN (STABILITY FUNCTIONS).....	7
2.2. TOWER MODELING.....	8
3. FORMULATION OF ELEMENTS	13
3.1. TOWER ELEMENTS.....	14
3.1.1. STRAIGHT SHAFT	14
3.1.2. TOWER TAPERED SHAFT	22
3.2. INSULATOR STRING	33
3.3. CABLE.....	37
3.4. SPRING ELEMENT	39
4. VALIDATION OF PROGRAM.....	41
4.1. ACCEPTANCE CRITERIA	41
4.2. EXAMPLES.....	43
5. COMPUTATIONAL MODELING.....	56
5.1. TOWER PROPERTIES	56
5.2. TOWER SYSTEM MODELS	59
5.3. BOUNDARY CONDITIONS	60
5.4. NONLINEAR STATIC ANALYSIS.....	62
5.4.1. LOAD CASES	63
5.5. DYNAMIC ANALYSIS.....	65
5.5.1. FREE VIBRATION	65

5.5.2.	TIME STEPPING TECHNIQUE	65
5.5.3.	DAMPING MATRIX	67
5.5.4.	WIND LOAD	69
5.5.4.1.	WIND SPEED	70
5.5.4.1.1.	MEAN WIND SPEED	71
5.5.4.1.2.	TURBULENCE WIND SPEED	72
6.	ANALYSIS RESULTS	82
6.1.	ISOLATED TOWER (MODEL 1 AND MODEL 2)	82
6.1.1.	STATIC DISPLACEMENTS	82
6.1.2.	FREE VIBRATION	88
6.2.	TRANSMISSION SYSTEM	91
6.2.1.	FREE VIBRATION	91
6.2.1.1.	MODEL 2 AND MODEL 3	91
6.2.1.2.	MODEL 3 AND MODEL 4	94
6.2.1.3.	MODEL 4 AND MODEL 5	96
6.2.1.4.	MODEL 4 AND MODEL 6	99
6.2.1.5.	MODEL 6 AND MODEL 7	103
6.2.1.6.	MODEL 6 AND MODEL 8	108
6.2.2.	DYNAMIC ANALYSIS	111
6.2.2.1.	COMPARISON OF MODEL 2 AND MODEL 4	112
6.2.2.2.	COMPARISON OF MODELS 3, 4, 5 AND 6	114
7.	SUMMARY, CONCLUSIONS AND RECOMMENDATIONS	119
7.1.	CONCLUSIONS	119
7.2.	RECOMMENDATION FOR FUTURE WORK	121
	REFERENCES	122
	APPENDIX - A	129
	APPENDIX – B	158

List of Figures

- Figure 1.1 - Transmission line system.
- Figure 1.2 - Transmission tower.
- Figure 3.1 - Representation of a tower segment by a tapered beam-column element.
- Figure 3.2 - Straight shaft segment.
- Figure 3.3 - Torsion Stiffness.
- Figure 3.4 - Diagonal effect.
- Figure 3.5 - Tapered shaft segment.
- Figure 3.6 - Deformed beam-column element.
- Figure 3.7 - Sway effect.
- Figure 3.8 - Insulator string.
- Figure 3.9 - Cable element.
- Figure 4.1 - Example No. 12.
- Figure 4.2 - Response of the systems shown in Figure 4.1 using Newmark-L option in SADAP.
- Figure 4.3 - Response of the systems shown in Figure 4.1 using time-stepping technique in MathCAD.
- Figure 4.4 - Cable element (Example 13).
- Figure 4.5 - Results from SADAP.
- Figure 4.6 - Cable element (Example 14).
- Figure 4.7 - Tapered tower (example 15).
- Figure 4.8 - x displacement of the tapered tower.

- Figure 4.9 - y displacement of the tapered tower.
- Figure 4.10 - z displacement of the tapered tower.
- Figure 4.11 - The 1st flexural natural frequency and mode shape of the detailed and the simplified tapered towers.
- Figure 4.12 - The 2nd flexural natural frequency and mode shape of the detailed and the simplified tapered towers.
- Figure 4.13 - The 3rd flexural natural frequency and mode shape of the detailed and the simplified tapered towers.
- Figure 4.14 - The 4th flexural natural frequency and mode shape of the detailed and the simplified tapered towers.
- Figure 5.1 - Tower A-402M.
- Figure 5.2 - A simplified model of an A-402M tower.
- Figure 5.3 - Transmission system models.
- Figure 5.4 - Boundary conditions in the study.
- Figure 5.5 - Nomenclatures of the loading in Table 5.3.
- Figure 5.6 - Controlled nodes where the loadings are applied in detailed and simplified tower models (representatively only).
- Figure 5.7 - Newmark Method.
- Figure 5.8 - Drag factors and areas of the tower zones.
- Figure 5.9 - Wind speed.
- Figure 5.10 - Variation of mean wind speed along the tower height.
- Figure 5.11 - Wind spectrum versus frequency.
- Figure 5.12 - Wind generation flowchart.

Figure 5.13 - Turbulence wind speed sample.

Figure 5.14 - Turbulence wind speed at a maximum time of 2 seconds.

Figure 5.15 - Top view of the transmission tower system.

Figure 5.16 - Wind speed in zones 1 and 2.

Figure 6.1 - (a) Model 1 and (b) Model 2.

Figure 6.2 - Load Case 1, x displacement of the top of the tower.

Figure 6.3 - Load Case 1, y displacement of the top of the tower.

Figure 6.4 - Load Case 1, x displacement of the left cross arm.

Figure 6.5 - Load Case 1, y displacement of the left cross arm.

Figure 6.6 - Load Case 1, x displacement of the right cross arm.

Figure 6.7 - Load Case 1, y displacement of the right cross arm.

Figure 6.8 - Load Case 2, x displacement of the top of the tower.

Figure 6.9 - Load Case 2, y displacement of the top of the tower.

Figure 6.10 - Load Case 2, z displacement of the top of the tower.

Figure 6.11 - Load Case 2, x displacement of the left cross arm.

Figure 6.12 - Load Case 2, y displacement of the left cross arm.

Figure 6.13 - Load Case 2, z displacement of the left cross arm.

Figure 6.14 - Load Case 2, x displacement of the right cross arm.

Figure 6.15 - Load Case 2, y displacement of the right cross arm.

Figure 6.16 - Load Case 2, z displacement of the right cross arm.

Figure 6.17 - (a) Model 2 and (b) Model 3.

Figure 6.18 - (a) Model 3 and (b) Model 4.

Figure 6.19 - (a) Model 4 and (b) Model 5.

Figure 6.20 - (a) Model 4 and (b) Model 6.

Figure 6.21 - (a) Model 6 and (b) Model 7.

Figure 6.22 - (a) Model 6 and (b) Model 8.

Figure 6.23 - (a) Model 2 and (b) Model 4.

Figure 6.24 - Displacement-time history at the top of the tower for Model 2.

Figure 6.25 - Displacement-time history at the top of the tower for Model 4.

Figure 6.26 - FFT of the displacement at the top of the tower for Model 2.

Figure 6.27 - FFT of the displacement at the top of the tower for Model 4.

Figure 6.28 - Computational Models.

Figure 6.29 - Displacement at the top of the tower for Model 3 (node 47).

Figure 6.30 - Displacement at the top of the tower for Model 4 (node 47).

Figure 6.31 - Displacement at the top of the tower for Model 5 (node 47).

Figure 6.32 - Displacement at the top of the tower for Model 6 (node 47).

Figure 6.33 - Displacement at the top of the tower for Models 4 and 5 (node 47).

Figure 6.34 - FFT of the tower for Model 3.

Figure 6.35 - FFT of the tower for Model 4.

Figure 6.36 - FFT of the tower for Model 5.

Figure 6.37 - FFT of the tower for Model 6.

List of Tables

Table 4.1 - Summary of examples.

Table 4.2 - Natural frequencies of the cable shown in Figure 4.6.

Table 4.3 - Applied force on the models in Figure 4.7.

Table 5.1- Properties of the conductors, ground wires and guyed cables.

Table 5.2 - Properties of the springs.

Table 5.3 - Load cases.

Table 6.1 - Percentage difference of displacements between the Models 1 and 2
for Load Case 1.

Table 6.2 - Percentage difference of displacements between the Models 1 and 2
for Load Case 2.

Table 6.3 - Comparison of mode shapes between Model 1 and Model 2.

Table 6.4 - Frequencies and mode shapes of Model 2 and Model 3.

Table 6.5 - Frequencies and mode shapes of Model 3 and Model 4.

Table 6.6 - Frequencies and mode shapes of Model 4 and Model 5.

Table 6.7 - Frequencies and mode shapes of Model 4 and Model 6.

Table 6.8 - Frequencies and mode shapes of Model 6 and Model 7.

Table 6.9 - Frequencies and mode shapes of Model 6 and Model 8.

List of abbreviations

ASCE	American Society of Civil Engineers
FE	Finite Element
FEA	Finite Element Analysis
DOF	Degree of freedom

List of symbols

Chapter 3

A	Cross-sectional area
A_L	Cross-sectional area of the longitudinal bars
AUX	Auxiliary value
b_{top}	Width at the top of the tapered element
b_{bottom}	Width at the bottom of the element
b_y	Width of the element in the y-x plane
b_z	Width of the element in the z-x plane
DX, DY, DZ	Distance between nodes in the x-, y- and z-direction respectively
E	Modulus of elasticity
E_{eq}	Equivalent modulus of elasticity of the cable
e	Axial displacement
$\{F\}$	Force vector
F_D	Force in the diagonal bar in the axial direction
$F_{D,y}$	Force in the diagonal bar in the y-direction
$F_{D,z}$	Force in the diagonal bar in the z-direction

F_w	Wind load
f_1, f_2, f_3	Flexibility coefficients using stability functions
f_D	Flexibility coefficient due to diagonal bar effect
G	Shear modulus
g	Gravity
H'	Pretension on the cable
I_y	Moment of inertia in the y direction
I_z	Moment of inertia in the z direction
J_x	Torsional moment of inertia
$[K]$	Stiffness matrix
$[K_L]$	Linear stiffness matrix
$[K_{NL}]$	Nonlinear stiffness matrix
k_T	Torsion stiffness
KUX, KUY,	Stiffness coefficients of the spring element
KUZ, KRX,	Stiffness coefficients of the spring element
KRY, KRZ	Stiffness coefficients of the spring element
L	Length of the element (distance between nodes)
L_c	Deformed length of the cable
L_D	Length of the diagonal bars
L_i	Length of the insulator
$[M]$	Mass matrix
P	Axial force
q_x	Dead load of the cable on the local x-direction

q_z	Dead load of the cable on the local z-direction
S_1, S_2, S_3	Stiffness coefficients using stability functions
T	Torsional moment
u_D	Axial displacement of the diagonal
W_i	Weight of the insulator
W_c	Weight of the cable
β	Tapered parameter or rotation due to torsion
η	Displacement due to torsion
ρ	Density or $\sqrt{P/EI}$
ν	Poisson's ratio
Δ	Displacement due to sway effect

Chapter 4

d_0	Initial sag of the cable
d_f	Final sag of the cable
f	Frequency in Hz
H_0	Initial horizontal tension component of the cable
H_f	Final horizontal tension component of the cable
$P.D.$	Percentage of difference
T_0	Initial tension in the cable
T_f	Final tension in the cable
λ	Dimensionless parameter related to cable properties
ω	Frequency in rad/s

Chapter 5

$a_0, a_1, a_2,$	Newmark constants
$a_3, a_4, a_5,$	Newmark constants
a_6, a_7	Newmark constant
$[C]$	Damping matrix
$C_{v1,v2}$	Cross covariance function
C_{df}	Drag factor
$\{\hat{F}\}$	Effective force vector (Newmark method)
k	Kaimal constant
$[\hat{K}]$	Effective stiffness matrix (Newmark method)
k_{g1}, k_{g2}	Stiffness of the ground wire
k_{c1}, k_{c2}	Stiffness of the conductor
$NSPEC$	Number of divisions of the spectrum
R_s	Ratio of the net projected area and the gross projected area
$Rv(\tau)$	Autocorrelation function
$S_v(f)$	Wind spectrum
t	Time
u_*	Friction Velocity
$\{u\}$	Displacement vector
$\{\dot{u}\}$	Velocity vector
$\{\ddot{u}\}$	Acceleration vector

\bar{V}	Mean wind speed
\bar{V}_{10}	Mean wind speed at 10 meters height
$\overline{V^2}$	Mean square value
v_1	Wind speed in zone 1
v_2	Wind speed in zone 2
V_{rms}	Root mean square
$V(t)$	Wind speed
$v(t)$	Turbulence wind speed
α, δ	Newmark constants
α, β	Rayleigh damping parameters
$\{\Delta u\}$	Incremental displacement vector
Δf	Frequency increment
ΔS	Distance between zones
ξ_i	Modal damping
$\{\phi\}$	Mode shape vector
σ_v^2	Variance
σ_v	Standard deviation
τ	Time variable
θ_i	Random angle with uniform distribution from 0 to 2π

1. INTRODUCTION

1.1. GENERAL

Transmission line systems play an important role in society; a failure in these systems causing an interruption in the energy supply can cause severe social and economic losses. To guarantee stability and low cost of maintenance, these systems need to be well designed.

In the past, in the United States, the majority of the state laws required that the transmission line system should be designed at a minimum to meet the requirements of the National Electrical Safety Code (NESC), which mainly covers electrical design of the transmission lines, however, it also contains a part of the structural loads and overload capacity factors. Some designers felt that the NESC code was too conservative, while others adopted procedures well above the minimum requirement. This inconsistency led to the development of in-house design criteria and guidelines. All this caused a large variation in the design (see reference ASCE, 1984 for details), and led to an unreliable or costly structures. In 1984, the American Society of Civil Engineers (ASCE) published a set of guidelines for determining the structural loads of the transmission towers. Though it created uniformity in the design procedure, these guidelines however were based on simplified assumptions due to the lack of computational structural programs. Structures built with such simplifications should be reviewed for safety now that the numerical analysis is much more advanced.

It is always of interest to engineers to design a transmission line system with the maximum span length possible. With the use of advanced computational programs, the structural analysis can be very sophisticated. This allows a significant increase of the span size and a reduction on the transmission system cost. Nonetheless, some precautions need to be taken in the construction of a numerical model that closely represents a real structure.

The design of transmission line systems (Figure 1.1) has always been a highlighted topic in structural engineering. In the past, towers were designed based on static load cases. The conductors and the tower were treated as independent units. The load resultants from the conductors were applied directly to the tower's members. Such simplifications could have a negative impact in today's economy. It was estimated that a failure of a transmission tower could cost one million US dollars per kilometer of line (Albermani et al., 2008) without including economic damages due to lack of electrical power.

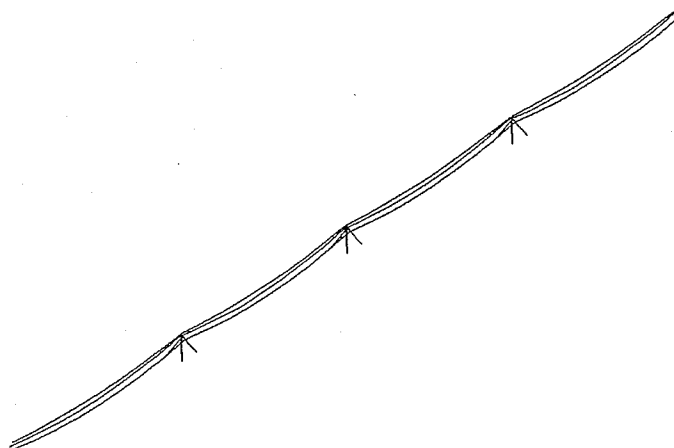


Figure 1.1 - Transmission line system.

Most transmission towers are constructed as steel latticed structures. In general, as for any tall and slender structure, the design of a transmission line system is governed by wind loads (Shehata et al., 2005). Therefore, due to the low natural frequencies of the system, a dynamic analysis is required. Most of the dynamic analyses of a transmission system are usually carried out by modeling the tower as an isolated structure as shown in Figure 1.2. This is not accurate since it has been proven that the dynamic characteristics of the whole system and the lateral movement of the conductors must be taken into account in the analysis. The dynamic effects that the conductor and insulator strings have on the vibration of the tower cannot be simply represented as lumped masses on the tower.

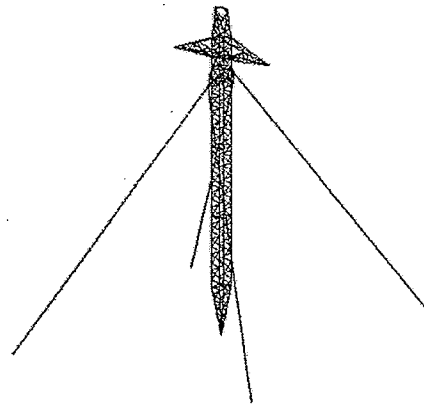


Figure 1.2 - Transmission tower.

The work in this thesis is entirely theoretical. It involves the development of a computer program based on the direct stiffness method. The program was validated through comparison with existing finite element (FE) programs, published or theoretical results. Several examples are included in this thesis

which demonstrates the effectiveness and the accuracy of the developed program.

1.2.OBJECTIVES

To date, the analysis of transmission line systems has generally focused on the analysis of isolated towers with the conductors acting as discrete loads on the tower at the connection points. Such a mathematical model may be used for static analysis of the system. In dynamic analysis, however, the effects that the conductors and the adjacent towers have on the response of the system are significant and must be considered in the analysis of the system. To obtain an accurate prediction of the response, the whole system, including the towers and the conductors, must be used in the analysis. Depending on the number of spans used in the analysis, this can be limited by the capacity of the computer. The problem can be alleviated by using an appropriate simplified element to model the tower. Hence, the goals of this study are

- To develop a reliable simplified tower model so that dynamic analysis of a transmission line system which includes several spans can be performed with limited computer capacity,
- To perform parametrical studies on the effects of the number of towers in the model, and
- To investigate the effect of the end restrains on dynamic response of the tower system.

1.3. OUTLINE OF THE THESIS

This thesis consists of seven chapters. In chapter 2 a literature review of the beam-column element formulated using stability functions and the computational models for the tower analysis used by previous researchers is presented.

In chapter 3 the details of the element formulations (tapered and straight tower element, insulator string, cable, and spring elements) used in the program are discussed.

In chapter 4 the validation of the elements is performed. A number of examples used to verify the Finite Element Program (SADAP – Static and Dynamic Analysis Program) are also included.

In chapter 5 the numerical models and loads used in this study are described.

The results from the analyses for both the isolated tower and the transmission system are discussed in chapter 6. Finally, chapter 7 includes a number of conclusions and recommendations for future research.

1.4. SCOPES OF THE RESEARCH

The scopes of the current research are

- A non-linear static analysis of transmission tower is restricted to an isolated tower for the purpose of verification of the proposed simplification.

- Only geometrical non-linearity is taken into account.
- The dynamic analysis is limited to a linear formulation due to computational constraints.
- Buckling of an individual member is not taken into consideration in the formulation of the simplified element.

2. LITERATURE REVIEW

2.1. BEAM-COLUMN (STABILITY FUNCTIONS)

There are several methods to derive the stiffness matrix of a beam-column element. One of them is through the use of modified slope-deflection equations, called Stability Functions. This method is widely used in the analysis of steel structures using Finite Element Analysis (FEA).

The Stability Functions Theory is more attractive than a standard energy method, because; requires fewer elements to predict buckling loads (Landesmann, 2007), uses only one stiffness matrix to describe the linear and the nonlinear behavior, easy to incorporate the plastic hinge theory and etc.

There are a large number of publications describing the use of the Stability Functions. One in particular is by Kim et al. (2001-A). Their derivation of the stability functions incorporated shear deformation, the tangent modulus of elasticity to account for gradual yielding due to residual stresses, the parabolic functions for gradual yielding due to flexure, and Orbison's full plastification surface of cross-section. The inelastic formulations are recommended only for compact steel sections. Kim et al. (2001-B) extended their formulation to incorporate the lateral torsional buckling. Later, Kim et al. (2006) performed an inelastic dynamic analysis of the three dimensional steel frames using stability functions. They archived good results when compared with commercial FE program (Abaqus).

2.2. TOWER MODELING

One of the earliest studies related to the analysis of transmission line is Bissiri and Landau in 1947. They investigated the influence of the cable rupture on subsequent line spans of a transmission line system. The cables were considered to have a catenary profile, the insulator strings were assumed as rigid body elements and the towers as fixed supports. Their research focused on calculating the cable tensile force based on static equilibrium and they presented hand calculation procedures for the analysis.

Cohen and Perrin (1957-A) described the procedure to calculate wind loads as static forces on guyed towers. They presented drag and lifting coefficients for towers of different types and shapes, as well as gust factors and a formulation for the change in wind speed with altitude. They extended their research and performed a simplified non-linear static analysis of guyed towers (Cohen and Perrin, 1957-B). Though this method was a simplified method, and was very efficient considering the computational limitations. The tower shaft was represented by equivalent beam-column elements and the guyed cables by non-linear springs.

Mozer et al. (1977) developed simplified procedure to calculate longitudinal forces due to a broken conductor wire or unbalanced ice load. They formulated an equivalent stiffness coefficient for the insulator string assuming small rotations. The accuracy of their procedure was verified by comparing their numerical result with the results from several static small scale experimental

tests. They also performed small scale dynamic tests and concluded that the dynamic characteristics of the tower-cable system are influenced from the impact load due to a wire rupture.

Peyrot et al. (1981) used a nonlinear elastic catenary cable element to analyze cross rope suspension transmission line structures. They performed a nonlinear static analysis using only one cable element per conductor's spans. The tower mast was modeled as a rigid body element. A static condensation was applied to reduce the degrees-of-freedom (DOF) of the mast. They, however, did not verify their analysis results.

To reduce the DOF of a transmission tower, Trainor et al. (1985) used a beam-column element that represents both straight and tapered tower shaft and calculated natural frequencies of the structure. They assumed the mass of the structure to be constant even when the tower's shaft was tapered.

Mathur et al. (1987) demonstrated that the towers, insulator strings, and conductors must be integrated as a whole in order to obtain an accurate dynamic analysis of a transmission tower system. Desai et al. (1994) analyzed galloping of a transmission line with ice on the conductors. In their study, the tower-line system was modeled considering multiple spans and the cable as a three-node isoparametric finite element. They concluded that a multi-span model is required to estimate galloping modes; severe galloping amplitudes can lead to a progressive failure of the towers.

Rodrigues (1999) studied the collapse of a transmission tower due to wind load and demonstrated that, even without the rupture of the conductor wire, the tower can fail due to dynamic wind load because of the low natural frequencies of the structure. A system of one tower, insulator strings and two cable spans was used in the analysis. The end towers were modeled as a linear spring element.

Lei, Y. H. and Chien, Y. L. (2005) studied the response of a transmission line system to seismic load, considering both material and geometric nonlinearities. Their model consisted of 3 towers, 4 conductor spans (4 cable elements per span) and springs to represent the end towers restrains. The stiffness of the springs was chosen to be equal to 1.5 times the stiffness of one tower, measured in each respective direction. No indication of modeling the insulator strings was reported. They concluded the importance to consider the conductors in the dynamic analysis of the transmission line system.

Using ANSYS, Oliveira (2006) investigated the collapse of one of the towers studied by Rodrigues (1999) using a non-linear static and dynamic analysis. He modeled the end towers using dynamic condensation available in ANSYS (therefore assumed that those towers have a linear behavior). He concluded that the tower can fail due to a wind load before a wire rupture and that the tower-line system presented lower natural frequencies than the isolated tower, as the initial frequencies of the tower-line were governed by the conductors' properties.

Oliveira et al. (2007) analyzed several guyed towers using three different models to investigate which model best represented the towers. The first model consisted only of truss elements (in this model, the use of dummy bars with low stiffness was required to stabilize the structure); the second model consisted of beam elements assuming rigid connections; and the third model considered the main elements as beams and the diagonals as trusses. In their study, the comparison between models was done considering a static linear and non-linear analysis, a dynamic based on free vibration, and a stability analysis. They concluded that the lateral displacement of the tower due to wind loads was not a function of the element type, but the stresses from the truss and the other two models were considerably different. They also concluded that the model using only beam elements can lead to a higher buckling load when compared with the combined truss and beam model. They recommended using the model that considered the main elements as beams and the diagonals as trusses to the analysis of guyed towers. This recommendation is used in this study.

Junior et al. (2007) studied the effect of a cable rupture on transmission lines using Central Finite Difference to integrate the equations of motion in the time domain. The geometric and material nonlinearities were included in the model. They investigated a 138kV transmission line, which consisted of eight detailed towers, nine cable spans (20 cable elements per span), and insulator strings. All modeled only using truss elements. They concluded that the standard cable rupture approach (equivalent static load) can be unsafe, depending on the transmission line model.

In the analysis of a transmission line system, the number of spans is defined by a case by case basis. It is very time consuming to run a multi-span model, and simplifications are still required to be able to perform a parametric study on the effects of the number and length of conductors spans. Zhang and Rattanawangcharoen (2008), investigated the dynamic characteristics of a single guyed tower, and a system made by three towers and four conductor's spans using a uniform non-linear beam-column element to simulate the tower shaft. A catenary cable element was also used to simulate the conductors, the ground wires and the guyed cables (only one cable element per span). They concluded that the system of towers has additional modes of vibration when compared with an isolated tower, which depend on the span length, and can have an important effect in the dynamic response. Therefore, multi-spans models should be considered for a more reliable analysis.

3. FORMULATION OF ELEMENTS

In the analysis of the transmission line system, a model consisting of one isolated tower is not sufficient to predict the dynamic behavior of the structural system. The consideration of the subsequent towers is necessary. However, a model consisting of more than one tower is extremely computational time consuming and sometimes even impossible. There are basically three different techniques to solve this problem. In the first technique, the extremity towers were modeled as simple mass-spring-damper elements as it was done at Rodrigues (1999). In this method, the spring stiffness is obtained by applying a unit force at the end of the insulator string elements and then inverting the resulting displacement. The second method is to use static condensation as done by Oliveira (2006) thus reducing the DOF of the structure. Even though these methods are very efficient, the adjacent towers can only be considered to have a linear behavior and only natural frequencies corresponding to the remaining DOFs were considered. The studies using these two methods were considered only two cable spans models.

The third technique is to simulate parts of the tower as a single element reducing the degree of freedom of the system therefore reducing the analysis complexity, as shown in Figure 3.1. Even though the analysis is simplified, the element is able to represent the non-linear static and dynamic behaviour of the structure.

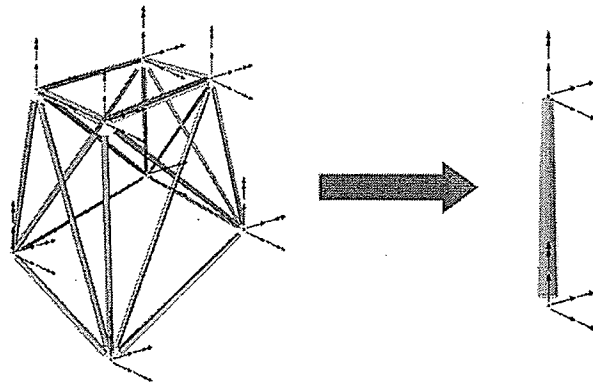


Figure 3.1 - Representation of a tower segment by a tapered beam-column element.

3.1. TOWER ELEMENTS

3.1.1. STRAIGHT SHAFT

The tower shaft (Figure 3.2) will be modeled similarly to a regular beam-column element with equivalent geometric properties.

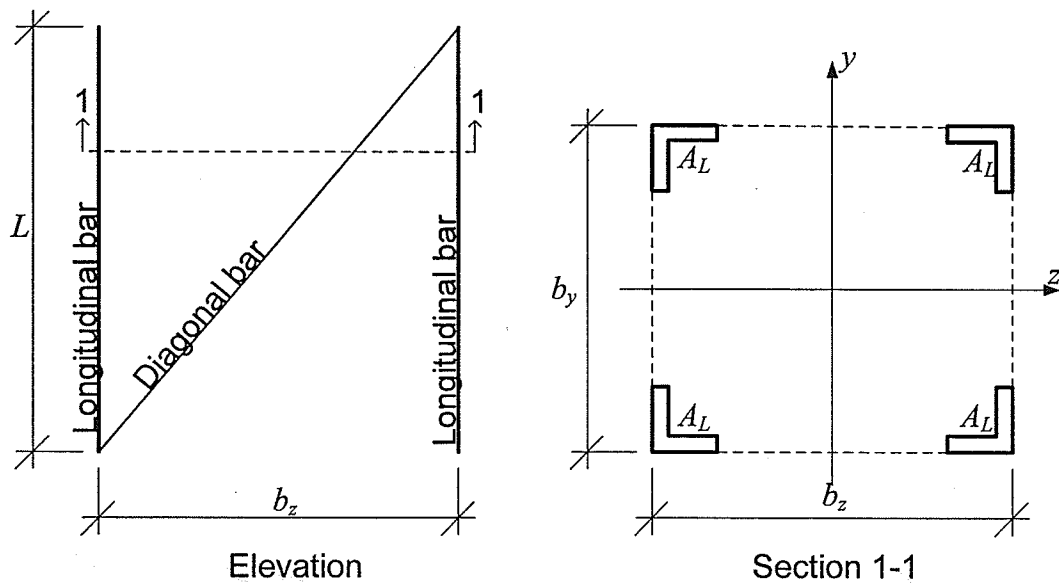


Figure 3.2 - Straight shaft segment.

The torsion stiffness, k_T , is considered to be provided exclusive by the diagonal bars, as shown in Figure 3.3. The formulation is given by Eqn. (3.1).

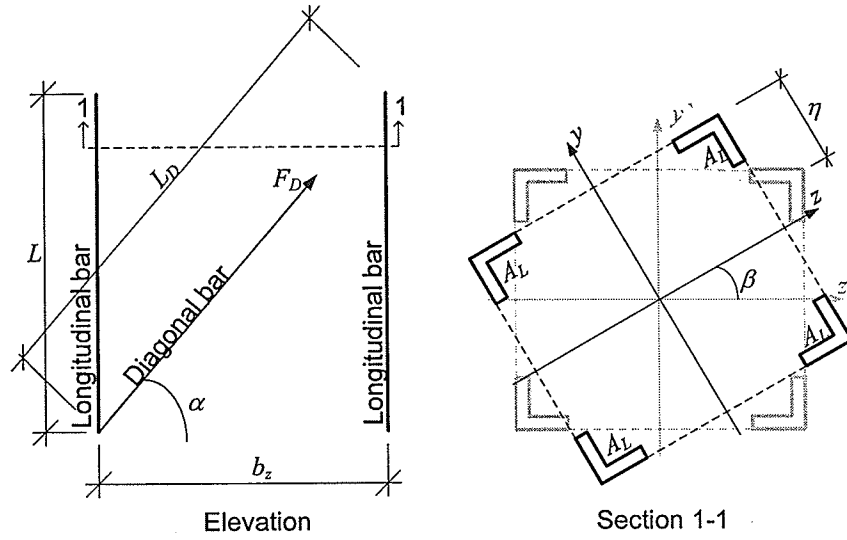


Figure 3.3 - Torsion Stiffness

$$\eta = \sin(\beta) \frac{\sqrt{b_y^2 + b_z^2}}{2} \approx \beta \frac{\sqrt{b_y^2 + b_z^2}}{2}$$

$$F_D = \frac{E \cdot A_D}{L_D} \eta \cos(\alpha)$$

$$F_{D,y} = \frac{E \cdot A_D}{L_{D,y}} \eta \cos^2(\alpha_y)$$

$$F_{D,z} = \frac{E \cdot A_D}{L_{D,z}} \eta \cos^2(\alpha_z)$$

$$T = F_{D,z} b_y + F_{D,y} b_z$$

$$T = EA_D \beta \frac{\sqrt{b_y^2 + b_z^2}}{2} \left(\frac{b_y \cos^2(\alpha_z)}{L_{D,z}} + \frac{b_z \cos^2(\alpha_y)}{L_{D,y}} \right)$$

$$k_T = \frac{T}{\beta} = EA_D \frac{\sqrt{b_y^2 + b_z^2}}{2} \left(\frac{b_z^2 b_y}{(\sqrt{b_z^2 + L^2})^3} + \frac{b_y^2 b_z}{(\sqrt{b_y^2 + L^2})^3} \right) \quad (3.1)$$

where A_D is the area of one diagonal, F_D is the force in the diagonal bar and T is the torsional moment.

Therefore the linear stiffness matrix, K_L , considering the torsion stiffness is given by:

$$K_L = \begin{bmatrix} \frac{EA}{L} & 0 & 0 & 0 & 0 & 0 & -\frac{EA}{L} & 0 & 0 & 0 & 0 & 0 \\ 0 & \frac{12EI_z}{L^3} & 0 & 0 & 0 & \frac{6EI_z}{L^2} & 0 & -\frac{12EI_z}{L^3} & 0 & 0 & 0 & \frac{6EI_z}{L^2} \\ 0 & 0 & \frac{12EI_y}{L^3} & 0 & -\frac{6EI_y}{L^2} & 0 & 0 & 0 & -\frac{12EI_y}{L^3} & 0 & -\frac{6EI_y}{L^2} & 0 \\ 0 & 0 & 0 & k_T & 0 & 0 & 0 & 0 & 0 & -k_T & 0 & 0 \\ 0 & 0 & -\frac{6EI_y}{L^2} & 0 & \frac{4EI_y}{L} & 0 & 0 & 0 & \frac{6EI_y}{L^2} & 0 & \frac{2EI_y}{L} & 0 \\ 0 & \frac{6EI_z}{L^2} & 0 & 0 & 0 & \frac{4EI_z}{L} & 0 & -\frac{6EI_z}{L^2} & 0 & 0 & 0 & \frac{2EI_z}{L} \\ -\frac{EA}{L} & 0 & 0 & 0 & 0 & 0 & \frac{EA}{L} & 0 & 0 & 0 & 0 & 0 \\ 0 & -\frac{12EI_z}{L^3} & 0 & 0 & 0 & -\frac{6EI_z}{L^2} & 0 & \frac{12EI_z}{L^3} & 0 & 0 & 0 & -\frac{6EI_z}{L^2} \\ 0 & 0 & -\frac{12EI_y}{L^3} & 0 & \frac{6EI_y}{L^2} & 0 & 0 & 0 & \frac{12EI_y}{L^3} & 0 & \frac{6EI_y}{L^2} & 0 \\ 0 & 0 & 0 & -k_T & 0 & 0 & 0 & 0 & 0 & k_T & 0 & 0 \\ 0 & 0 & -\frac{6EI_y}{L^2} & 0 & \frac{2EI_y}{L} & 0 & 0 & 0 & \frac{6EI_y}{L^2} & 0 & \frac{4EI_y}{L} & 0 \\ 0 & \frac{6EI_z}{L^2} & 0 & 0 & 0 & \frac{2EI_z}{L} & 0 & -\frac{6EI_z}{L^2} & 0 & 0 & 0 & \frac{4EI_z}{L} \end{bmatrix} \quad (3.2)$$

$$A = 4A_L$$

$$I_y = A_L b_z^2$$

$$I_z = A_L b_y^2$$

$$k_T = EA_D \frac{\sqrt{b_y^2 + b_z^2}}{2} \left(\frac{b_z^2 b_y}{(\sqrt{b_z^2 + L^2})^3} + \frac{b_y^2 b_z}{(\sqrt{b_y^2 + L^2})^3} \right) \quad (3.3)$$

A modification on the stiffness matrix (Eqn. 3.2) is required to take into account the effect of the diagonal bars. These bars are considered to resist in the shear deformation only. The flexibility coefficient, f_D , is given by:

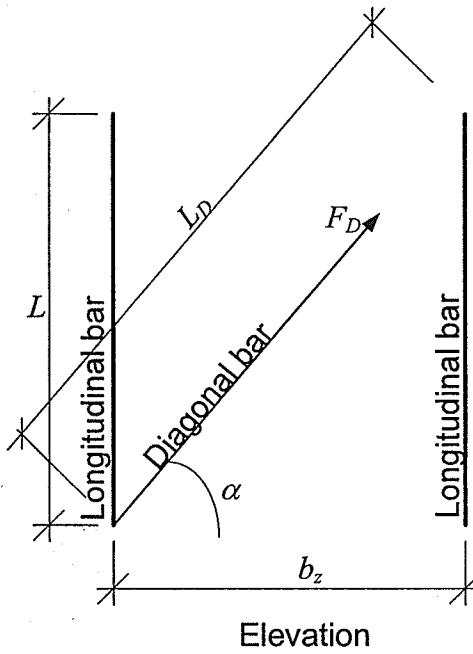


Figure 3.4 - Diagonal effect.

$$F_{Dz} = \frac{2A_D E}{L_{Dz}} u_{Dz}$$

$$F_z = \frac{2A_D E}{L_{Dz}} \cos^2(\alpha_z) u_z$$

Setting $u_z = 1$

$$k_{Dz} = \frac{2A_D E}{L_{Dz}} \cos^2(\alpha_z) \quad (3.4)$$

$$f_{Dz} = k_{Dz}^{-1} = \frac{L_{Dz}}{2A_D E} \frac{1}{\cos^2(\alpha_z)}$$

$$f_{Dz} = \frac{L_{Dz}}{2A_D E} \left(\frac{b_z}{L_{Dz}} \right)$$

If the shear deformation is considered, a new stiffness matrix consists of columns and rows 2 to 6 and 8 to 12, except 4 and 10 of the linear stiffness matrix in Eqn. 3.2 is inverted and the shear deformation is added. After this step, the matrix is re-inverted and the remaining coefficients are calculated by equilibrium of the element (Pinto, 2006-A; Pinto, 2006-B). The steps in this formulation are as follows,

$$\begin{bmatrix} k_{2,2} & k_{2,6} \\ k_{6,2} & k_{6,6} \end{bmatrix}_{\text{with shear deformation}} = \left(\begin{bmatrix} k_{2,2} & k_{2,6} \\ k_{6,2} & k_{6,6} \end{bmatrix}^{-1} + \begin{bmatrix} f_{D2,2} & 0 \\ 0 & 0 \end{bmatrix} \right)^{-1}$$

$$\begin{bmatrix} k_{8,8} & k_{8,12} \\ k_{12,8} & k_{12,12} \end{bmatrix}_{\text{with shear deformation}} = \left(\begin{bmatrix} k_{8,8} & k_{8,12} \\ k_{12,8} & k_{12,12} \end{bmatrix}^{-1} + \begin{bmatrix} f_{D8,8} & 0 \\ 0 & 0 \end{bmatrix} \right)^{-1}$$

$$k_{2,8} = k_{8,2} = -k_{2,2}$$

$$k_{2,12} = k_{12,2} = k_{2,2} - k_{2,6}$$

$$k_{6,8} = k_{8,6} = -k_{2,6}$$

$$k_{6,12} = k_{12,6} = k_{2,6}L - k_{6,6}$$

$$f_{D2,2} = f_{D8,8} = \frac{L_{D_z}}{2EA_D \left(\frac{b_y}{L_{D_z}} \right)^2}$$

$$L_{D_z} = \sqrt{b_y^2 + L^2}$$

$$\begin{bmatrix} k_{3,3} & k_{3,5} \\ k_{5,3} & k_{5,5} \end{bmatrix}_{\text{with shear deformation}} = \left(\begin{bmatrix} k_{3,3} & k_{3,5} \\ k_{5,3} & k_{5,5} \end{bmatrix}^{-1} + \begin{bmatrix} f_{D3,3} & 0 \\ 0 & 0 \end{bmatrix} \right)^{-1}$$

$$\begin{bmatrix} k_{9,9} & k_{9,11} \\ k_{11,9} & k_{11,11} \end{bmatrix}_{\text{with shear deformation}} = \left(\begin{bmatrix} k_{9,9} & k_{9,11} \\ k_{11,9} & k_{11,11} \end{bmatrix}^{-1} + \begin{bmatrix} f_{D9,9} & 0 \\ 0 & 0 \end{bmatrix} \right)^{-1}$$

$$k_{3,9} = k_{9,3} = -k_{3,3}$$

$$k_{3,11} = k_{11,3} = -k_{3,3}L - k_{3,5}$$

$$k_{5,9} = k_{9,5} = -k_{3,5}$$

$$k_{5,11} = k_{11,5} = -k_{3,5}L - k_{5,5}$$

(3.5)

$$f_{D3,3} = f_{D9,9} = \frac{L_{D_y}}{2EA_D \left(\frac{b_z}{L_{D_y}} \right)^2}$$

$$L_{D_y} = \sqrt{b_z^2 + L^2}$$

The new coefficients should substitute the ones in the previous presented linear stiffness matrix (Eqn. 3.2).

Besides the previous matrix, it is required the addition of a non-linear stiffness matrix, K_{NL} , to account for geometric non-linearity. The Non-linear stiffness matrix is given by,

$$K_{NL} = \begin{bmatrix} 0 & 0 & 0 & 0 & 0 & 0 & 0 & 0 & 0 & 0 & 0 & 0 \\ 0 & \frac{6P}{5L} & 0 & 0 & 0 & \frac{P}{10} & 0 & -\frac{6P}{5L} & 0 & 0 & 0 & \frac{P}{10} \\ 0 & 0 & \frac{6P}{5L} & 0 & -\frac{P}{10} & 0 & 0 & 0 & -\frac{6P}{5L} & 0 & -\frac{P}{10} & 0 \\ 0 & 0 & 0 & 0 & 0 & 0 & 0 & 0 & 0 & 0 & 0 & 0 \\ 0 & 0 & -\frac{P}{10} & 0 & \frac{2LP}{15} & 0 & 0 & 0 & \frac{P}{10} & 0 & -\frac{PL}{30} & 0 \\ 0 & \frac{P}{10} & 0 & 0 & 0 & \frac{2LP}{15} & 0 & -\frac{P}{10} & 0 & 0 & 0 & -\frac{PL}{30} \\ 0 & 0 & 0 & 0 & 0 & 0 & 0 & 0 & 0 & 0 & 0 & 0 \\ 0 & -\frac{6P}{5L} & 0 & 0 & 0 & -\frac{P}{10} & 0 & \frac{6P}{5L} & 0 & 0 & 0 & -\frac{P}{10} \\ 0 & 0 & -\frac{6P}{5L} & 0 & \frac{P}{10} & 0 & 0 & 0 & \frac{6P}{5L} & 0 & \frac{P}{10} & 0 \\ 0 & 0 & 0 & 0 & 0 & 0 & 0 & 0 & 0 & 0 & 0 & 0 \\ 0 & 0 & \frac{P}{10} & 0 & -\frac{PL}{30} & 0 & 0 & 0 & \frac{P}{10} & 0 & \frac{2LP}{15} & 0 \\ 0 & \frac{P}{10} & 0 & 0 & 0 & -\frac{PL}{30} & 0 & -\frac{P}{10} & 0 & 0 & 0 & \frac{2LP}{15} \end{bmatrix} \quad (3.6)$$

The axial force P is the average axial force in the two node of the element; it is calculated in the subroutine that calculates the elements forces, thus it is considered equal to zero for the first load step. The axial force is defined as positive if the element is in tension.

The mass is assumed uniformly distributed along the element length. Therefore, the consistent mass matrix of a uniform beam-column will be used, and is given by:

$$M = AUX \begin{bmatrix} 140 & 0 & 0 & 0 & 0 & 0 & 70 & 0 & 0 & 0 & 0 & 0 \\ 0 & 156 & 0 & 0 & 0 & 22L & 0 & 54 & 0 & 0 & 0 & -13L \\ 0 & 0 & 156 & 0 & -22L & 0 & 0 & 0 & 54 & 0 & 13L & 0 \\ 0 & 0 & 0 & \frac{140J_x}{4A_L} & 0 & 0 & 0 & 0 & 0 & \frac{70J_x}{4A_L} & 0 & 0 \\ 0 & 0 & -22L & 0 & 4L^2 & 0 & 0 & 0 & -13L & 0 & -3L^2 & 0 \\ 0 & 22L & 0 & 0 & 0 & 4L^2 & 0 & 13L & 0 & 0 & 0 & -3L \\ 70 & 0 & 0 & 0 & 0 & 0 & 140 & 0 & 0 & 0 & 0 & 0 \\ 0 & 54 & 0 & 0 & 0 & 13L & 0 & 156 & 0 & 0 & 0 & -22L \\ 0 & 0 & 54 & 0 & -13L & 0 & 0 & 0 & 156 & 0 & 22L & 0 \\ 0 & 0 & 0 & \frac{70J_x}{4A_L} & 0 & 0 & 0 & 0 & 0 & \frac{140J_x}{4A_L} & 0 & 0 \\ 0 & 0 & 13L & 0 & -3L^2 & 0 & 0 & 0 & 22L & 0 & 4L^2 & 0 \\ 0 & -13L & 0 & 0 & 0 & -3L & 0 & -22L & 0 & 0 & 0 & 4L^2 \end{bmatrix} \quad (3.7)$$

where

$$AUX = \frac{\left(4A_L\rho + \frac{4A_D L_D \rho}{L}\right)L}{420} \quad (3.8)$$

$$J_x = I_y + I_z$$

$$L_D = \frac{\sqrt{b_z^2 + L^2} + \sqrt{b_y^2 + L^2}}{2}$$

3.1.2. TOWER TAPERED SHAFT

The tapered shaft tower, Figure 3.5, is modeled with the same assumptions as the straight shaft, i.e. a beam-column element with equivalent geometric properties. The difference is that the inertias are not constant.

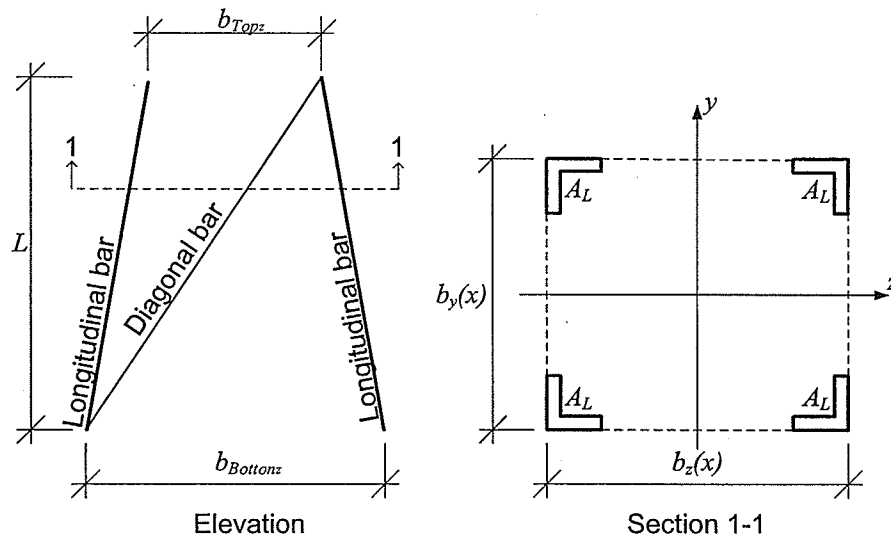


Figure 3.5 - Tapered shaft segment.

The equivalent section properties of the tapered element representing a lattice segment are defined as the following:

$$\begin{aligned}
 A &= 4A_L \\
 I_y(x) &= 4 \left[A_L \left(\frac{b_z(x)}{2} \right)^2 \right] = A_L [b_z(x)]^2 \\
 I_z(x) &= 4 \left[A_L \left(\frac{b_y(x)}{2} \right)^2 \right] = A_L [b_y(x)]^2 \\
 b_y(x) &= b_{Bottom_y} (1 - \beta_y x) \\
 b_z(x) &= b_{Bottom_z} (1 - \beta_z x) \\
 \beta &= \frac{b_{Bottom} - b_{Top}}{b_{Bottom} L}
 \end{aligned}
 \tag{3.9}$$

Similar to the case of a straight shaft, the area of the diagonal bars, A_D is not considered, as they are only assumed to resist shear.

As can be seen that the inertia is not constant along the element length, a formulation for the stiffness matrix of a tapered beam-column is presented in the following:

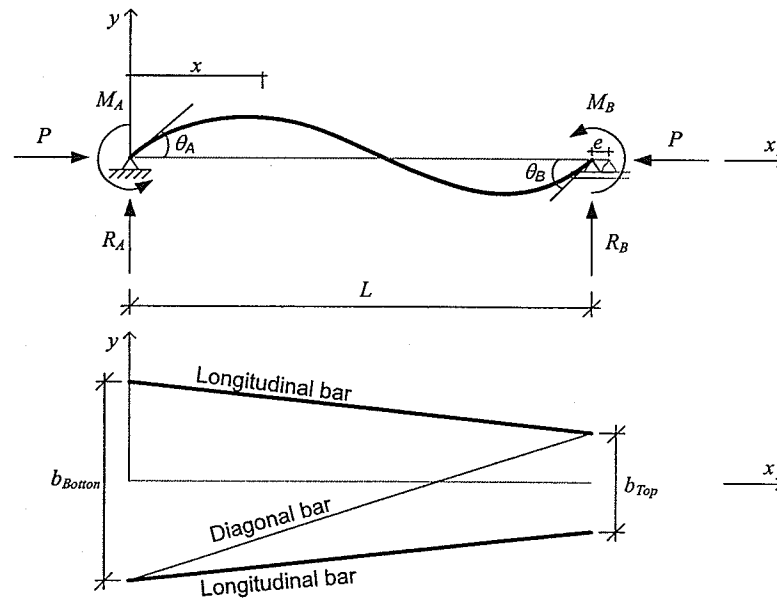


Figure 3.6 - Deformed beam-column element.

Consider a simple supported beam in the xy -plane with varying moment of inertia along its length subjected to end moments and a compressive force as shown in Figure 3.6.

$$\begin{aligned}
 EI_z(x) \frac{\partial^2 y(x)}{\partial x^2} &= M(x) \\
 EI_z(x) \frac{\partial^2 y(x)}{\partial x^2} &= R_A x - M_A - Py(x) \\
 EI_z(x) \frac{\partial^2 y(x)}{\partial x^2} &= \frac{M_A + M_B}{L} x - M_A - Py(x) \tag{3.10} \\
 \frac{\partial^2 y(x)}{\partial x^2} &= \frac{\frac{(M_A + M_B)x}{L} - M_A}{EI_z(x)} - \frac{Py(x)}{EI_z(x)} \\
 \frac{\partial^2 y(x)}{\partial x^2} &= \frac{\frac{(M_A + M_B)x}{L} - M_A}{EI_{Bottom} (1 + \beta x)^2} - \frac{\rho^2 y(x)}{(1 + \beta x)^2}
 \end{aligned}$$

where $\rho = \sqrt{\frac{|P|}{EI_{Bottom}}}$.

Solving the differential equation for displacement together with the boundary conditions $y(0) = 0$ and $y(L) = 0$, the slope of the beam is obtained to be:

$$\begin{aligned}
\frac{\partial y(x)}{\partial x} = \theta(x) = & -\frac{1}{2} \frac{\left(x + \frac{1}{\beta} \right)^{\frac{1-\beta+\sqrt{\beta^2-4\rho^2}}{2}} \left(\beta + \sqrt{\beta^2-4\rho^2} \right) \left[\left(\frac{L\beta+1}{\beta} \right)^{\frac{1-\beta+\sqrt{\beta^2-4\rho^2}}{2}} M_A + \left(\frac{1}{\beta} \right)^{\frac{1-\beta+\sqrt{\beta^2-4\rho^2}}{2}} M_B \right]}{\beta \left(x + \frac{1}{\beta} \right) \rho^2 EI_{Bottom} \sqrt{\frac{L\beta}{\beta}} \sqrt{\frac{1}{\beta}} \left[\left(\frac{L\beta+1}{\beta} \right)^{\frac{1-\sqrt{\beta^2-4\rho^2}}{2}} \left(\frac{1}{\beta} \right)^{\frac{1-\sqrt{\beta^2-4\rho^2}}{2}} - \left(\frac{1}{\beta} \right)^{\frac{1-\sqrt{\beta^2-4\rho^2}}{2}} \left(\frac{L\beta+1}{\beta} \right)^{\frac{1-\sqrt{\beta^2-4\rho^2}}{2}} \right]} \\
& + \frac{1}{2} \frac{\left(x + \frac{1}{\beta} \right)^{\frac{1-\beta-\sqrt{\beta^2-4\rho^2}}{2}} \left(\beta - \sqrt{\beta^2-4\rho^2} \right) \left[\left(\frac{L\beta+1}{\beta} \right)^{\frac{1-\beta-\sqrt{\beta^2-4\rho^2}}{2}} M_A + \left(\frac{1}{\beta} \right)^{\frac{1-\beta-\sqrt{\beta^2-4\rho^2}}{2}} M_B \right]}{\beta \left(x + \frac{1}{\beta} \right) \rho^2 EI_{Bottom} \sqrt{\frac{L\beta}{\beta}} \sqrt{\frac{1}{\beta}} \left[\left(\frac{L\beta+1}{\beta} \right)^{\frac{1-\sqrt{\beta^2-4\rho^2}}{2}} \left(\frac{1}{\beta} \right)^{\frac{1-\sqrt{\beta^2-4\rho^2}}{2}} - \left(\frac{1}{\beta} \right)^{\frac{1-\sqrt{\beta^2-4\rho^2}}{2}} \left(\frac{L\beta+1}{\beta} \right)^{\frac{1-\sqrt{\beta^2-4\rho^2}}{2}} \right]} \\
& + \frac{M_A + M_B}{\rho^2 LEI_{Bottom}}
\end{aligned} \tag{3.11}$$

Rearranging the solutions and calculating for the nodes:

$$\begin{aligned}
 \theta_A = \theta(0) &= \left[\frac{\beta^2 \left[\left(\frac{1}{\beta} \right)^{a+b} \left(L + \frac{1}{\beta} \right)^{a-b} (a+b) - \left(\frac{1}{\beta} \right)^{a-b} \left(L + \frac{1}{\beta} \right)^{a+b} (a-b) \right]}{P\sqrt{L\beta+1} \left[\left(L + \frac{1}{\beta} \right)^b \left(\frac{1}{\beta} \right)^{-b} - \left(\frac{1}{\beta} \right)^b \left(L + \frac{1}{\beta} \right)^{-b} \right]} + \frac{1}{P.L} \right] M_A \\
 &+ \left[\frac{2\beta b}{P\sqrt{L\beta+1} \left[\left(L + \frac{1}{\beta} \right)^b \left(\frac{1}{\beta} \right)^{-b} - \left(\frac{1}{\beta} \right)^b \left(L + \frac{1}{\beta} \right)^{-b} \right]} + \frac{1}{PL} \right] M_B = f_1 M_A + f_2 M_B \\
 \theta_B = \theta(L) &= \left[\frac{2\beta b}{P\sqrt{L\beta+1} \left[\left(L + \frac{1}{\beta} \right)^b \left(\frac{1}{\beta} \right)^{-b} - \left(\frac{1}{\beta} \right)^b \left(L + \frac{1}{\beta} \right)^{-b} \right]} + \frac{1}{PL} \right] M_A \\
 &+ \left[\frac{\beta \left[\left(L + \frac{1}{\beta} \right)^{a+b} (a+b) \left(\frac{1}{\beta} \right)^{a-b} - \left(L + \frac{1}{\beta} \right)^{a-b} (a-b) \left(\frac{1}{\beta} \right)^{a+b} \right]}{P\sqrt{L\beta+1} \left[\left(L + \frac{1}{\beta} \right)^b \left(\frac{1}{\beta} \right)^{-b} - \left(\frac{1}{\beta} \right)^b \left(L + \frac{1}{\beta} \right)^{-b} \right]} + \frac{1}{PL} \right] M_B = f_2 M_A + f_3 M_B
 \end{aligned} \tag{3.12}$$

For compression ($P > 0$):

$$\begin{aligned}
 b &= \frac{\sqrt{\beta^2 - 4\rho^2}}{2\beta} \\
 a &= \frac{1}{2}
 \end{aligned} \tag{3.13}$$

For tension ($P < 0$):

$$\begin{aligned}
 b &= \frac{\sqrt{\beta^2 + 4\rho^2}}{2\beta} \\
 a &= \frac{1}{2}
 \end{aligned} \tag{3.14}$$

Eqn. 3.12 can be written in the matrix form as:

$$\begin{aligned} \begin{Bmatrix} \theta_A \\ \theta_B \end{Bmatrix} &= \begin{bmatrix} f_1 & f_2 \\ f_2 & f_3 \end{bmatrix} \begin{Bmatrix} M_A \\ M_B \end{Bmatrix} \\ \begin{Bmatrix} M_A \\ M_B \end{Bmatrix} &= \begin{bmatrix} f_1 & f_2 \\ f_2 & f_3 \end{bmatrix}^{-1} \begin{Bmatrix} \theta_A \\ \theta_B \end{Bmatrix} = \begin{bmatrix} S_1 & S_2 \\ S_2 & S_3 \end{bmatrix} \begin{Bmatrix} \theta_A \\ \theta_B \end{Bmatrix} \end{aligned} \quad (3.15)$$

where S_1 , S_2 , and S_3 are stiffness coefficients obtained numerically. Similar procedure is carried out for the element in the xz -plane. As well, the same method can be used for zero axial force members.

Consider a member with ends having relative transverse displacement of Δ as shown in Figure 3.7 (Chen and Lui, 1991).

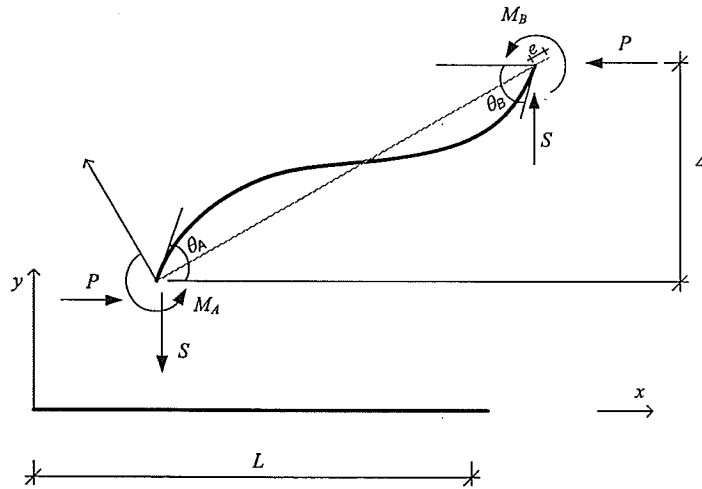


Figure 3.7 - Sway effect.

The end moments can be written as:

$$\begin{aligned} M_A &= S_1 \left[\theta_A - \tan^{-1} \left(\frac{\Delta}{L} \right) \right] + S_2 \left[\theta_B - \tan^{-1} \left(\frac{\Delta}{L} \right) \right] \\ M_B &= S_2 \left[\theta_A - \tan^{-1} \left(\frac{\Delta}{L} \right) \right] + S_3 \left[\theta_B - \tan^{-1} \left(\frac{\Delta}{L} \right) \right] \end{aligned} \quad (3.16)$$

For small $\frac{\Delta}{L}$:

$$\begin{aligned} M_A &= S_1\theta_A + S_2\theta_B - (S_1 + S_2)\frac{\Delta}{L} \\ M_B &= S_2\theta_A + S_3\theta_B - (S_2 + S_3)\frac{\Delta}{L} \end{aligned} \quad (3.17)$$

From equilibrium:

$$\begin{aligned} SL + P\Delta + M_A + M_B &= 0 \\ S &= -\frac{P\Delta + M_A + M_B}{L} \\ S &= -\frac{1}{L} \left[S_1\theta_A + S_2\theta_B - (S_1 + S_2)\frac{\Delta}{L} + S_2\theta_A + S_3\theta_B - (S_2 + S_3)\frac{\Delta}{L} + P\Delta \right] \\ S &= \left[-\left(\frac{S_1 + S_2}{L}\right)\theta_A - \left(\frac{S_2 + S_3}{L}\right)\theta_B + \left(\frac{S_1 + 2S_2 + S_3}{L^2} + \frac{P}{L}\right)\Delta \right] \end{aligned} \quad (3.18)$$

Arranging for a matrix form:

$$\begin{Bmatrix} M_A \\ M_B \\ S \\ P \end{Bmatrix} = \begin{bmatrix} S_1 & S_2 & -\frac{S_1 + S_2}{L} & 0 \\ S_2 & S_3 & -\frac{S_2 + S_3}{L} & 0 \\ -\frac{S_1 + S_2}{L} & -\frac{S_2 + S_3}{L} & \frac{S_1 + 2S_2 + S_3 - PL}{L^2} & 0 \\ 0 & 0 & 0 & \frac{EA}{L} \end{bmatrix} \begin{Bmatrix} \theta_A \\ \theta_B \\ \Delta \\ e \end{Bmatrix} \quad (3.19)$$

The torsion stiffness is calculated with the same procedure as the tower straight shaft, assuming an average tower width. With the expansion for the z direction, the stiffness matrix becomes:

$$K = \begin{bmatrix} k_{1,1} & 0 & 0 & 0 & 0 & 0 & k_{1,7} & 0 & 0 & 0 & 0 & 0 \\ 0 & k_{2,2} & 0 & 0 & 0 & k_{2,6} & 0 & k_{2,8} & 0 & 0 & 0 & k_{2,12} \\ 0 & 0 & k_{3,3} & 0 & k_{3,5} & 0 & 0 & 0 & k_{3,9} & 0 & k_{3,11} & 0 \\ 0 & 0 & 0 & k_{4,4} & 0 & 0 & 0 & 0 & 0 & k_{4,10} & 0 & 0 \\ 0 & 0 & k_{5,3} & 0 & k_{5,5} & 0 & 0 & 0 & k_{5,9} & 0 & k_{5,11} & 0 \\ 0 & k_{6,2} & 0 & 0 & 0 & k_{6,6} & 0 & k_{6,8} & 0 & 0 & 0 & k_{6,12} \\ k_{7,1} & 0 & 0 & 0 & 0 & 0 & k_{7,7} & 0 & 0 & 0 & 0 & 0 \\ 0 & k_{8,2} & 0 & 0 & 0 & k_{8,6} & 0 & k_{8,8} & 0 & 0 & 0 & k_{8,12} \\ 0 & 0 & k_{9,3} & 0 & k_{9,5} & 0 & 0 & 0 & k_{9,9} & 0 & k_{9,11} & 0 \\ 0 & 0 & 0 & k_{10,4} & 0 & 0 & 0 & 0 & 0 & k_{10,10} & 0 & 0 \\ 0 & 0 & k_{11,3} & 0 & k_{11,5} & 0 & 0 & 0 & k_{11,9} & 0 & k_{11,11} & 0 \\ 0 & k_{12,2} & 0 & 0 & 0 & k_{12,6} & 0 & k_{12,8} & 0 & 0 & 0 & k_{12,12} \end{bmatrix}$$

$$k_{1,1} = k_{7,7} = -k_{1,7} = -k_{7,1} = \frac{4EA_L}{L}$$

$$k_{2,2} = -k_{2,8} = -k_{8,2} = k_{8,8} = \frac{S_{1z} + 2S_{2z} + S_{3z} - PL}{L^2}$$

$$k_{2,6} = k_{6,2} = -k_{6,8} = -k_{8,6} = \frac{S_{1z} + S_{2z}}{L}$$

$$k_{2,12} = k_{12,2} = -k_{8,12} = -k_{12,8} = \frac{S_{2z} + S_{3z}}{L}$$

$$k_{6,6} = S_{1z}$$

$$k_{6,12} = k_{12,6} = S_{2z}$$

$$k_{12,12} = S_{3z}$$

$$k_{4,4} = -k_{4,10} = -k_{10,4} = k_{10,10} = EA_D \frac{\sqrt{b_y^2 \text{ aver} + b_z^2 \text{ aver}}}{2} \left[\frac{b_z^2 \text{ aver} b_y \text{ aver}}{\left(\sqrt{L^2 + b_z^2 \text{ aver}}\right)^3} + \frac{b_y^2 \text{ aver} b_z \text{ aver}}{\left(\sqrt{L^2 + b_y^2 \text{ aver}}\right)^3} \right] \quad (3.20)$$

$$k_{3,3} = -k_{3,9} = -k_{9,3} = k_{9,9} = \frac{S_{1y} + 2S_{2y} + S_{3y} - PL}{L^2}$$

$$-k_{3,5} = -k_{5,3} = k_{5,9} = k_{9,5} = \frac{S_{1y} + S_{2y}}{L}$$

$$-k_{3,11} = -k_{11,3} = k_{9,11} = k_{11,9} = \frac{S_{2y} + S_{3y}}{L}$$

$$k_{5,5} = S_{1z}$$

$$k_{5,11} = k_{11,5} = S_{2z}$$

$$k_{11,11} = S_{3z}$$

$$I_y = A_1 b_z^2 \text{Bottom}$$

$$I_z = A_1 b_y^2 \text{Bottom}$$

$$a = \frac{1}{2}$$

$$\beta_y = \frac{b_z \text{Top} - b_z \text{Bottom}}{b_z \text{Bottom} L}$$

$$\beta_z = \frac{b_y \text{Top} - b_y \text{Bottom}}{b_y \text{Bottom} L}$$

$$\text{if } \left(-10^{-7} \text{ or } -\frac{EI_{\min}}{L^2} 10^{-5} \right) < P < \left(10^{-7} \text{ or } \frac{EI_{\min}}{L^2} 10^{-5} \right)$$

$$f_{1i} = \frac{L^2 \beta_i^2 + 2L\beta_i - 2\ln(L\beta_i + 1)(L\beta_i + 1)}{L^2 EI_i \beta_i^3}$$

$$f_{2i} = \frac{2L\beta_i - \ln(L\beta_i + 1)(L\beta_i + 2)}{L^2 EI_i \beta_i^3}$$

$$f_{3i} = \frac{\frac{2L\beta_i}{L\beta_i + 1} + \frac{(L\beta_i)^2}{L\beta_i + 1} - 2\ln(L\beta_i + 1)}{L^2 EI_i \beta_i^3}$$

$$\text{if } P < \left(-10^{-7} \text{ or } -\frac{EI_{\min}}{L^2} 10^{-5} \right)$$

$$b_i = \frac{\sqrt{\beta_i^2 + 4 \frac{|P|}{EI_i}}}{2\beta_i}$$

$$\text{if } P > \left(10^{-7} \text{ or } \frac{EI_{\min}}{L^2} 10^{-5} \right)$$

$$b_i = \frac{\sqrt{\beta_i^2 - 4 \frac{|P|}{EI_i}}}{2\beta_i}$$

$$f_{1i} = \frac{\beta_i^2 \left[\left(\frac{1}{\beta_i} \right)^{a+b_i} \left(L + \frac{1}{\beta_i} \right)^{a-b_i} (a+b_i) - \left(\frac{1}{\beta_i} \right)^{a-b_i} \left(L + \frac{1}{\beta_i} \right)^{a+b_i} (a-b_i) \right]}{P \sqrt{L\beta_i + 1} \left[\left(L + \frac{1}{\beta_i} \right)^b \left(\frac{1}{\beta_i} \right)^{-b} - \left(\frac{1}{\beta_i} \right)^b \left(L + \frac{1}{\beta_i} \right)^{-b} \right]} + \frac{1}{PL}$$

$$f_{2i} = \frac{2\beta_i b_i}{P \sqrt{L\beta_i + 1} \left[\left(L + \frac{1}{\beta_i} \right)^b \left(\frac{1}{\beta_i} \right)^{-b} - \left(\frac{1}{\beta_i} \right)^b \left(L + \frac{1}{\beta_i} \right)^{-b} \right]} + \frac{1}{PL}$$

$$f_{3i} = \frac{\beta_i \left[\left(L + \frac{1}{\beta_i} \right)^{a+b_i} (a+b_i) \left(\frac{1}{\beta_i} \right)^{a-b_i} - \left(L + \frac{1}{\beta_i} \right)^{a-b_i} (a-b_i) \left(\frac{1}{\beta_i} \right)^{a+b_i} \right]}{P \sqrt{L\beta_i + 1} \left[\left(L + \frac{1}{\beta_i} \right)^b \left(\frac{1}{\beta_i} \right)^{-b} - \left(\frac{1}{\beta_i} \right)^b \left(L + \frac{1}{\beta_i} \right)^{-b} \right] \left(L + \frac{1}{\beta_i} \right)} + \frac{1}{PL}$$

(3.21)

$$\begin{bmatrix} S_{1i} & S_{2i} \\ S_{2i} & S_{3i} \end{bmatrix} = \begin{bmatrix} f_{1i} & f_{2i} \\ f_{2i} & f_{3i} \end{bmatrix}^{-1}$$

If the shear deformation analysis is used, the same procedure used in the straight shaft element is adopted. The shear flexibility coefficients are obtained following the formulation in Eqn. 3.22.

$$\begin{bmatrix} k_{2,2} & k_{2,6} \\ k_{6,2} & k_{6,6} \end{bmatrix}_{\text{with shear deformation}} = \left(\begin{bmatrix} k_{2,2} & k_{2,6} \\ k_{6,2} & k_{6,6} \end{bmatrix}^{-1} + \begin{bmatrix} flexshear_{2,2} & 0 \\ 0 & 0 \end{bmatrix} \right)^{-1}$$

$$\begin{bmatrix} k_{8,8} & k_{8,12} \\ k_{12,8} & k_{12,12} \end{bmatrix}_{\text{with shear deformation}} = \left(\begin{bmatrix} k_{8,8} & k_{8,12} \\ k_{12,8} & k_{12,12} \end{bmatrix}^{-1} + \begin{bmatrix} flexshear_{8,8} & 0 \\ 0 & 0 \end{bmatrix} \right)^{-1}$$

$$k_{2,8} = k_{8,2} = -k_{2,2}$$

$$k_{2,12} = k_{12,2} = k_{2,2}L - k_{2,6}$$

$$k_{6,8} = k_{8,6} = -k_{2,6}$$

$$k_{6,12} = k_{12,6} = k_{2,6}L - k_{6,6}$$

$$flexshear_{2,2} = flexshear_{8,8} = \frac{L_{Dz}}{2EA_D \left(\frac{\left(\frac{b_{y\text{ Bottom}} + b_{y\text{ Top}}}{2} \right)^2}{L_{Dz}} \right)^2}$$

$$L_{Dz} = \sqrt{\left(\frac{b_{y\text{ Bottom}} + b_{y\text{ Top}}}{2} \right)^2 + L^2 + \left(\frac{b_{z\text{ Bottom}} - b_{z\text{ Top}}}{2} \right)^2}$$

$$\begin{bmatrix} k_{3,3} & k_{3,5} \\ k_{5,3} & k_{5,5} \end{bmatrix}_{\text{with shear deformation}} = \left(\begin{bmatrix} k_{3,3} & k_{3,5} \\ k_{5,3} & k_{5,5} \end{bmatrix}^{-1} + \begin{bmatrix} flexshear_{3,3} & 0 \\ 0 & 0 \end{bmatrix} \right)^{-1}$$

$$\begin{bmatrix} k_{9,9} & k_{9,11} \\ k_{11,9} & k_{11,11} \end{bmatrix}_{\text{with shear deformation}} = \left(\begin{bmatrix} k_{9,9} & k_{9,11} \\ k_{11,9} & k_{11,11} \end{bmatrix}^{-1} + \begin{bmatrix} flexshear_{9,9} & 0 \\ 0 & 0 \end{bmatrix} \right)^{-1}$$

$$k_{3,9} = k_{9,3} = -k_{3,3}$$

$$k_{3,11} = k_{11,3} = -k_{3,3}L - k_{3,5}$$

$$k_{5,9} = k_{9,5} = -k_{3,5}$$

$$k_{5,11} = k_{11,5} = -k_{3,5}L - k_{5,5}$$

$$flexshear_{3,3} = flexshear_{9,9} = \frac{L_{Dy}}{2EA_D \left(\frac{\left(\frac{b_{z\text{ Bottom}} + b_{z\text{ Top}}}{2} \right)^2}{L_{Dy}} \right)^2}$$

$$L_{Dy} = \sqrt{\left(\frac{b_{z\text{ Bottom}} + b_{z\text{ Top}}}{2} \right)^2 + L^2 + \left(\frac{b_{y\text{ Bottom}} - b_{y\text{ Top}}}{2} \right)^2}$$

(3.22)

The axial force P is the average axial force in the two nodes of the element; it is considered equal to zero for the first load step. The axial force is defined as negative if the element is in tension.

As the straight tower element, the mass is also considered to be constant along the element length and given by,

$$M = AUX \begin{bmatrix} 140 & 0 & 0 & 0 & 0 & 0 & 70 & 0 & 0 & 0 & 0 & 0 \\ 0 & 156 & 0 & 0 & 0 & 22L & 0 & 54 & 0 & 0 & 0 & -13L \\ 0 & 0 & 156 & 0 & -22L & 0 & 0 & 0 & 54 & 0 & 13L & 0 \\ 0 & 0 & 0 & \frac{140J_x}{4A_L} & 0 & 0 & 0 & 0 & 0 & \frac{70J_x}{4A_L} & 0 & 0 \\ 0 & 0 & -22L & 0 & 4L^2 & 0 & 0 & 0 & -13L & 0 & -3L^2 & 0 \\ 0 & 22L & 0 & 0 & 0 & 4L^2 & 0 & 13L & 0 & 0 & 0 & -3L \\ 70 & 0 & 0 & 0 & 0 & 0 & 140 & 0 & 0 & 0 & 0 & 0 \\ 0 & 54 & 0 & 0 & 0 & 13L & 0 & 156 & 0 & 0 & 0 & -22L \\ 0 & 0 & 54 & 0 & -13L & 0 & 0 & 0 & 156 & 0 & 22L & 0 \\ 0 & 0 & 0 & \frac{70J_x}{4A_L} & 0 & 0 & 0 & 0 & 0 & \frac{140J_x}{4A_L} & 0 & 0 \\ 0 & 0 & 13L & 0 & -3L^2 & 0 & 0 & 0 & 22L & 0 & 4L^2 & 0 \\ 0 & -13L & 0 & 0 & 0 & -3L & 0 & -22L & 0 & 0 & 0 & 4L^2 \end{bmatrix} \quad (3.23)$$

$$AUX = \frac{\left(4A_D\rho + \frac{4A_D L_D\rho}{L}\right)L}{420}$$

$$J_x = I_y + I_z$$

$$L_D = \frac{L_{Dy} + L_{Dz}}{2}$$

3.2. INSULATOR STRING

The insulator was modeled as a truss element as done by many researchers such as Rodrigues (1999) and Oliveira (2006). The stiffness matrix of a truss element is given in the Eqn. 3.24.

$$K_L = \frac{EA}{L} \begin{bmatrix} 1 & 0 & 0 & 0 & 0 & 0 & -1 & 0 & 0 & 0 & 0 & 0 \\ 0 & 0 & 0 & 0 & 0 & 0 & 0 & 0 & 0 & 0 & 0 & 0 \\ 0 & 0 & 0 & 0 & 0 & 0 & 0 & 0 & 0 & 0 & 0 & 0 \\ 0 & 0 & 0 & 10^{-10} & 0 & 0 & 0 & 0 & 0 & 0 & 0 & 0 \\ 0 & 0 & 0 & 0 & 10^{-10} & 0 & 0 & 0 & 0 & 0 & 0 & 0 \\ 0 & 0 & 0 & 0 & 0 & 10^{-10} & 0 & 0 & 0 & 0 & 0 & 0 \\ -1 & 0 & 0 & 0 & 0 & 0 & 1 & 0 & 0 & 0 & 0 & 0 \\ 0 & 0 & 0 & 0 & 0 & 0 & 0 & 0 & 0 & 0 & 0 & 0 \\ 0 & 0 & 0 & 0 & 0 & 0 & 0 & 0 & 0 & 0 & 0 & 0 \\ 0 & 0 & 0 & 0 & 0 & 0 & 0 & 0 & 0 & 10^{-10} & 0 & 0 \\ 0 & 0 & 0 & 0 & 0 & 0 & 0 & 0 & 0 & 0 & 10^{-10} & 0 \\ 0 & 0 & 0 & 0 & 0 & 0 & 0 & 0 & 0 & 0 & 0 & 10^{-10} \end{bmatrix} \quad (3.24)$$

However, it can be noticed that some of the diagonal terms in the above equation are zero. This causes numerical instability in the first step of calculation. To avoid this instability, the technique outlined by Mathur (1985) and Mathur, et al. (1987) will be used to evaluate the initial stiffness matrix. The formulation of this initial stiffness matrix is briefed in the followings.

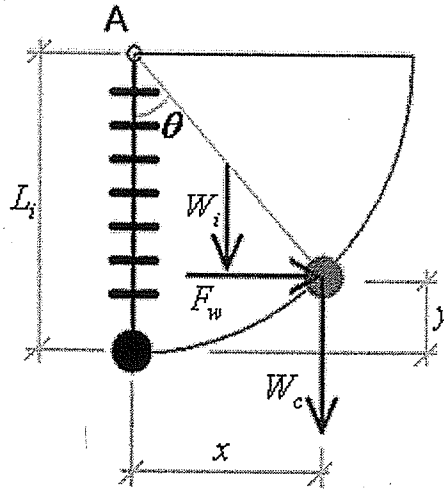


Figure 3.8 - Insulator string.

Consider an insulator string in Figure 3.8, the horizontal stiffness of the insulator string can be formulated using the moment equilibrium about the hinge A.

$$F_w(L_i - y) - \frac{W_i x}{2} - W_c x = 0$$

Solving for F_w yields:

$$F_w = \frac{x(W_i + 2W_c)}{2(L_i - y)} = \frac{x(W_i + 2W_c)}{2L_i[1 - 1 + \cos(\theta)]}$$

$$F_w = \frac{x(W_i + 2W_c)}{2L_i \cos\left[\sin^{-1}\left(\frac{x}{L_i}\right)\right]} = \frac{x(W_i + 2W_c)}{2L_i \sqrt{1 - \frac{x^2}{L_i^2}}} \quad (3.25)$$

where F_w is the wind force, W_i is the weight of the insulator string and is assumed to be uniformly distributed along the length, W_c is the weight of the cable, L_i is the length of the insulator, θ is the rotation at the hinge and x is the horizontal displacement of the cable. The stiffness matrix of the insulator string element for

the first step can therefore be written in the same form as the nonlinear stiffness matrix of an axial force member as follows:

$$K_{NL} = \begin{bmatrix} 0 & 0 & 0 & 0 & 0 & 0 & 0 & 0 & 0 & 0 & 0 & 0 \\ 0 & \frac{P}{L} & 0 & 0 & 0 & 0 & 0 & -\frac{P}{L} & 0 & 0 & 0 & 0 \\ 0 & 0 & \frac{P}{L} & 0 & 0 & 0 & 0 & 0 & -\frac{P}{L} & 0 & 0 & 0 \\ 0 & 0 & 0 & 0 & 0 & 0 & 0 & 0 & 0 & 0 & 0 & 0 \\ 0 & 0 & 0 & 0 & 0 & 0 & 0 & 0 & 0 & 0 & 0 & 0 \\ 0 & 0 & 0 & 0 & 0 & 0 & 0 & 0 & 0 & 0 & 0 & 0 \\ 0 & 0 & 0 & 0 & 0 & 0 & 0 & 0 & 0 & 0 & 0 & 0 \\ 0 & -\frac{P}{L} & 0 & 0 & 0 & 0 & 0 & \frac{P}{L} & 0 & 0 & 0 & 0 \\ 0 & 0 & -\frac{P}{L} & 0 & 0 & 0 & 0 & 0 & \frac{P}{L} & 0 & 0 & 0 \\ 0 & 0 & 0 & 0 & 0 & 0 & 0 & 0 & 0 & 0 & 0 & 0 \\ 0 & 0 & 0 & 0 & 0 & 0 & 0 & 0 & 0 & 0 & 0 & 0 \\ 0 & 0 & 0 & 0 & 0 & 0 & 0 & 0 & 0 & 0 & 0 & 0 \end{bmatrix} \quad (3.26)$$

The axial load P in the initial stiffness matrix, Eqn. 3.26, is represented by half of the weight of the insulator string plus the weight of the conductor span. The axial force is defined as positive if the element is in tension. The program recalculates the axial load P after the first step using the average of the axial forces at the end nodes.

The mass matrix of the insulator string is formulated using the consistent mass as carried out for a truss element. Eqn. 3.27 shows the mass matrix of the insulator string used in this study.

$$M = \frac{A\rho L}{6} \begin{bmatrix} 2 & 0 & 0 & 0 & 0 & 0 & 1 & 0 & 0 & 0 & 0 & 0 \\ 0 & 2 & 0 & 0 & 0 & 0 & 0 & 1 & 0 & 0 & 0 & 0 \\ 0 & 0 & 2 & 0 & 0 & 0 & 0 & 0 & 1 & 0 & 0 & 0 \\ 0 & 0 & 0 & 10^{-15} & 0 & 0 & 0 & 0 & 0 & 0 & 0 & 0 \\ 0 & 0 & 0 & 0 & 10^{-15} & 0 & 0 & 0 & 0 & 0 & 0 & 0 \\ 0 & 0 & 0 & 0 & 0 & 10^{-15} & 0 & 0 & 0 & 0 & 0 & 0 \\ 1 & 0 & 0 & 0 & 0 & 0 & 2 & 0 & 0 & 0 & 0 & 0 \\ 0 & 1 & 0 & 0 & 0 & 0 & 0 & 2 & 0 & 0 & 0 & 0 \\ 0 & 0 & 1 & 0 & 0 & 0 & 0 & 0 & 2 & 0 & 0 & 0 \\ 0 & 0 & 0 & 0 & 0 & 0 & 0 & 0 & 0 & 10^{-15} & 0 & 0 \\ 0 & 0 & 0 & 0 & 0 & 0 & 0 & 0 & 0 & 0 & 10^{-15} & 0 \\ 0 & 0 & 0 & 0 & 0 & 0 & 0 & 0 & 0 & 0 & 0 & 10^{-15} \end{bmatrix} \quad (3.27)$$

The linear stiffness matrix used in this study was taken from Hajdin, et al. (2000) while the nonlinear part was assumed to be the same as that for a truss element, Eqn. 3.26. Similarly, the mass matrix for the cable element was derived using the consistent mass and the resulting mass matrix is the same as Eqn. 3.27 for the insulator string element. The linear stiffness matrix is given by:

$$K_L = \frac{E_{eq}A}{L} \begin{bmatrix} 1 & 0 & 0 & 0 & 0 & 0 & -1 & 0 & 0 & 0 & 0 & 0 \\ 0 & 0 & 0 & 0 & 0 & 0 & 0 & 0 & 0 & 0 & 0 & 0 \\ 0 & 0 & 0 & 0 & 0 & 0 & 0 & 0 & 0 & 0 & 0 & 0 \\ 0 & 0 & 0 & 10^{-10} & 0 & 0 & 0 & 0 & 0 & 0 & 0 & 0 \\ 0 & 0 & 0 & 0 & 10^{-10} & 0 & 0 & 0 & 0 & 0 & 0 & 0 \\ 0 & 0 & 0 & 0 & 0 & 10^{-10} & 0 & 0 & 0 & 0 & 0 & 0 \\ -1 & 0 & 0 & 0 & 0 & 0 & 1 & 0 & 0 & 0 & 0 & 0 \\ 0 & 0 & 0 & 0 & 0 & 0 & 0 & 0 & 0 & 0 & 0 & 0 \\ 0 & 0 & 0 & 0 & 0 & 0 & 0 & 0 & 0 & 0 & 0 & 0 \\ 0 & 0 & 0 & 0 & 0 & 0 & 0 & 0 & 0 & 10^{-10} & 0 & 0 \\ 0 & 0 & 0 & 0 & 0 & 0 & 0 & 0 & 0 & 0 & 10^{-10} & 0 \\ 0 & 0 & 0 & 0 & 0 & 0 & 0 & 0 & 0 & 0 & 0 & 10^{-10} \end{bmatrix} \quad (3.28)$$

$$\alpha = \tan\left(\frac{|DY|}{\sqrt{DX^2 + DZ^2}}\right)$$

$$g = 9.81 \text{ m/s}^2$$

$$q_x = \rho Ag \sin(\alpha)$$

$$q_z = \rho Ag \cos(\alpha)$$

$$E_{eq}A = \frac{EA}{1 + \frac{EA}{24} \left((q_z L)^2 \frac{\left(2P - \frac{2q_x L}{3}\right)}{\left(P^2 - \frac{2q_x LP}{3} + \left(\frac{q_x L}{3}\right)^2\right)^2} \right)}$$

Similar to the case of the insulator string element, the linear stiffness matrix of the cable contain zero coefficients on the diagonal. Therefore, the nonlinear stiffness matrix was added in with the load P be the initial pretension in the cable for the first load step. P is recalculated in each step.

3.4. SPRING ELEMENT

The spring element was used at the terminations of the line representing the cables or the extremity towers. The mass and self-weight load of the spring element was assumed to be applied only on the unrestrained node (the element must be restrained at node 1 and the load must be applied at node 2). This element is the only one in the program library that can have zero length. All of its properties must be given in the global coordinate system.

The Stiffness matrix is given by:

$$K_L = \begin{bmatrix} KUX & 0 & 0 & 0 & 0 & 0 & -KUX & 0 & 0 & 0 & 0 & 0 \\ 0 & KUY & 0 & 0 & 0 & 0 & 0 & -KUY & 0 & 0 & 0 & 0 \\ 0 & 0 & KUZ & 0 & 0 & 0 & 0 & 0 & -KUZ & 0 & 0 & 0 \\ 0 & 0 & 0 & KRX & 0 & 0 & 0 & 0 & 0 & -KRX & 0 & 0 \\ 0 & 0 & 0 & 0 & KRY & 0 & 0 & 0 & 0 & 0 & -KRY & 0 \\ 0 & 0 & 0 & 0 & 0 & KRZ & 0 & 0 & 0 & 0 & 0 & -KRZ \\ -KUX & 0 & 0 & 0 & 0 & 0 & KUX & 0 & 0 & 0 & 0 & 0 \\ 0 & -KUY & 0 & 0 & 0 & 0 & 0 & KYY & 0 & 0 & 0 & 0 \\ 0 & 0 & -KUZ & 0 & 0 & 0 & 0 & 0 & KUZ & 0 & 0 & 0 \\ 0 & 0 & 0 & -KRX & 0 & 0 & 0 & 0 & 0 & KRX & 0 & 0 \\ 0 & 0 & 0 & 0 & -KRY & 0 & 0 & 0 & 0 & 0 & KRY & 0 \\ 0 & 0 & 0 & 0 & 0 & -KRZ & 0 & 0 & 0 & 0 & 0 & KRZ \end{bmatrix} \quad (3.29)$$

where KUX, KUY and KUZ are the translational stiffness coefficients in the global x-, y-, and z-directions, respectively, and KRX, KRY and KRZ are the rotational stiffness parameters which generally are zero. Note that although the rotational stiffness coefficients are theoretically equal to zero, small values should be input for numerical stability.

Since the mass of the spring is considered applied only on node 2 as stated, the Mass matrix, M , is given by,

$$M = MX \begin{bmatrix} 10^{-15} & 0 & 0 & 0 & 0 & 0 & 0 & 0 & 0 & 0 & 0 & 0 \\ 0 & 10^{-15} & 0 & 0 & 0 & 0 & 0 & 0 & 0 & 0 & 0 & 0 \\ 0 & 0 & 10^{-15} & 0 & 0 & 0 & 0 & 0 & 0 & 0 & 0 & 0 \\ 0 & 0 & 0 & 10^{-15} & 0 & 0 & 0 & 0 & 0 & 0 & 0 & 0 \\ 0 & 0 & 0 & 0 & 10^{-15} & 0 & 0 & 0 & 0 & 0 & 0 & 0 \\ 0 & 0 & 0 & 0 & 0 & 10^{-15} & 0 & 0 & 0 & 0 & 0 & 0 \\ 0 & 0 & 0 & 0 & 0 & 0 & 1 & 0 & 0 & 0 & 0 & 0 \\ 0 & 0 & 0 & 0 & 0 & 0 & 0 & 1 & 0 & 0 & 0 & 0 \\ 0 & 0 & 0 & 0 & 0 & 0 & 0 & 0 & 1 & 0 & 0 & 0 \\ 0 & 0 & 0 & 0 & 0 & 0 & 0 & 0 & 0 & 10^{-15} & 0 & 0 \\ 0 & 0 & 0 & 0 & 0 & 0 & 0 & 0 & 0 & 0 & 10^{-15} & 0 \\ 0 & 0 & 0 & 0 & 0 & 0 & 0 & 0 & 0 & 0 & 0 & 10^{-15} \end{bmatrix} \quad (3.30)$$

Where MX is the mass of the spring in tons.

4. VALIDATION OF PROGRAM

An in-house program, SADAP-Static and Dynamic Analysis Program, was developed using FORTRAN. All the elements described in the previous chapter were incorporated in the program. A series of test problems was created to verify all the elements and procedures of the program. The results were compared with results from other commercial FE programs, published or theoretical results. Only some of the examples are presented in this chapter. Other examples are included in the Appendix - B.

4.1. ACCEPTANCE CRITERIA

The program was considered acceptable if the difference between the program results and the available results did not exceed five percent for displacements and ten percent for internal forces. When the simplified tower models were verified with detailed tower models, the results were acceptable if the difference of the results did not exceed ten percent for displacements and natural frequencies values.

The percentage difference is calculated using the following formula (SAP2000, 2006):

$$P.D. = 100 \left(\frac{\text{Results from program}}{\text{Results from other source}} - 1 \right) \% \quad (4.1)$$

The maximum percentage difference of displacement and internal forces (when applicable) is provided in the end of each example.

The examples were divided into eight groups. Each group division was based on the element type. Table 4.1 summarizes all the examples.

Table 4.1 - Summary of examples.

Beam-column				
Example No.	Example name	Features tested	Analysis type	Method of Verification
1	General load 1	Automatic self weight	Linear static	Ansys version 11
		Concentrated load		Weaver and Gere, 1980 pages 344 to 357
2	Local axis	Rotation of the local axis	Linear static	Weaver and Gere, 1980 pages 344 to 357
3	Buckling of column	Nonlinear analysis	Nonlinear static	Theoretical results
4	Eigenvalue problem 1	Eigenvalue analysis	Eigenvalue	Militano, 2000 pages 32 to 35
5	Eigenvalue problem 2	Eigenvalue analysis with axial force	Eigenvalue	Przemieniecki, 1985 pages 403 to 406
6	Vibration 1	Dynamic solver	Linear dynamic	Battista, 2007-C page 138
Truss				
Example No.	Example name	Features tested	Analysis type	Method of Verification
7	General load 2	Automatic self weight	Linear static	Ansys version 11
		Concentrated load		Weaver and Gere, 1980 pages 343 to 345
8	Buckling	Nonlinear analysis	Nonlinear static	Theoretical results
9	Eigenvalue problem 3	Eigenvalue analysis	Eigenvalue	Mario Paz, 2004 page 434 to 437
Spring				
Example No.	Example name	Features tested	Analysis type	Method of Verification
10	General load 3	Automatic self weight	Linear static	Theoretical results
		Concentrated load		
11	Eigenvalue problem 4	Eigenvalue analysis	Eigenvalue	Theoretical results
12	Vibration 2	Dynamic solver	Linear dynamic	Theoretical results
Cable				
Example No.	Example name	Features tested	Analysis type	Method of Verification
13	General load 4	Automatic self weight	Nonlinear static	Theoretical results
		Concentrated load		
14	Eigenvalue problem 5	Eigenvalue analysis	Eigenvalue	Irvine, 1992 page 192
Tapered tower				
Example No.	Example name	Features tested	Analysis type	Method of Verification
15	General load 5	Automatic self weight	Nonlinear static	Frame and Truss element comparison
		Concentrated load		
16	Eigenvalue problem 6	Eigenvalue analysis	Eigenvalue	Frame and Truss element comparison
Beam-column (stability functions)				
Example No.	Example name	Features tested	Analysis type	Method of Verification
17	General load 6	Automatic self weight	Linear static	Ansys version 11
		Uniform distributed load		Weaver and Gere, 1980 pages 344 to 357
		Concentrated load		
18	Local axis	Rotation of the local axis	Linear static	Ansys version 11
19	Buckling of column	Nonlinear analysis	Nonlinear static	Theoretical results
20	Eigenvalue problem 7	Eigenvalue analysis	Eigenvalue	Militano, 2000 pages 32 to 35
21	Eigenvalue problem 8	Eigenvalue analysis with axial force	Eigenvalue	Przemieniecki, 1985 pages 403 to 406
22	Vibration 3	Dynamic solver	Linear dynamic	Battista, 2007-C page 138
Insulator string				
Example No.	Example name	Features tested	Analysis type	Method of Verification
23	General load 7	Automatic self weight	Nonlinear static	Theoretical results
		Concentrated load		
24	Eigenvalue problem 9	Eigenvalue analysis	Eigenvalue	Theoretical results
25	Vibration 4	Dynamic solver	Linear dynamic	Theoretical results
Straigh tower				
Example No.	Example name	Features tested	Analysis type	Method of Verification
26	General load 8	Automatic self weight	Nonlinear static	Frame and Truss element comparison
		Concentrated load		
27	Eigenvalue problem 8	Eigenvalue analysis	Eigenvalue	Frame and Truss element comparison

4.2. EXAMPLES

As stated, only some examples will be presented in this Chapter. The rests are included in the Appendix - B.

Example No. 11:

This example was chosen to verify the Eigenvalue analysis of the spring element. The results where compared with a theoretical analysis. The spring is directly attached to a mass, m of 5 tons. The properties of the spring are

$$K_{UX} = 30 \text{ kN/m} \quad K_{UY} = 20 \text{ kN/m} \quad K_{UZ} = 35 \text{ kN/m}$$

The natural frequencies of the system can be calculated as

$$\omega = \sqrt{\frac{k}{m}} = \left\{ \begin{array}{l} 2.44949 \\ 2.00000 \\ 2.64575 \end{array} \right\} \text{ rad/s}$$

The SADAP results:

MODE	MODAL MASS	FREQ[RAD]	FREQ[HZ]
1	5.00000	2.00000	0.31831
2	5.00000	2.44949	0.38985
3	5.00000	2.64575	0.42108

MODAL SHAPES							
MODAL SHAPE: 1							
NODE	DX	DY	DZ	RX	RY	RZ	
1	0.00000	0.00000	0.00000	0.00000	0.00000	0.00000	
2	0.00000	1.00000	0.00000	0.00000	0.00000	0.00000	

MODAL SHAPE: 2							
NODE	DX	DY	DZ	RX	RY	RZ	
1	0.00000	0.00000	0.00000	0.00000	0.00000	0.00000	
2	1.00000	0.00000	0.00000	0.00000	0.00000	0.00000	

MODAL SHAPE: 3							
NODE	DX	DY	DZ	RX	RY	RZ	
1	0.00000	0.00000	0.00000	0.00000	0.00000	0.00000	
2	0.00000	0.00000	1.00000	0.00000	0.00000	0.00000	

Here $P.D. = 0\%$

Example No. 12:

This example was chosen to verify the dynamic solver. Two systems, a SDOF and a 2DOF system, were used as shown in Figure 4.1. The results were compared with a theoretical and numerical analyses (Battista, 2007-A). The damping matrix is a Rayleigh type damping matrix, detailed in Chapter 5.

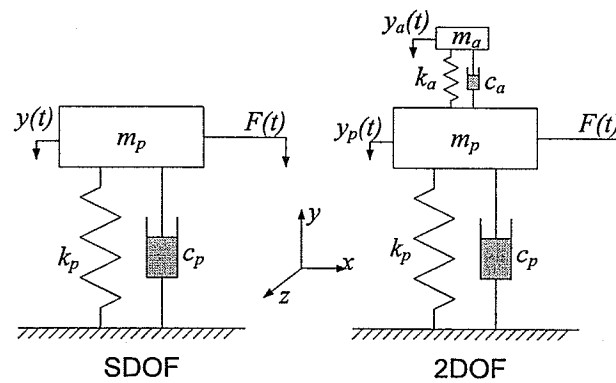


Figure 4.1 - Example No. 12.

The properties of the system are

$$\begin{aligned}
 m_p &= 5 \text{ tons} & k_p &= 20 \text{ kN/m} & \xi_p &= 0.01 \text{ (or } c_p = 0.04 \text{ kN-s/m)} \\
 m_a &= 0.05 \text{ tons} & k_a &= 0.19 \text{ kN/m} & \xi_a &= 0.0513 \text{ (or } c_a = 0.2 \text{ kN-s/m)}
 \end{aligned}$$

The applied force is described as

$$F(t) = F_0 \sin(\Omega t) = 1 \sin(2t) \text{ kN}$$

Theoretical vertical displacement for the SDOF in Figure 4.1(a) is

$$y_{\max} = \frac{F_0}{k_p} \frac{1}{\sqrt{\left[1 - \left(\frac{\Omega}{w}\right)^2\right]^2 + \left(2\xi \frac{\Omega}{w}\right)^2}} = \frac{1}{20} \frac{1}{\sqrt{\left[1 - \left(\frac{2}{2}\right)^2\right]^2 + \left(2(0.01)\left(\frac{2}{2}\right)\right)^2}} = 2.5 \text{ m}$$

The result from the program, shown in Figure 4.2, is identical to the theoretical value. The results of both systems, Figure 4.2, are also compared with the results from the time-stepping technique using MathCAD, shown in Figure 4.3. The $P.D._{\max} = 1.03\%$.

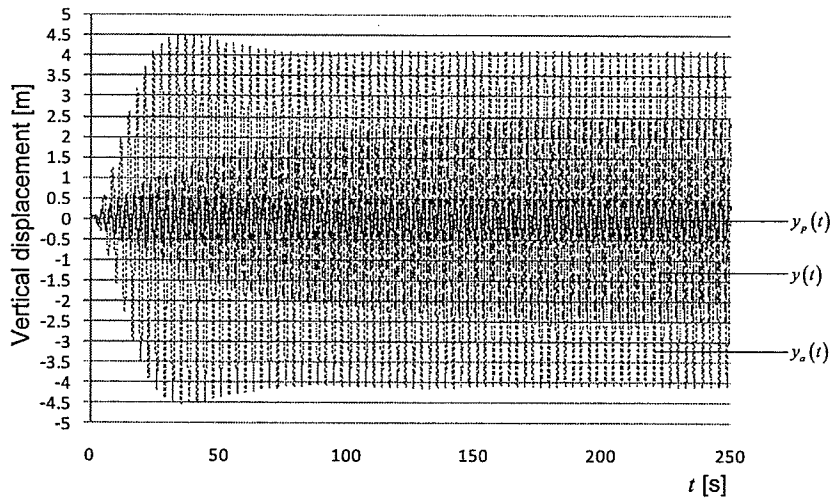


Figure 4.2 - Response of the systems shown in Figure 4.1 using Newmark-L option in SADAP.

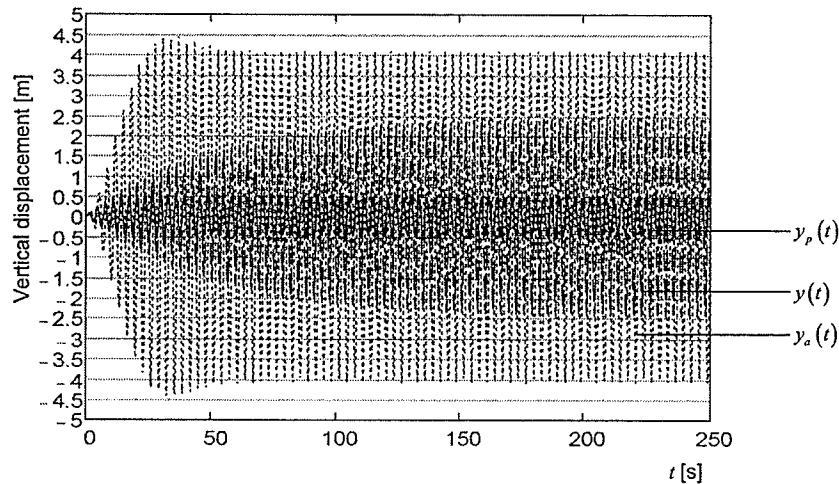


Figure 4.3 - Response of the systems shown in Figure 4.1 using time-stepping technique in MathCAD.

Example No. 13:

This example, Figure 4.4, was chosen to verify the static analysis of the cable element. The properties of the cable and the applied force are:

$$L = 100 \text{ m} \quad E = 200 \text{ GPa} \quad A = 1 \times 10^{-3} \text{ m}^2$$

$$\rho = 10 \text{ tons/m}^3 \quad H_0 = 9.81 \text{ kN} \quad F = 15.0 \text{ kN}$$

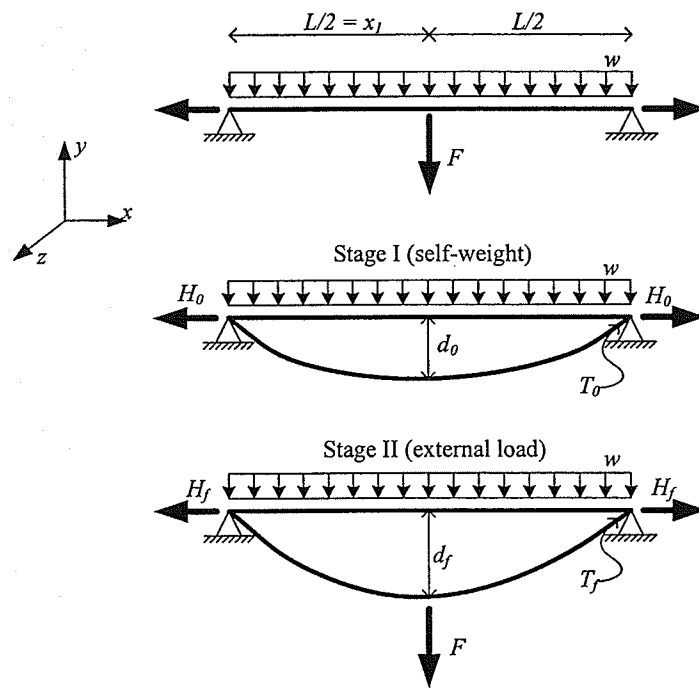


Figure 4.4 - Cable element (Example 13).

The results were compared with theoretical results. Theoretical results can be evaluated as follows (Sussekind, 1982; Irvine, 1974):

$$d_0 = \frac{wL^2}{8H_0} = 12.5 \text{ m}$$

$$T_0 = \sqrt{H_0^2 + \left(\frac{wL}{2}\right)^2} = 10.96791 \text{ kN}$$

$$L_c = L \left[1 + 8 \left(\frac{d_0}{L} \right)^2 \right] = 112.5 \text{ m}$$

$$\lambda = \sqrt{\frac{\left(\frac{w \cdot H_0}{L} \right)^2 L}{\frac{H_0 L_c}{EA}}} = 134.618$$

$$\begin{aligned} \left(\frac{H_f - H_0}{H_0} \right)^3 + \left(2 + \frac{\lambda^2}{24} \right) \left(\frac{H_f - H_0}{H_0} \right)^2 + \left(1 + \frac{\lambda^2}{12} \right) \left(\frac{H_f - H_0}{H_0} \right) + \\ - \frac{\lambda^2}{2} \left[\left(\frac{x_1}{L} \right) - \left(\frac{x_1}{L} \right)^2 \right] \left(\frac{F}{wL} \right) \left[1 + \left(\frac{F}{wL} \right) \right] = 0 \end{aligned}$$

$$H_f = 34.76131 \text{ kN}$$

$$d_f = \frac{\frac{wL}{2} + F}{4H_f} = 14.31391 \text{ m}$$

$$T_f = \sqrt{H_f^2 + \left(\frac{wL}{2} + \frac{F}{2} \right)^2} = 36.90844 \text{ kN}$$

The results from the program are shown in Figure 4.5. As can be seen in the figure, the $P.D._{MAX} = 0.92\%$

LOAD STEP= 1

CABLE ELEMENTS INTERNAL FORCES: (TENSION +)

ELEM.	N NODE 1	N NODE 2
1	10.968	10.477
2	10.477	10.112
3	10.112	9.8863
4	9.8863	9.8100
5	9.8100	9.8863
6	9.8863	10.112
7	10.112	10.477
8	10.477	10.968

SUPPORT REACTIONS:

NODE	RX	RY	RZ	MX	MY	MZ
1	-9.8100	4.9050	0.0000	0.0000	0.0000	0.0000
9	9.8100	4.9050	0.0000	0.0000	0.0000	0.0000

DISPLACEMENTS:

NODE	TRANS.X	TRANS.Y	TRANS.Z	ROT.X	ROT.Y	ROT.Z
1	0.00000000	0.00000000	0.00000000	0.00000000	0.00000000	0.00000000
2	0.00000000	-5.48875000	0.00000000	0.00000000	0.00000000	0.00000000
3	0.00000000	-9.37500000	0.00000000	0.00000000	0.00000000	0.00000000
4	0.00000000	-11.71875000	0.00000000	0.00000000	0.00000000	0.00000000
5	0.00000000	-12.50000000	0.00000000	0.00000000	0.00000000	0.00000000
6	0.00000000	-11.71875000	0.00000000	0.00000000	0.00000000	0.00000000
7	0.00000000	-9.37500000	0.00000000	0.00000000	0.00000000	0.00000000
8	0.00000000	-5.48875000	0.00000000	0.00000000	0.00000000	0.00000000
9	0.00000000	0.00000000	0.00000000	0.00000000	0.00000000	0.00000000

LOAD STEP= 101

CABLE ELEMENTS INTERNAL FORCES: (TENSION +)

ELEM.	N NODE 1	N NODE 2
1	37.247	36.756
2	36.813	36.447
3	36.410	36.185
4	36.043	35.966
5	35.966	36.043
6	36.185	36.410
7	36.447	36.813
8	36.756	37.247

SUPPORT REACTIONS:

NODE	RX	RY	RZ	MX	MY	MZ
1	-35.058	12.405	0.0000	0.0000	0.0000	0.0000
9	35.058	12.405	0.0000	0.0000	0.0000	0.0000

TOTAL DISPLACEMENTS:

NODE	TRANS.X	TRANS.Y	TRANS.Z	ROT.X	ROT.Y	ROT.Z
1	0.00000000	0.00000000	0.00000000	0.00000000	0.00000000	0.00000000
2	0.443900603	-4.345603348	0.00000000	0.00000000	0.00000000	0.00000000
3	0.492037631	-8.126599955	0.00000000	0.00000000	0.00000000	0.00000000
4	0.289226460	-11.409259954	0.00000000	0.00000000	0.00000000	0.00000000
5	0.000000000	-14.249168061	0.00000000	0.00000000	0.00000000	0.00000000
6	-0.289226460	-11.409259954	0.00000000	0.00000000	0.00000000	0.00000000
7	-0.492037631	-8.126599955	0.00000000	0.00000000	0.00000000	0.00000000
8	-0.443900603	-4.345603348	0.00000000	0.00000000	0.00000000	0.00000000
9	0.000000000	0.000000000	0.000000000	0.000000000	0.000000000	0.000000000

Figure 4.5 - Results from SADAP.

Example No. 14:

This example, Figure 4.6, was chosen to verify the Eigenvalue analysis of the cable element. The cable is pretensioned with a force $H = 9.81 \text{ kN}$. The geometry and mechanical properties of the cable are the same as in previous example.

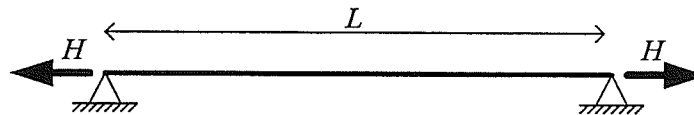


Figure 4.6 - Cable element (Example 14).

The natural frequency of the cable can be calculated as (Irvine, 1992)

$$\omega_n = \frac{n\pi}{L} \sqrt{\frac{H}{A\rho}} = 0.9839757n \text{ rad/s}$$

The first five natural frequencies of a cable are

$$\omega = \left\{ \begin{array}{l} 0.98398 \\ 1.96795 \\ 2.95193 \\ 3.93590 \\ 4.91988 \end{array} \right\} \text{ rad/s}$$

The SADAP results are given in Table 4.2.

Table 4.2 - Natural frequencies of the cable shown in Figure 4.6.

Mode	Frequency [rad/s]									
	Exact	4 Elements	<i>P.D.</i>	8 Elements	<i>P.D.</i>	16 Elements	<i>P.D.</i>	32 Elements	<i>P.D.</i>	
1	0.98398	1.00942	2.59%	0.99031	0.64%	0.98556	0.16%	0.98437	0.04%	
2	1.96795	2.16998	10.27%	2.01884	2.59%	1.98062	0.64%	1.97111	0.16%	
3	2.95193	3.52630	19.46%	3.12407	5.83%	2.99477	1.45%	2.96261	0.36%	
4	3.93590	-	-	4.33995	10.27%	4.03768	2.59%	3.96124	0.64%	
5	4.91988	-	-	5.67498	15.35%	5.11903	4.05%	4.96941	1.01%	

It can be seen that the maximum *P.D.* is 1% using 32 elements.

Example No. 15:

This example, Figure 4.7, was chosen to verify the static analysis of the tapered element. Two models of tower were created: a simplified model using tapered element described in Chapter 3 and a detailed model using beam and truss elements. The properties of the models are:

For longitudinal bars:

$$E = 210 \text{ GPa} \quad \nu = 0.3 \quad A = 1.00 \times 10^{-03} \text{ m}^2 \quad \rho = 7.86 \text{ ton/m}^3$$

$$I_x = 2.45 \times 10^{-06} \text{ m}^4 \quad I_y = 1.23 \times 10^{-06} \text{ m}^4 \quad I_z = 1.23 \times 10^{-06} \text{ m}^4$$

For diagonal and horizontal bars:

$$E = 210 \text{ GPa} \quad A = 5.00 \times 10^{-04} \text{ m}^2 \quad \rho = 7.86 \text{ ton/m}^3$$

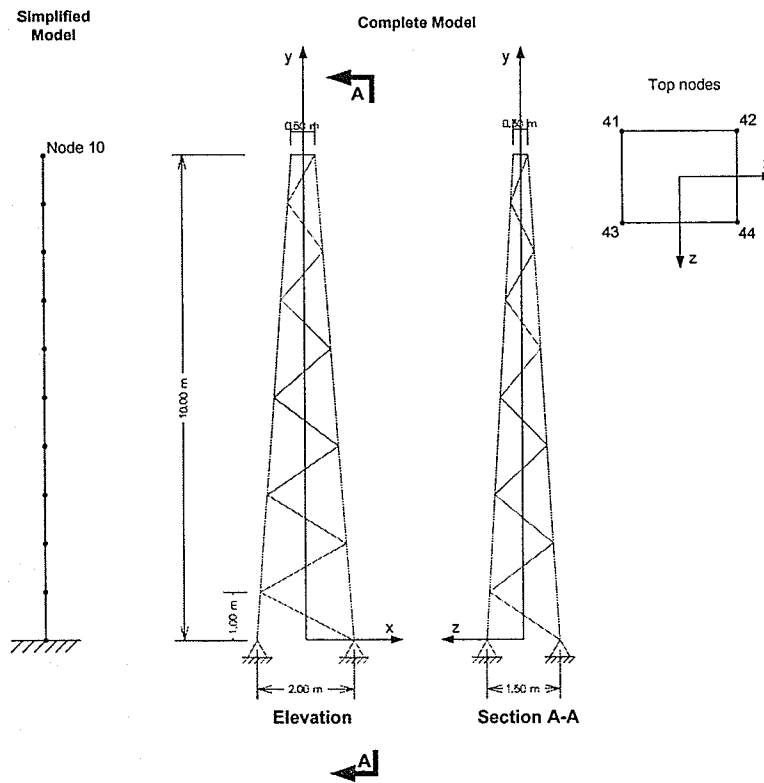


Figure 4.7 - Tapered tower (example 15).

The applied force in Table 4.3 was chosen to be close to critical buckling load (calculated based on a non-linear stability analysis) of the tower to verify the behavior of the simplified element.

Table 4.3 - Applied force on the models in Figure 4.7.

Model	Node	Fx	Fy	Fz	Mx	My	Mz
		kN	kN	kN	kNm	kNm	kNm
Complete Model	41	20	-400	5	0	0	0
	42	20	-400	5	0	0	0
	43	20	-400	5	0	0	0
	44	20	-400	5	0	0	0
Simpl. Model	10	80	-1600	20	0	0	0

The comparison between the results of models in this example is described in Figures 4.8 to 4.10. The maximum *P.D.* are 7.50% (without the shear deformation option on) and 6.11% (with the shear deformation option on).

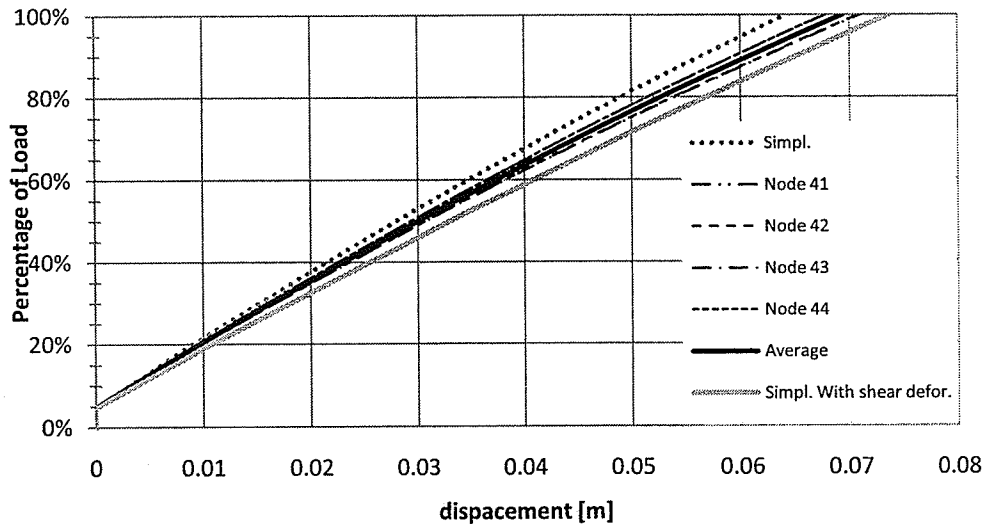


Figure 4.8 - x displacement of the tapered tower.

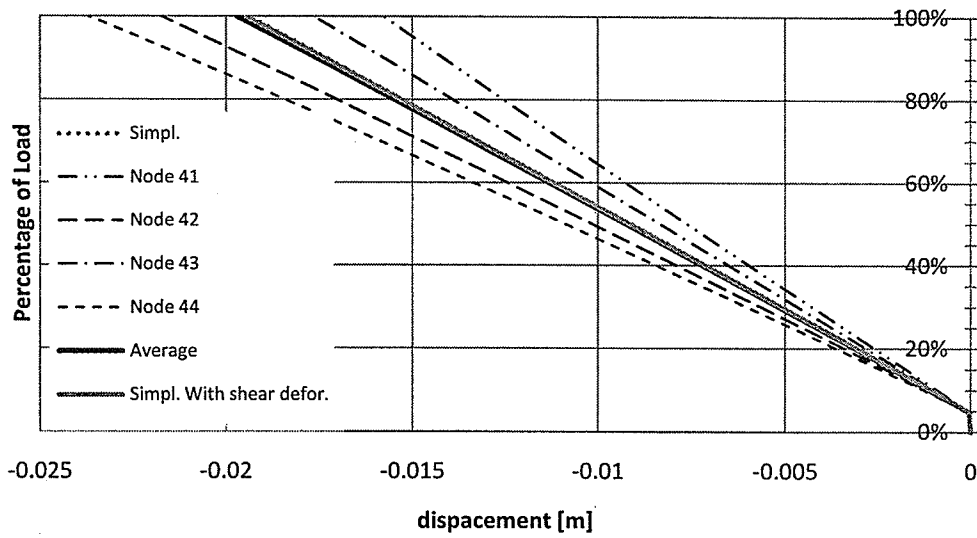


Figure 4.9 - y displacement of the tapered tower.

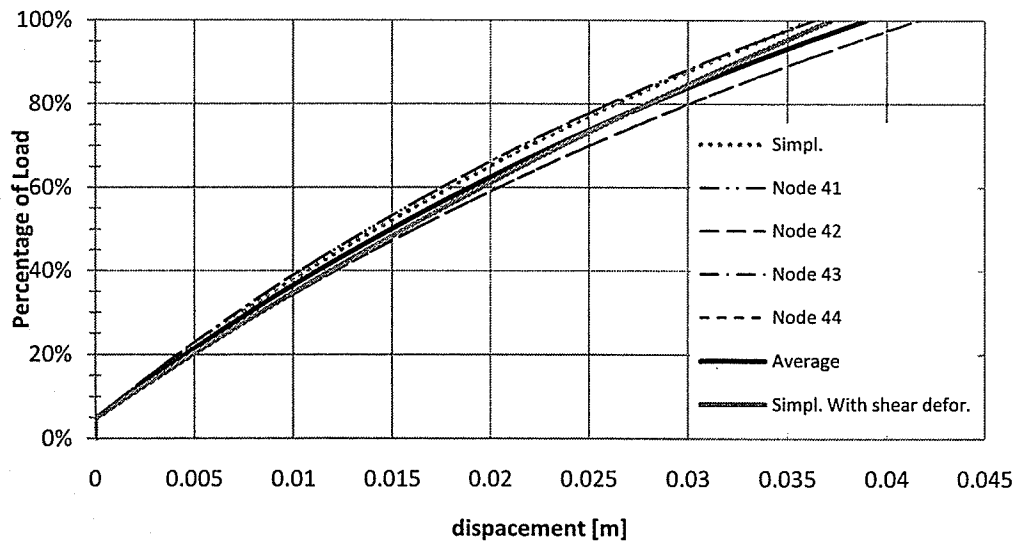


Figure 4.10 - z displacement of the tapered tower.

Example No. 16:

This example was chosen to verify the Eigenvalue analysis of a tapered tower element. The same geometric and material properties from previous example were used in this verification. The Figures 4.11 to 4.14 illustrate the mode shapes of the structures. The corresponding *P.D.* are 4.72%, 7.19%, 3.78% and 6.83% for the first four flexural mode shapes, respectively.

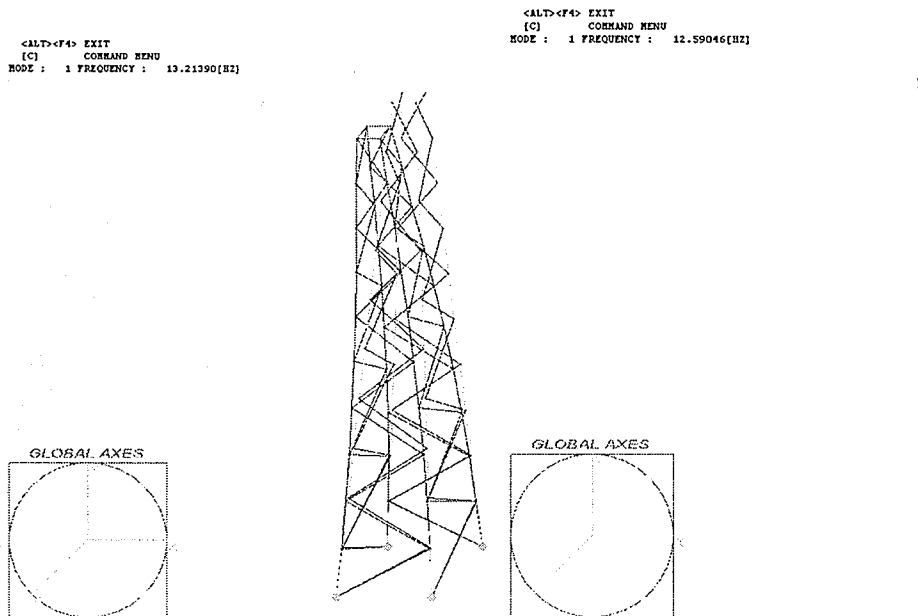


Figure 4.11 - The 1st flexural natural frequency and mode shape of the detailed and the simplified tapered towers.

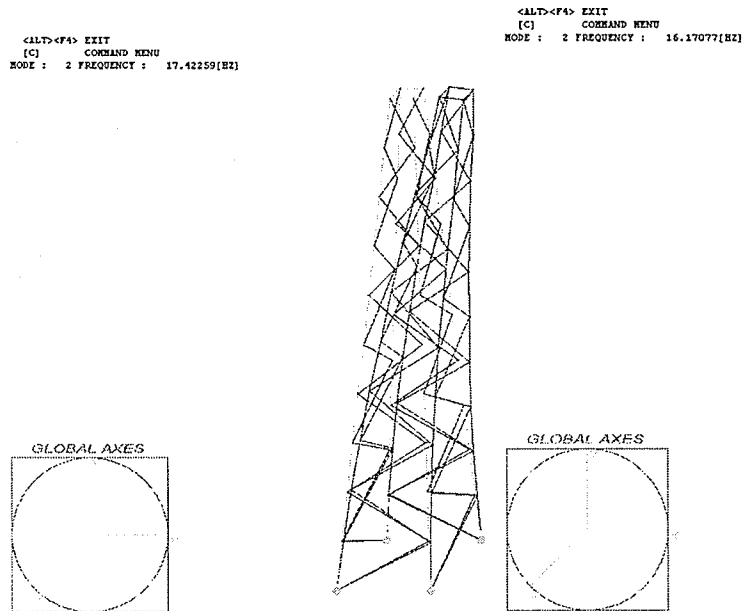


Figure 4.12 - The 2nd flexural natural frequency and mode shape of the detailed and the simplified tapered towers.

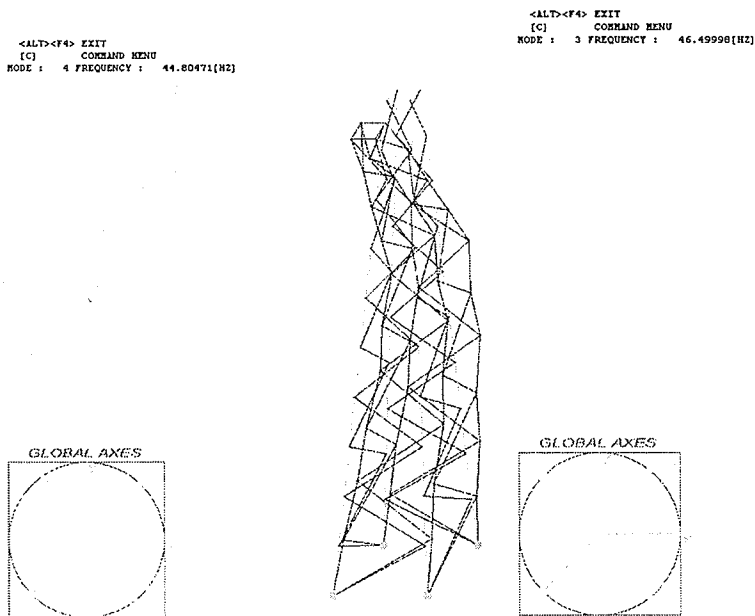


Figure 4.13 - The 3rd flexural natural frequency and mode shape of the detailed and the simplified tapered towers.

<ALT><F4> EXIT
(C) * COMMAND MENU
MODE : 6 FREQUENCY : 51.97570(HZ)

<ALT><F4> EXIT
(C) * COMMAND MENU
MODE : 4 FREQUENCY : 55.52431(HZ)

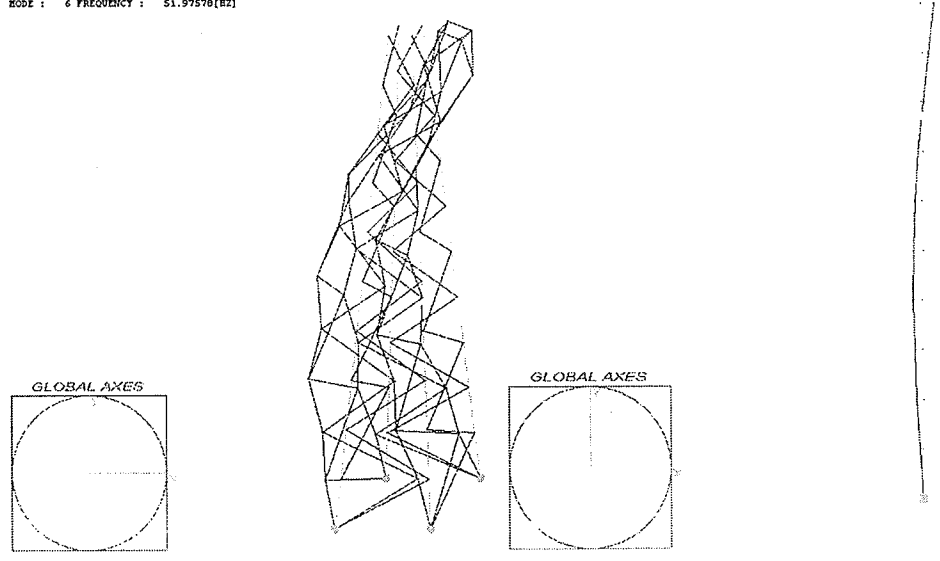


Figure 4.14 - The 4th flexural natural frequency and mode shape of the detailed and the simplified tapered towers.

5. COMPUTATIONAL MODELING

The present chapter describes the numerical model of the research. The analyzed tower was designated A-402M, a modification of the original A-402-0 tower. The whole A-402-0 tower shaft is tapered but the A-402M shaft is straight with the exception of the top and the base segments of the tower.

5.1. TOWER PROPERTIES

The geometric properties of the A402-M tower are illustrated in Figure 5.1. The tower includes four guy cables of a double ½ inch diameter grade 220 galvanized steel wire. All members are made of steel with E of 200 GPa, $\nu = 0.3$, and $\rho = 7.86 \text{ ton/m}^3$. The properties of the cables are listed in Table 5.1 (Horr et al., 2004; Shehata and Damatty, 2006).

Table 5.1- Properties of the conductors, ground wires and guyed cables.

	Conductor	Ground wire	Guyed cable
Horizontal span (m)	480	480	24.16
Effective Diameter (mm)	40.64	9.00	11.10
Effective Area (m ²)	1.2972E-03	6.3617E-05	9.6774E-05
Density (ton/m ³)	2.2765	6.25	7.86
Weight (N/m)	28.97	3.90	7.46
Modulus of Elasticity (kN/m ²)	6.23E+07	1.86E+08	1.86E+08
Sag (m)	20.00	13.54	0.24
Pretension per cable (kN)	41.72	8.30	13.34

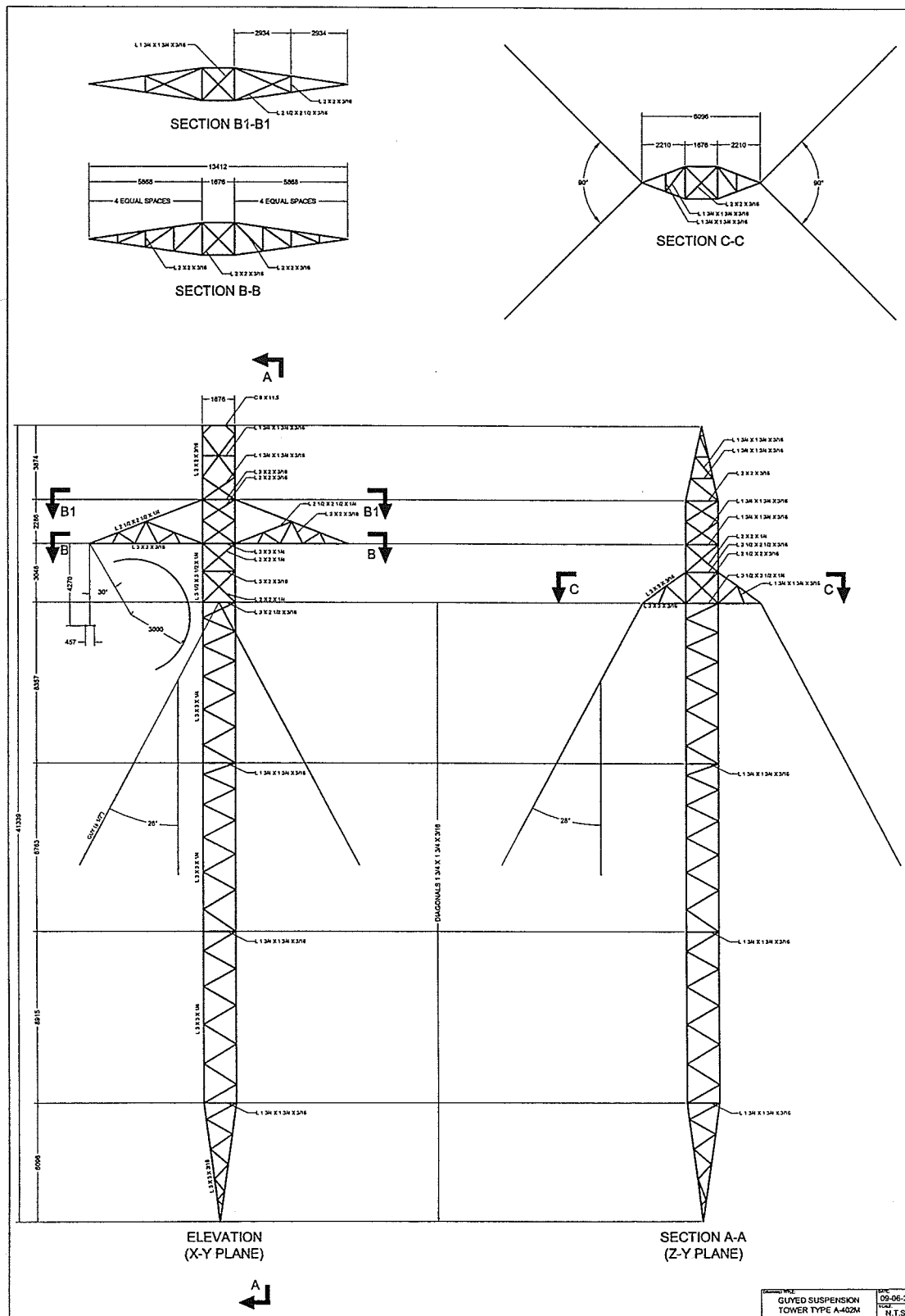


Figure 5.1 - Tower A-420M

The simplified tower was modeled using the equivalent properties (Chapter 3) of the detailed A-402M tower. The Figure 5.2 was extracted directly from the program.

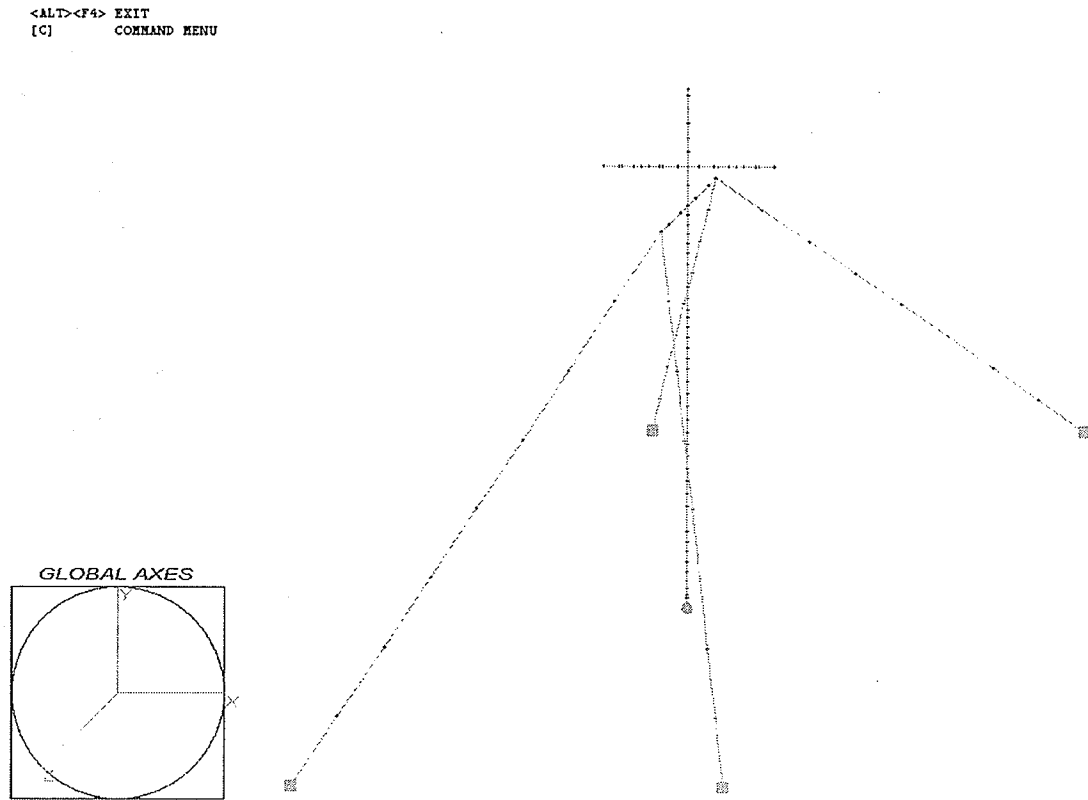


Figure 5.2 - A simplified model of an A-402M tower.

5.2. TOWER SYSTEM MODELS

The transmission system constitutes of one ground wire for lightning protection connecting at the top of each tower, and four conductors (bundled together as one single equivalent conductor) connected to the insulator strings which are 4.27 meter in length. These insulator strings are connected to the tower at the cross arms. Eight models are investigated in this study as illustrated in Figure 5.3.

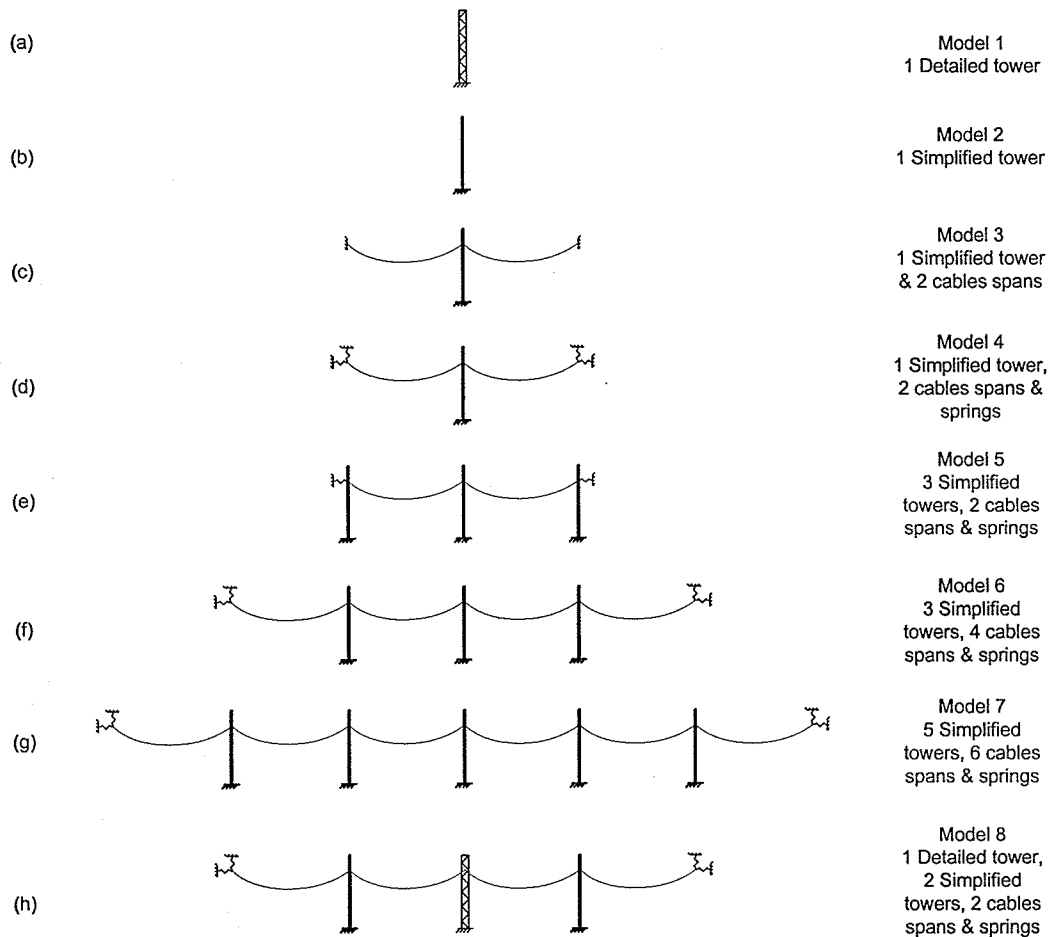


Figure 5.3 - Transmission system models.

Model 1 (A-402M tower - Figure 5.1) and Model 2 (simplified A-402M tower - Figure 5.2) were used to investigate if the simplified model is able to describe with accuracy the detailed tower.

Model 3 was created to verify the effect of the conductors and ground wires in the transmission system on the response of the tower and the tower's dynamic characteristics.

Models 4 and 5 were created to investigate the boundary condition at the termination of the cables.

Models 6 and 7 were used to investigate the effect of number of cable spans on the natural frequencies and the mode shapes of the system.

Model 8 was created to study the use of a combination of the model containing both the detailed and the simplified towers.

5.3. BOUNDARY CONDITIONS

One of the modeling questions is the effects of the boundary conditions on the response of the system. In this study, three boundary conditions will be investigated:

- Conductors and ground wires at the extremity towers, as well as the extremity towers are represented by fix supports – Figure 5.4(a);

- Conductors and ground wires at the extremity towers, as well as the extremity towers are represented by two linear springs – Figure 5.4(b); and
- Conductors and ground wires at the extremity towers are represented by a linear spring – Figure 5.4(c).

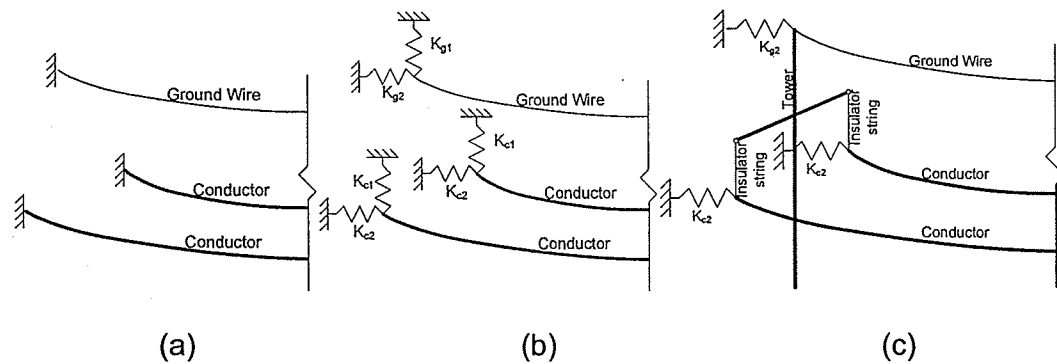


Figure 5.4 - Boundary conditions in the study

K_{g1} is calculated by applying a unit load on the tip of the simplified tower model in the three directions (x,y,z) and inverting the corresponding displacement. K_{g2} is calculated based on a stiffness of a cable with the same properties of the ground wire. K_{c1} is calculated using the same technique used in evaluating K_{g1} while K_{c2} is obtained from the stiffness of a conductor. Note that the load is applied at the end of the insulator string (the node connecting to the cables) and not directly on the tower in the calculation of K_{c1} . The mass of the springs are considered zero for those DOFs corresponding to the subscript 1 stiffness and half the mass of a cable span for those DOFs corresponding to the subscript 2 stiffness. The properties of the springs are listed in Table 5.2.

Table 5.2 - Properties of the springs.

Spring	KUX	KUY	KUZ	KRX	KRY	KRZ	MASS
	kN/m	kN/m	kN/m	kNm	kNm	kNm	ton
K _{g1}	2.0175E+02	1.6827E+04	3.4950E+02	N/A ¹	N/A ¹	N/A ¹	0.0000E+00
K _{c1}	6.5135E+00	2.6421E+02	6.5135E+00	N/A ¹	N/A ¹	N/A ¹	0.0000E+00
K _{g2}	1.7300E-02	1.7300E-02	3.5006E+00	N/A ²	N/A ²	N/A ²	9.5400E-02
K _{c2}	1.7380E-01	1.7380E-01	1.7841E+01	N/A ¹	N/A ¹	N/A ¹	1.4151E+00

(¹ The stiffness can be any positive value and will not affect the results because neither the insulator string nor the cable can resist rotations; ² The stiffness must be a very small number for Model 5 because end towers resist certain rotations. In this study, the value was set to 1.0E-06 kNm)

5.4. NONLINEAR STATIC ANALYSIS

The geometric nonlinear analysis was carried out for Model 1 and Model 2 to investigate the efficiency of the proposed nonlinear stiffness formulation for the simplified tower when compared with the detailed model. Twenty one load-steps were used in the analysis. Self-weight and pretension force were applied in the first step. The external load cases were applied in the subsequent steps.

In each load step, Eqn (5.1) was calculated and the displacement was evaluated using Eqn. (5.2) (Battista, 2007-B).

$$[K]\{\Delta u_i\} = \{\Delta F_i\} \quad (5.1)$$

$$\{u_i\} = \{u_{i-1}\} + \{\Delta u_i\} \quad (5.2)$$

where $[K]$ is the nonlinear stiffness matrix, $\{\Delta u_i\}$ is the incremental displacement vector, $\{\Delta F_i\}$ is the force vector of the current step, and $\{u_i\}$ is the updated displacement vector.

The analysis was performed using a modified Cholesky factorization method together with a bandwidth solver.

5.4.1. LOAD CASES

Two of the seven load cases used in the original A-402 tower verification report (Appendix 2A - Disney and Parker, 2007) are presented here. The two selected load cases are listed in Table 5.3. The nomenclatures used in the table are referred to in the Figure 5.5 and the node numbers where the loads are applied are shown in Figure 5.6. For the detailed model, the load at the top of the tower was applied at the centre node.

Table 5.3 - Load cases.

LOAD CASE 1						
		kN		kN		kN
Ground Wire	V1	-8.3800	L1	8.4960	T1	0.0000
Conductor 1	V2	-70.4780	L2	32.4360	T2	0.0000
Conductor 2	V3	-70.4780	L3	32.4360	T3	0.0000
LOAD CASE 2						
		kN		kN		kN
Ground Wire	V1	2.8470	L1	1.9570	T1	2.1260
Conductor 1	V2	-43.4010	L2	18.7710	T2	9.2660
Conductor 2	V3	-43.4010	L3	18.7710	T3	9.2660

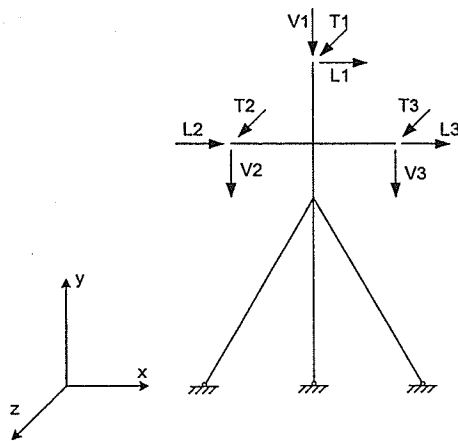


Figure 5.5 - Nomenclatures of the loading in Table 5.3.

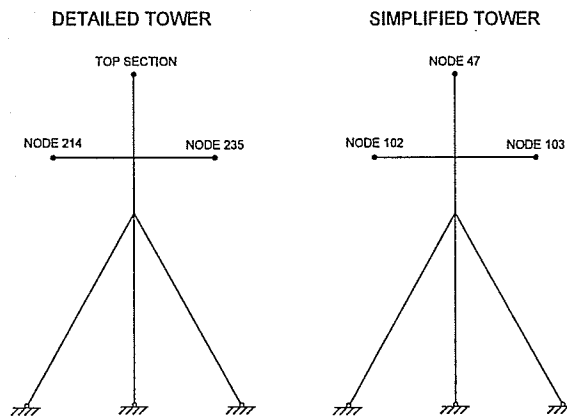


Figure 5.6 - Controlled nodes where the loadings are applied in detailed and simplified tower models (representatively only).

In addition to the loads from the conductors and ground wire, a self-weight of all elements and pretension on the guyed cables were also included in the analysis for both models. These pretension and self-weights were not factored.

5.5. DYNAMIC ANALYSIS

5.5.1. FREE VIBRATION

The free vibration analysis of the towers was performed to verify the mass matrix of the structure. The analysis was carried out after static analysis of the structures due to self-weight and pretension was done. The eigenvalue problem is in the form of (Chopra, 1995; Clough and Penzien, 1993; Craig, 1981; Timoshenko et al., 1974):

$$([K] - \omega_i^2 [M])\{\phi_i\} = 0 \quad (5.3)$$

A nontrivial solution $\{\phi_i\} \neq 0$ requires that the determinant of the coefficient matrix be zero, i.e.

$$|[K] - \omega_i^2 [M]| = 0 \quad (5.4)$$

where $[K]$ is the global non-linear stiffness matrix, $[M]$ is the global mass matrix, ω_i is the i^{th} -natural circular frequency and $\{\phi_i\}$ is the i^{th} modal shape of the structure.

5.5.2. TIME STEPPING TECHNIQUE

The free vibration analysis performed in previous section was carried out only to (a) verify the mass matrix as mentioned as well as to (b) construct the damping matrix of the structure and (c) preliminary investigate the effects of cables and number of span on the natural frequencies of the structures. Although modal superposition analysis of the structure can be carried out in dynamic analysis, time-stepping technique was chosen in this study to avoid the needs to

parametrically study the number of mode shapes required in the modal superposition analysis.

There are a number of numerical techniques for dynamic analysis of a structure, the Newmark method with $\alpha = 0.25$ and $\delta = 0.5$, an average acceleration, was chosen in this study. This is because the method is unconditionally stable. The method is described as shown in Figure 5.7 (Bathe, 1996):

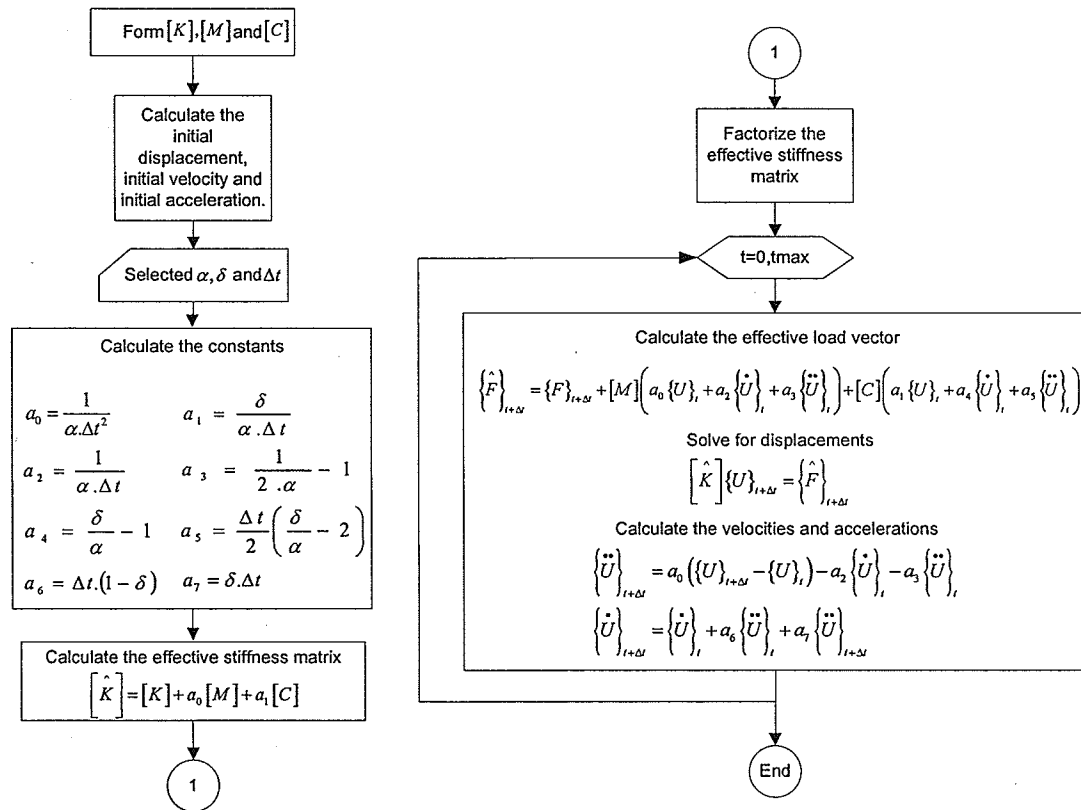


Figure 5.7 - Newmark Method.

5.5.3. DAMPING MATRIX

The damping in the structure dissipates energy, i.e. it changes kinetic or potential energy into heat. The dissipation of energy is a very complex issue and there are several mathematical formulations for damping force. In the field of structural dynamics, damping force is usually assumed to be proportional to the velocity and in opposite direction of the motion. This type of damping is called viscous damping (Paz and Leigh, 2004).

Usually damping of a structure is defined by experimental results. When no experimental values are given, the value of 2% damping ratio for steel bolted structures is recommended (Battista et al., 2003; Rodrigues, 1999; Oliveira, 2006). In the Newmark method, a damping matrix, $[C]$, is required. Commonly, the damping matrix can be calculated using a Rayleigh damping formulation. The method assumes damping matrix to be proportional to the mass and the stiffness matrix of the structure. When the structure has low fundamental natural frequencies (lower than 1 Hz), the damping matrix can assume to be proportional to the mass matrix only. On the other hands, when the structure has high fundamental natural frequencies (much higher than 1 Hz), the damping matrix can assume to be proportional to the stiffness matrix only (Battista R.C, 2007-C). In this study, the Rayleigh type damping matrix is used and the damping matrix has the form of (Bathe, 1996; Paz and Leigh, 2004; Oliveira, 2006)

$$[C] = \alpha[M] + \beta[K] \quad (5.5)$$

The coefficients α and β can be expressed as a function of the i^{th} frequencies ω_i and i^{th} modal damping ratios ξ_i by

$$\xi_i = \frac{\alpha}{2\omega_i} + \frac{\beta\omega_i}{2} \quad (5.6)$$

Rearranging the previous equation, it leads to:

$$\alpha = 2\xi_i\omega_i - \beta\omega_i^2 \quad (5.7)$$

$$\beta = \frac{2\xi_j}{\omega_j} - \frac{\alpha}{\omega_j^2} = \frac{2(\xi_j\omega_j - \xi_i\omega_i)}{\omega_j^2 - \omega_i^2} \quad (5.8)$$

Oliveira (2006) recommended that the frequencies ω_i and ω_j should be chosen as the extremes of the design frequency range. He assumed a uniform damping ratio. The recommendation as well as the assumption was used in this study. ω_j of 119.2207 rad/s (18.9746 Hz) was used for all models, except for Model 2, in the calculation. This is because all the models have that frequency within the vicinity of the specified value and the change in the value does not have an effect on the resulting damping matrix. The choice of ω_i , however, has the effect on the resulting damping matrix. Therefore, specific values for individual model were chosen as listed.

$$\omega_{iModel\ 3} = 0.7414 \text{ rad/s}(0.1180 \text{ Hz})$$

$$\omega_{iModel\ 4} = 0.7212 \text{ rad/s}(0.1148 \text{ Hz})$$

$$\omega_{iModel\ 5} = 0.7207 \text{ rad/s}(0.1147 \text{ Hz})$$

$$\omega_{iModel\ 6} = 0.7106 \text{ rad/s}(0.1131 \text{ Hz})$$

The Rayleigh damping parameters for Model 3, 4, 5 and 6 are respectively:

$$\begin{aligned}
\beta_{Model\ 3} &= 3.33 \times 10^{-4} \quad , \quad \alpha_{Model\ 3} = 0.029473 \\
\beta_{Model\ 4} &= 3.33 \times 10^{-4} \quad , \quad \alpha_{Model\ 4} = 0.028676 \\
\beta_{Model\ 5} &= 3.33 \times 10^{-4} \quad , \quad \alpha_{Model\ 5} = 0.028642 \\
\beta_{Model\ 6} &= 3.34 \times 10^{-4} \quad , \quad \alpha_{Model\ 6} = 0.028259
\end{aligned}$$

For Model 2 which does not have conductors, ω_i and ω_j were chosen to be

$$\begin{aligned}
\omega_i &= 9.5186 \text{ rad/s} (1.5149 \text{ Hz}) \\
\omega_j &= 115.0535 \text{ rad/s} (18.3113 \text{ Hz})
\end{aligned}$$

The Rayleigh damping parameters for Model 2 are:

$$\beta = 3.210 \times 10^{-4} \quad , \quad \alpha = 0.35165$$

5.5.4. WIND LOAD

In this study, dynamic effects of wind load will be considered, this is mainly because wind load is harmful for structures with low natural frequency such as transmission tower system (lower than 1 Hz). The wind pressure can be calculated by the following formula (Blessmann, 2005):

$$p(t) = \frac{\rho}{2} [V(t)]^2 C_{df} \tag{5.9}$$

where $p(t)$ is the wind pressure in N/m^2 , ρ is the specific density of the air (can be assumed equal to 1.226 kg/m^3), $V(t)$ is the wind speed in m/s , and C_{df} is the drag factor. According to the CSA S37-01 (2001) standard, the drag factor for latticed square towers can be defined by the following equation:

$$C_{df} = 4.0(R_s)^2 + 5.9(R_s) + 4.0 \tag{5.10}$$

where R_s is defined as the ratio of the net projected area of a surface of the structure facing the wind and the gross area of that surface. In calculation of R_s , the tower was divided into seven zones as illustrated in Figure 5.8.

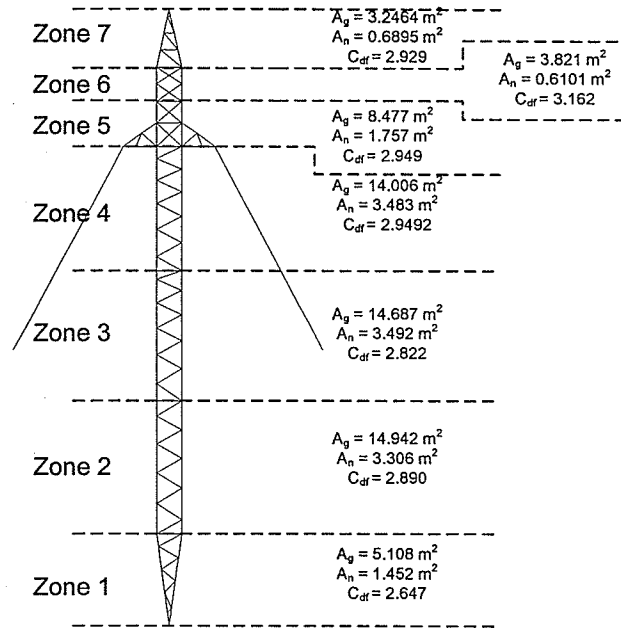


Figure 5.8 - Drag factors and areas of the tower zones.

The drag factors for the conductors and ground wires were used as 1.10 and 1.25 respectively as adopted by Rodrigues (1999).

5.5.4.1. WIND SPEED

The wind speed $V(t)$ can be separated into two parts, one due to an average or mean wind speed \bar{V} and the other due to turbulence $v(t)$ as illustrated in Figure 5.9.

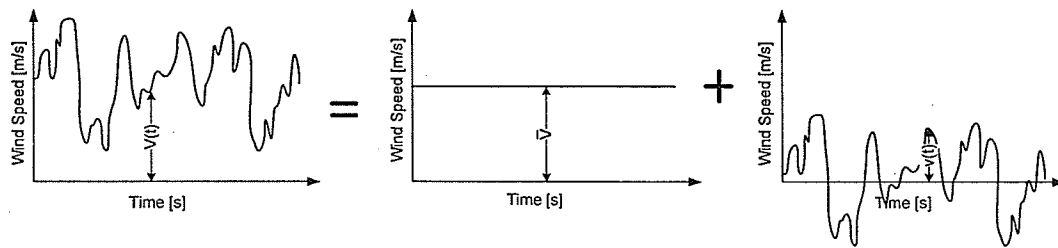


Figure 5.9 - Wind speed.

$$V(t) = \bar{V} + v(t) \quad (5.11)$$

5.5.4.1.1. MEAN WIND SPEED

The static wind pressure for Winnipeg, Manitoba, class A terrain is 450 Pa (Ochonski, 2008) at 10 meters height. Therefore a mean wind speed at 10 m height \bar{V}_{10} to generate this pressure is equal to 27.09 m/s. This speed value was used to generate the turbulence speed. The mean wind speed is not constant with the height as illustrated in the Figure 5.10. Most standards recommend a mean wind speed that follows a logarithmic or an exponential rule. In this study, the exponential formulation was used.

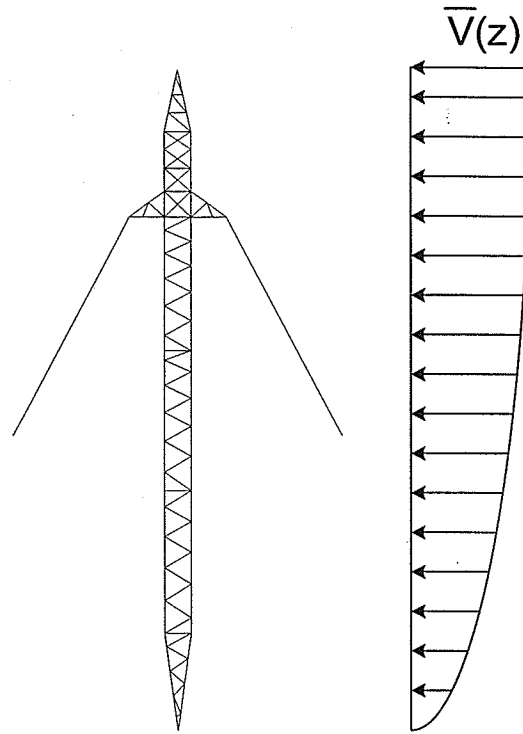


Figure 5.10 - Variation of mean wind speed along the tower height.

$$\bar{V}(z) = V_{10} \left(\frac{z}{10} \right)^p \quad (5.12)$$

where z is the height above the ground and p usually depends on the shape of the terrain (the value of 0.2 was used in the study).

5.5.4.1.2. TURBULENCE WIND SPEED

Even though the turbulence wind speed is a random process, it has a degree of regularity and can be treated as stationary and ergodic process (Rodrigues, 1999) in statistical point of view. It is stationary because the statistical parameters are time invariants. It is ergodic because these parameters when calculated for any sample with respect to time will be the same across the

total collection of samples (Paz and Leigh, 2004). Some of the important statistical parameters in the wind engineering are (Blessmann, 2005 and Oliveira, 2006):

- Mean value:

$$\bar{V} = \lim_{T \rightarrow \infty} \frac{1}{T} \int_0^T V(t) dx \quad (5.13)$$

- Mean square value:

$$\overline{V^2} = \lim_{T \rightarrow \infty} \frac{1}{T} \int_0^T (V(t))^2 dx \quad (5.14)$$

- Root mean square:

$$V_{rms} = \sqrt{\overline{V^2}} \quad (5.15)$$

- Variance:

$$\sigma_v^2 = \lim_{T \rightarrow \infty} \frac{1}{T} \int_0^T (V(t) - \bar{V})^2 dx \quad (5.16)$$

- Standard deviation:

$$\sigma_v = \sqrt{\sigma_v^2} \quad (5.17)$$

In the present study, the turbulent wind speed $v(t)$ was generated with a zero mean. Therefore, \bar{V} equals to zero, $\overline{V^2}$ equals to σ_v^2 and V_{rms} equals to σ_v .

In case of a random phenomenon, the fluctuations consist of a random process with a continuum distribution over the frequencies f . This continuum spectrum, also called spectral density of the variance $S_v(f)$ and is defined as:

$$\sigma_v^2 = \int_0^{\infty} S_v(f) df \quad (5.18)$$

There are a large number of mathematical formulations for this spectrum, with different parameters, but none of them represent the totality of the samples (Blessmann, 2005). The spectrum used in this study is the Kaimal spectrum and was chosen because it is also a function of height (Blessmann, 1995 and Oliveira, 2006).

$$S_v(f) = \frac{200u_*^2 Y_1(z, f)}{(1 + 50Y_1(z, f))^{5/3} f} \quad (5.19)$$

$$Y_1(z, f) = z \frac{f}{\bar{V}(z)}$$

where $\bar{V}(z)$ is an hourly average wind speed at a height of z ; u_* is the friction velocity. $\bar{V}(z)$ and u_* are given in m/s. Those two parameters are described by

$$\bar{V}(z) = V_{10} \left(\frac{z}{10} \right)^p$$

$$u_* = k \frac{\bar{V}(z)}{\ln \left(\frac{z}{z_0} \right)} \quad (5.20)$$

The parameter k is the Karman constant and is equal to 0.4; z_0 is a direct function of the height of the obstacles. B.J. Vickery suggested a value of 1/20 times the average height of the obstacles to be used for z_0 (Blessmann, 1995). In urban areas, the value of z_0 can range from 0.2 m. to 4 m. In this study, the value of 0.07 m was used to be conservative. The plot of wind spectrum with frequency, Eqn. (5.19), is shown in Figure 5.11.

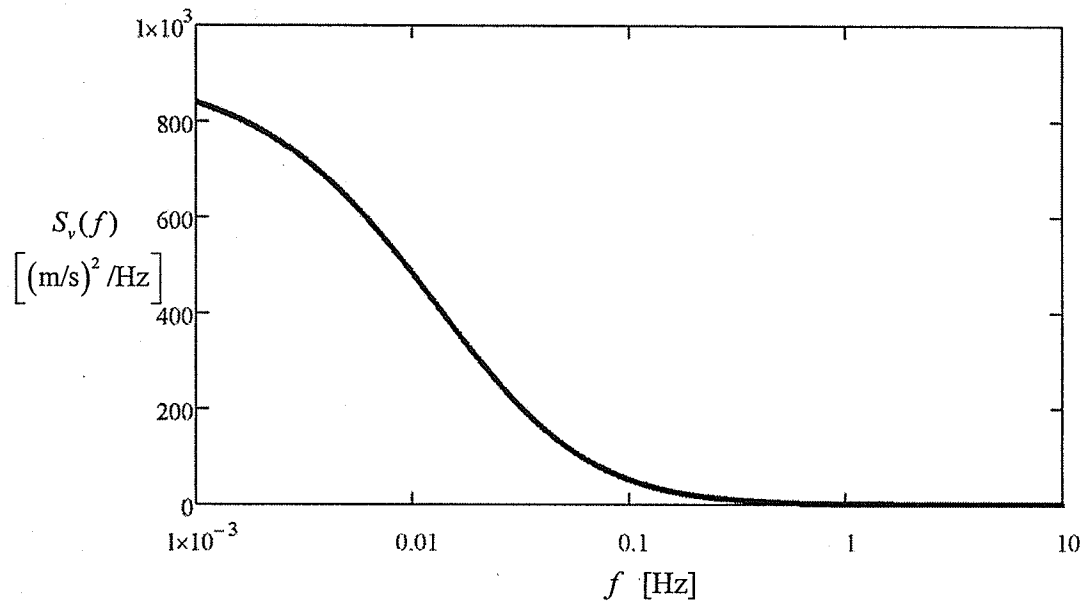


Figure 5.11 - Wind spectrum versus frequency.

It can be seen from the figure that the wind spectrum has very low values for frequencies higher than 1 Hz.

The autocorrelation function is also a very important statistical parameter since it defines the dependence of a fluctuation value at time t and a fluctuation value at time $t + \tau$ for the same sample (Blessmann, 1995; Blessmann, 2005; Oliveira, 2006). Mathematically it is defined as:

$$R_v(\tau) = \lim_{T \rightarrow \infty} \frac{1}{T} \int_0^T v(t)v(t+\tau)dt \quad (5.21)$$

The complete spectral density $\dot{S}_v^*(f)$ of the fluctuations of the wind speed is the Fourier transformer of the autocorrelation $R_v(\tau)$, and can be given by:

$$\dot{S}_v^*(f) = \int_{-\infty}^{+\infty} R_v(\tau)e^{-i2\pi f\tau}d\tau \quad (5.22)$$

where $S_v(f) = 2\dot{S}_v(f)$. This function can also be related with the spectral density by the inverse Fourier transformer formula:

$$R_v(\tau) = \int_{-\infty}^{\infty} \dot{S}_v(f) e^{i2\pi f\tau} df = 2 \int_0^{\infty} \dot{S}_v(f) e^{i2\pi f\tau} df$$

$$R_v(\tau) = 2 \int_0^{\infty} \dot{S}_v(f) \cos(2\pi f\tau) df \quad (5.23)$$

This can be rearranged as

$$R_v(\tau) = \int_0^{\infty} S_v(f) \cos(2\pi f\tau) df \quad (5.24)$$

The last statistical parameter used in this study to generate wind turbulence is the cross covariance which is a function that relates a sample v_1 measured at time t with another sample v_2 measured at time $t + \tau$ at a fixed distance. It is given by

$$C_{v_1, v_2}(\tau) = \lim_{T \rightarrow \infty} \frac{1}{T} \int_0^T v_1(t) v_2(t + \tau) dt \quad (5.25)$$

The cross covariance can also be expressed as a Fourier transformer. In the present work, the wind load was applied at the same time for all loaded nodes, therefore $\tau = 0$. This simplification, according to Oliveira (2006), leads to

$$C_{v_1, v_2}(0) = \int_{-\infty}^{+\infty} S_v(f) e^{-fC} df \quad (5.26)$$

According to Simiu (1986) the parameter C can be found from

$$C = \frac{\sqrt{[C_y^2 (y_2 - y_1)^2 + C_z^2 (z_2 - z_1)^2]}}{V_{10}} \quad (5.27)$$

where $y_2 - y_1$ is the horizontal distance between samples, $z_2 - z_1$ is the vertical distance between samples, and C_y and C_z are exponential decay coefficients that are determined experimentally. Conservative values of 16 and 10 for C_y and C_z , respectively, were used as suggested by Simiu (1986).

There are several methods to generate the wind speed. In this study, the formulation adopted by Oliveira (2006) was used. Only one wind speed is generated in this method and is given by a summation of harmonic functions as:

$$v(t) = \sum_{i=1}^{NSPEC} \sqrt{2S_v(f_i)\Delta f} \cos(2\pi f_i t + \theta_i) \quad (5.28)$$

where Δf is the frequency increment, θ_i is a random angle from 0 to 2π , and $NSPEC$ is the number of division of the spectrum. The formulation is calculated in FORTRAN. The flowchart of the calculation is shown in Figure 5.12. Figure 5.13 shows the wind profile generated by the code and Figure 5.14 shows the zoom of the wind profile for the first two seconds. Figure 5.14 shows that the wind profile constructed is actually a smooth continuous curve and not a piecewise curve. The wind profile obtained was only at a single location. To determine the loads on nodes along the cable, autocorrelation (Eqn. 5.24) and cross covariance (Eqn. 5.26) were used (Oliveira, 2006). Note that the cross covariance relates two different samples at different locations while the autocorrelation relates the same sample at different time. Therefore, in order to determine the wind profile at a different location from the known wind profile, the cross covariance is first calculated using the distance between the two locations. Then the time required

to produce the autocorrelation to have the same value as that of the cross covariance is determined. This time represents the lag in the arrival time of the same sample at the second location.

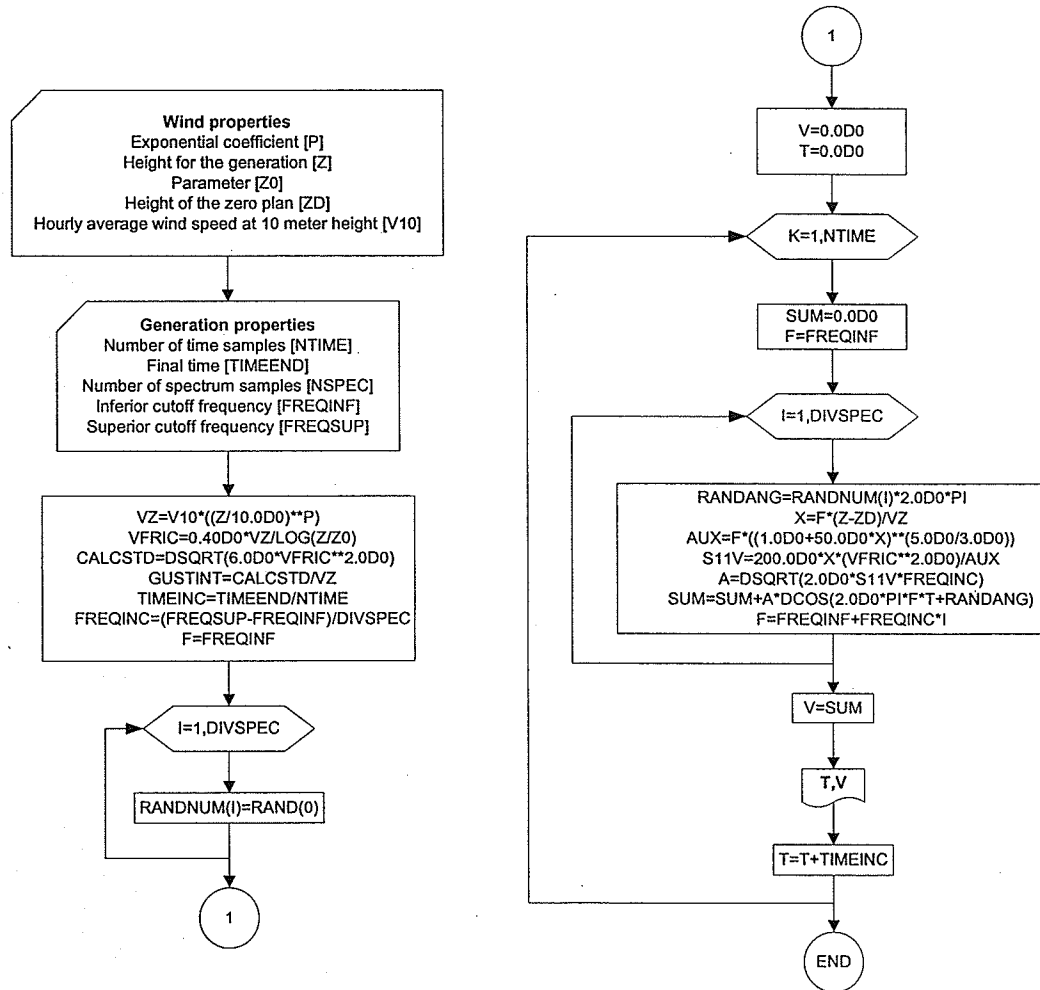


Figure 5.12 - Wind generation flowchart.

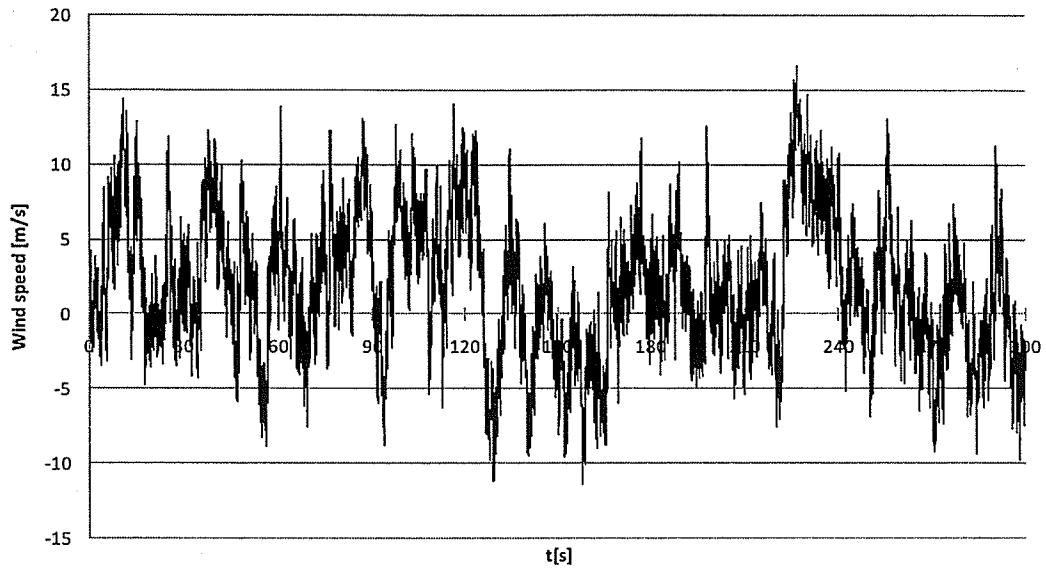


Figure 5.13 - Turbulence wind speed sample.

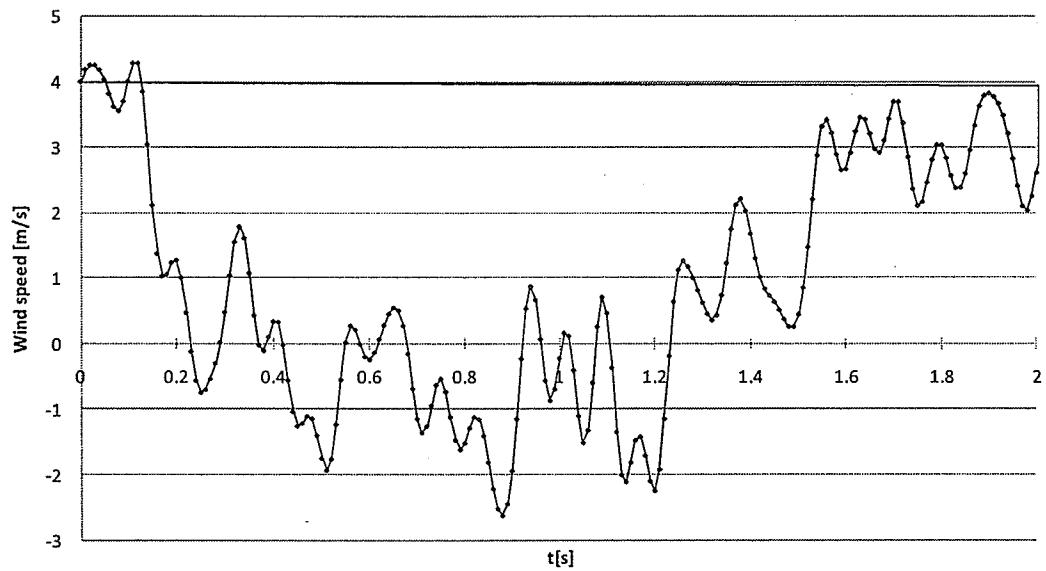


Figure 5.14 - Turbulence wind speed at a maximum time of 2 seconds.

In this study, a transmission line span is 480 meters long and is divided into seventeen equal spaced distances (ΔS) of 60 meters. Note that there are eight cable elements per span, as illustrated in Figure 5.15. As previously stated,

the wind profile in Figure 5.13 or 5.14 is assumed to be at the boundary nodes (zone 1 in Figure 5.15). To obtain the time lag of the wind profile in zone 2, ΔS apart, the cross covariance is calculated to be, Eqn. (5.26):

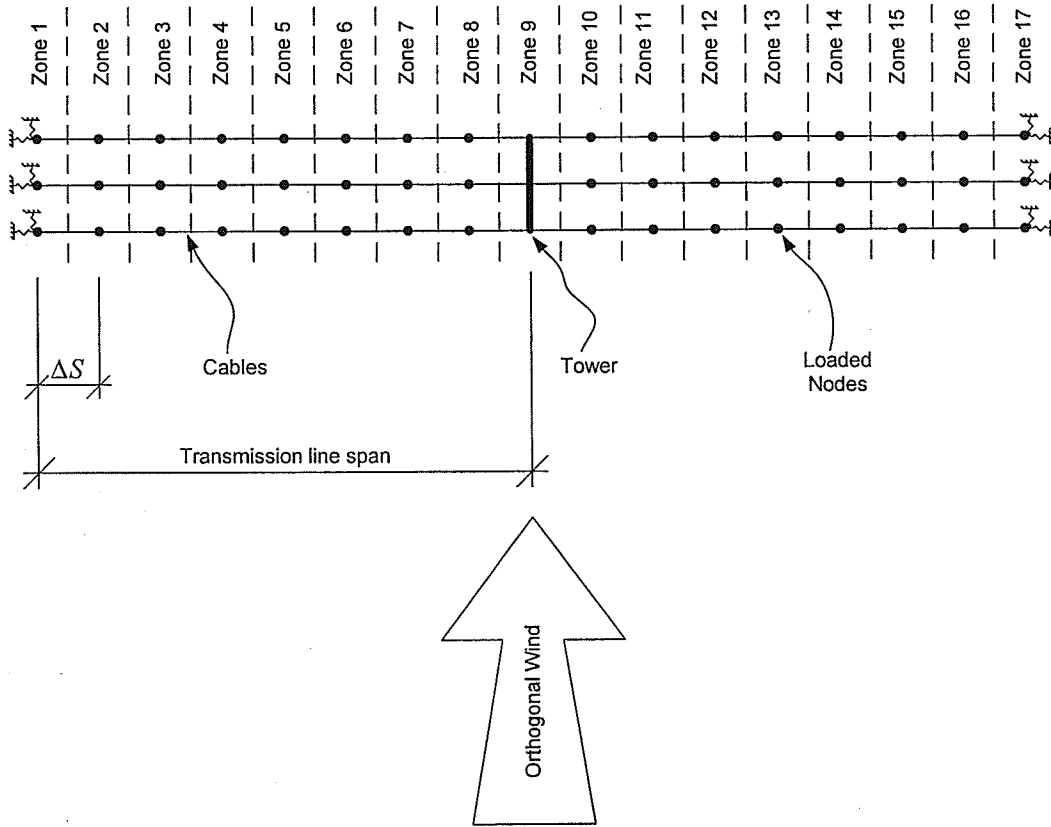


Figure 5.15 - Top view of the transmission tower system.

$$C_{v_1, v_2}(60 \text{ m}) = \int_{-\infty}^{+\infty} S_v(f) e^{-fC} df = 10.27 \text{ [m}^2/\text{s}^2] \quad (5.29)$$

The time required to provide the autocorrelation to have the same value as this calculated cross covariance is determined using Eqn. (5.24), i.e.

$$R_v(4.89 \text{ s}) = \int_0^{\infty} S_v(f) \cos(2\pi f\tau) df = 10.28 \text{ [m}^2/\text{s}^2] \quad (5.30)$$

This means that the wind profile in zone 2 is 4.89 seconds behind the wind profile in zone 1. The plots of the wind profiles in zone 1 and zone 2 are shown in Figure 5.16.

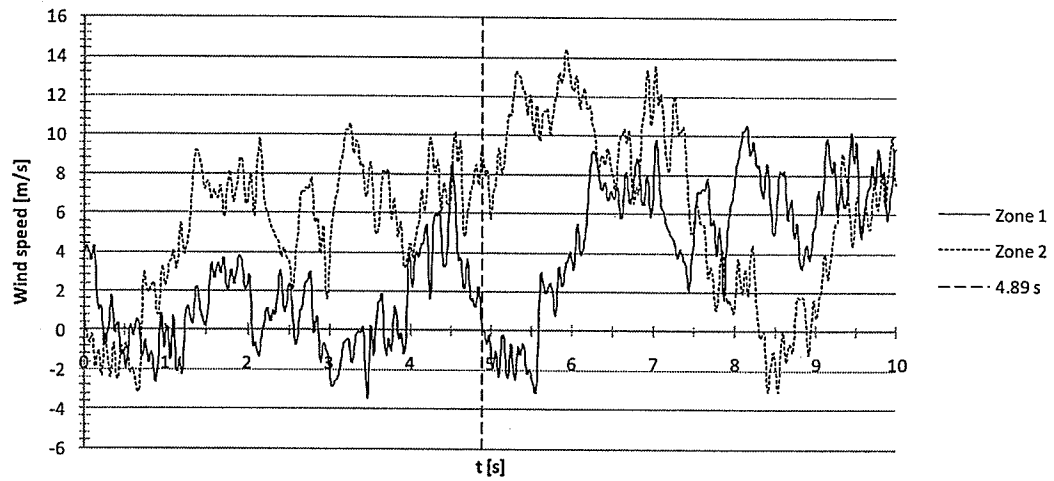


Figure 5.16 - Wind speed in zones 1 and 2.

6. ANALYSIS RESULTS

6.1. ISOLATED TOWER (MODEL 1 AND MODEL 2)

The comparison of the displacements from the static analyses was made at the controlled nodes shown in Figure 5.6 for Models 1 – a detailed model and 2 – a simplified model (Figure 6.1a, and 6.1b, respectively). For the detailed model, Figure 6.1a, the average displacement of all the nodes on the top of the tower was used. In the dynamic analysis, only the natural frequencies of the main structure were compared. All the frequencies corresponding to the members in detailed model were not included in the comparison.

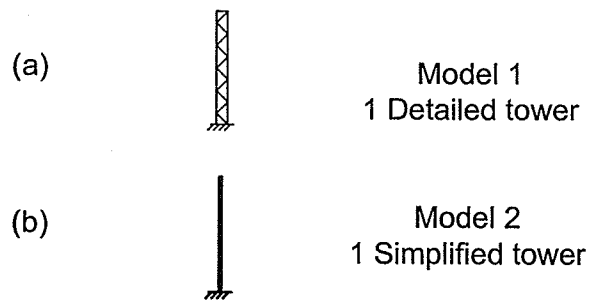


Figure 6.1 - (a) Model 1 and (b) Model 2.

6.1.1. STATIC DISPLACEMENTS

Figures 6.12 to 6.16 illustrate the displacements at the observed locations. Tables 6.1 and 6.2 summarize the differences between the maximum displacements of the detailed and the simplified models for load cases 1 and 2, respectively. Note that although there was no load in the z-direction for load case 1, there was some small z-displacement for the detailed model (3×10^{-4} m in comparison to 0.4m) because of the asymmetrical configuration of the diagonals.

- Load Case 1 Results:

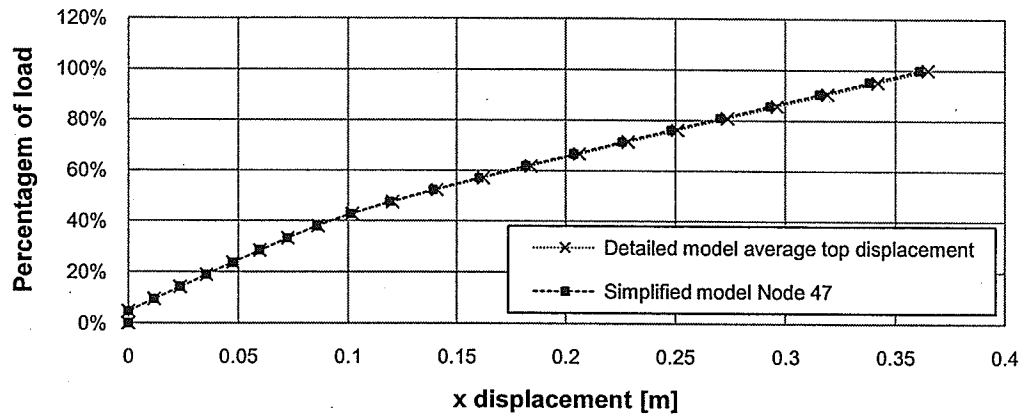


Figure 6.2 - Load Case 1, x displacement of the top of the tower.

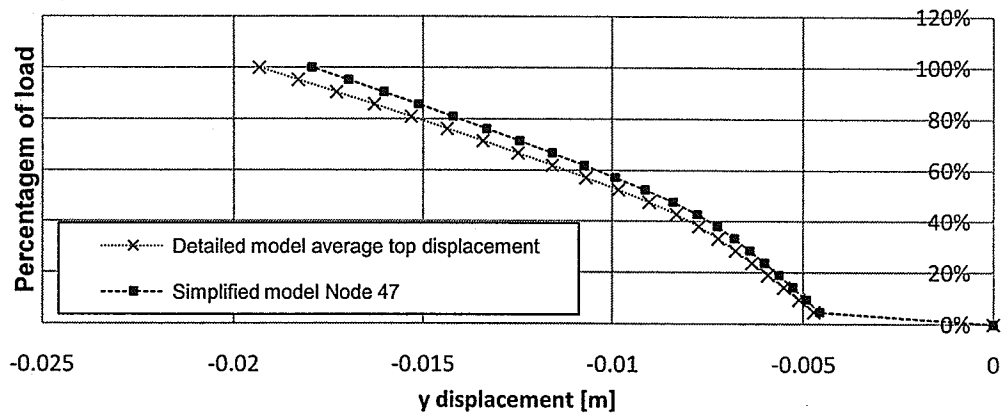


Figure 6.3 - Load Case 1, y displacement of the top of the tower.

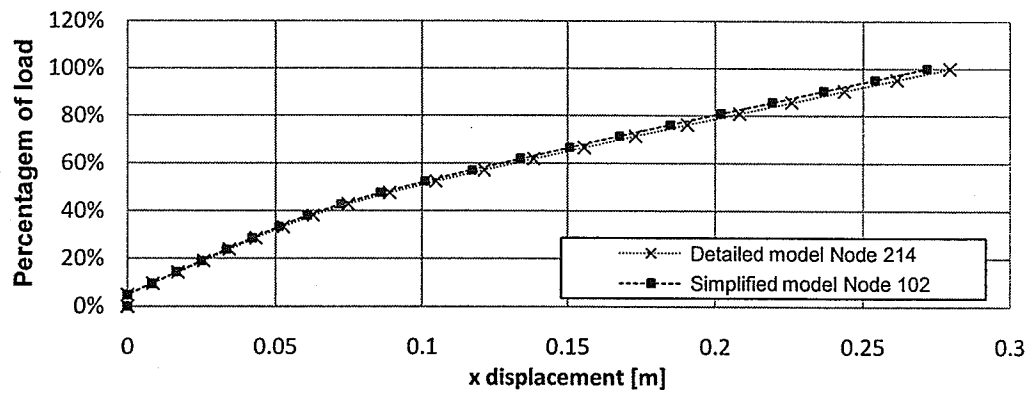


Figure 6.4 - Load Case 1, x displacement of the left cross arm.

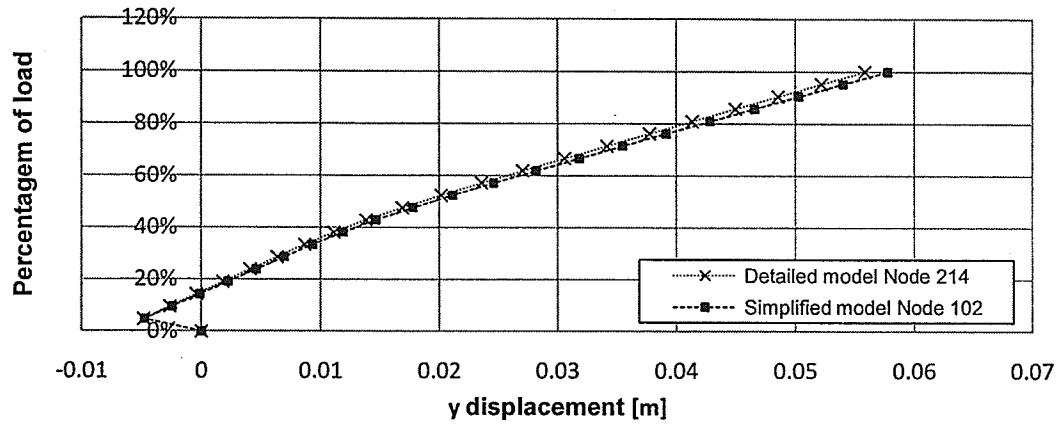


Figure 6.5 - Load Case 1, y displacement of the left cross arm.

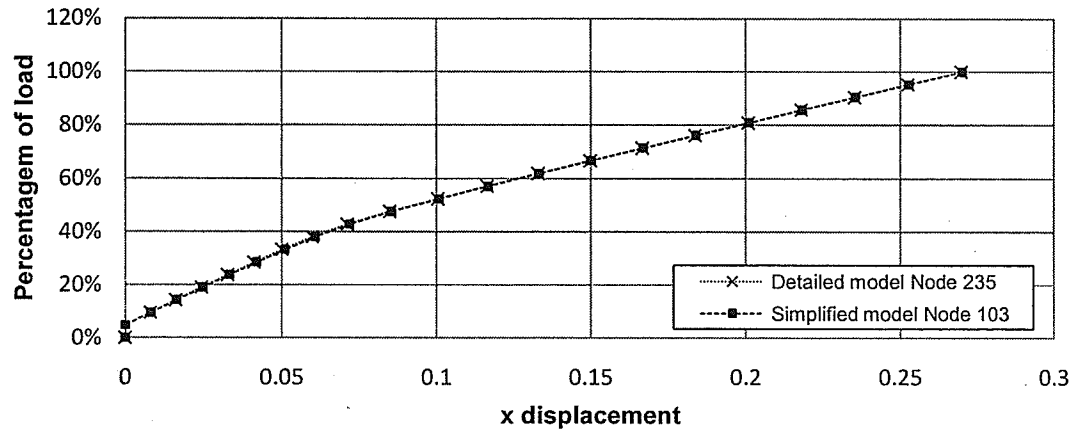


Figure 6.6 - Load Case 1, x displacement of the right cross arm.

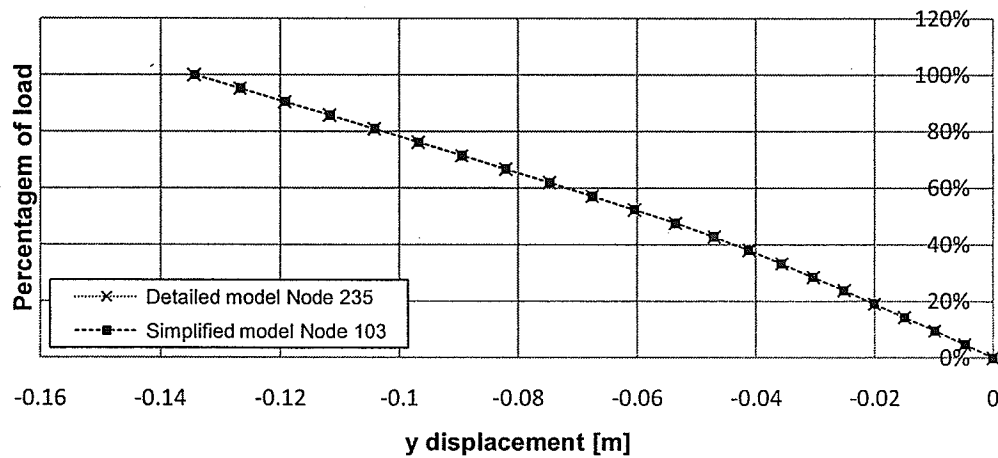


Figure 6.7 - Load Case 1, y displacement of the right cross arm.

Table 6.1 - Percentage difference of displacements between the Models 1 and 2
for Load Case 1.

<i>P.D.</i> (Final displacement)		
NODE (simplified model)	X	Y
47	-1.09%	-7.18%
102	-2.79%	3.43%
103	0.15%	-0.09%

- Load Case 2 results:

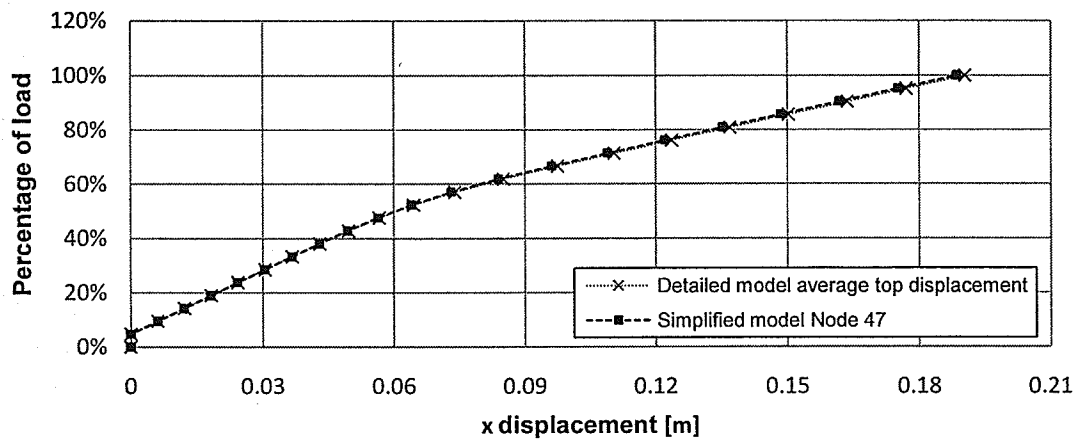


Figure 6.8 - Load Case 2, x displacement of the top of the tower.

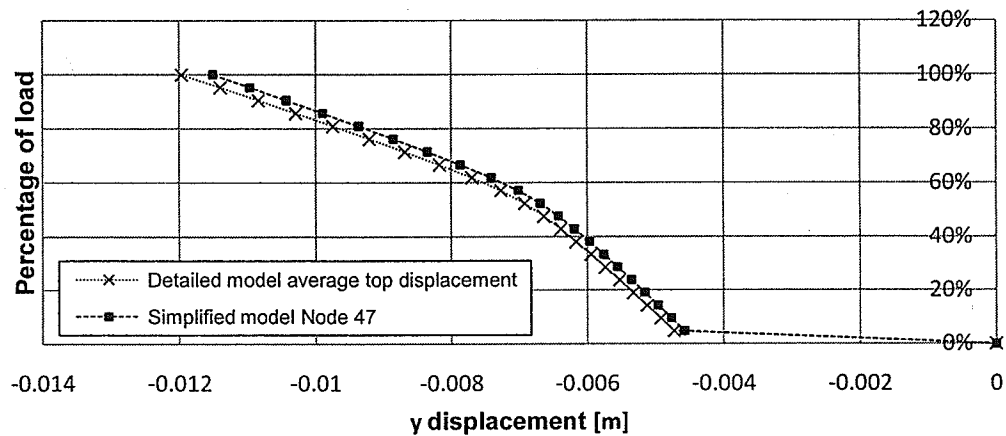


Figure 6.9 - Load Case 2, y displacement of the top of the tower.

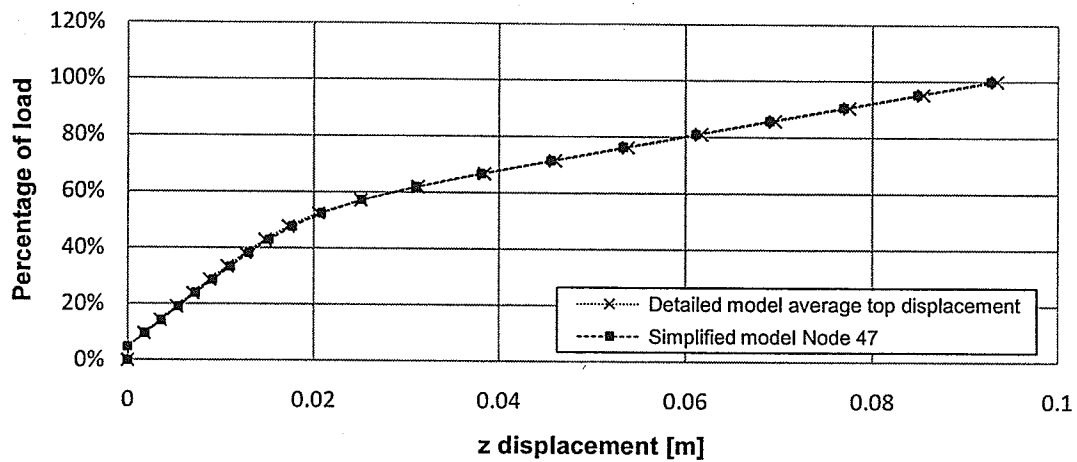


Figure 6.10 - Load Case 2, z displacement of the top of the tower.

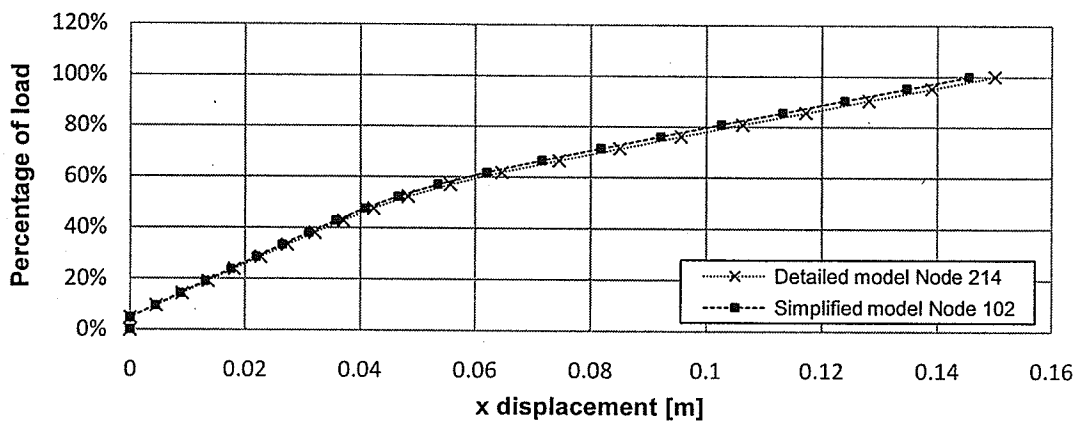


Figure 6.11 - Load Case 2, x displacement of the left cross arm.

Load Case 2

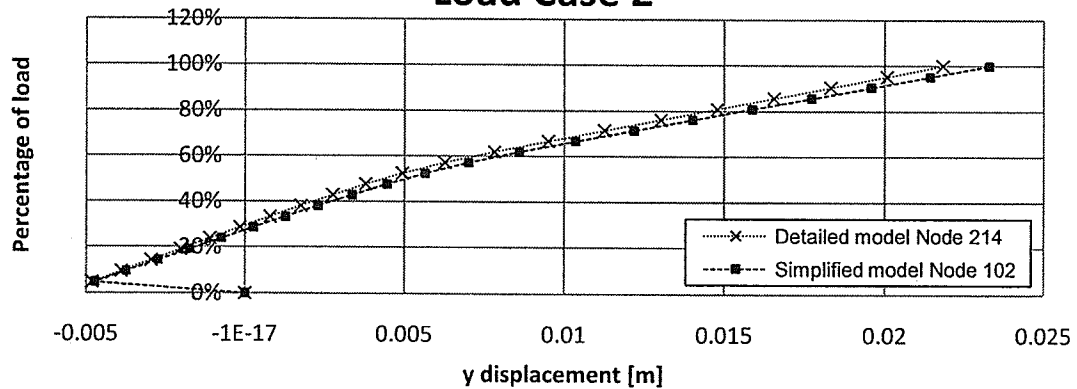


Figure 6.12 - Load Case 2, y displacement of the left cross arm.

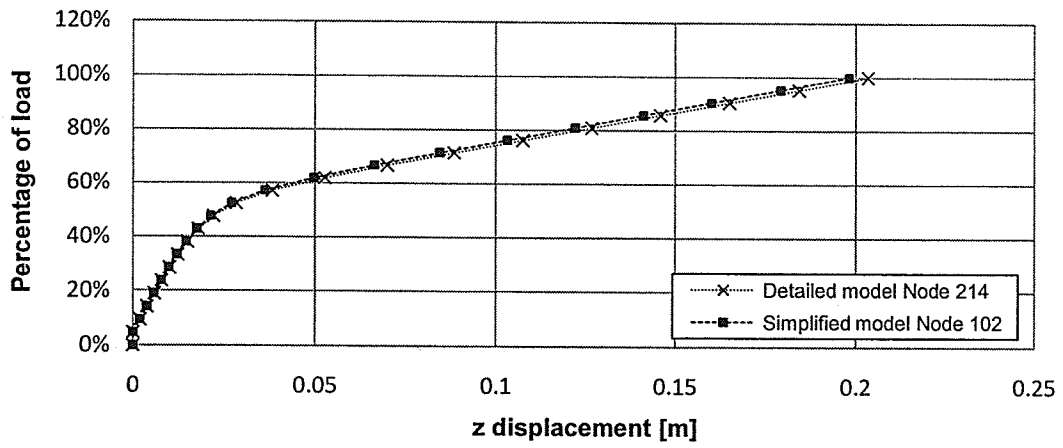


Figure 6.13 - Load Case 2, z displacement of the left cross arm.

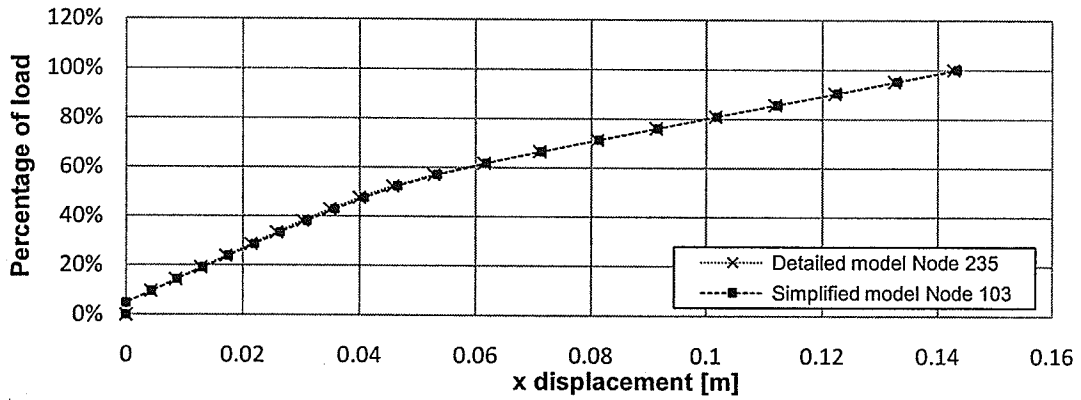


Figure 6.14 - Load Case 2, x displacement of the right cross arm.

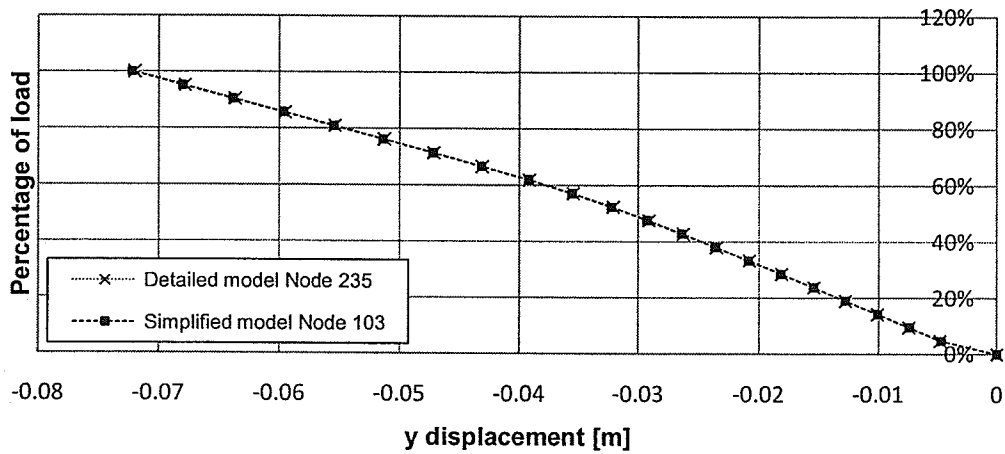


Figure 6.15 - Load Case 2, y displacement of the right cross arm.

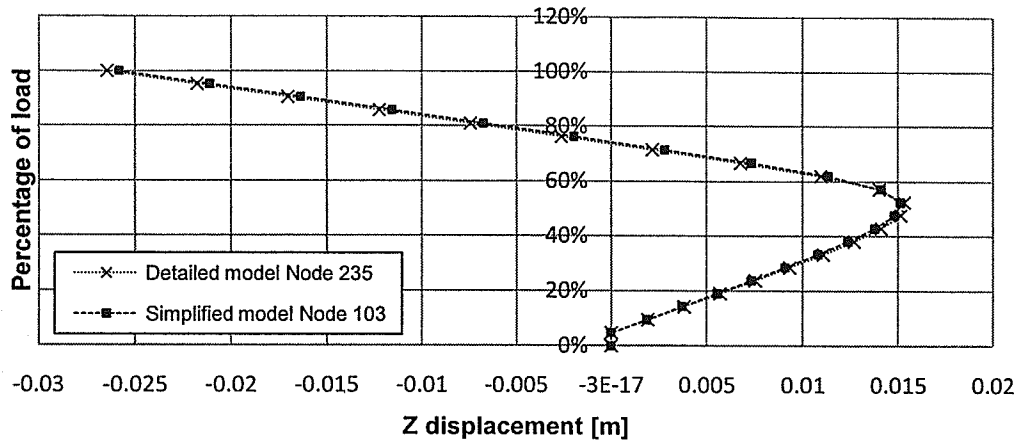


Figure 6.16 - Load Case 2, z displacement of the right cross arm.

Table 6.2 - Percentage difference of displacements between the Models 1 and 2 for Load Case 2.

<i>P.D.</i> (Final displacement)			
NODE (simplified model)	X	Y	Z
47	-0.98%	-3.80%	-0.69%
102	-3.03%	6.66%	-2.60%
103	0.44%	0.32%	-2.35%

Figures 6.2 to 6.16 show that the simplified model gives 7% error of the displacements of the detailed model. Tables 6.1 to 6.2 illustrate that the *P.D.* between the two results for final displacements are within 10%. This clearly indicates that the simplified model can represent the detailed model in the non-linear analysis.

6.1.2. FREE VIBRATION

For the free vibration analysis, the computational runtime of Model 1 was 1 hour and 6 minutes and that of Model 2 was 2 minutes and 28 seconds. In this study, only the first forty modes were investigated. Several of them correspond to

the vibration of guy wires only and would not be of interest in this thesis. The first fourteen mode shapes relating to the tower mast are presented in a graphic form in the Appendix - A. The mode shapes are normalized to have the maximum value of unity.

Table 6.3 summarizes the mode shapes of both models. The symbols LB, TB, T, and X represent the lateral bending, transverse bending, torsion, and no movement of the tower mast (the magnitudes of the mode shape at the top are less than 0.001 for translation and 0.00015 for rotation), respectively. The plus sign indicates that the amplitudes of the mode shape at the top are greater than 0.1 for translations and 0.015 for rotations. When there is no plus sign and no X sign, the amplitudes of the mode shape at the top for translation are in between 0.01 and 0.1 with those associating with the rotation are in between 0.015 and 0.0015. When there is an X sign in front of the symbol, the magnitudes of the mode shapes at the top are between 0.01 and 0.001 for translation and 0.0015 and 0.00015 for rotation. The darker color of the shade indicates the higher amplitude of the mode shape. Only LB, TB and T modes were compared between the two models.

Table 6.3 - Comparison of mode shapes between Model 1 and Model 2.

Detailed Tower (Model 1)					Simplified Tower (Model 2)				
MODE	FREQ[HZ]	Lateral	Transversal	Torsion	MODE	FREQ[HZ]	Lateral	Transversal	Torsion
1	1.50257	LB	X	X	1	1.51493	LB	X	X
2	1.50382	X	TB	X	2	1.51619	X	TB	X
3	1.50579	X	X	T	3	1.51813	X	X	T
4	1.51131	X	X	X	4	1.52369	X	X	X
5	1.51689	X	TB	X	5	1.52964	X	TB	X
6	1.52002	LB	X	X	6	1.53251	LB	X	X
7	1.52155	X	X	T	7	1.53400	X	X	T
8	1.52577	X	X	X	8	1.53847	X	X	X
9	2.30032	X/LB	TB+	X	9	2.31917	X	TB+	X
10	2.42060	LB+	X	X	10	2.45239	LB+	X	X
11	3.04877	X	X	T+	11	3.07444	X	X	T+
12	3.08061	X	X/TB	X	12	3.10586	X	X/TB	X
13	3.08070	X	X	X	13	3.10601	X	X	X
14	3.08093	X	X	X	14	3.10617	X	X	X
15	3.08095	X	X	X	15	3.10617	X	X	X
16	3.08095	X	X	X	16	3.10619	X	X	X
17	3.09350	X/LB	TB	X	17	3.11851	X	TB	X
18	3.09400	LB	X	X	18	3.12040	LB	X	X
19	3.55151	LB+	X	X/T	20	3.65619	LB+	X	X
20	3.57424	X/LB	X	T+	19	3.63406	X	X	T+
21	4.44293	X	TB+	X	21	4.56100	X	TB+	X
22	4.76743	X	X	X	22	4.80668	X	X	X
23	4.76766	X	X	X	23	4.80670	X	X	X
24	4.76810	X	X	X	24	4.80715	X/LB	X	X
25	4.76813	X	X	X/T	25	4.80717	X	X	X/T
26	4.76950	X	TB	X	26	4.80927	X	X/TB	X
27	4.77091	LB	X	X	27	4.81025	LB	X	X
28	4.77356	X	TB	X	28	4.81381	X	TB	X
29	4.77998	X	X	T	29	4.82022	X	X	T
30	6.62264	X	X	X	30	6.67706	X	X	X
31	6.62274	X	X/TB	X	31	6.67725	X	X/TB	X
32	6.62320	X	X	X	32	6.67746	X	X	X
33	6.62320	X	X	X	33	6.67746	X	X	X
34	6.62323	X	X	X	34	6.67746	X	X	X
35	6.62458	LB	X	X	35	6.67927	LB	X	X
36	6.62518	X	TB	X	36	6.67959	X	TB	X
37	6.62926	X	X	T	37	6.68426	X	X	T
38	8.65794	X	TB	X	38	8.72986	X	TB	X
39	8.65920	LB	X	X	40	8.73102	LB	X	X
40	8.65970	X	X	X	39	8.73088	X	X	X

Table 6.3 shows that both models have similar frequencies and the corresponding mode shapes. This demonstrates that the simplified model can represent the detailed model in the dynamic analysis if chosen to.

6.2. TRANSMISSION SYSTEM

An accurate dynamic analysis of a transmission system cannot be attained without considering the effects of the insulator strings, the conductors and the ground wires. The best and simplest technique is to include the insulator strings, the conductors and the ground wires in the model. According to Oliveira (2006), the addition of the insulator strings, the conductors and the ground wires would reduce natural frequencies of the tower because these structures have very low stiffness compared to the mass. According to past literature, a required number of tower spans in the model depends on the system characteristics, load type and the direction of the load. A cascade failure analysis for example, requires a large number of spans. On the other hand, a wind load analysis may require lesser number of spans. In this study, in order to appreciate the effects of the insulator strings, conductors, and the ground wires, as well as the number of the spans, on the dynamic characteristics of the transmission system, free vibration of the system with different number of spans is investigated.

6.2.1. FREE VIBRATION

6.2.1.1. MODEL 2 AND MODEL 3

The objective for this comparison is to investigate the effects of the insulator strings, the conductors and the ground wire cables on the dynamic properties of the transmission system. Figure 6.17 illustrates the models used in this part of study.

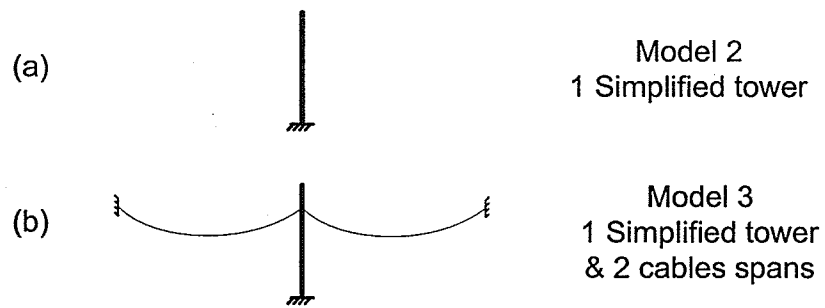


Figure 6.17 - (a) Model 2 and (b) Model 3.

Table 6.4 shows a comparison between the natural frequencies and mode shapes of models 2 and 3. It can be seen from the table that there are mode shapes associating to lower frequencies present for model 3. These frequencies are the direct effects of the addition to the system of the cables and insulators that have low stiffness to mass ratio.

Table 6.4 - Frequencies and mode shapes of Model 2 and Model 3.

1 simplified tower without cables (Model 2)					1 simplified tower with cables (Model 3)				
MODE	FREQ[HZ]	LATERAL	TRANSVERSAL	TORSION	MODE	FREQ[HZ]	LATERAL	TRANSVERSAL	TORSION
					1	0.11800	X/LB	X	X
					5	0.13260	X	X	T
					6	0.13328	X	X/TB	X
					9	0.24016	LB	X	X
					11	0.25152	X/LB	X	X
					19	0.30850	X/LB	X	X
					21	0.34674	X	TB	X
					22	0.35670	X/LB	X	X
					25	0.37140	LB	X	X
					27	0.39259	X	X	X/T
					31	0.47733	X/LB	X	X
					33	0.49941	X	X/TB	X
					34	0.50009	LB	X	X
					37	0.51626	LB	X	X
					39	0.54369	LB	X	X
					47	0.66310	X/LB	X	X
					49	0.67737	LB	X	X
					51	0.71278	X	X	X/T
					55	0.71649	LB	X	X
					57	0.85100	LB	X	X
					59	0.86708	X/LB	X	X
					61	0.86922	X	X/TB	X
					63	0.88449	LB	X	X
					69	1.01321	LB	X	X
					71	1.03135	LB	X	X
					79	1.07766	X/LB	X	X
					81	1.23918	LB	X	X
					87	1.45979	LB	X	X
					88	1.46103	X	TB	X
					89	1.46249	X	X	T
					91	1.47363	X	TB	X
					92	1.47587	LB	X	X
					93	1.47760	X	X	T
					95	2.33027	X/LB	TB+	X
					96	2.44590	LB+	X	T
					97	2.46023	LB+	X/TB	T+
					98	2.46411	LB	TB	T
					99	2.97109	X	X	T+
					100	2.99021	X	X/TB	X
					105	3.00298	LB	X	X
					106	3.00371	X	TB	X
					107	3.21603	LB+	X	X
					108	3.74297	X	X	T+
					109	4.11614	X	TB+	X
					114	4.62867	X	X/TB	X
					115	4.62892	X	TB	X/T
					116	4.63057	X/LB	X/TB	X
					117	4.63062	X/LB	X/TB	X
					118	4.64375	X	X	T
					119	4.79046	LB+	X	X
1	1.51493	LB	X	X					
2	1.51619	X	TB	X					
3	1.51813	X	X	T					
5	1.52964	X	TB	X					
6	1.53251	LB	X	X					
7	1.53400	X	X	T					
9	2.31917	X	TB+	X					
10	2.45239	LB+	X	X					
11	3.07444	X	X	T+					
12	3.10586	X	X/TB	X					
17	3.11851	X	TB	X					
18	3.12040	LB	X	X					
20	3.65619	LB+	X	X					
19	3.63406	X	X	T+					
21	4.56100	X	TB+	X					
29	4.82022	X	X	T					

6.2.1.2. MODEL 3 AND MODEL 4

As mentioned in Section 5.3, different boundary conditions will be investigated. In this section, the use of spring or fixed supports, Figure 6.18, to represent the boundary conditions is studied here. The processing time of Model 3 and Model 4 are practically the same (7 minutes and 41 seconds). Table 6.5 shows the free vibration analysis of the two models. It can be seen that some of the frequencies and the corresponding mode shapes are the same. However, it is expected that Model 4 should represent a more realistic environment of the system than Model 3 since Model 3 assumes that the end towers have infinity stiffness. Therefore, the use of Model 3 not only does not save computational time but also does not represent an actual situation. This type of supports should be avoided in the analysis as, depending on the load, might not predict the actual response of the structure.

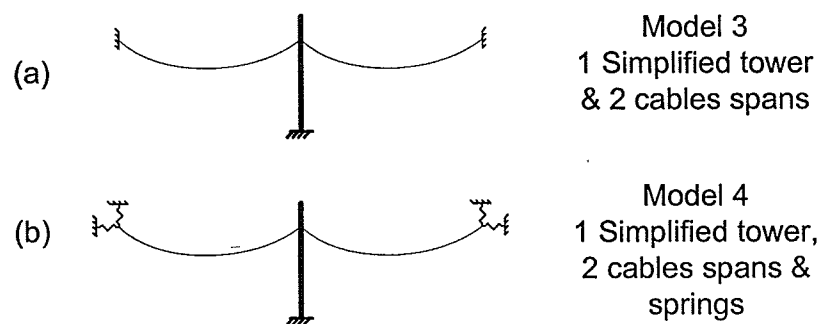


Figure 6.18 - (a) Model 3 and (b) Model 4.

Table 6.5 - Frequencies and mode shapes of Model 3 and Model 4.

1 simplified tower with cables (Model 3)					1 simplified tower with cables and springs (Model 4)				
MODE	FREQ[HZ]	LATERAL	TRANSVERSAL	TORSION	MODE	FREQ[HZ]	LATERAL	TRANSVERSAL	TORSION
1	0.11800	X/LB	X	X	1	0.11479	X/LB	X	X
5	0.13260	X	X	T	5	0.13209	X	X	T
6	0.13328	X	X/TB	X	6	0.13266	X	X/TB	X
11	0.25152	X/LB	X	X	9	0.17643	X/LB	X	X
9	0.24016	LB	X	X	11	0.22976	LB	X	X
					15	0.25074	X	X	X/T
					17	0.25148	X/LB	X	X
19	0.30850	X/LB	X	X	21	0.30847	X/LB	X	X
25	0.37140	LB	X	X	23	0.32562	LB	X	X
21	0.34674	X	TB	X	27	0.34038	X	TB	X
22	0.35670	X/LB	X	X					
27	0.39259	X	X	X/T					
					29	0.39087	X	X	T
					30	0.39114	X	X/TB	X
					31	0.39279	LB	X	X
					33	0.39953	LB	X	X
					35	0.40776	X	X	T
					36	0.40926	X	TB	X
31	0.47733	X/LB	X	X	39	0.47730	X/LB	X	X
33	0.49941	X	X/TB	X	41	0.49752	X	X/TB	X
34	0.50009	LB	X	X					
37	0.51626	LB	X	X	43	0.52730	LB	X	X
39	0.54369	LB	X	X	45	0.54300	LB	X	X
					47	0.54591	X	X	X/T
					48	0.54593	X	X/TB	X
47	0.66310	X/LB	X	X	53	0.66303	X/LB	X	X
49	0.67737	LB	X	X	55	0.68389	LB	X	X
55	0.71649	LB	X	X	57	0.71084	LB	X	X
51	0.71278	X	X	X/T	59	0.71240	X	X	X/T
57	0.85100	LB	X	X	63	0.85482	LB	X	X
59	0.86708	X/LB	X	X	65	0.86700	X/LB	X	X
61	0.86922	X	X/TB	X	67	0.86909	X	X/TB	X
63	0.89449	LB	X	X	69	0.88389	LB	X	X
					71	0.88550	X	X	X/T
69	1.01321	LB	X	X	75	1.01463	LB	X	X
71	1.03135	LB	X	X	77	1.03091	LB	X	X
79	1.07766	X/LB	X	X	85	1.07758	X/LB	X	X
81	1.23918	LB	X	X	87	1.23917	LB	X	X
87	1.45979	LB	X	X	93	1.45953	LB	X	X
88	1.46103	X	TB	X	94	1.46090	X	TB	X
89	1.46249	X	X	T	95	1.46243	X	X	T
91	1.47363	X	TB	X	97	1.47349	X	TB	X
92	1.47587	LB	X	X	98	1.47570	LB	X	X
93	1.47760	X	X	T	99	1.47754	X	X	T
					101	1.66845	LB+	X	X
					103	2.09114	X	X	T
					104	2.09114	X	X/TB	X
					105	2.11617	LB+	X	X
95	2.33027	X/LB	TB+	X	107	2.32845	X	TB+	X/T
96	2.44590	LB+	X	T	108	2.46103	LB+	X	X
97	2.46023	LB+	X/TB	T+					
98	2.46411	LB	TB	T					
99	2.97109	X	X	T+	109	2.97079	X	X	T+
100	2.99021	X	X/TB	X	110	2.99005	X	X/TB	X
106	3.00371	X	TB	X	115	3.00345	X	TB	X
105	3.00298	LB	X	X	116	3.00455	LB	X	X
107	3.21603	LB+	X	X	117	3.30127	LB+	X	X
108	3.74297	X	X	T+	118	3.56804	X	X	T+
					119	3.57596	X	TB	X
					120	3.74983	X	X	T+
109	4.11614	X	TB+	X	121	4.00869	X	TB+	X
					125	4.62800	X/LB	X/TB	X/T
114	4.62867	X	X/TB	X					
115	4.62892	X	TB	X/T					
116	4.63057	X/LB	X/TB	X	126	4.62824	X	X/TB	X
117	4.63062	X/LB	X/TB	X	127	4.63043	X/LB	X/TB	X
					128	4.63061	LB	X	X/T
118	4.64375	X	X	T	129	4.64314	X	X	T
119	4.79046	LB+	X	X	132	5.43560	LB+	X	X

6.2.1.3. MODEL 4 AND MODEL 5

In this section, the investigation is carried out to verify if the end towers are needed in the model to provide a more realistic system (Figure 6.19b). The results of the inclusion of the end towers in comparison to the use of spring representing end towers will be discussed.

The processing times to analyze Models 4 and 5 are 7 minutes and 41 seconds and 1 hour and 50 minutes, respectively. Table 6.6 illustrates the natural frequencies and the mode shapes of each model. It can be noticed the appearance of new mode shapes for frequencies above 1.2 Hz. With only a free vibration analysis, it is expected the dynamic response of the system can be different depending on the loading. The dynamic analyses of the two systems will be carried out in the later part of this thesis.

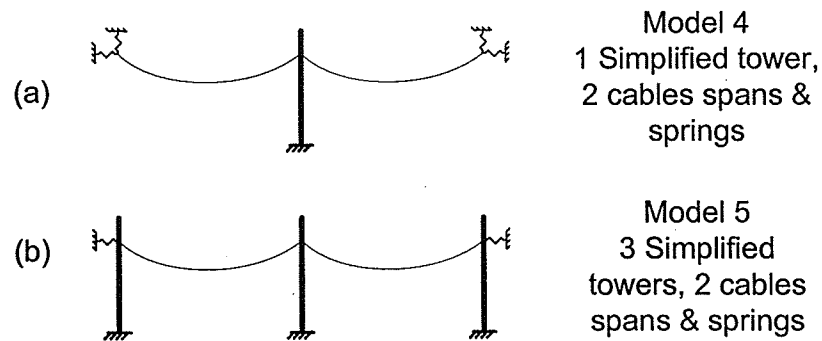


Figure 6.19 - (a) Model 4 and (b) Model 5.

Table 6.6 - Frequencies and mode shapes of Model 4 and Model 5.

1 simplified tower with 2 cables spans (Model 4)					3 simplified towers with 2 cables spans (Model 5)				
MODE	FREQ[HZ]	LATERAL	TRANSVERSAL	TORSION	MODE	FREQ[HZ]	LATERAL	TRANSVERSAL	TORSION
1	0.11479	X/LB	X	X	1	0.11465	X/LB	X	X
5	0.13209	X	X	T	5	0.13204	X	X	T
6	0.13266	X	X/TB	X	6	0.13269	X	X/TB	X
9	0.17643	X/LB	X	X	9	0.17513	X/LB	X	X
11	0.22976	LB	X	X	11	0.22906	LB	X	X
15	0.25074	X	X	X/T	15	0.25064	X	X	X/T
17	0.25148	X/LB	X	X	17	0.25141	X/LB	X	X
21	0.30847	X/LB	X	X	21	0.30847	X/LB	X	X
23	0.32562	LB	X	X	23	0.32199	LB	X	X
27	0.34038	X	TB	X	27	0.34057	X	TB	X
29	0.39087	X	X	T	29	0.39018	X	X	T
30	0.39114	X	X/TB	X	30	0.39104	X	X/TB	X
31	0.39279	LB	X	X	31	0.3926	LB	X	X
33	0.39953	LB	X	X	33	0.39757	LB	X	X
35	0.40776	X	X	T	35	0.40294	X	X	T
36	0.40926	X	TB	X	36	0.40756	X	TB	X
39	0.47730	X/LB	X	X	39	0.4773	X/LB	X	X
41	0.49752	X	X/TB	X	41	0.49753	X	X/TB	X
43	0.52730	LB	X	X	43	0.52694	LB	X	X
45	0.54300	LB	X	X	45	0.54282	LB	X	X
47	0.54591	X	X	X/T	47	0.54566	X	X	X/T
48	0.54593	X	X/TB	X	48	0.54607	X	X/TB	X
53	0.66303	X/LB	X	X	53	0.66302	X/LB	X	X
55	0.68389	LB	X	X	55	0.68378	LB	X	X
57	0.71084	LB	X	X	57	0.71059	LB	X	X
59	0.71240	X	X	X/T	59	0.71215	X	X	X/T
63	0.85482	LB	X	X	63	0.85476	LB	X	X
65	0.86700	X/LB	X	X	65	0.86699	X/LB	X	X
67	0.86909	X	X/TB	X	67	0.86909	X	X/TB	X
69	0.88389	LB	X	X	69	0.8836	LB	X	X
71	0.88550	X	X	X/T	71	0.88522	X	X	X/T
75	1.01463	LB	X	X	75	1.01461	LB	X	X
77	1.03091	LB	X	X	77	1.03076	LB	X	X
85	1.07758	X/LB	X	X	85	1.07755	X/LB	X	X
87	1.23917	LB	X	X	87	1.2391	LB	X	X
					93	1.45669	X/LB	X	X
					94	1.45699	X	X/TB	X
93	1.45953	LB	X	X	95	1.45955	LB	X	X
94	1.46090	X	TB	X	96	1.46085	X	TB	X
					97	1.4617	X	X/TB	X/T
95	1.46243	X	X	T	98	1.46246	X	X	T
					99	1.46361	X	X	X/T
97	1.47349	X	TB	X	105	1.47308	X/LB	TB	X
					106	1.47352	X/LB	X/TB	X/T
					107	1.47425	LB	X/TB	X/T
					108	1.47462	X/LB	X	X
98	1.47570	LB	X	X	110	1.47571	LB	X	X/T
99	1.47754	X	X	T	111	1.47757	X/LB	X	T
					112	1.47816	X	X/TB	X
					113	1.47878	X/LB	X	X/T
					116	1.48249	X	X/TB	X
101	1.66845	LB+	X	X	117	1.60801	LB+	X/TB	X
					118	1.67296	X/LB	X/TB	X/T
					119	1.7253	X	X/TB	X
					120	1.75116	LB+	X/TB	X
103	2.09114	X	X	T					
104	2.09114	X	X/TB	X					
105	2.11617	LB+	X	X					
107	2.32845	X	TB+	X/T					
108	2.46103	LB+	X	X	121	2.33072	LB+	TB+	X
					122	2.36068	LB	TB	T
					123	2.45848	LB+	TB	X
					124	2.51648	X/LB	X/TB	X/T
					125	2.51715	LB	X/TB	X
					126	2.52982	X/LB	X/TB	X

Table 6.6 (cont'd) - Frequencies and mode shapes of Model 4 and Model 5.

1 simplified tower with 2 cables spans (Model 4)					3 simplified towers with 2 cables spans (Model 5)				
MODE	FREQ[HZ]	LATERAL	TRANSVERSAL	TORSION	MODE	FREQ[HZ]	LATERAL	TRANSVERSAL	TORSION
					127	2.55731	X	X/TB	X
					128	2.68401	LB	TB	T
					129	2.91021	LB	X/TB	X/T
					130	2.96855	X/LB	X/TB	T
109	2.97079	X	X	T+	131	2.9737	X/LB	X/TB	T
					132	2.97566	X/LB	X/TB	T
					133	2.98476	X/LB	X/TB	T
					134	2.98845	X/LB	X/TB	X/T
					135	2.98997	X/LB	X/TB	X/T
110	2.99005	X	X/TB	X	136	2.99018	X	X/TB	X
					137	2.99026	X	X/TB	X/T
					138	2.9903	X	X/TB	X/T
					139	2.99032	X	X/TB	X/T
					142	2.99042	X	X	X/T
					143	2.99043	X/LB	X	X/T
					144	2.99046	X/LB	X/TB	X/T
					145	2.9905	X/LB	X/TB	X
					146	2.9907	X/LB	X/TB	X
					147	3.00159	LB	X/TB	X/T
					148	3.00326	LB	TB	X/T
115	3.00345	X	TB	X	149	3.00423	LB	X	X/T
116	3.00455	LB	X	X	150	3.00473	X	X/TB	X/T
					151	3.00499	LB	X/TB	X/T
					152	3.00673	X/LB	X/TB	X/T
117	3.30127	LB+	X	X	153	3.30233	LB+	TB	X
118	3.56804	X	X	T+	154	3.55604	X/LB	TB	T+
119	3.57596	X	TB	X	155	3.58193	X	TB	X/T
					156	3.74954	X	X/TB	T+
120	3.74983	X	X	T+	157	3.83988	X/LB	TB+	T
					158	4.0916	X/LB	TB	X/T
121	4.00869	X	TB+	X	159	4.19418	LB	TB+	T
					160	4.24228	LB	TB+	X
					161	4.508	X/LB	TB+	T
					162	4.51347	X/LB	TB	X
					163	4.53014	LB	TB+	T
128	4.63061	LB	X	X/T	164	4.59302	LB	TB	X/T
					165	4.62179	X	TB	X/T
					166	4.62285	X/LB	TB	X
					167	4.62533	X	X/TB	X/T
					168	4.62709	X/LB	TB	X/T
					169	4.62723	X	TB	T
					170	4.62726	X/LB	TB	X/T
					171	4.62792	X/LB	X	X
126	4.62824	X	X/TB	X	172	4.628	X	X/TB	X
125	4.62800	X/LB	X/TB	X/T	173	4.62808	X/LB	X/TB	X/T
					174	4.62824	X	X/TB	X
					175	4.62829	X/LB	TB	X/T
127	4.63043	X/LB	X/TB	X	176	4.62837	X/LB	X/TB	X
					177	4.62874	X/LB	TB	X/T
					178	4.62924	X/LB	TB	X/T
					179	4.62994	X	X/TB	X/T
					180	4.63021	X/LB	X/TB	X/T
					181	4.63043	X/LB	TB	X/T
					182	4.63067	X/LB	TB	T
					183	4.6309	X/LB	TB	X/T
					184	4.63291	X/LB	X/TB	X/T
					185	4.63322	X/LB	X/TB	X/T
129	4.64314	X	X	T	186	4.64331	X	X/TB	T
					187	4.64637	X/LB	TB	X/T
					188	5.2937	LB	TB	X/T
132	5.43560	LB+	X	X	189	5.40686	LB+	TB	X/T

6.2.1.4. MODEL 4 AND MODEL 6

This section investigates the influence of using more than two conductors' spans in the analysis of the transmission system as shown in Figure 6.20.

The processing time for Model 6 is 2 hours and 37 minutes, which is twenty times greater than Model 4. Table 6.7 shows the natural frequencies and the mode shapes of the two models. The increase in the number of cable spans increases the number of frequencies and mode shapes as expected. Similar to the previous section, the inclusion of more spans might affect the dynamic response of the system. However, the effects will depend on the nature of the loading.

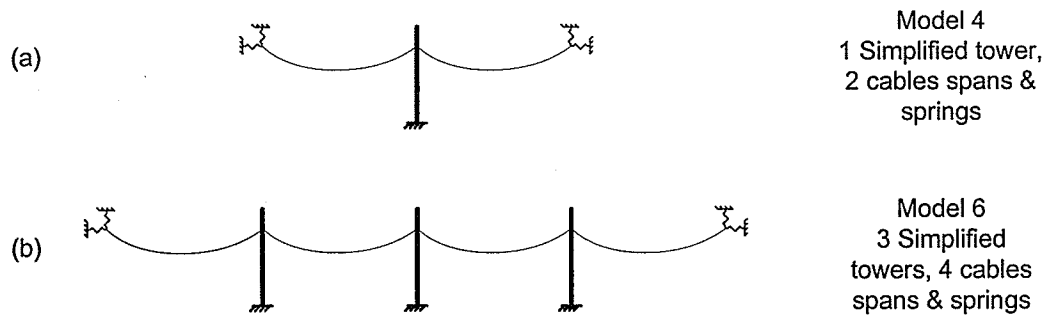


Figure 6.20 - (a) Model 4 and (b) Model 6.

Table 6.7 - Frequencies and mode shapes of Model 4 and Model 6.

1 simplified tower with 2 cable spans (Model 4)					3 simplified towers with 4 cable spans (Model 6)				
MODE	FREQ[HZ]	LATERAL	TRANSVERSAL	TORSION	MODE	FREQ[HZ]	LATERAL	TRANSVERSAL	TORSION
1	0.11479	X/LB	X	X	1	0.11311	X/LB	X	X
					5	0.11981	X/LB	X	X
					9	0.13024	X	X	T
					10	0.13063	X	X/TB	X
					11	0.13232	X/LB	X	X
5	0.13209	X	X	T	13	0.14095	X	X	T
6	0.13266	X	X/TB	X	14	0.14231	X	X/TB	X
9	0.17643	X/LB	X	X					
					19	0.20561	LB	X	X
11	0.22976	LB	X	X	21	0.22879	LB	X	X
					25	0.24078	LB	X	X
15	0.25074	X	X	X/T	29	0.24981	X	X	X/T
					30	0.24989	X	X/TB	X
17	0.25148	X/LB	X	X	31	0.25122	X/LB	X	X
21	0.30847	X/LB	X	X	35	0.2523	X/LB	X	X
					41	0.30846	X/LB	X	X
23	0.32562	LB	X	X					
					45	0.32919	X/LB	X	X
27	0.34038	X	TB	X	49	0.33759	X	TB	X
					51	0.34935	X	TB	T
					52	0.35054	X	X/TB	X
30	0.39114	X	X/TB	X	53	0.35322	X	X/TB	X
31	0.39279	LB	X	X	55	0.3617	LB	X	X
33	0.39953	LB	X	X	59	0.39159	LB	X	X
29	0.39087	X	X	T					
					61	0.39255	X	X	X/T
					63	0.39325	X/LB	X	X
					65	0.39375	X	X	X/T
35	0.40776	X	X	T					
					67	0.40888	X/LB	X	X
36	0.40926	X	TB	X					
39	0.4773	X/LB	X	X	71	0.47727	X/LB	X	X
					73	0.47738	X/LB	X	X
41	0.49752	X	X/TB	X	75	0.4967	X	X/TB	X
43	0.5273	LB	X	X	77	0.4993	LB	X	X
48	0.54593	X	X/TB	X	79	0.50086	X	X/TB	X
45	0.543	LB	X	X	83	0.54256	LB	X	X
					87	0.54382	X/LB	X	X
					89	0.54482	X/LB	X	X
47	0.54591	X	X	X/T	91	0.54597	X	X	X/T
					95	0.65514	LB	X	X
53	0.66303	X/LB	X	X	101	0.66299	X/LB	X	X
					103	0.66315	X/LB	X	X
55	0.68389	LB	X	X	107	0.70659	LB	X	X
57	0.71084	LB	X	X	109	0.70964	LB	X	X
59	0.7124	X	X	X/T	111	0.71111	X	X	X/T
					113	0.71208	LB	X	X
					115	0.71275	X	X	X/T
63	0.85482	LB	X	X	119	0.82681	LB	X	X
65	0.867	X/LB	X	X	123	0.8669	X/LB	X	X
					125	0.86714	X/LB	X	X
67	0.86909	X	X/TB	X	127	0.86903	X	X/TB	X
					129	0.86932	X	X/TB	X
					131	0.87812	LB	X	X
69	0.88389	LB	X	X	133	0.88344	LB	X	X
					137	0.88467	X/LB	X	X
71	0.8855	X	X	X/T	139	0.88588	X	X	X/T
75	1.01463	LB	X	X	143	0.99679	LB	X	X

Table 6.7 (cont'd) - Frequencies and mode shapes of Model 4 and Model 6.

1 simplified tower with 2 cable spans (Model 4)					3 simplified towers with 4 cable spans (Model 6)				
MODE	FREQ[HZ]	LATERAL	TRANSVERSAL	TORSION	MODE	FREQ[HZ]	LATERAL	TRANSVERSAL	TORSION
					147	1.02802	X/LB	X	X
					149	1.03054	X/LB	X	X
					153	1.03139	X/LB	X	X
77	1.03091	LB	X	X					
85	1.07758	X/LB	X	X	163	1.07747	X/LB	X	X
					164	1.07757	X/LB	X	X
					165	1.07761	X/LB	X	X
					167	1.08311	LB+	X	X
87	1.23917	LB	X	X	169	1.23571	LB	X/TB	X
					170	1.23931	X/LB	X/TB	X
					171	1.24343	LB	X	X
93	1.45953	LB	X	X	183	1.45967	LB	X	X/T
					184	1.45979	LB	X/TB	X
					185	1.46053	X	X/TB	X/T
94	1.4609	X	TB	X					
95	1.46243	X	X	T	186	1.46191	X	X/TB	T
					187	1.46282	X	X	X/T
					188	1.46374	X	X/TB	X/T
					189	1.46385	X	X/TB	X/T
					190	1.46418	X	X	X/T
					191	1.46471	X	X	X/T
97	1.47349	X	TB	X	195	1.47394	X/LB	TB	X/T
					197	1.47506	X/LB	X/TB	X/T
98	1.4757	LB	X	X	198	1.47577	LB	X	X
					200	1.47584	LB	X	X
99	1.47754	X	X	T	201	1.47754	X	X/TB	T
					202	1.47772	X	X	X/T
101	1.66845	LB+	X	X					
					207	1.90072	X/LB	TB	T+
					208	1.96226	X/LB	TB	T
					209	2.09231	LB	X/TB	X/T
103	2.09114	X	X	T					
104	2.09114	X	X/TB	X					
105	2.11617	LB+	X	X					
					211	2.12153	X/LB	TB	T
					212	2.14258	X/LB	TB	X/T
107	2.32845	X	TB+	X/T					
					213	2.41159	LB+	TB	T+
108	2.46103	LB+	X	X	214	2.4181	LB+	TB	T
					215	2.44534	LB+	TB+	T+
					216	2.45347	LB+	TB+	T
					217	2.47328	LB	TB+	T+
					218	2.74288	X/LB	TB	X/T
					219	2.83602	LB+	TB	T
					220	2.96513	LB	X/TB	X/T
109	2.97079	X	X	T+					
					221	2.98303	X/LB	X/TB	T
					222	2.98431	X	X/TB	T
					223	2.98547	X	X/TB	T
					224	2.98574	X/LB	X/TB	T
					225	2.98722	X/LB	X/TB	X/T
					226	2.98767	LB	X/TB	X/T
					227	2.98824	X/LB	X/TB	X/T
					228	2.98985	X/LB	X	X/T
					229	2.99002	X/LB	X	X
110	2.99005	X	X/TB	X					
					230	2.99009	X/LB	X/TB	X/T
					231	2.99015	X	X/TB	T
					232	2.99018	X/LB	X/TB	X/T
					233	2.99022	X	X	X/T

Table 6.7 (cont'd) - Frequencies and mode shapes of Model 4 and Model 6.

1 simplified tower with 2 cable spans (Model 4)					3 simplified towers with 4 cable spans (Model 6)				
MODE	FREQ[HZ]	LATERAL	TRANSVERSAL	TORSION	MODE	FREQ[HZ]	LATERAL	TRANSVERSAL	TORSION
					234	2.99029	X	X/TB	X
					235	2.9904	X	X/TB	X
					237	2.99208	X/LB	X/TB	X/T
					238	2.99859	LB	TB	T
					239	2.99984	X/LB	TB	T
115	3.00345	X	TB	X					
					240	3.0046	LB	TB	X
					241	3.00744	LB	X/TB	X/T
116	3.00455	LB	X	X	242	3.00934	LB	X	X/T
					243	3.01098	LB	X/TB	X/T
					244	3.02001	X/LB	X/TB	X/T
					245	3.31602	LB+	TB	T
117	3.30127	LB+	X	X	246	3.31947	LB+	X/TB	T
					247	3.45039	LB+	TB	T+
118	3.56804	X	X	T+					
119	3.57596	X	TB	X					
120	3.74983	X	X	T+					
					248	3.88121	LB	TB	T+
					249	3.90759	X/LB	TB+	T+
121	4.00869	X	TB+	X	250	4.0574	X/LB	X/TB	T+
					251	4.1187	LB	TB+	T+
					252	4.15369	X/LB	TB+	T+
					253	4.2482	X/LB	TB+	T+
					254	4.53041	X/LB	TB	T
					255	4.54471	X/LB	TB+	T+
					256	4.57044	X/LB	TB	T+
					257	4.58462	X/LB	TB	T+
					258	4.59225	X/LB	TB	T+
					259	4.60443	X/LB	TB	T
					260	4.6104	X	TB	T
					261	4.61633	X	TB	T
					262	4.61749	X/LB	TB	T
					263	4.61996	X/LB	X/TB	T
					264	4.62414	X/LB	X/TB	T+
					265	4.62633	X	X/TB	X/T
					266	4.6267	X/LB	X/TB	X
					267	4.62715	X/LB	X/TB	X/T
					268	4.62781	X/LB	X	T
125	4.628	X/LB	X/TB	X/T	269	4.62802	X/LB	X/TB	X
126	4.62824	X	X/TB	X					
					270	4.62833	X/LB	X/TB	X/T
					271	4.62853	X/LB	X/TB	X/T
					272	4.62855	X/LB	TB	T
					273	4.62861	X/LB	X/TB	T
					274	4.62906	X/LB	X/TB	T
					275	4.6297	X	X/TB	T
					276	4.63016	X/LB	TB	X/T
127	4.63043	X/LB	X/TB	X					
128	4.63061	LB	X	X/T					
					277	4.63093	X/LB	TB	X/T
129	4.64314	X	X	T	278	4.63113	X/LB	X	T
					279	4.82113	X/LB	X/TB	T
					280	4.89927	X/LB	TB	T+
					281	5.09098	LB+	TB+	T+
132	5.4356	LB+	X	X					

6.2.1.5. MODEL 6 AND MODEL 7

An additional cable spans (Figure 6.21) is investigated in this section. The processing time for the analysis of Model 7 is 18 hours and 4 minutes, approximately seven times of that required for Model 6. The comparison of natural frequencies and mode shapes of the two models is shown in Table 6.8. It can be seen the increase in the number of cable spans generates new frequencies and mode shapes. These new mode shapes will affect the dynamic response of the system. However, the effects might depend on the nature of the loading.

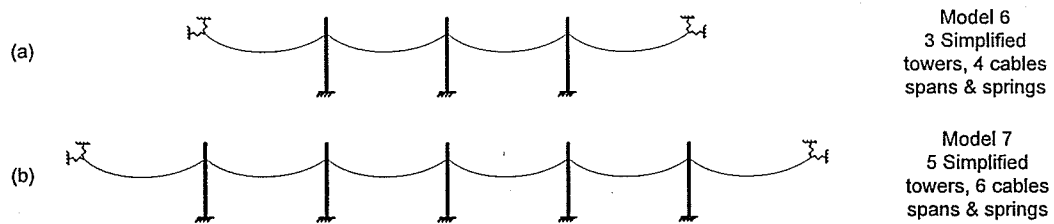


Figure 6.21 - (a) Model 6 and (b) Model 7.

Table 6.8 - Frequencies and mode shapes of Model 6 and Model 7.

3 simplified towers with 4 cable spans (Model 6)					5 simplified towers with 6 cable spans (Model 7)				
MODE	FREQ[HZ]	LATERAL	TRANSVERSAL	TORSION	MODE	FREQ[HZ]	LATERAL	TRANSVERSAL	TORSION
1	0.11311	X/LB	X	X	1	0.11262	X/LB	X	X
5	0.11981	X/LB	X	X	5	0.11654	X/LB	X	X
					9	0.12195	X/LB	X	X
					13	0.13008	X	X	X/T
10	0.13063	X	X/TB	X	14	0.13038	X	X/TB	X
11	0.13232	X/LB	X	X	15	0.13083	X/LB	X	X
9	0.13024	X	X	T	17	0.13259	X	X/TB	T
14	0.14231	X	X/TB	X	18	0.13303	X	X/TB	X
					19	0.13698	X/LB	X	X
13	0.14095	X	X	T	27	0.15171	X	X	T
					28	0.15352	X	X/TB	X
19	0.20561	LB	X	X	29	0.22454	LB	X	X
21	0.22879	LB	X	X	31	0.22848	LB	X	X
25	0.24078	LB	X	X	35	0.23479	LB	X	X
					39	0.24682	X/LB	X	X
					40	0.24693	X	X	X
29	0.24981	X	X	X/T	41	0.24904	X	X	X/T
30	0.24989	X	X/TB	X					
31	0.25122	X/LB	X	X	43	0.25117	X/LB	X	X
35	0.2523	X/LB	X	X	46	0.25161	X/LB	X	X
					53	0.25352	X/LB	X	X
41	0.30846	X/LB	X	X	61	0.30846	X/LB	X	X
45	0.32919	X/LB	X	X	67	0.32631	X	X/TB	T
49	0.33759	X	TB	X	68	0.32874	X	TB	X/T
					69	0.32946	X/LB	X	X
51	0.34935	X	TB	T					
52	0.35054	X	X/TB	X	73	0.34013	X	X/TB	X/T
53	0.35322	X	X/TB	X	75	0.34695	X	X/TB	X
					77	0.3556	X	X/TB	X
55	0.3617	LB	X	X	78	0.356	LB	X	X
					83	0.3766	LB	X	X
59	0.39159	LB	X	X	87	0.39026	LB	X	X
61	0.39255	X	X	X/T	89	0.39176	X	X	X/T
					91	0.39235	X/LB	X	X
65	0.39375	X	X	X/T	93	0.39277	X	X	X/T
63	0.39325	X/LB	X	X	95	0.39342	X/LB	X	X
67	0.40888	X/LB	X	X	99	0.40976	X/LB	X	X
71	0.47727	X/LB	X	X	103	0.47727	X/LB	X	X
73	0.47738	X/LB	X	X	105	0.47734	X/LB	X	X
75	0.4967	X	X/TB	X					
77	0.4993	LB	X	X	109	0.49371	LB	X	X
					111	0.49719	X	X/TB	X/T
					113	0.49954	X	X/TB	X
79	0.50086	X	X/TB	X	115	0.50252	X	X/TB	X
					117	0.50489	X	X	X/T
					119	0.51923	LB	X	X
83	0.54256	LB	X	X	123	0.54248	LB	X	X
					124	0.5429	X	X	X/T
					125	0.54328	LB	X	X
87	0.54382	X/LB	X	X	131	0.54404	X/LB	X	X
91	0.54597	X	X	X/T	133	0.546	X	X	X/T
89	0.54482	X/LB	X	X	135	0.54798	X/LB	X	X
95	0.65514	LB	X	X	139	0.64872	LB	X	X
101	0.66299	X/LB	X	X	148	0.663	X/LB	X	X
103	0.66315	X/LB	X	X	150	0.66308	X/LB	X	X
107	0.70659	LB	X	X	155	0.6794	LB	X	X
111	0.71111	X	X	X/T	157	0.69684	X	X	X/T
109	0.70964	LB	X	X	159	0.70749	LB	X	X
115	0.71275	X	X	X/T	161	0.71054	X/LB	X	X/T
110	0.71047	X	X	X	162	0.71125	X/LB	X	X
113	0.71208	LB	X	X	163	0.71125	LB	X	X
					164	0.7115	X/LB	X	X
					169	0.7125	X/LB	X	X

Table 6.8 (cont'd) - Frequencies and mode shapes of Model 6 and Model 7.

3 simplified towers with 4 cable spans (Model 6)					5 simplified towers with 6 cable spans (Model 7)				
119	0.82681	LB	X	X	175	0.82007	LB	X	X
					177	0.83452	X	X	X/T
					179	0.85224	LB	X	X
					181	0.85393	LB	X/TB	X/T
123	0.8669	X/LB	X	X	183	0.86705	X/LB	X	X
125	0.86714	X/LB	X	X	185	0.86719	X/LB	X	X
127	0.86903	X	X/TB	X	188	0.86907	X	X/TB	X
129	0.86932	X	X/TB	X	190	0.86921	X	X/TB	X
137	0.88467	X/LB	X	X	197	0.88326	X/LB	X	X
131	0.87812	LB	X	X	198	0.88335	LB	X	X
139	0.88588	X	X	X/T	200	0.88374	X	X	X/T
133	0.88344	LB	X	X	201	0.88428	LB	X	X
					211	0.88789	LB	X	X
143	0.99679	LB	X	X	213	0.9924	LB	X	X
					217	1.01369	LB	X	X
					219	1.0238	X	X	X/T
147	1.02802	X/LB	X	X	221	1.03065	X/LB	X	X
149	1.03054	X/LB	X	X	223	1.0308	LB	X	X
					225	1.03109	X/LB	X	X
153	1.03139	X/LB	X	X	230	1.03157	X/LB	X	X
163	1.07747	X/LB	X	X	243	1.07752	X/LB	X	X
164	1.07757	X/LB	X	X	245	1.07763	X/LB	X	X
165	1.07761	X/LB	X	X					
167	1.08311	LB+	X	X					
					249	1.23549	LB	X	X/T
					250	1.23771	LB	X	X/T
171	1.24343	LB	X	X	251	1.23957	LB	X	X/T
170	1.23931	X/LB	X/TB	X	252	1.24273	X/LB	X/TB	X/T
169	1.23571	LB	X/TB	X	253	1.24436	LB	X/TB	X
					271	1.42351	LB	TB	T
183	1.45967	LB	X	X/T					
184	1.45979	LB	X/TB	X	272	1.45977	LB	X	X
185	1.46053	X	X/TB	X/T	273	1.45993	X	X/TB	X
					274	1.4603	X/LB	X	X
					275	1.46109	X/LB	X	X/T
					276	1.46148	X	X/TB	X/T
					277	1.46154	X/LB	TB	T
186	1.46191	X	X/TB	T	278	1.46232	X	X/TB	T
187	1.46282	X	X	X/T	279	1.46386	X	X/TB	X
188	1.46374	X	X/TB	X/T	280	1.46451	X	X/TB	X/T
189	1.46385	X	X/TB	X/T	281	1.46473	X	X/TB	X/T
190	1.46418	X	X	X/T	283	1.4655	X	X	X/T
191	1.46471	X	X	X/T					
195	1.47394	X/LB	TB	X/T	293	1.47505	X/LB	TB	X/T
197	1.47506	X/LB	X/TB	X/T	294	1.47534	X/LB	X/TB	X
198	1.47577	LB	X	X	295	1.47569	LB	X/TB	X/T
200	1.47584	LB	X	X					
					296	1.476	X/LB	X/TB	X/T
					297	1.47606	X	X/TB	X/T
					298	1.4763	X/LB	X/TB	X/T
					299	1.47633	X/LB	X	X/T
					300	1.47644	X	X/TB	X/T
					301	1.47769	X	X/TB	X/T
					302	1.47793	X	X	X/T
201	1.47754	X	X/TB	T	303	1.47847	X	X/TB	T
202	1.47772	X	X	X/T	304	1.48008	X	X	X/T
207	1.90072	X/LB	TB	T+					
208	1.96226	X/LB	TB	T					
					313	2.00235	LB+	TB	T
209	2.09231	LB	X/TB	X/T	314	2.03963	LB	X/TB	X
					315	2.09349	X	X/TB	T
					316	2.09543	X	X/TB	X/T
211	2.12153	X/LB	TB	T					
212	2.14258	X/LB	TB	X/T					

Table 6.8 (cont'd) - Frequencies and mode shapes of Model 6 and Model 7.

3 simplified towers with 4 cable spans (Model 6)					5 simplified towers with 6 cable spans (Model 7)				
					317	2.13189	LB+	X/TB	X
					318	2.17589	X/LB	X	X/T
214	2.4184	LB+	TB	T	319	2.45087	LB+	TB	X/T
213	2.41159	LB+	TB	T+	320	2.50532	LB+	TB	T
217	2.47328	LB	TB+	T+	321	2.51309	LB	TB+	T+
215	2.44534	LB+	TB+	T+	322	2.5367	LB+	TB+	T+
216	2.45347	LB+	TB+	T					
					323	2.62919	LB	X/TB	T+
					324	2.63776	LB	TB	T+
					325	2.6451	LB	TB	T+
					326	2.68475	LB	TB	T
					327	2.80199	LB	TB	T
218	2.74288	X/LB	TB	X/T					
					328	2.93527	LB	X/TB	T
					329	2.94636	X/LB	X	T
					330	2.94855	LB	X	T
220	2.96513	LB	X/TB	X/T	331	2.97616	LB	X	X/T
221	2.98303	X/LB	X/TB	T	332	2.97727	X	X/TB	T
					333	2.97791	LB	TB	X/T
222	2.98431	X	X/TB	T	334	2.98303	X/LB	X/TB	T
					335	2.98451	X/LB	X/TB	X/T
223	2.98547	X	X/TB	T	336	2.98544	X/LB	X/TB	T
					337	2.98605	LB	X/TB	T
224	2.98574	X/LB	X/TB	T	338	2.98666	X/LB	X/TB	T
					339	2.98822	X	X/TB	X/T
226	2.98767	LB	X/TB	X/T					
225	2.98722	X/LB	X/TB	X/T	340	2.98993	X/LB	X/TB	X/T
227	2.98824	X/LB	X/TB	X/T	341	2.99001	X/LB	X/TB	X/T
228	2.98985	X/LB	X	X/T	342	2.99031	X/LB	X	X/T
229	2.99002	X/LB	X	X	343	2.99035	X/LB	X	X
					344	2.99036	X	X/TB	X
					345	2.99037	X	X	X/T
					346	2.99042	X/LB	X	X/T
					347	2.99042	X	X/TB	X
230	2.99009	X/LB	X/TB	X/T	348	2.99043	X/LB	X/TB	X/T
					349	2.99043	X/LB	X/TB	X/T
					350	2.99043	X/LB	X	X/T
					351	2.99048	X/LB	X/TB	X/T
					352	2.99056	X	X/TB	X/T
					353	2.99058	X/LB	X	X
					354	2.99066	X/LB	X	X/T
					355	2.99066	X/LB	X/TB	X/T
					356	2.99115	X/LB	X	X
					357	2.99129	X/LB	X	X/T
					358	2.99141	X/LB	X/TB	X/T
					359	2.99189	X/LB	X/TB	X
231	2.99015	X	X/TB	T	360	2.99202	X/LB	X	T
232	2.99018	X/LB	X/TB	X/T	361	2.99348	X/LB	X/TB	X/T
219	2.83602	LB+	TB	T	362	2.99471	LB+	TB	T
233	2.99022	X	X	X/T	363	2.99777	X/LB	X	X/T
234	2.99029	X	X/TB	X					
235	2.9904	X	X/TB	X					
236	2.99045	X	X	X					
237	2.99208	X/LB	X/TB	X/T	364	2.99964	X/LB	X	X/T
241	3.00744	LB	X/TB	X/T	365	3.0045	LB	X/TB	X/T
239	2.99984	X/LB	TB	T	366	3.00479	X/LB	X/TB	T
242	3.00934	LB	X	X/T	367	3.00642	LB	X	T
243	3.01098	LB	X/TB	X/T	368	3.00926	LB	X/TB	T
					369	3.06744	LB+	X/TB	T
					370	3.07231	LB+	TB	T
238	2.99859	LB	TB	T	371	3.11405	LB	TB	T
240	3.0046	LB	TB	X					
244	3.02001	X/LB	X/TB	X/T					
245	3.31602	LB+	TB	T					

Table 6.8 (cont'd) - Frequencies and mode shapes of Model 6 and Model 7.

3 simplified towers with 4 cable spans (Model 6)					5 simplified towers with 6 cable spans (Model 7)				
246	3.31947	LB+	X/TB	T					
247	3.45039	LB+	TB	T+	372	3.42938	LB+	TB	T+
					373	3.52462	LB	X/TB	X/T
					374	3.58762	LB	TB	T+
					375	3.58975	LB+	TB	T+
					376	3.61996	LB	TB+	T+
249	3.90759	X/LB	TB+	T+	377	3.65214	LB+	TB+	T+
248	3.88121	LB	TB	T+	378	3.864	LB	TB+	T+
250	4.0574	X/LB	X/TB	T+					
251	4.1187	LB	TB+	T+					
252	4.45369	X/LB	TB+	T+					
253	4.2482	X/LB	TB+	T+	379	4.27499	X/LB	TB+	T+
					380	4.30225	LB	TB+	T+
255	4.54471	X/LB	TB+	T+	381	4.30959	LB	TB+	T+
					382	4.33252	X/LB	TB	T
254	4.53041	X/LB	TB	T	383	4.55354	X/LB	TB	T
256	4.57044	X/LB	TB	T+	384	4.55648	X/LB	TB	T+
257	4.58462	X/LB	TB	T+	385	4.58788	LB	X/TB	T+
258	4.59225	X/LB	TB	T+					
					386	4.61386	X/LB	X/TB	T
					387	4.61741	LB	X/TB	T
261	4.61633	X	TB	T	388	4.61769	X/LB	TB	X/T
259	4.60443	X/LB	TB	T	389	4.61797	LB	TB	T
260	4.6104	X	TB	T	390	4.6186	X	TB	T
					391	4.62303	X/LB	X/TB	X/T
263	4.61996	X/LB	X/TB	T	392	4.62348	X/LB	X/TB	T
					393	4.62511	X	X/TB	T
264	4.62414	X/LB	X/TB	T+					
262	4.61749	X/LB	TB	T	394	4.62559	X/LB	TB	X/T
265	4.62633	X	X/TB	X/T	395	4.62665	X/LB	X/TB	X/T
266	4.6267	X/LB	X/TB	X	396	4.62684	X	X/TB	X
267	4.62715	X/LB	X/TB	X/T	397	4.62691	X/LB	X/TB	T
268	4.62781	X/LB	X	T	398	4.62692	X	X/TB	T
					399	4.6272	X	X/TB	X/T
					400	4.62739	X	X	X/T
					401	4.62767	X	X/TB	X/T
					402	4.62776	X/LB	X/TB	T
269	4.62802	X/LB	X/TB	X	403	4.62786	X/LB	X/TB	X/T
					404	4.62794	X	X/TB	X/T
					405	4.62797	X	X	T
					406	4.62814	X	X/TB	X/T
					407	4.62823	X	X/TB	X/T
					408	4.62825	X/LB	X/TB	X/T
270	4.62833	X/LB	X/TB	X/T	409	4.62825	X/LB	X/TB	X/T
271	4.62853	X/LB	X/TB	X/T	410	4.62835	X/LB	X/TB	X/T
274	4.62906	X/LB	X/TB	T	411	4.62836	X	X/TB	T
272	4.62855	X/LB	TB	T	412	4.62858	X/LB	TB	T
273	4.62861	X/LB	X/TB	T	413	4.62871	X/LB	X/TB	T
275	4.6297	X	X/TB	T	414	4.62875	X	X/TB	T
					415	4.62879	X/LB	X	X/T
278	4.63113	X/LB	X	T	416	4.62909	X/LB	X	T
					417	4.62927	X/LB	X/TB	T
276	4.63016	X/LB	TB	X/T	418	4.62931	X/LB	TB	T
277	4.63093	X/LB	TB	X/T	419	4.62934	X/LB	TB	T
					420	4.62956	X/LB	X/TB	X
279	4.82113	X/LB	X/TB	T	421	4.62957	X/LB	X/TB	T
					422	4.62984	X/LB	X/TB	X/T
					423	4.63552	X/LB	TB	T
					424	4.75234	LB	TB	T
					425	4.77214	LB	TB	X/T
280	4.89927	X/LB	TB	T+	426	4.91953	LB	TB+	T+
281	5.09098	LB+	TB+	T+	427	4.96511	LB+	TB+	T+

6.2.1.6. MODEL 6 AND MODEL 8

The use of detailed tower modeling is investigated in three spans transmission system as shown in Figure 6.22(b). The objective is to study the difference between using a detailed tower modeling and simplified tower modeling. The processing time for the free vibration analysis of Model 8 is 12 hours and 45 minutes while that of Model 6 is 2 hours and 37 minutes. Table 6.9 shows the natural frequencies and the mode shapes of the two models. It is evident that both of the systems have almost the same natural frequencies and mode shapes (1.05% error for the first 200 modes).

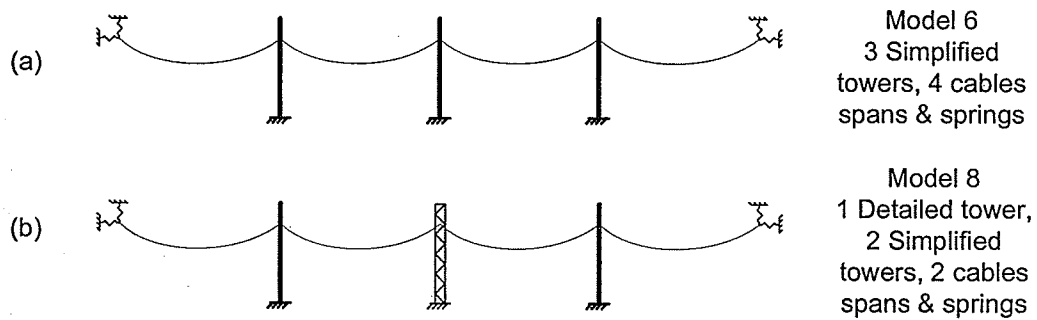


Figure 6.22 - (a) Model 6 and (b) Model 8.

Table 6.9 - Frequencies and mode shapes of Model 6 and Model 8.

3 simplified tower with 4 cable spans (Model 6)					1 detailed and 2 simplified towers with 4 cable spans (Model 8)				
MODE	FREQ(HZ)	LATERAL	TRANSVERSE	TORSION	MODE	FREQ(HZ)	LATERAL	TRANSVERSE	TORSION
1	0.11311	X/LB	X	X	1	0.11311	X/LB	X	X
5	0.11981	X/LB	X	X	5	0.11981	X/LB	X	X
9	0.13024	X	X	T	9	0.13024	X	X	T
10	0.13063	X	X/TB	X	10	0.13064	X	X/TB	X
11	0.13232	X/LB	X	X	11	0.13234	X/LB	X	X
13	0.14095	X	X	T	13	0.14096	X	X	T
14	0.14231	X	X/TB	X	14	0.14232	X	X/TB	X
19	0.20561	LB	X	X	19	0.20562	LB	X	X
21	0.22879	LB	X	X	21	0.22879	LB	X	X
25	0.24078	LB	X	X	25	0.24078	LB	X	X
29	0.24981	X	X	X/T	29	0.24982	X	X	X/T
30	0.24989	X	X/TB	X	30	0.24989	X	X/TB	X
31	0.25122	X/LB	X	X	31	0.25121	X/LB	X	X
35	0.2523	X/LB	X	X	35	0.2523	X/LB	X	X
41	0.30846	X/LB	X	X	41	0.30846	X/LB	X	X
45	0.32919	X/LB	X	X	45	0.32919	X/LB	X	X
49	0.33759	X	TB	X	49	0.33821	X	X/TB	X
51	0.34935	X	TB	T	51	0.34956	X	TB	T
52	0.35054	X	X/TB	X	52	0.35054	X	X/TB	X/T
53	0.35322	X	X/TB	X	53	0.35323	X	X/TB	X
55	0.3617	LB	X	X	55	0.3617	LB	X	X
59	0.39159	LB	X	X	59	0.39156	LB	X	X
61	0.39255	X	X	X/T	61	0.39256	X	X	X/T
63	0.39325	X/LB	X	X	63	0.39325	X/LB	X	X
65	0.39375	X	X	X/T	65	0.39376	X	X	X/T
67	0.40888	X/LB	X	X	67	0.40888	X/LB	X	X
71	0.47727	X/LB	X	X	71	0.47727	X/LB	X	X
73	0.47738	X/LB	X	X	73	0.47738	X/LB	X	X
75	0.4967	X	X/TB	X	75	0.49683	X	X/TB	X
77	0.4993	LB	X	X	77	0.4993	LB	X	X
79	0.50086	X	X/TB	X	79	0.50091	X	X/TB	X
83	0.54256	LB	X	X	83	0.54254	LB	X	X
87	0.54382	X/LB	X	X	87	0.54381	X/LB	X	X
89	0.54482	X/LB	X	X	89	0.54482	X/LB	X	X
91	0.54597	X	X	X/T	91	0.54597	X	X	X/T
92	0.546	X	X/TB	X	92	0.546	X	X/TB	X
95	0.65514	LB	X	X	95	0.65513	LB	X	X
101	0.66299	X/LB	X	X	101	0.66299	X/LB	X	X
103	0.66315	X/LB	X	X	103	0.66315	X/LB	X	X
107	0.70659	LB	X	X	107	0.70659	LB	X	X
109	0.70964	LB	X	X	109	0.70962	LB	X	X
111	0.71111	X	X	X/T	111	0.71111	X	X	X/T
113	0.71208	LB	X	X	113	0.71207	LB	X	X
115	0.71275	X	X	X/T	115	0.71275	X	X	X/T
119	0.82681	LB	X	X	119	0.8268	LB	X	X
123	0.8669	X/LB	X	X	123	0.8669	X/LB	X	X
125	0.86714	X/LB	X	X	125	0.86713	X/LB	X	X
127	0.86903	X	X/TB	X	127	0.86904	X	X/TB	X
129	0.86932	X	X/TB	X	129	0.86932	X	X/TB	X
131	0.87812	LB	X	X	131	0.87812	LB	X	X
133	0.88344	LB	X	X	133	0.8834	LB	X	X
137	0.88467	X/LB	X	X	137	0.88466	X/LB	X	X
139	0.88588	X	X	X/T	139	0.88588	X	X	X/T
143	0.99679	LB	X	X	143	0.99678	LB	X	X
147	1.02802	X/LB	X	X	147	1.02802	X/LB	X	X
149	1.03054	X/LB	X	X	149	1.03053	X/LB	X	X
153	1.03139	X/LB	X	X	153	1.03138	X/LB	X	X
163	1.07747	X/LB	X	X	163	1.07746	X/LB	X	X
164	1.07757	X/LB	X	X	164	1.07754	X/LB	X	X
165	1.07761	X/LB	X	X	165	1.07761	X	X	X
167	1.08311	LB	X	X	167	1.08253	LB	X	X
168	1.11625	X/LB	X	X	168	1.11625	X/LB	X	X
169	1.23571	LB	X/TB	X	169	1.23573	LB	X	X
170	1.23931	X/LB	X/TB	X	170	1.23946	X	X	X/T
171	1.24343	LB	X	X	171	1.24354	LB	X	X
183	1.45967	LB	X	X/T	183	1.44538	LB	X/TB	X
184	1.4464	X/LB	TB	X	184	1.4464	X/LB	TB	X

Table 6.9 (cont'd) - Frequencies and mode shapes of Model 6 and Model 8.

3 simplified tower with 4 cable spans (Model 6)					1 detailed and 2 simplified towers with 4 cable spans (Model 8)				
MODE	FREQ[HZ]	LATERAL	TRANSVERSE	TORSION	MODE	FREQ[HZ]	LATERAL	TRANSVERSE	TORSION
186	1.46191	X	X/TB	T	185	1.44797	X	X	T
195	1.47394	X/LB	TB	X/T	187	1.45863	X	TB	X
188	1.46374	X	X/TB	X/T	188	1.46006	X/LB	X	X/T
184	1.45979	LB	X/TB	X	189	1.46118	LB	X	X/T
189	1.46385	X	X/TB	X/T	190	1.46149	X/LB	X	T
190	1.46418	X	X	X/T	191	1.46196	X/LB	X	T
191	1.46471	X	X	X/T					
185	1.46053	X	X/TB	X/T	199	1.47506	X	X/TB	X
187	1.46282	X	X	X/T	202	1.47618	X/LB	X/TB	X
197	1.47506	X/LB	X/TB	X/T					
198	1.47577	LB	X	X					
200	1.47584	LB	X	X					
201	1.47754	X	X/TB	T					
202	1.47772	X	X	X/T					
207	1.90072	X/LB	TB	T+	207	1.90821	X/LB	TB	T+
208	1.96226	X/LB	TB	T	208	1.96215	X	TB	X/T
209	2.09231	LB	X/TB	X/T	209	2.09212	LB+	X	X
211	2.12153	X/LB	TB	T	211	2.12096	X	X/TB	T
212	2.14258	X/LB	TB	X/T	212	2.14253	X	TB	X
213	2.42159	LB+	TB	T+	213	2.31055	LB	TB+	X
214	2.43181	LB+	TB	T	214	2.39577	LB+	X/TB	X/T
215	2.44534	LB+	TB+	T+	215	2.47318	LB	TB	T
216	2.45347	LB+	TB+	T	216	2.49592	LB	TB	T
217	2.47328	LB	TB+	T+					
218	2.74288	X/LB	TB	X/T	217	2.72093	X/LB	TB	X/T
219	2.83602	LB+	TB	T	218	2.81769	LB+	X/TB	T
223	2.98547	X	X/TB	T	219	2.90248	X/LB	X	T
221	2.98303	X/LB	X/TB	T	220	2.91087	X/LB	X/TB	T
222	2.98431	X	X/TB	T	221	2.9215	X/LB	X/TB	T
220	2.96513	LB	X/TB	X/T	222	2.92781	LB	X	X/T
240	3.0046	LB	TB	X	223	2.94323	LB	TB	X/T
225	2.98722	X/LB	X/TB	X/T	224	2.94924	X	X/TB	X
224	2.98574	X/LB	X/TB	T	225	2.95624	X/LB	X/TB	T
231	2.99015	X	X/TB	T	226	2.95967	X	X/TB	T
234	2.99029	X	X/TB	X	227	2.96046	X	X/TB	X
238	2.99859	LB	TB	T	228	2.97361	LB	TB	X/T
226	2.98767	LB	X/TB	X/T	229	2.97764	LB	X/TB	X
227	2.98824	X/LB	X/TB	X/T	230	2.98196	X/LB	X/TB	X
228	2.98985	X/LB	X	X/T	231	2.98198	X/LB	X/TB	X
230	2.99009	X/LB	X/TB	X/T	232	2.9832	X/LB	X/TB	X
229	2.99002	X/LB	X	X	233	2.98738	X/LB	X	X
232	2.99018	X/LB	X/TB	X/T	234	2.98898	X/LB	X	X/T
237	2.99208	X/LB	X/TB	X/T	235	2.98961	X/LB	X	X
233	2.99022	X	X	X/T	237	2.99019	X/LB	X	X/T
244	3.02001	X/LB	X/TB	X/T	240	2.9903	X/LB	X	X
					241	2.99144	X/LB	X/TB	X
					242	2.99244	X/LB	X/TB	X/T
239	2.99984	X/LB	TB	T					
					243	3.0049	X/LB	X/TB	X/T
235	2.9904	X	X/TB	X	244	3.01127	X	X/TB	X
241	3.00744	LB	X/TB	X/T					
242	3.00934	LB	X	X/T					
243	3.01098	LB	X/TB	X/T					
245	3.31602	LB+	TB	T	247	3.39438	LB+	TB	T
246	3.31947	LB+	X/TB	T	245	3.32917	LB+	TB	T+
247	3.45039	LB+	TB	T+	246	3.3424	LB	TB	T+
248	3.86121	LB	TB	T+	248	3.68182	X/LB	TB	T+
249	3.90759	X/LB	TB+	T+	249	3.85162	X	TB+	T+
250	4.0574	X/LB	X/TB	T+					
					250	4.08873	LB	TB+	T
251	4.1187	LB	TB+	T+	251	4.11836	LB	TB+	T+
252	4.15369	X/LB	TB+	T+	252	4.16673	LB	TB+	T+
253	4.2482	X/LB	TB+	T+	253	4.38103	X/LB	TB+	T
254	4.53041	X/LB	TB	T	254	4.51686	X/LB	TB	T
255	4.54471	X/LB	TB+	T+					
256	4.57044	X/LB	TB	T+					
					255	4.57472	X/LB	TB	X/T
					256	4.58077	X	X	X/T
257	4.58462	X/LB	TB	T+	257	4.5818	X/LB	TB	T

Table 6.9 (cont'd) - Frequencies and mode shapes of Model 6 and Model 8.

3 simplified tower with 4 cable spans (Model 6)					1 detailed and 2 simplified towers with 4 cable spans (Model 8)				
MODE	FREQ(HZ)	LATERAL	TRANSVERSE	TORSION	MODE	FREQ(HZ)	LATERAL	TRANSVERSE	TORSION
258	4.59225	X/LB	TB	T+	258	4.58255	X/LB	X/TB	X
259	4.60443	X/LB	TB	T	259	4.58344	X/LB	TB	T
263	4.61996	X/LB	X/TB	T	260	4.58381	X/LB	X/TB	T
260	4.6104	X	TB	T	261	4.58513	X/LB	X/TB	T
264	4.62414	X/LB	X/TB	T+	262	4.59667	X/LB	TB	T
261	4.61633	X	TB	T	263	4.5993	X/LB	TB	T
262	4.61749	X/LB	TB	T	264	4.61731	X/LB	TB	T
268	4.62781	X/LB	X	T	265	4.62464	X	X/TB	T
265	4.62633	X	X/TB	X/T	266	4.62535	X	X/TB	X/T
266	4.6267	X/LB	X/TB	X	267	4.627	X/LB	X/TB	X/T
267	4.62715	X/LB	X/TB	X/T	268	4.62739	X	X/TB	X
269	4.62802	X/LB	X/TB	X	269	4.62754	X/LB	X/TB	X/T
270	4.62833	X/LB	X/TB	X/T	270	4.62785	X	X/TB	X
277	4.63093	X/LB	TB	X/T	271	4.62796	X	X/TB	X
273	4.62861	X/LB	X/TB	T	272	4.62816	X/LB	TB	X/T
276	4.63016	X/LB	TB	X/T	273	4.62838	X	X/TB	X/T
271	4.62853	X/LB	X/TB	X/T	274	4.62854	X/LB	X/TB	X/T
274	4.62906	X/LB	X/TB	T	275	4.62861	X	X/TB	X/T
275	4.6297	X	X/TB	T	276	4.6291	X/LB	X/TB	X/T
278	4.63113	X/LB	X	T	277	4.62955	X	X/TB	T
272	4.62855	X/LB	TB	T	278	4.65223	X/LB	TB	T
279	4.82113	X/LB	X/TB	T	279	4.90296	X/LB	TB	X/T
280	4.89927	X/LB	TB	T+	280	5.05534	LB	TB	X/T
281	5.09098	LB+	TB+	T+	281	5.07832	LB+	TB	T

6.2.2. DYNAMIC ANALYSIS

It can be seen from the previous sections that the addition of number of towers and cables spans introduces new frequencies and mode shapes to the system. The scope of this research is focused on if there is a change in the response caused by the use of different number cable spans and boundary conditions. Due to computational restraint the analysis will be limited only on Models 2, 3, 4, 5 and 6. Only transverse wind load is considered in this study.

The dynamic analysis is performed with a time increment equal to 0.001 seconds from 0 seconds to 600 seconds (10 minutes). The initial 2 minutes will not be analyzed to avoid any kind of unwanted vibration due to fast application of

the load. The processing time for Model 2 is 11 hours 57 minutes, Model 3 and Model 4 - 25 hours 38 minutes, and Model 5 - 4 days 21 hours and 21 minutes. For Model 6, the analysis was carried out on the civil engineering department server – Minerva, which required approximately 5 days to run.

6.2.2.1. COMPARISON OF MODEL 2 AND MODEL 4

Model 2 contains only a single tower while Model 4 includes cables in the system (Figure 6.23). In order to compare the results, the same loading is applied only on the tower. Figures 6.24 and 6.25 show the displacement-time histories of node 47 (the top of the tower) for Models 2 and 4, respectively. It can be seen that the maximum displacements at the top of the tower for Models 2 and 4 are 0.113 and 0.156 meters, respectively. The difference is approximately 28%. Here, even the loads on the cables were not considered, Model 4 provides higher displacement.

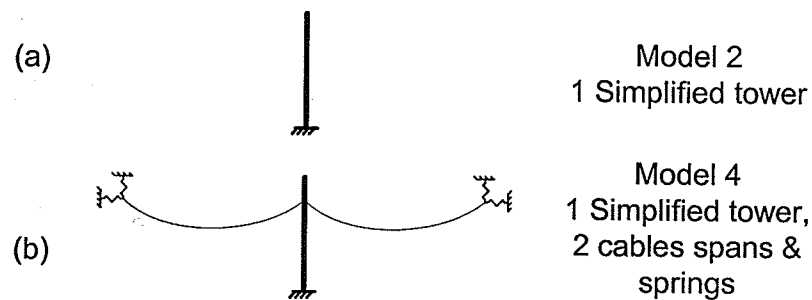


Figure 6.23 - (a) Model 2 and (b) Model 4.

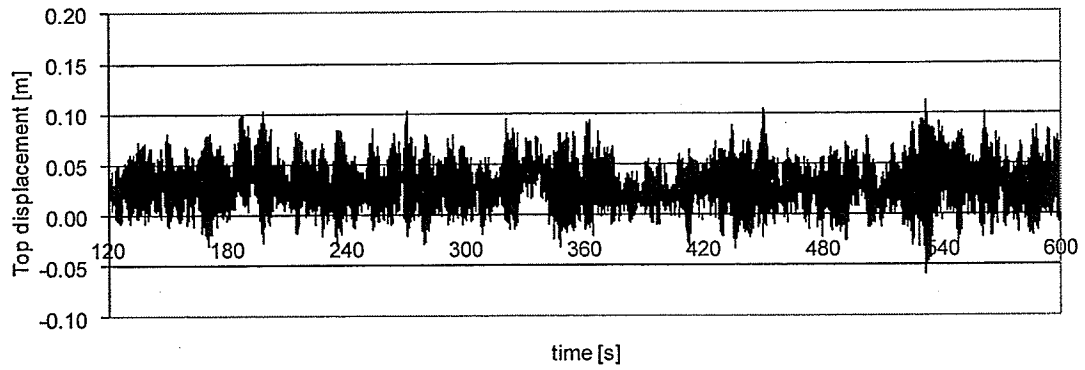


Figure 6.24 - Displacement-time history at the top of the tower for Model 2.

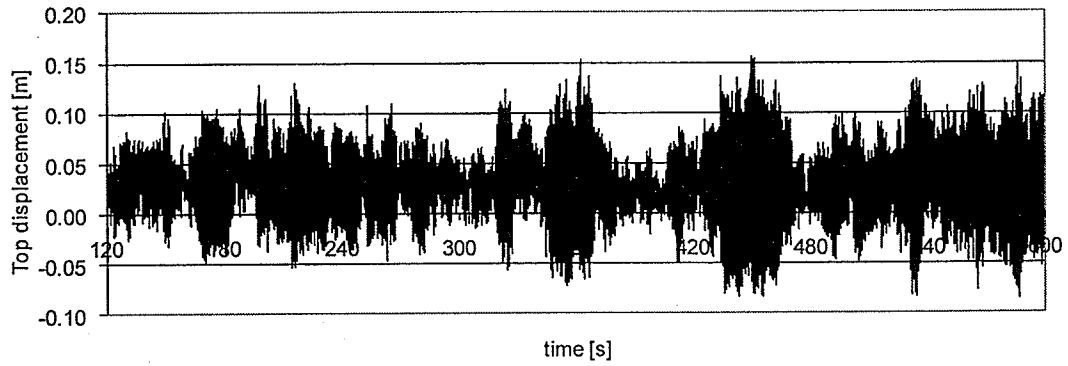


Figure 6.25 - Displacement-time history at the top of the tower for Model 4.

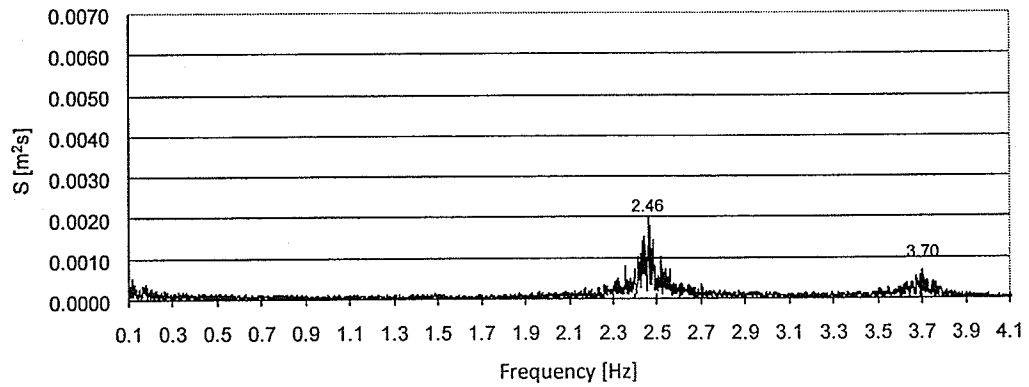


Figure 6.26 - FFT of the displacement at the top of the tower for Model 2.

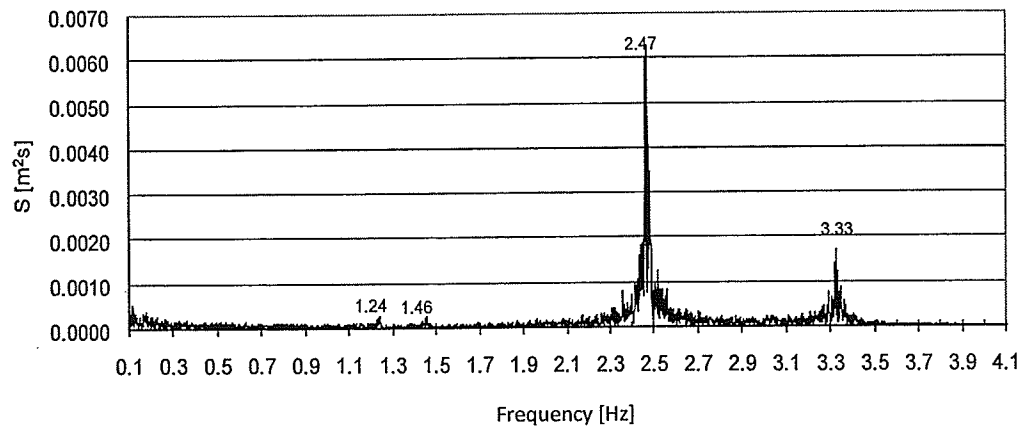


Figure 6.27 - FFT of the displacement at the top of the tower for Model 4.

The Fast Fourier Transforms (FFT) of the responses are shown in Figures 6.26 and 6.27, for Models 2 and 4, respectively. It can be seen that lower frequencies that appear in Model 4 (Table 6.5) do not contribute much to the response of the tower. As stated, the loadings are applied only on the tower.

6.2.2.2. COMPARISON OF MODELS 3, 4, 5 AND 6

For convenience, Figure 6.28 shows models 3, 4, 5 and 6. Here the wind load is applied on the central two cables spans and on the central tower. Figures 6.29 to 6.32 present the displacement at the top of the central tower of the four models. It can be seen that the maximum displacements of all the models are not much different (0.424, 0.419, 0.421 and 0.429 meters for models 3, 4, 5 and 6, respectively). Figure 6.33 compares the displacements at the top of the central tower of models 4 and 5. The figure shows that the results from the two models are almost identical (maximum difference is 0.5%). This means that the end springs can be used to represent end towers in this case.

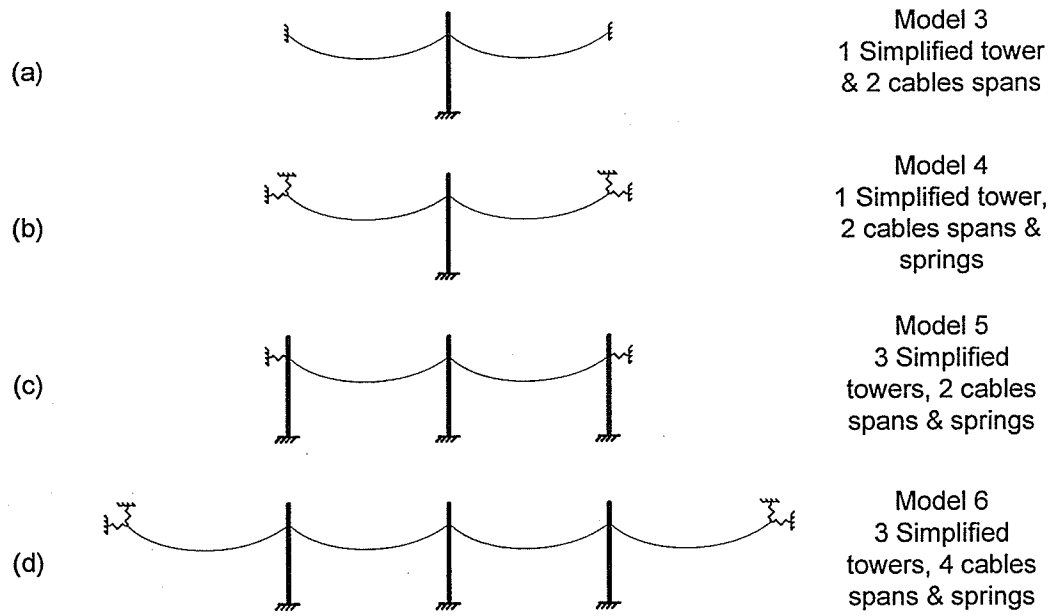


Figure 6.28 - Computational Models.

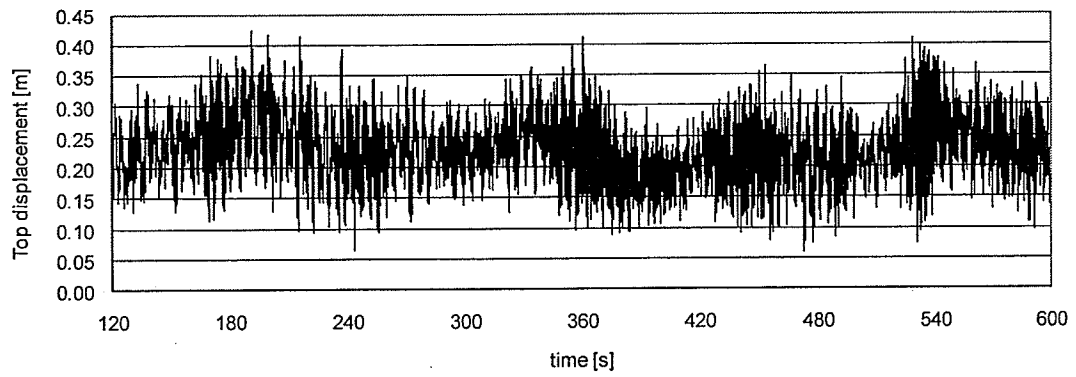


Figure 6.29 - Displacement at the top of the tower for Model 3 (node 47).

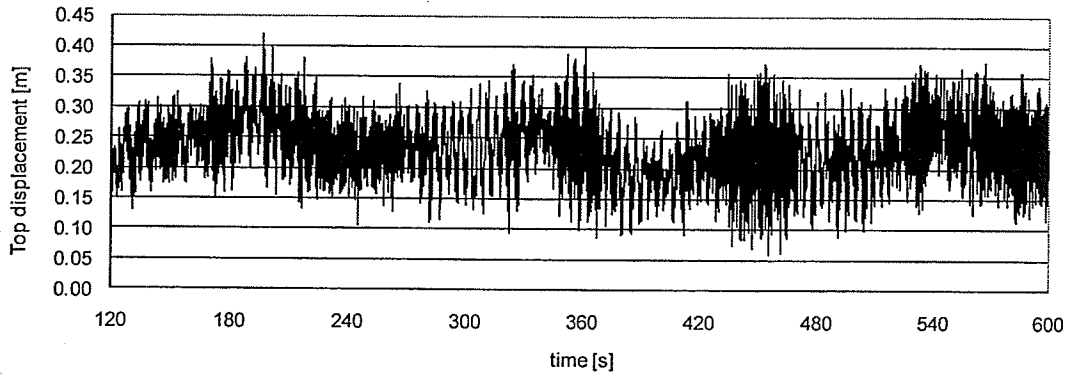


Figure 6.30 - Displacement at the top of the tower for Model 4 (node 47).

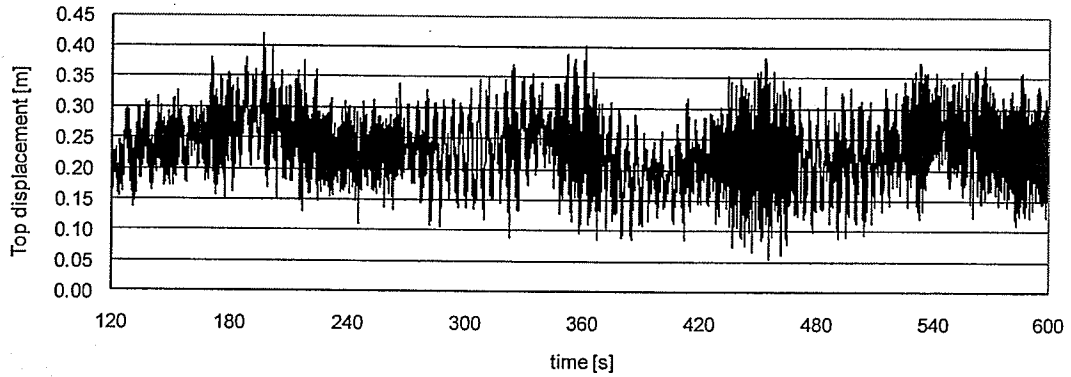


Figure 6.31 - Displacement at the top of the tower for Model 5 (node 47).

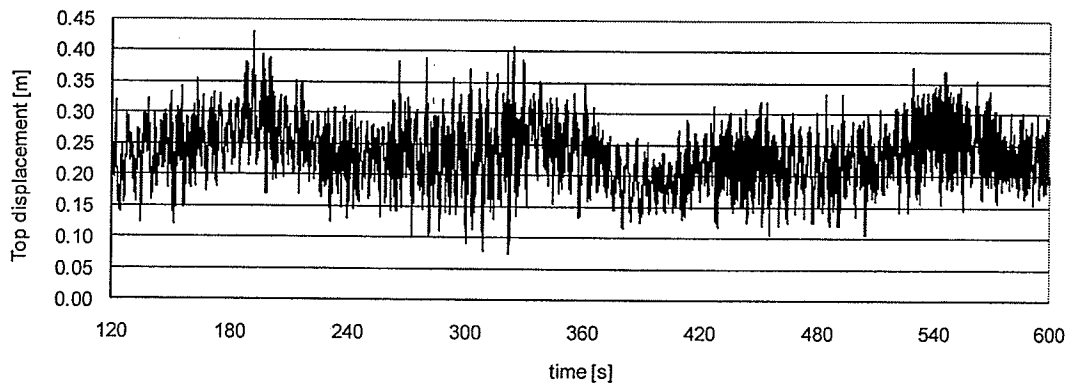


Figure 6.32 - Displacement at the top of the tower for Model 6 (node 47).

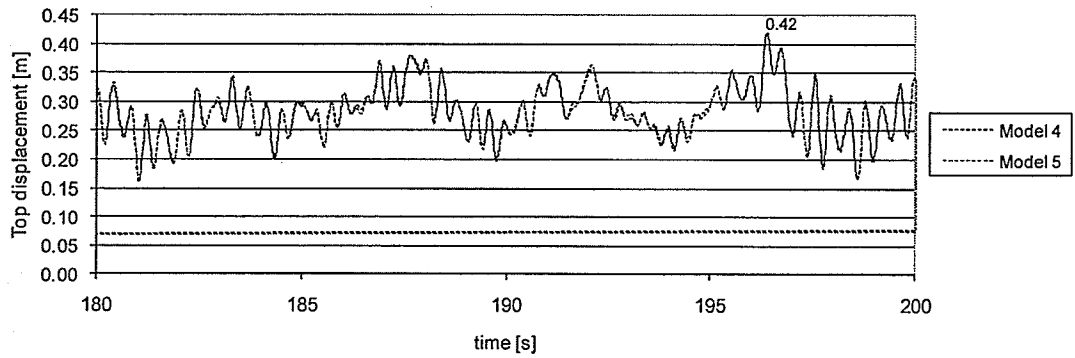


Figure 6.33 - Displacement at the top of the tower for Models 4 and 5 (node 47).

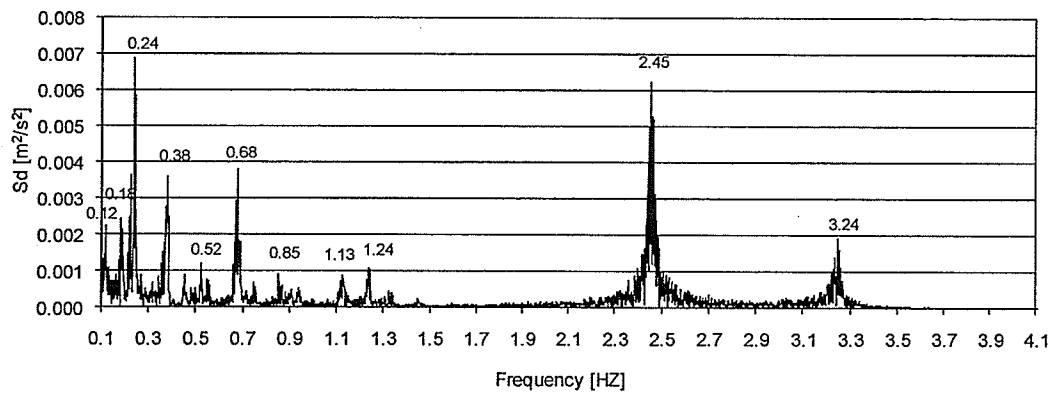


Figure 6.34 - FFT of the tower for Model 3.

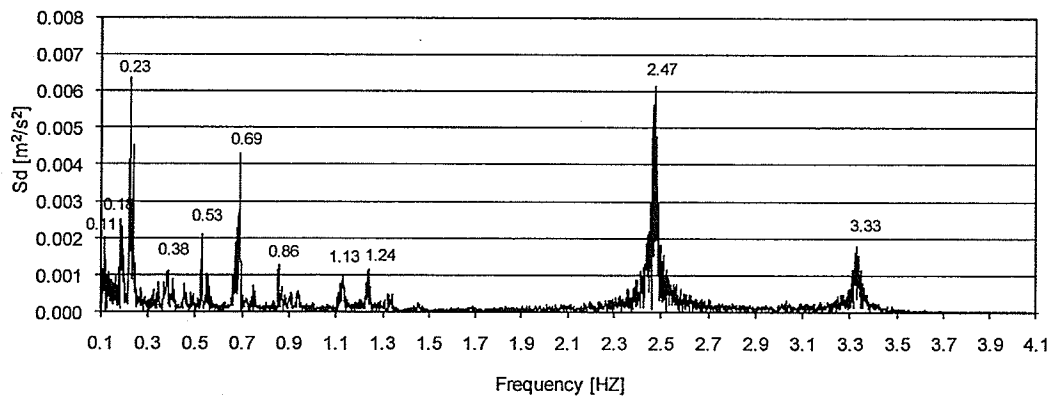


Figure 6.35 - FFT of the tower for Model 4.

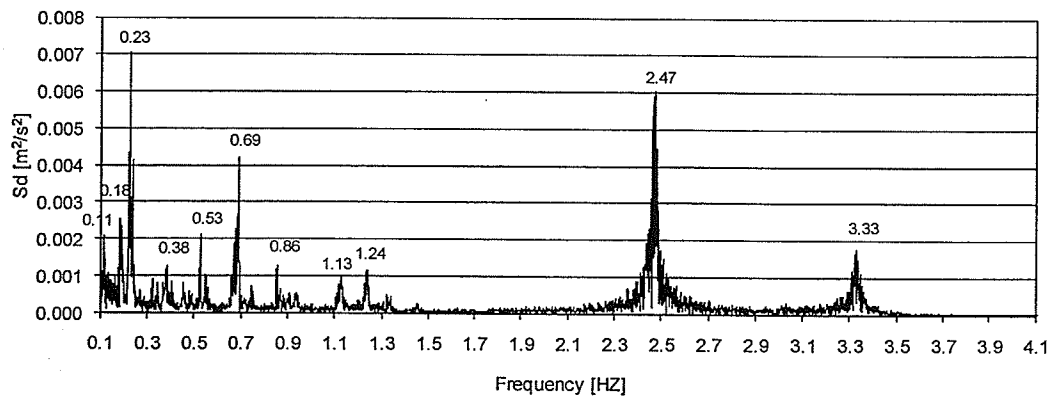


Figure 6.36 - FFT of the tower for Model 5.

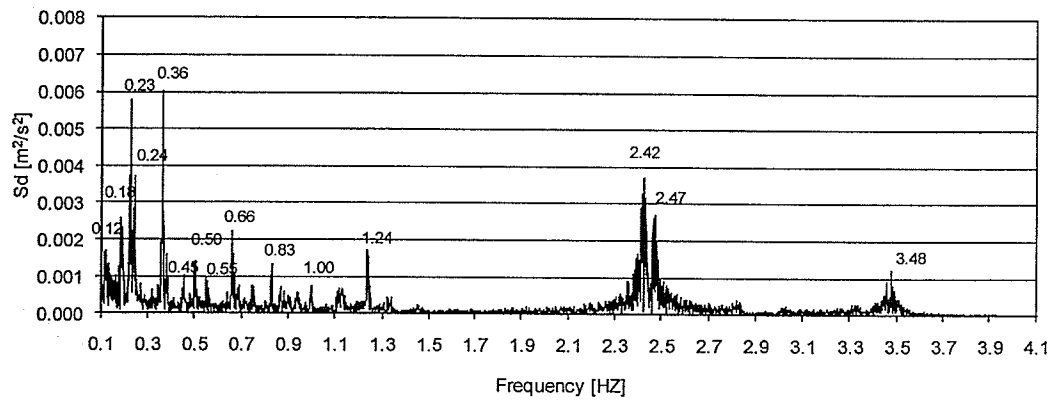


Figure 6.37 - FFT of the tower for Model 6.

The FFTs of all the responses are presented in Figures 6.34 to 6.37. The FFTs confirm the frequencies of the tower calculated in the free vibration reported previously (Section 6.2.1). Similar main frequencies are observed in all the models.

7. SUMMARY, CONCLUSIONS AND RECOMMENDATIONS

7.1. CONCLUSIONS

A finite element program called SADAP was developed for the analysis of a transmission tower line system. The program is capable of carrying out both geometric non-linear static and dynamic analyses and it was validated using the available theoretical and numerical results. This program contains linear and non-linear commonly used and simplified beam-column elements, cable element, truss element and spring element. The simplified beam-column elements were specially formulated here to represent a tower mast, both straight and tapered. These simplified elements include a torsional stiffness provided by diagonal bracings.

In this study, the developed program was used to:

- a) Evaluate the differences of modeling full detailed towers and the proposed simplified elements in the analyses;
- b) Investigate the importance of the boundary conditions on both free vibration and wind induced dynamic responses of the transmission system; and,
- c) Examine the importance of the number of cable spans on the dynamic behaviour of a transmission line system;

The study showed that:

- a) The proposed simplified element can be effectively used to model a tower in linear static, non-linear static and dynamic analyses of a transmission line system;
- b) The results from using the simplified model in the non-linear static analysis of an isolated tower are within 7% of the results obtained using a detailed model;
- c) The first forty natural frequencies of an isolated tower modeling using the simplified model are within 3% of those of a tower modeling in detail;
- d) The increase in the number of cable spans introduces new mode shapes, which will have dynamic effects on the response of the tower system depending on the nature of the loading. For the wind loading used in this study, i.e. wind perpendicular to the line, these modes do not appear to have any effect on the dynamic response of the system;
- e) In conducting the dynamic analysis of the tower, the conductor spans must be incorporated in the model as it affects the dynamic properties of the system;
- f) End spring elements can be used to replace the end towers for a linear dynamic analysis with the wind load in this study; and,
- g) For the wind load considered, two cable spans are sufficient to represent the response of the transmission line system.

7.2. RECOMMENDATION FOR FUTURE WORK

The author recommends the following for future research:

- a) Evaluate if intermediate towers can also be replaced by spring elements;
- b) Perform a non-linear interactive dynamic analysis considering the orthogonal wind load. Nonetheless, in such sophisticated analysis, a high efficient cluster would be needed;
- c) Investigate the number of cable spans considering both a linear and a non-linear dynamic analysis applying wind loadings in different directions;
- d) Consider the buckling of one tower leg in the simplified element for post-buckling analysis, such as in the cascade failure analysis; and,
- e) Investigate the possibility of reducing the vibration of the transmission tower line by adding a control mass-spring-damper (as in example 12) or a pendulum system to the tower.

REFERENCES

- Albermani F., Kitipornchai S., and Chan R.W.K. 2008. "Failure analysis of transmission towers". *Engineering Failure Analysis*. 1-7.
- American Society of Civil Engineering. 1984. "Guidelines for Transmission Line Structural Loading". New York.
- ANSYS. 2004. "Theory Reference". Release 9.0, Ansys Inc.
- Bathe K.J. 1996. "Finite Element Procedures". New Jersey: Prentice Hall.
- Battista R.C. 2007. Class notes "Reduction and Control of Vibration in Structures" (in Portuguese). Federal University of the State of Rio de Janeiro.
- Battista R.C. 2007. Class notes "Structural Analysis I" (in Portuguese). Federal University of the State of Rio de Janeiro.
- Battista R.C. 2007. Class notes "Structural Dynamics" (in Portuguese). Federal University of the State of Rio de Janeiro.
- Battista R.C., Rodrigues R.S., and Pfeil M.S. 2003. "Dynamic behavior and stability of transmission line towers under wind forces". *Wind Engineering*. 1051-1067.
- Bissiri A. and Landau M. 1947. "Broken Conductor Effect on Sags in Suspension Spans". *AIEE*. 66: 1181-1188.
- Blessmann J. 1995. "The wind in the Structural Engineering" (in Portuguese). Editora da Universidade/UFRGS.

- Blessmann J. 2005. "Introduction of the studies of dynamic wind actions" (in Portuguese). Editora da Universidade/UFRGS.
- Chen W.F, and Lui E.M. 1991. "Stability Design of Steel Frames". Library of Congress Cataloging-in-Publication Data.
- Chopra A.K. 1995. "Dynamics of Structures – Theory and Application to Earthquake Engineering". Prentice-Hall Inc.
- Clough R.W. and Penzien J. 1993. "Dynamics of Structures". McGraw-Hill Inc.
- Cohen E and Perrin H. 1957. "Design of Multi-level Guyed Towers: Wind Load". Journal of the Structural Division, ASCE. 83: 1-29.
- Cohen E and Perrin H. 1957. "Design of Multi-level Guyed Towers: Structural Analysis". Journal of the Structural Division, ASCE. 83: 1-29.
- Craig R.R. 1981. "Structural Dynamics". New York: John J. S.
- CSA-S37-01. 2001. "Antennas, Towers and Antenna-Supporting Structures", Canadian Standard Association.
- Desai Y.M., Yu P., Popplewell N., and Shah A.H. 1994. "Finite Element Modeling of Transmission Line Galloping". Computer & Structures. 57(3): 407-420.
- Disney P., and Parker G. 2005. "The Appraisal of Manitoba Hydro A-402 Guyed Suspension Towers Under High Intensity Winds". Manitoba Hydro technical report, appendix 2A.

- Hajdin N., Michaltsos G.T. and Konstantakopoulos T.G. 2000. "About the equivalent modulus of elasticity of cables of cables-stayed bridges". The scientific journal FACTA UNIVERSITATIS. 569-575.
- Horr A.M., Yibulayin A., and Disney P. 2004. "Nonlinear spectral dynamic analysis of guyed towers. Part II: Manitoba towers case study". Canadian Journal of Civil Engineering. 31: 1061-1076.
- Irvine M. 1992. "Cable Structures". New York: Dover Publication Inc.
- Irvine M. 1974. "Studies in the Static and Dynamics of Simple Cable Systems". Pasadena, California.
- Junior J.K, Miguel L.F.F, Menezes R.C.R., Miguel L.F.F. and Alva G.M.S. 2007. "Analysis of the behavior of towers of a segment of TL subjected to a dynamic load due to cable rupture" (in Portuguese). Mecanica Computacional. XXVI: 247-257.
- Kim S.E., Ngo-Huu C., and Lee D.H. 2005. "Second-order inelastic dynamic analysis of 3-D steel frames". Solids and Structures. 43: 1693-1709.
- Kim S.E., Lee J. and Park J.S. 2001. "3-D second-order plastic-hinge analysis accounting for lateral torsional buckling". Solids and Structures. 39: 2109-2128.
- Kim S.E., Park M.H. and Choi S.H. 2001. "Direct design of three-dimensional frames using practical advanced analysis". Engineering Structures. 23: 1491-1502.

- Landesmann A. 2007. Class notes "Steel Structures" (in Portuguese). Federal University of the State of Rio de Janeiro.
- Lei Y.H. and Chien Y.L. 2005. "Seismic Analysis of Transmission Towers Considering both Geometric and Material Nonlinearities". *Tamkang Journal of Science and Engineering*. 1(8): 29-42.
- Levy R. and Spillers W.R. 2003. "Analysis of Geometrically Nonlinear Structures". Kluwer Academic Publishers.
- Mathur R.K. 1985. "Structural Dynamic Characteristics of Transmission Systems". Master of Science Thesis – University of Manitoba.
- Mathur R.K., Shah A.H., Trainor P.G.S., and Popplewell N. 1987. "Dynamics of a Guyed Transmission Tower System". *IEEE Transactions of Power Delivery*. PWRD-2(3): 908-916.
- Militano G. 2000. "Computer-Aided Free Vibration Analysis of Guyed Towers". Master of Science thesis, University of Manitoba.
- Mozer J.D., Pohlman J.C., and Fleming J.F. 1977. "Longitudinal Load Analysis of Transmission Line Systems". *IEEE Transactions of Power Delivery*. PWRD-96(5): 1657-1665.
- Ochonski, A. 2008. "Development of Latticed Towers Using Advanced Composite Materials". Doctor of Philosophy thesis, University of Manitoba.

Oliveira M.I.R. 2006. "Structural Analysis of Energy Transmission Towers Subjected to Dynamic Effects Induced by Wind" (in Portuguese). Master of Science thesis, University of the State of Rio de Janeiro.

Oliveira M.I.R, Silva J.G.S., Vellasco P.C.G.S., Andrade S.A.L. and Lima L.R.O. 2007. "Structural Analysis of Guyed Steel Telecommunication Towers for Radio Antennas". Journal of the Brazilian Society of Mechanical Sciences and Engineering. 29(2): 185-195.

Paz M. and Leigh W. 2004. "Structural Dynamics – Theory and Computation". Springer Science+Business Media Inc.

Peyrot A.H., Lee J.W., Jensen G.H. and Osteraas J.D. 1981. "Application of cable elements concept to a transmission line with cross rope suspension structures". IEEE Transactions on Power Apparatus and Systems. PAS-100(7): 3254-3262.

Pinto P.S. 2006. Class notes "Structural Analysis I" (in Portuguese). University of the State of Rio de Janeiro.

Pinto P.S. 2006. Class notes "Structural Analysis II" (in Portuguese). University of the State of Rio de Janeiro.

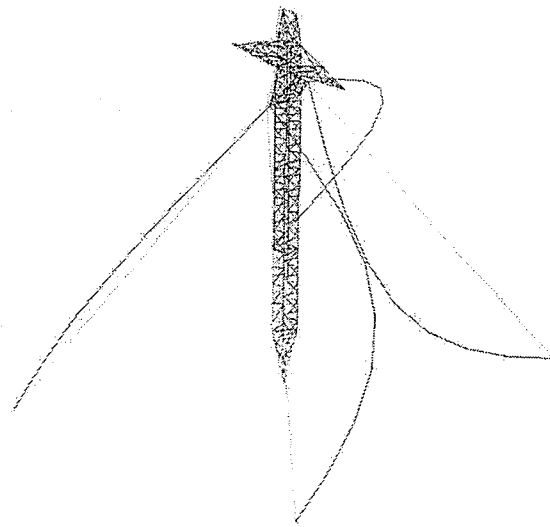
Przemieniecki J.S. 1985. "Theory of Matrix Structural Analysis". New York: Dover Publications Inc.

- Rodrigues R.S. 1999. "Collapse of TEE Towers under Action of Wind" (in Portuguese). Master of Science Thesis – COPPE/Federal University of the State of Rio de Janeiro.
- SAP2000, 2008. "Analysis Verification Examples", Computer and Structures Inc.
- Shehata A.Y., and El Damatty A.A. 2006. "Assessment of the Failure of an Electrical Transmission Line Due to a Downburst Event". *Electrical Transmission Line*. 27-38.
- Shehata A.Y., El Damatty A.A., and Savory E. 2005. "Finite element modeling of transmission line under downburst wind loading". *Finite Element in Analysis and Design*. 42: 71-89.
- Simiu E. 1986. "Wind Effect on Structures". John Wiley & Sons.
- Sussekind J.C. 1982. "Structural Analysis Course – Volume III". Porto Alegre: Globo.
- Tainor P.G.S, Popplewell N., Shah A.H.W and Wong C.K. 1985. "Estimation of Fundamental Dynamic Characteristics of Transmission Towers". *IEEE Transactions on Power Apparatus and Systems*. PAS-104(3): 681-689.
- Timoshenko S., Young D.H. and Weaver W.JR. 1974. "Vibration Problems in Engineering". John J.S.
- Weaver W.JR. and Gere J.M. 1980. "Matrix Analysis of Framed Structures". D. Van Nostrand Company.

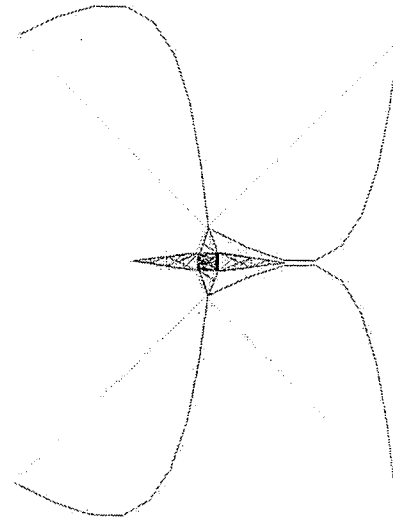
Zhang Qi W., and Rattanawangcharoen N. 2008. "The Analysis of a Transmission Guyed Tower Line System Subjected to Downburst Wind". Manitoba Hydro final report.

APPENDIX - A

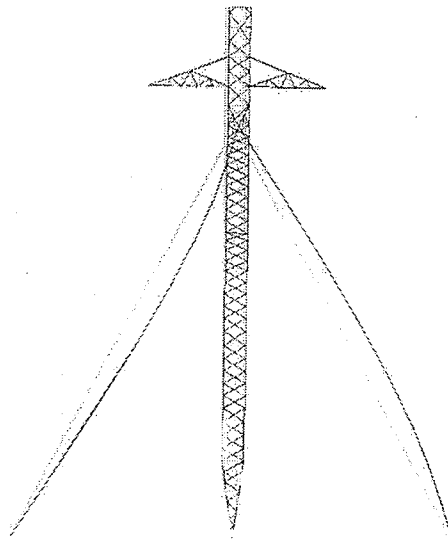
The fundamental model shapes of the detailed (Model 1) and simplified (Model 2) isolated towers (excluding the mode shapes corresponding to only cable movements)



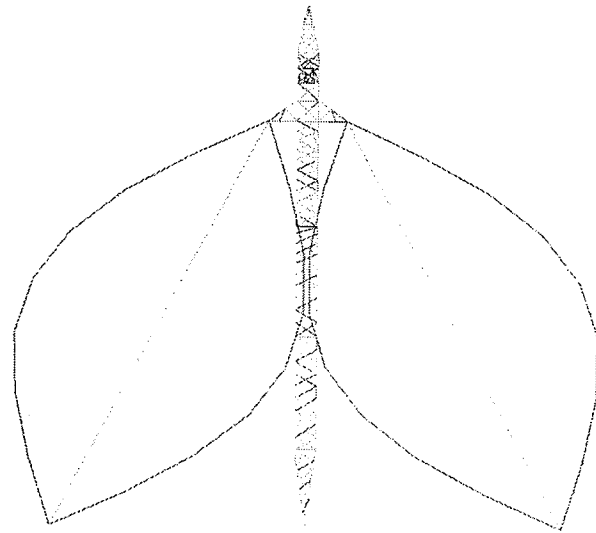
Three dimensional view



Top view

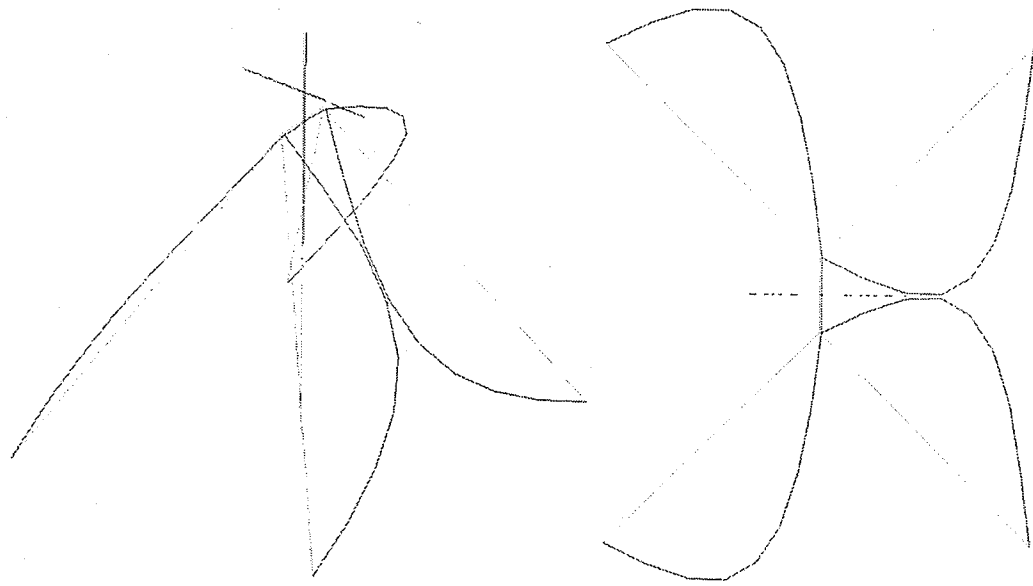


Lateral view



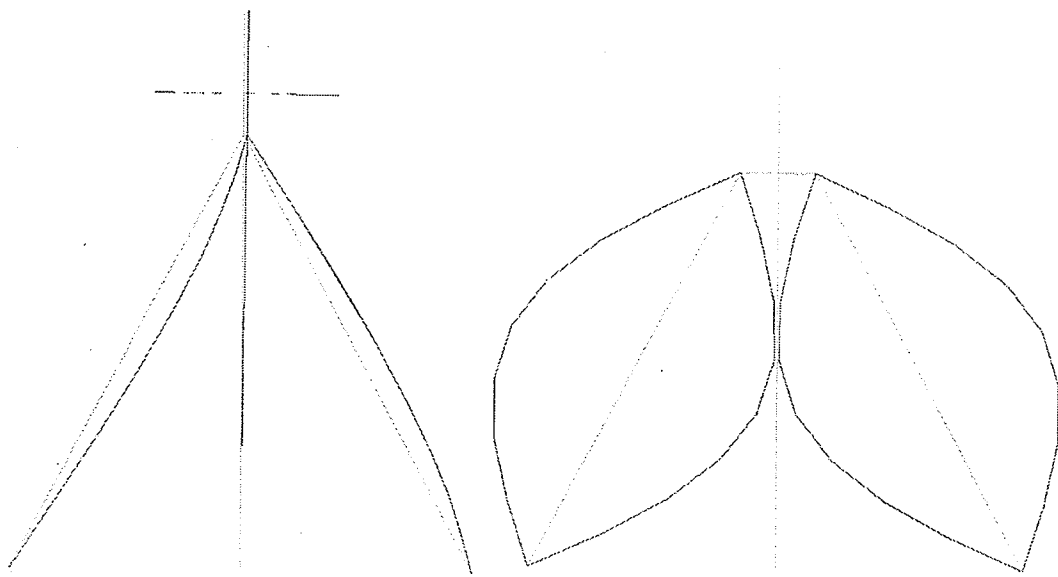
Transversal view

Figure A.1 - 1st Mode shape of Model 1 (frequency=1.50 Hz) (magnification: $\times 10$).



Three dimensional view

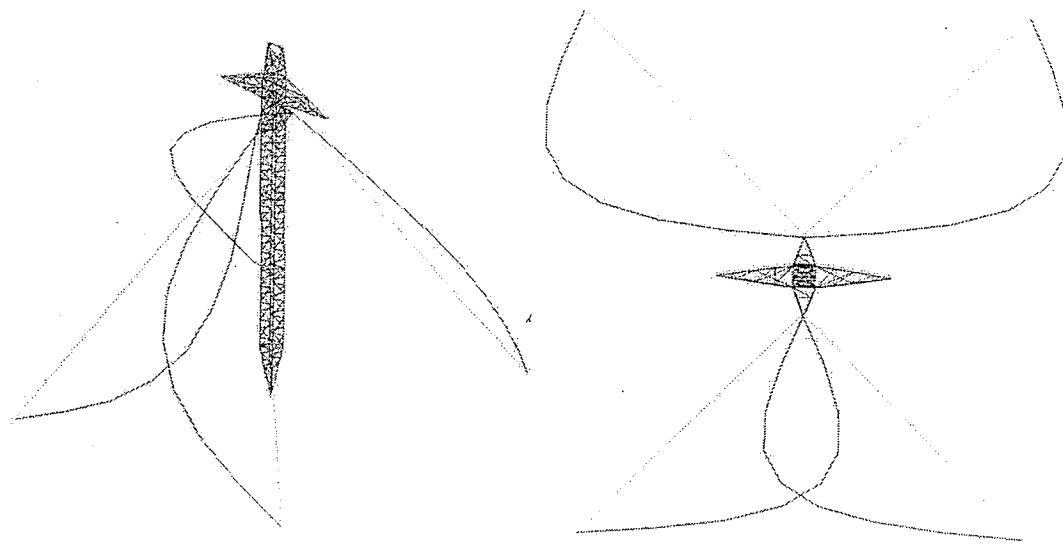
Top view



Lateral view

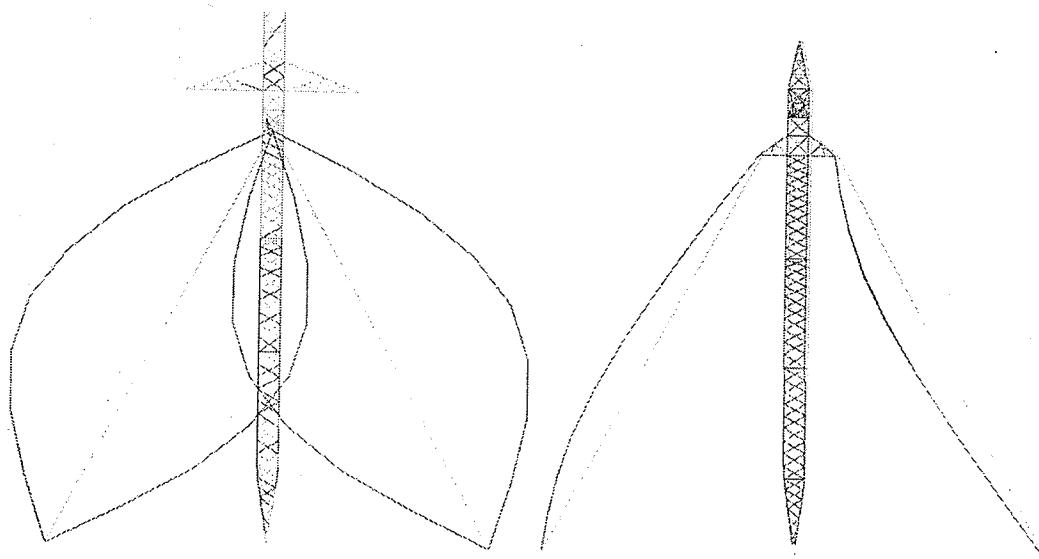
Transversal view

Figure A.2 - 1st Mode shape of Model 2 (frequency=1.51 Hz) (magnification: $\times 10$).



Three dimensional view

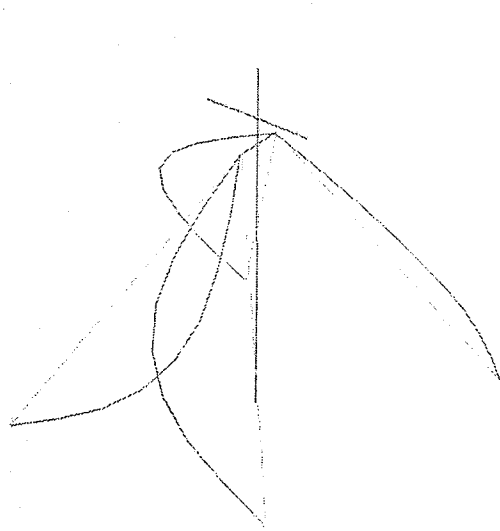
Top view



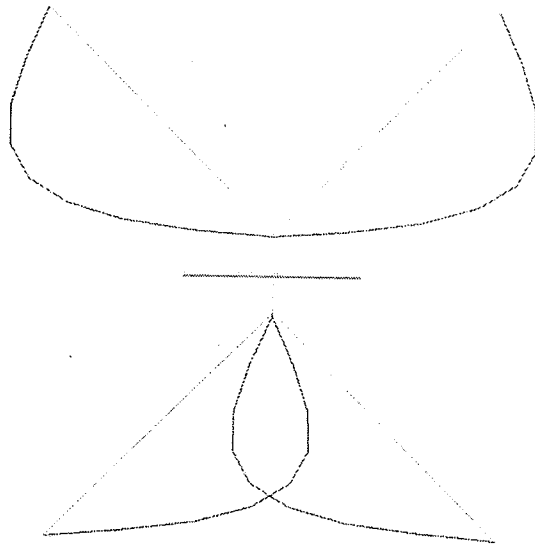
Lateral view

Transversal view

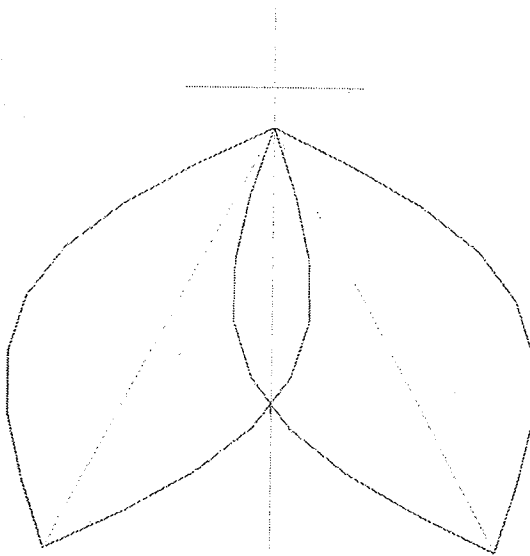
Figure A.3 - 2nd Mode shape of Model 1 (frequency=1.50 Hz) (magnification: ×10).



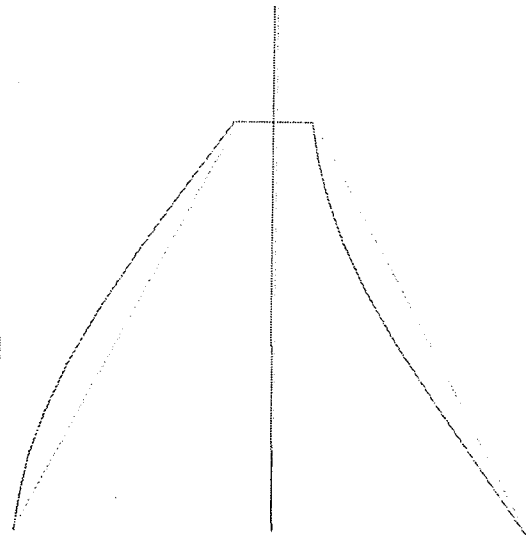
Three dimensional view



Top view

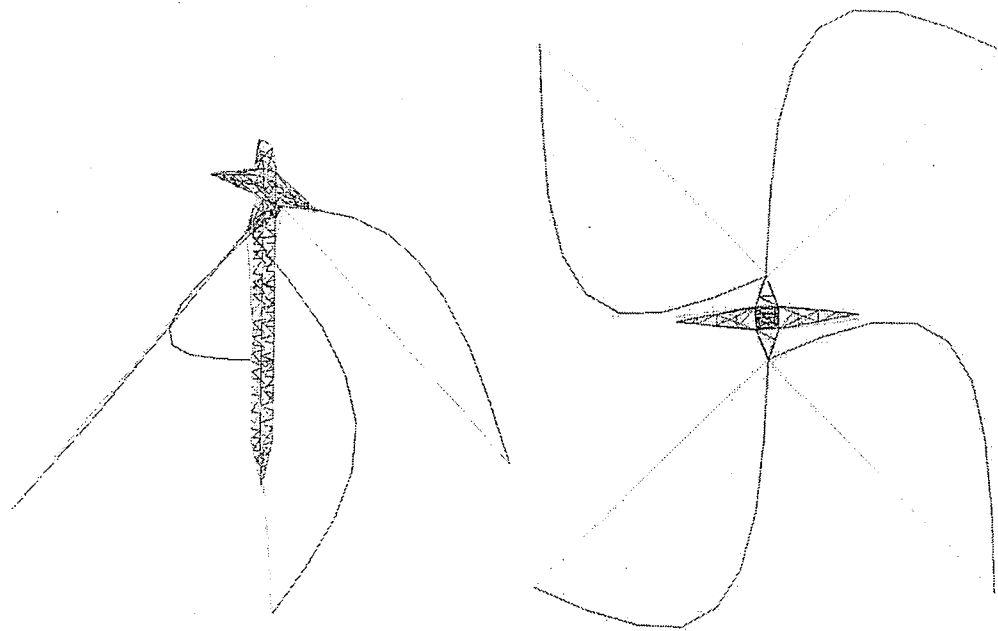


Lateral view



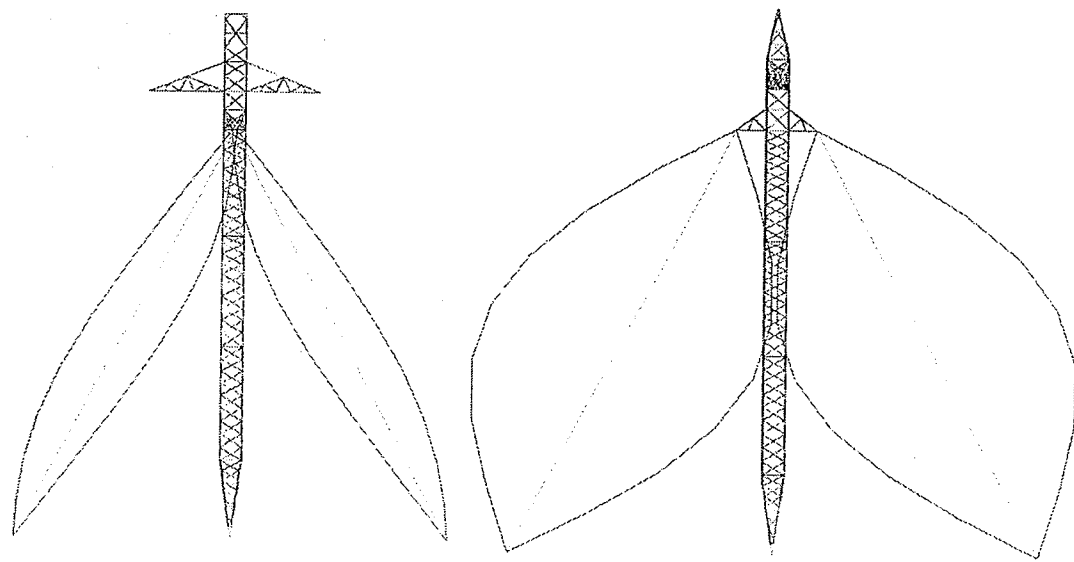
Transversal view

Figure A.4 - 2nd Mode shape of Model 2 (frequency=1.52 Hz) (magnification: $\times 10$).



Three dimensional view

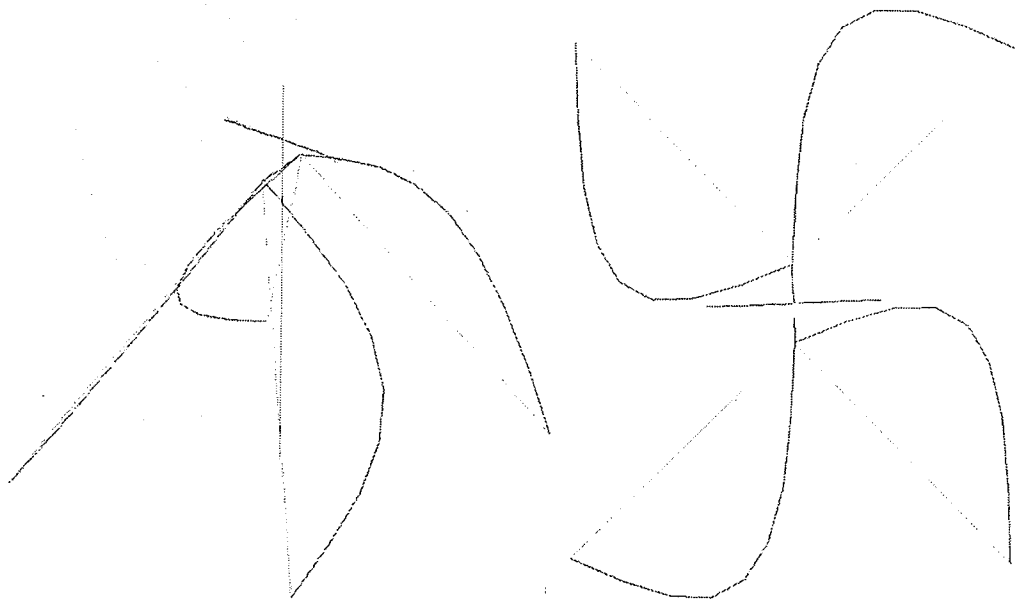
Top view



Lateral view

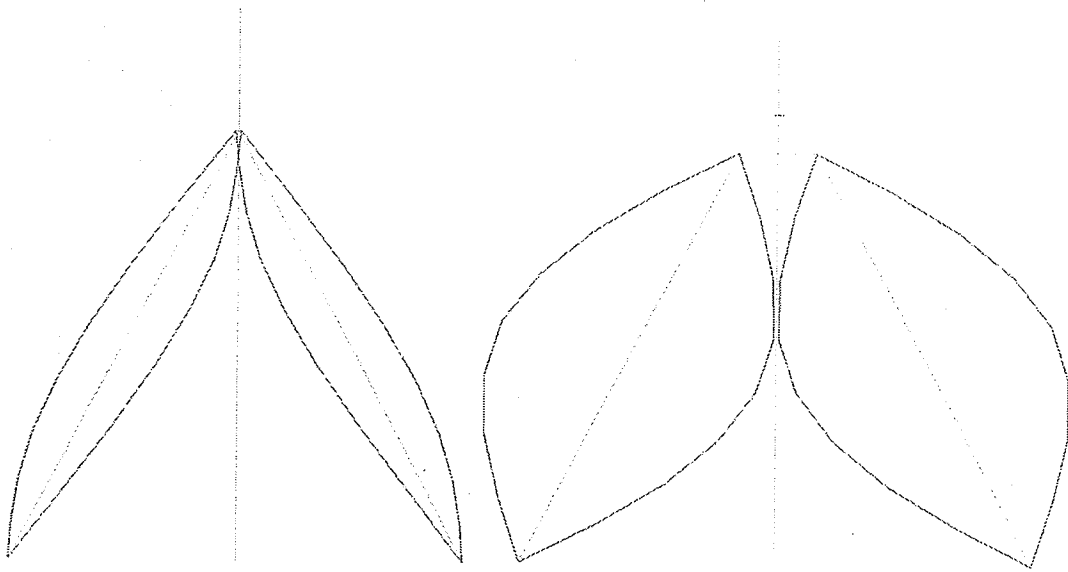
Transversal view

Figure A.5 - 3rd Mode shape of Model 1 (frequency=1.51 Hz) (magnification: $\times 10$).



Three dimensional view

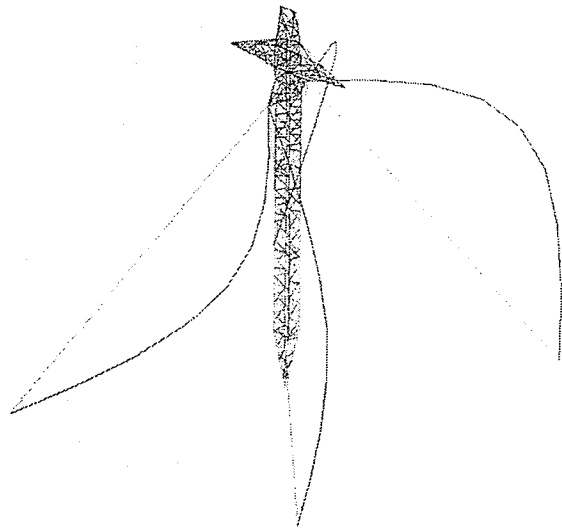
Top view



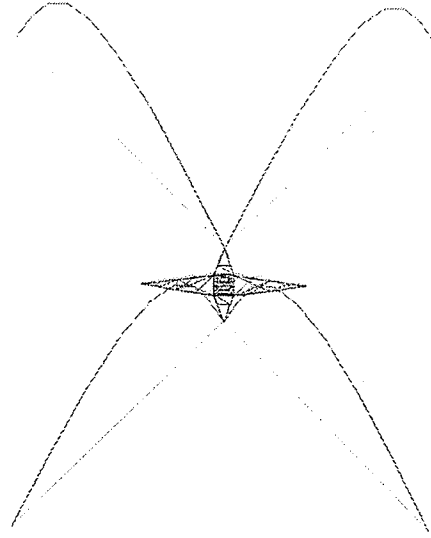
Lateral view

Transversal view

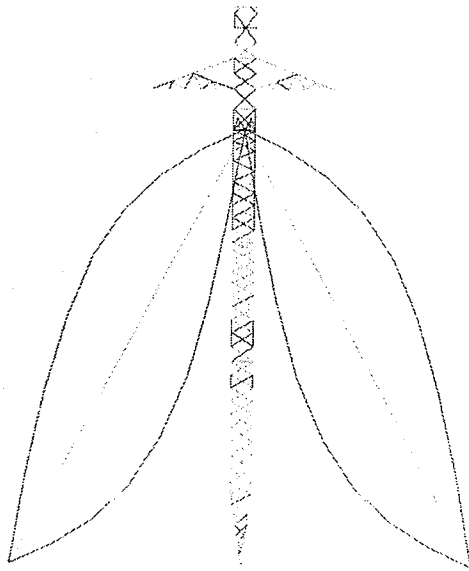
Figure A.6 - 3rd Mode shape of Model 2 (frequency=1.52 Hz) (magnification: $\times 10$).



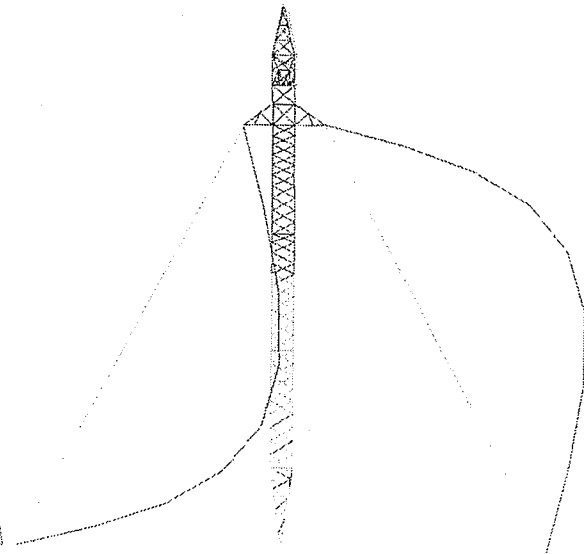
Three dimensional view



Top view

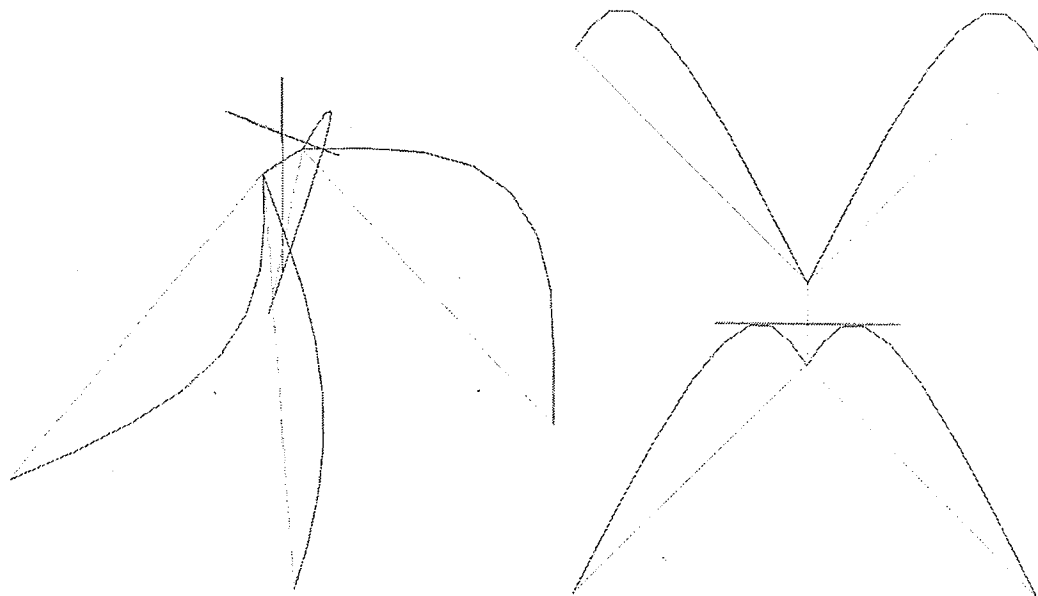


Lateral view



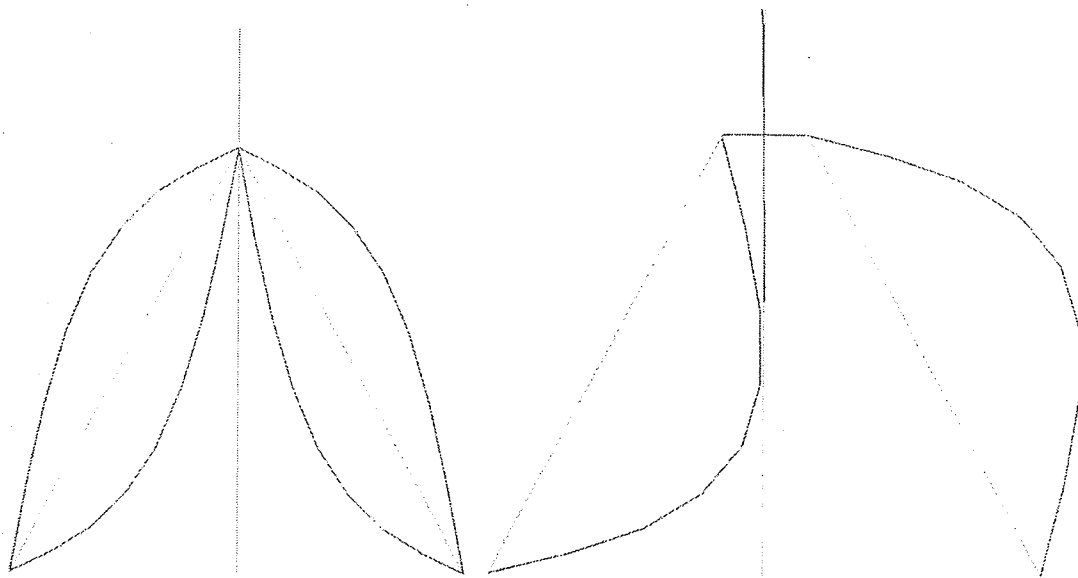
Transversal view

Figure A.7 - 5th Mode shape of Model 1 (frequency=1.52 Hz) (magnification: $\times 10$).



Three dimensional view

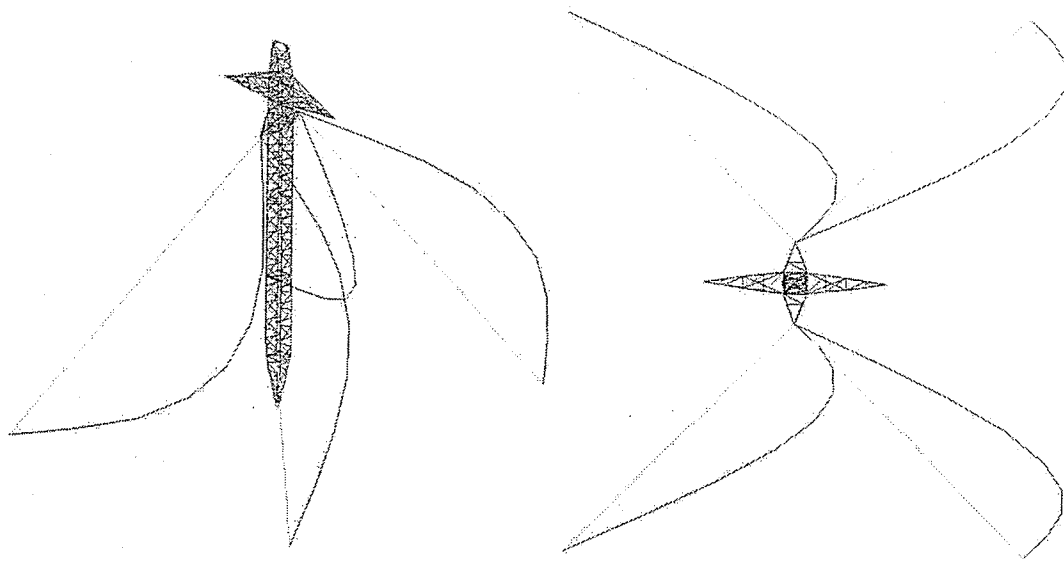
Top view



Lateral view

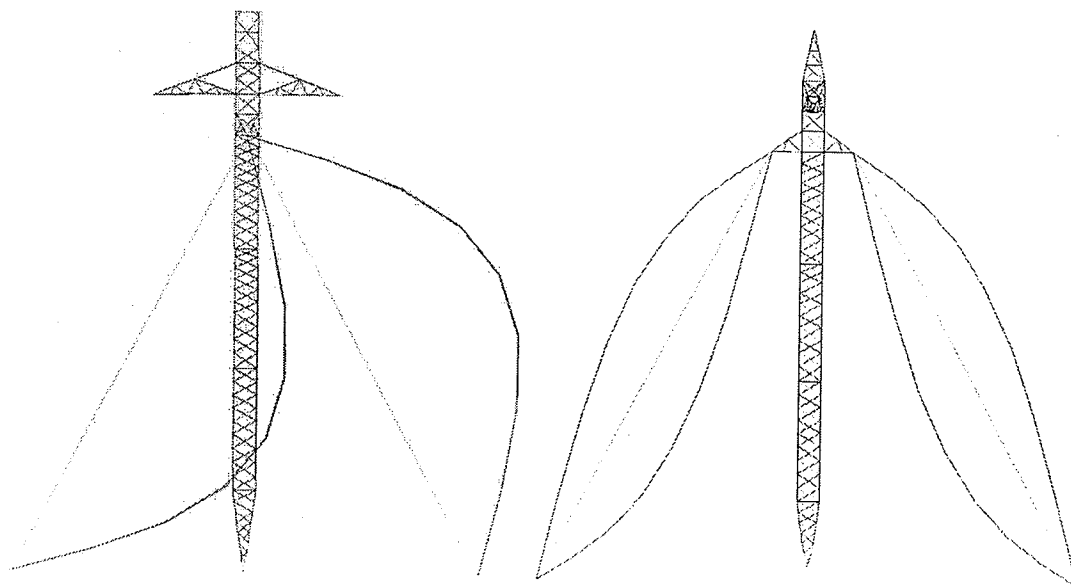
Transversal view

Figure A.8 - 5th Mode shape of Model 2 (frequency=1.53 Hz) (magnification: ×10).



Three dimensional view

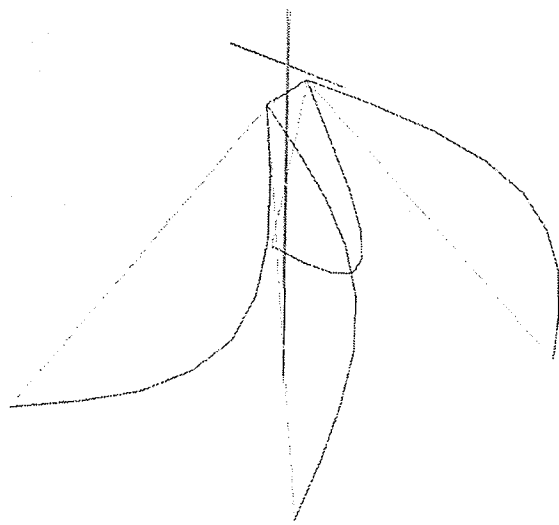
Top view



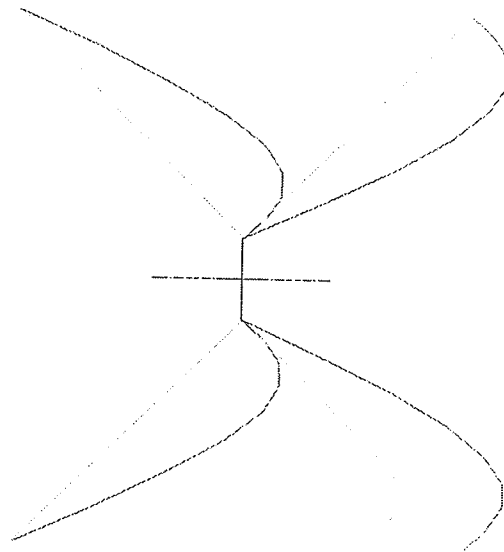
Lateral view

Transversal view

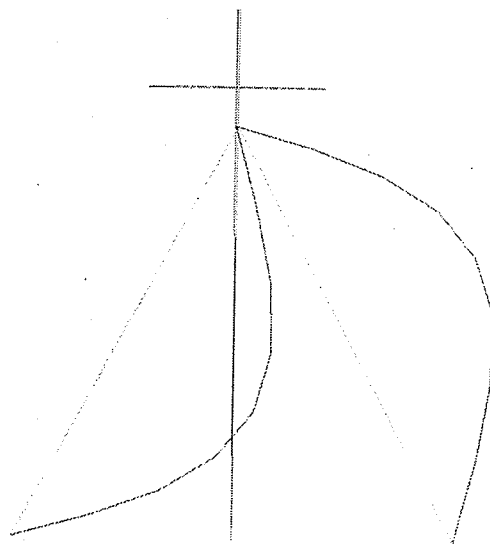
Figure A.9 - 6th Mode shape of Model 1 (frequency=1.52 Hz) (magnification: $\times 10$).



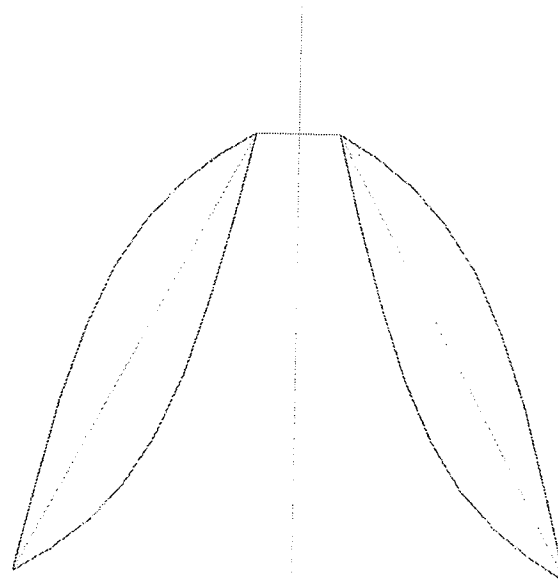
Three dimensional view



Top view

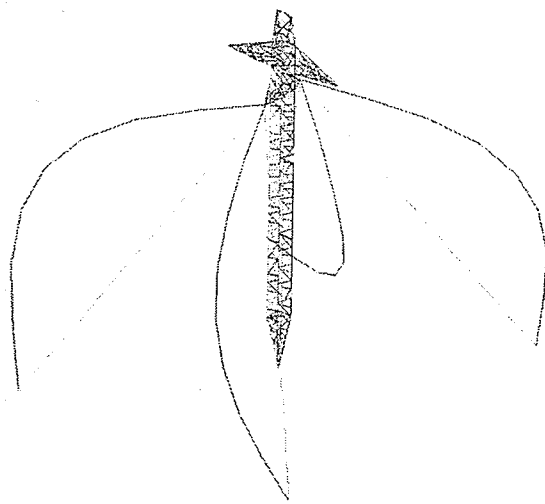


Lateral view

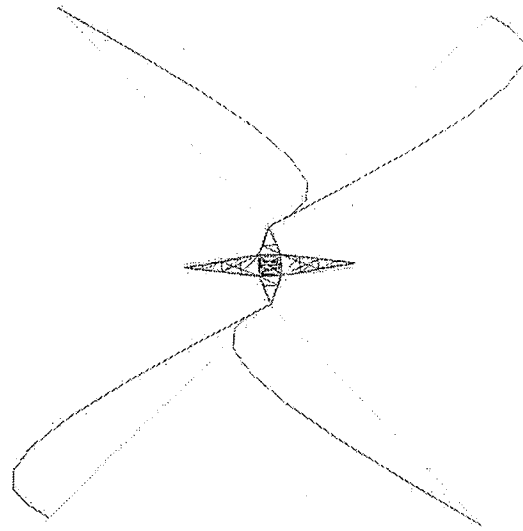


Transversal view

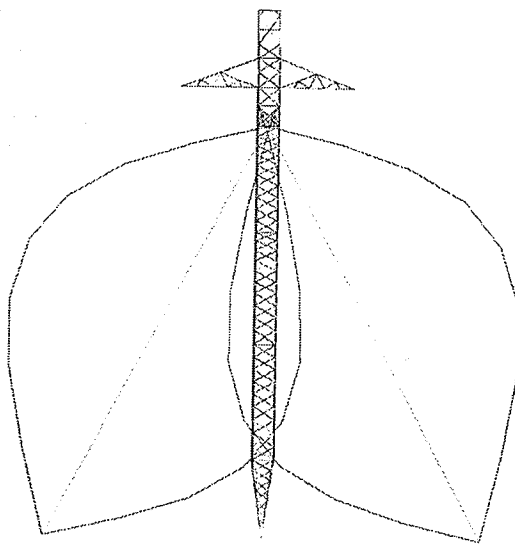
Figure A.10 - 6th Mode shape of Model 2 (frequency=1.53 Hz) (magnification: $\times 10$).



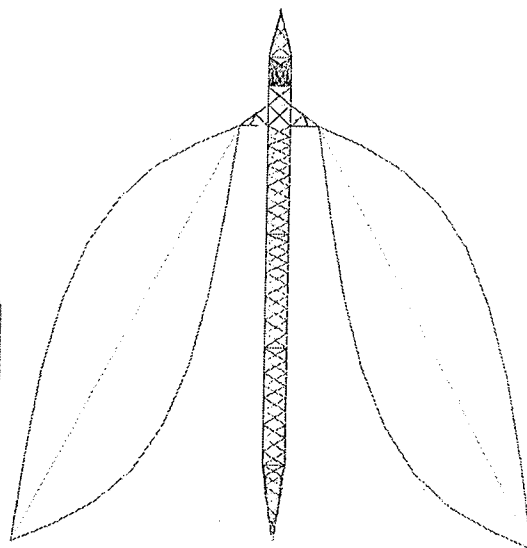
Three dimensional view



Top view

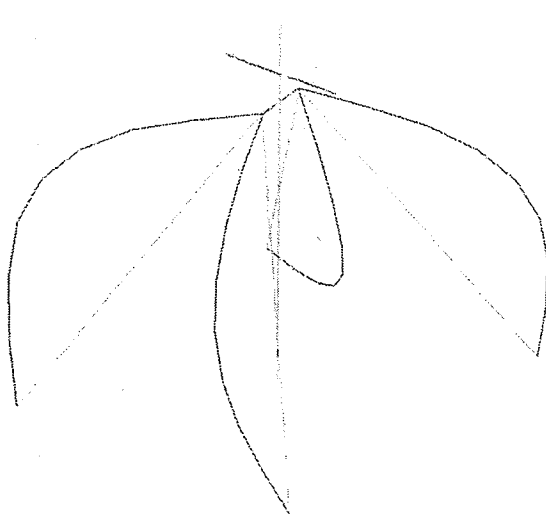


Lateral view

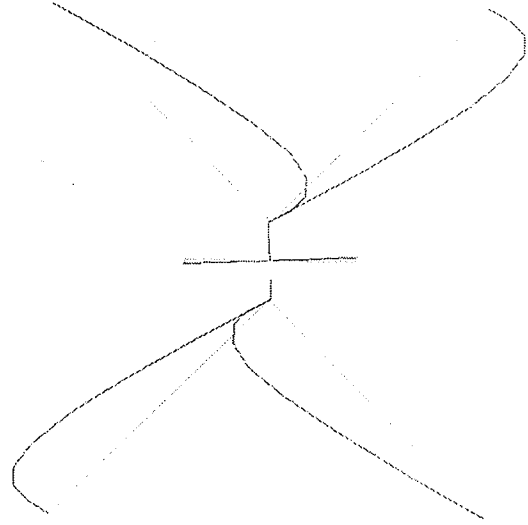


Transversal view

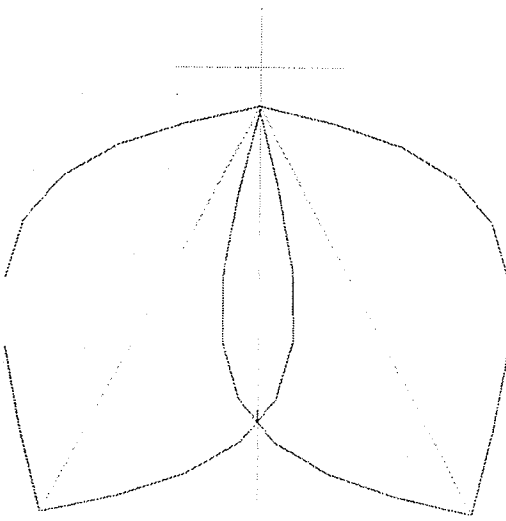
Figure A.11 - 7th Mode shape of Model 1 (frequency=1.52 Hz) (magnification: $\times 10$).



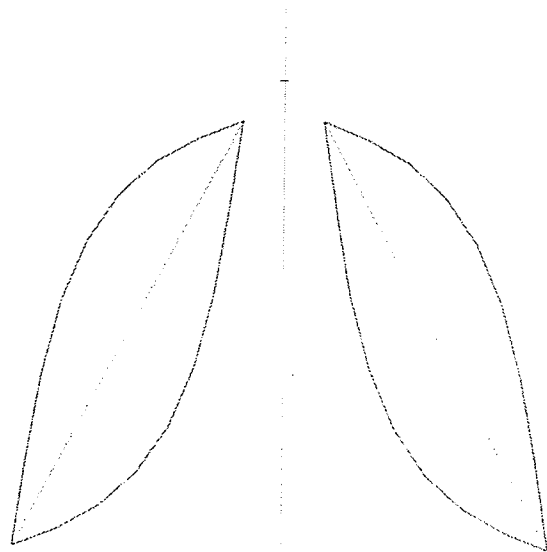
Three dimensional view



Top view

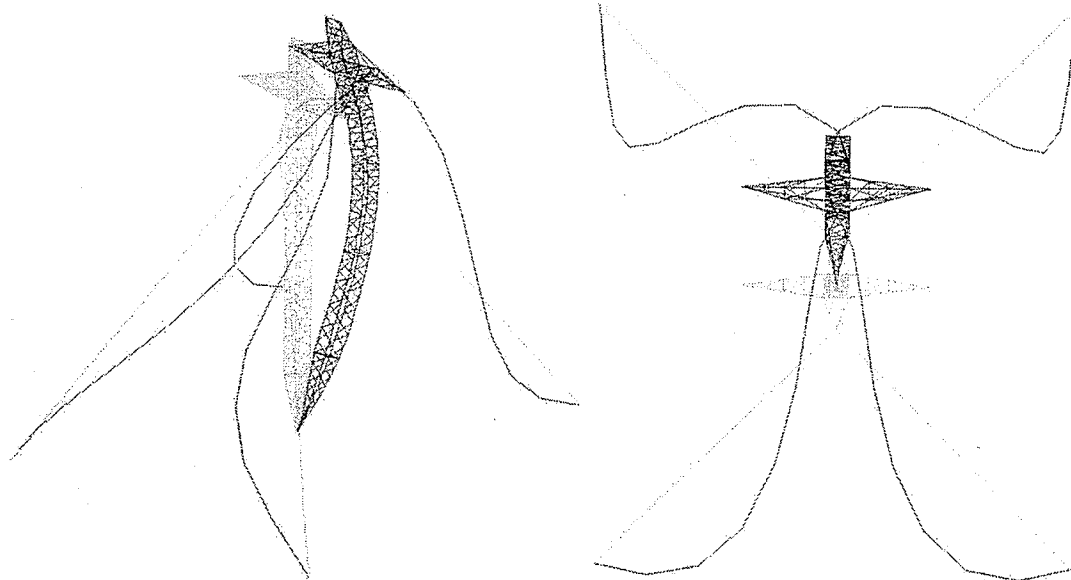


Lateral view



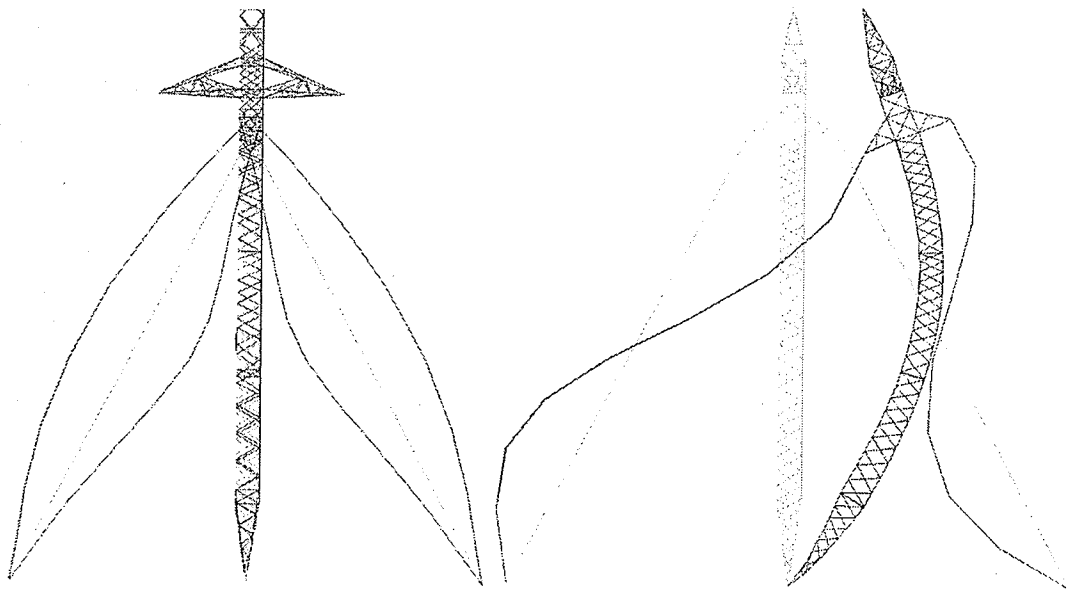
Transversal view

Figure A.12 - 7th Mode shape of Model 2 (frequency=1.53 Hz) (magnification: $\times 10$).



Three dimensional view

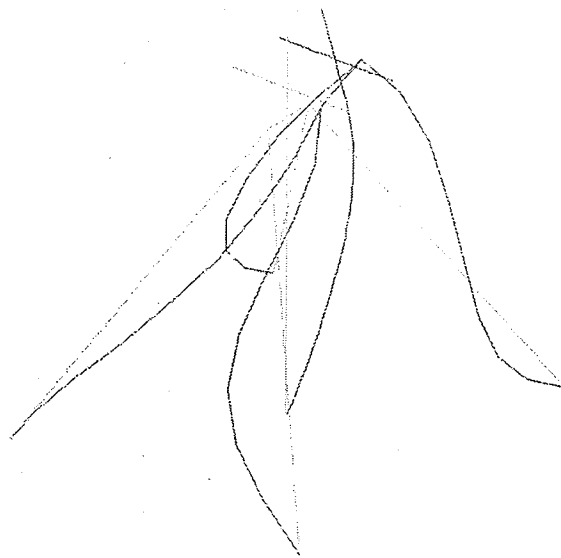
Top view



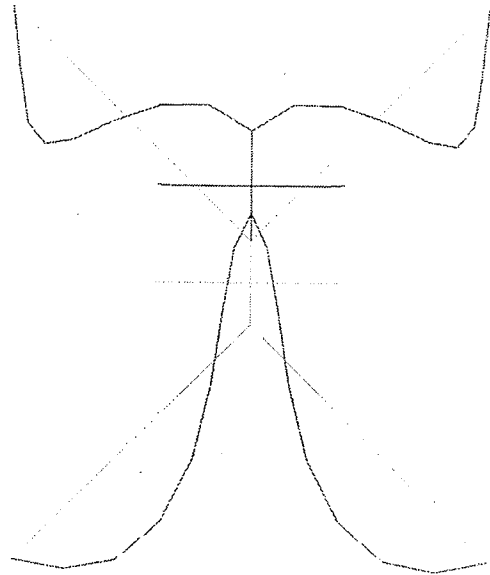
Lateral view

Transversal view

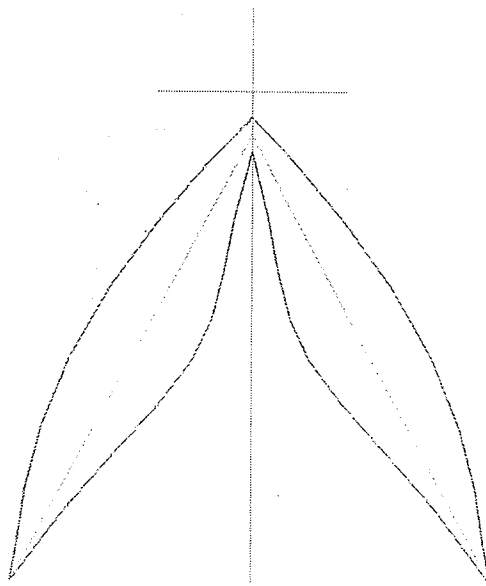
Figure A.13 - 9th Mode shape of Model 1 (frequency=2.30 Hz) (magnification: $\times 10$).



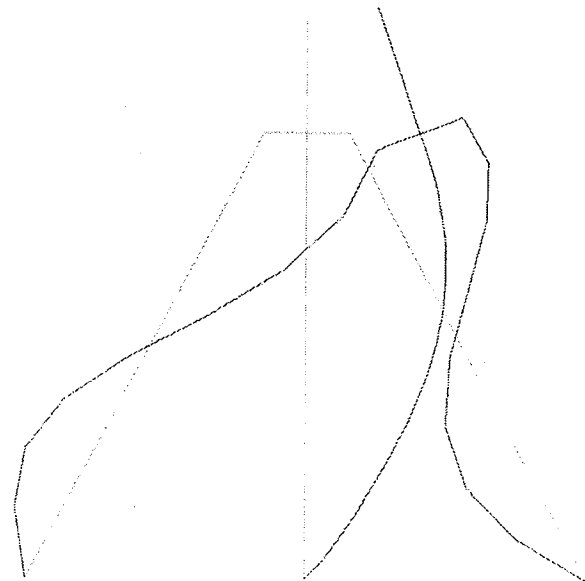
Three dimensional view



Top view

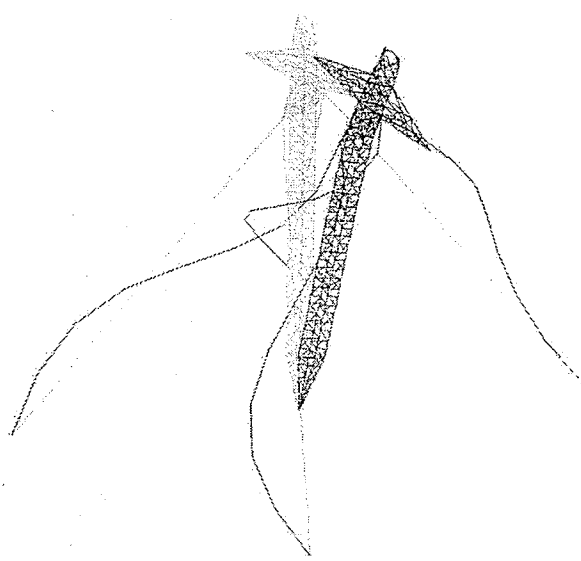


Lateral view

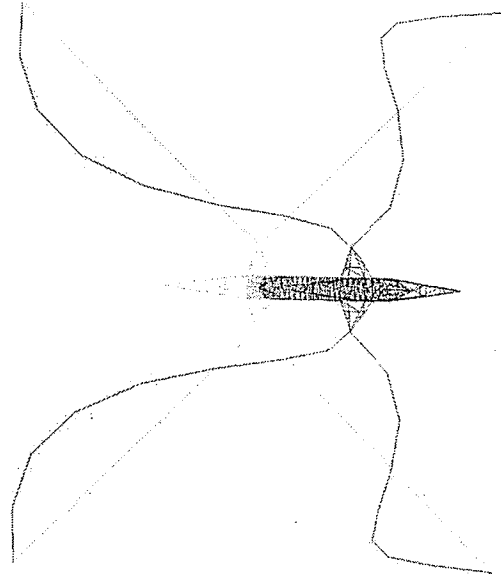


Transversal view

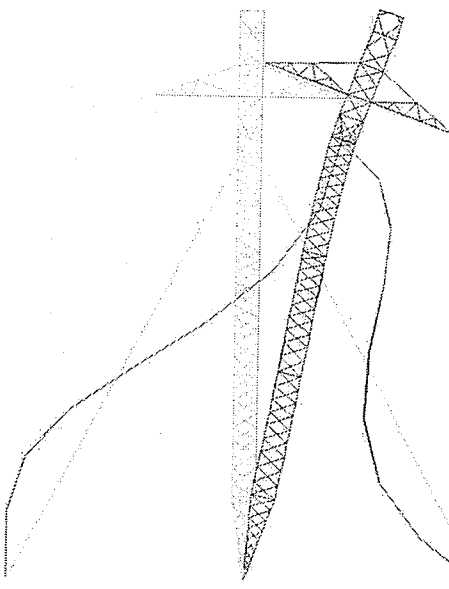
Figure A.14 - 9th Mode shape of Model 2 (frequency=2.32 Hz) (magnification: $\times 10$).



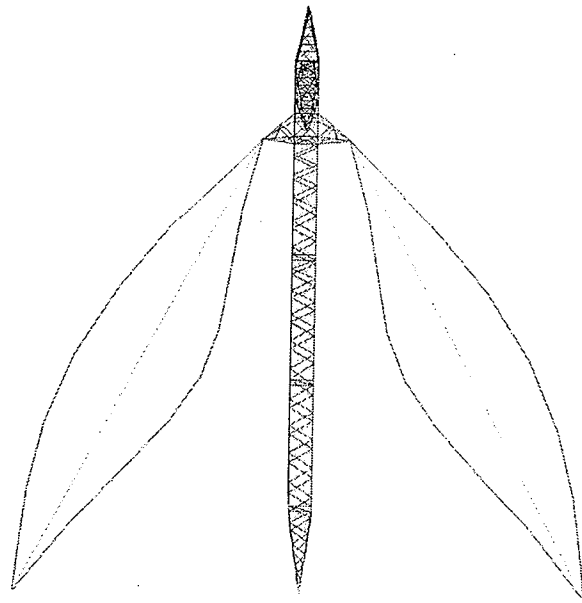
Three dimensional view



Top view



Lateral view



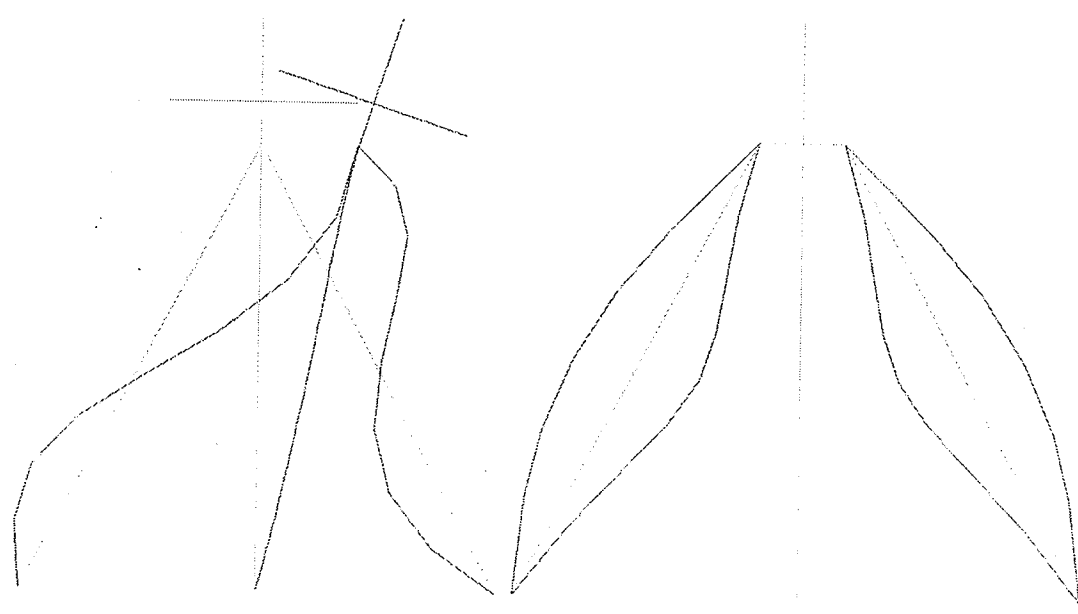
Transversal view

Figure A.15 - 10th Mode shape of Model 1 (frequency=2.42 Hz) (magnification: $\times 10$).



Three dimensional view

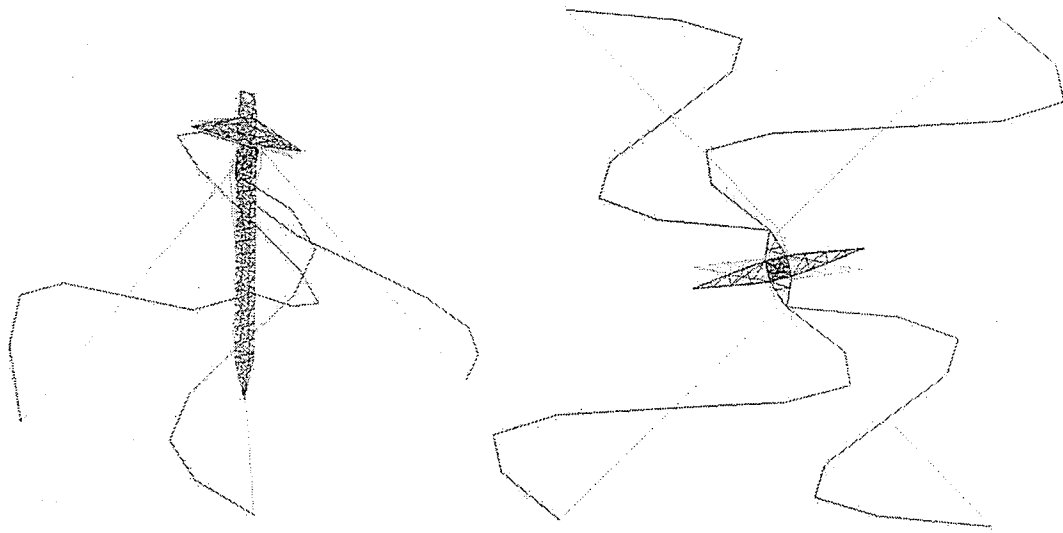
Top view



Lateral view

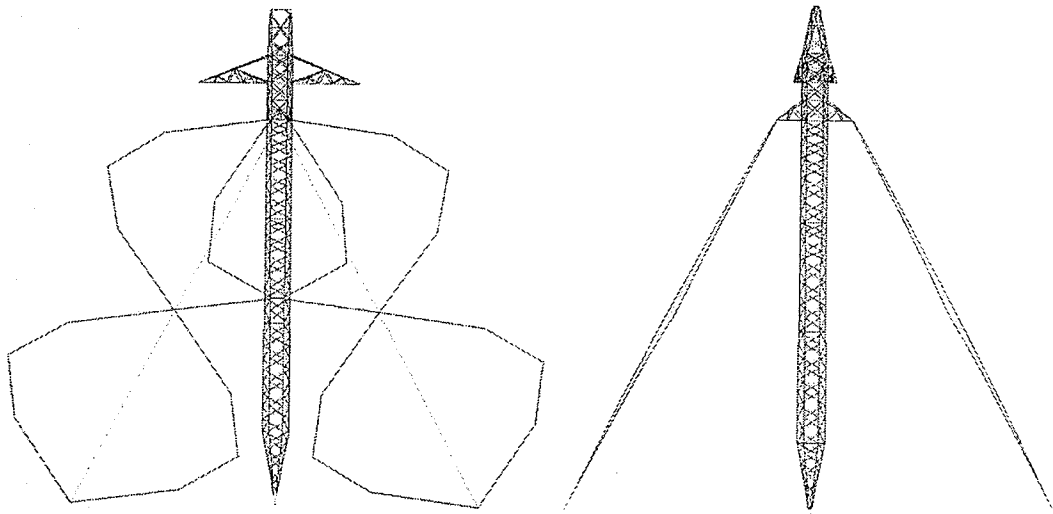
Transversal view

Figure A.16 - 10th Mode shape Model 2 (frequency=2.45 Hz) (magnification: ×10).



Three dimensional view

Top view



Lateral view

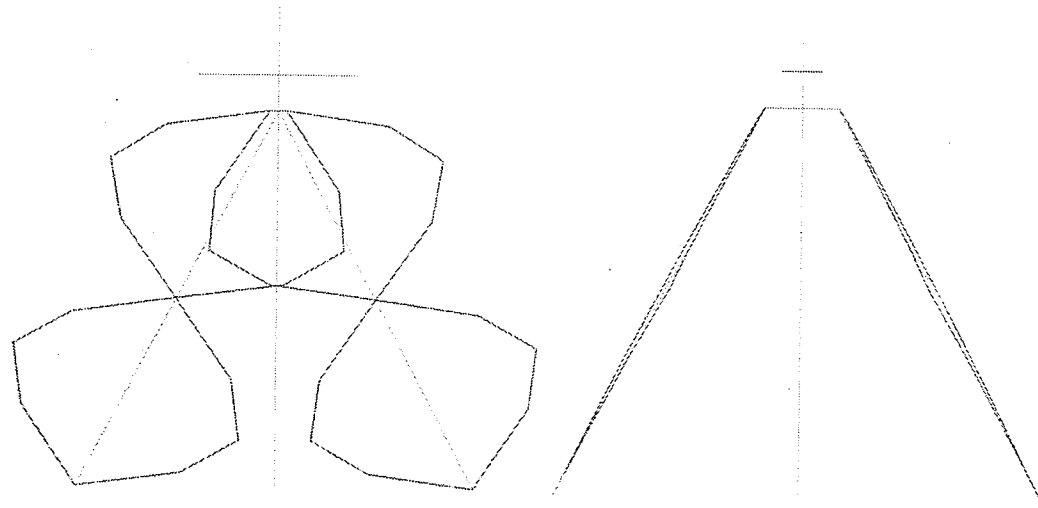
Transversal view

Figure A.17 - 11th Mode shape of Model 1 (frequency=3.05 Hz) (magnification: $\times 10$).



Three dimensional view

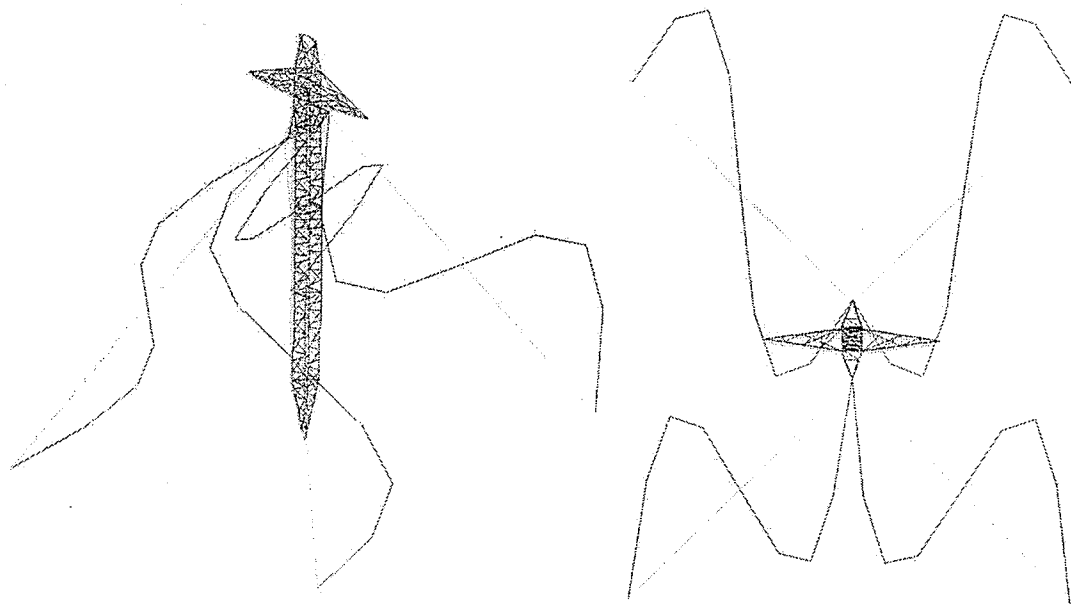
Top view



Lateral view

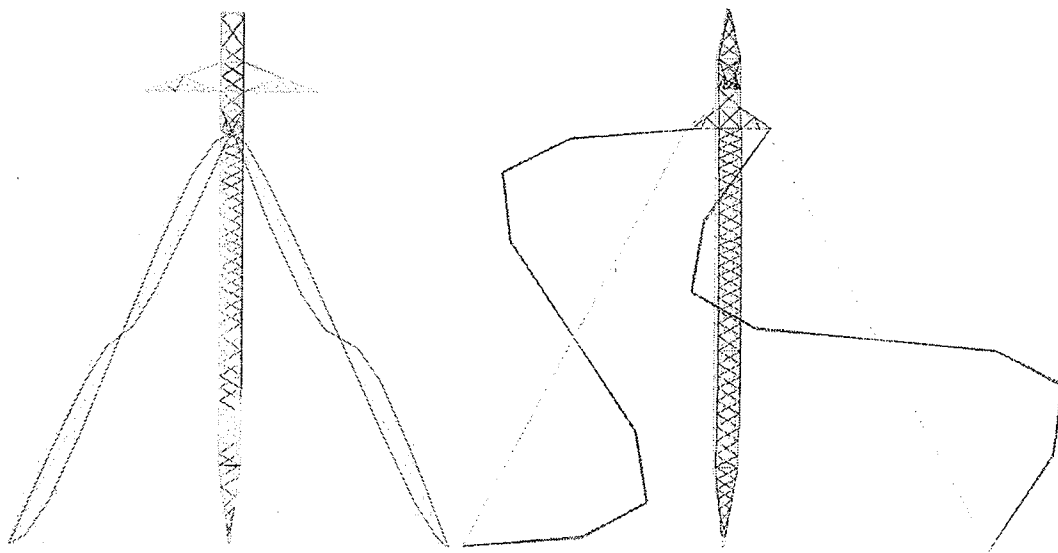
Transversal view

Figure A.18 - 11th Mode shape 11 of Model 2 (frequency=3.07 Hz) (magnification: $\times 10$).



Three dimensional view

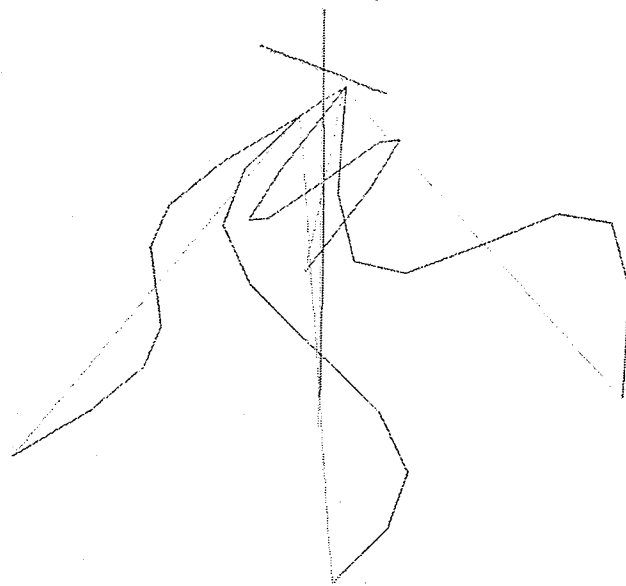
Top view



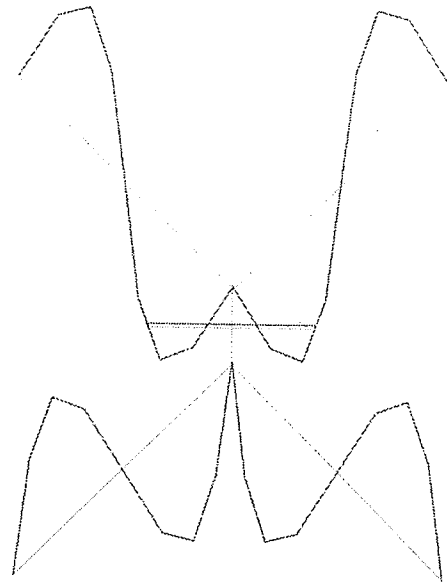
Lateral view

Transversal view

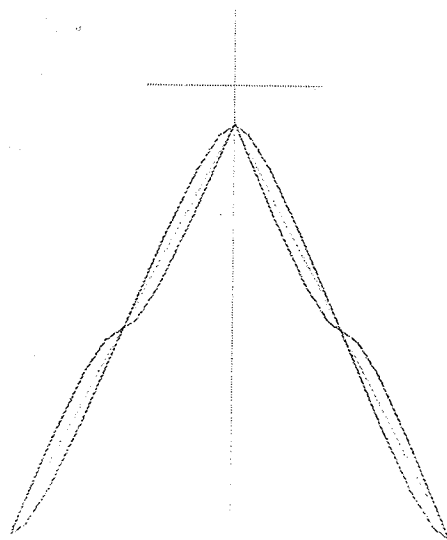
Figure A.19 - 17th Mode shape of Model 1 (frequency=3.09 Hz) (magnification: $\times 10$).



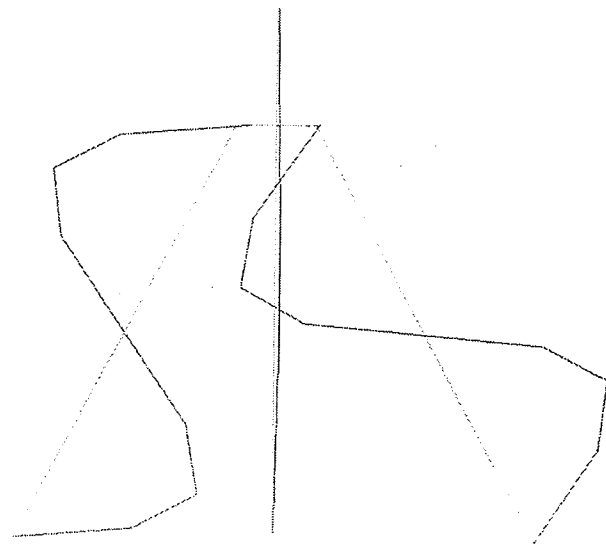
Three dimensional view



Top view

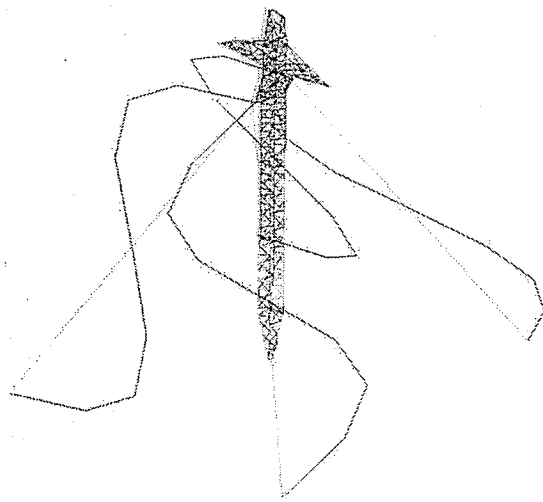


Lateral view

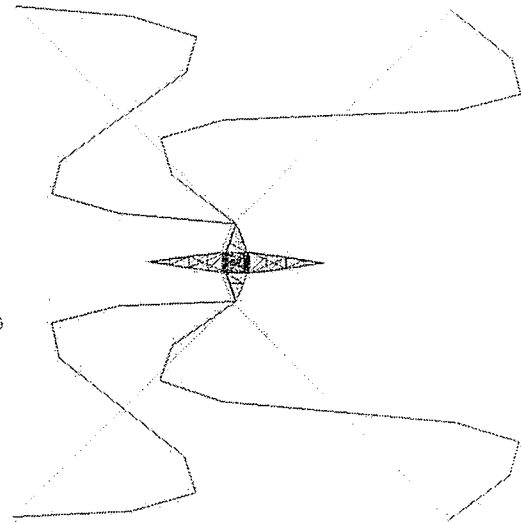


Transversal view

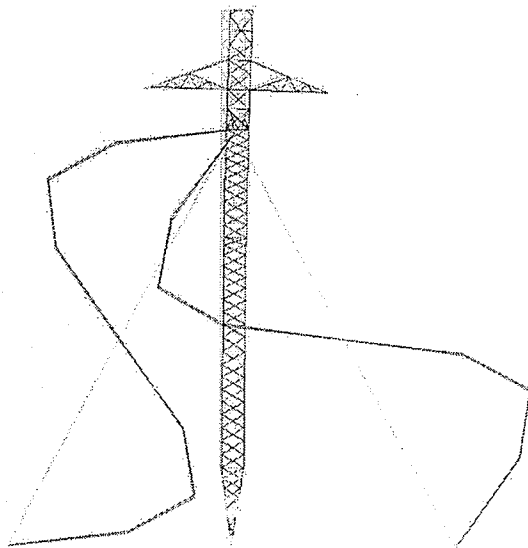
Figure A.20 - 17th Mode shape of Model 2 (frequency=3.12 Hz) (magnification: $\times 10$).



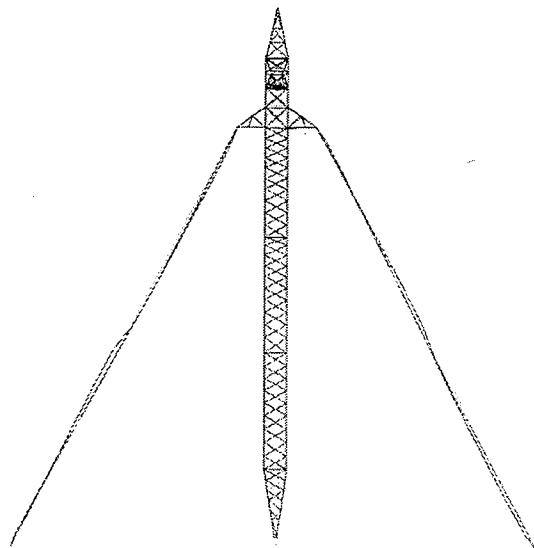
Three dimensional view



Top view

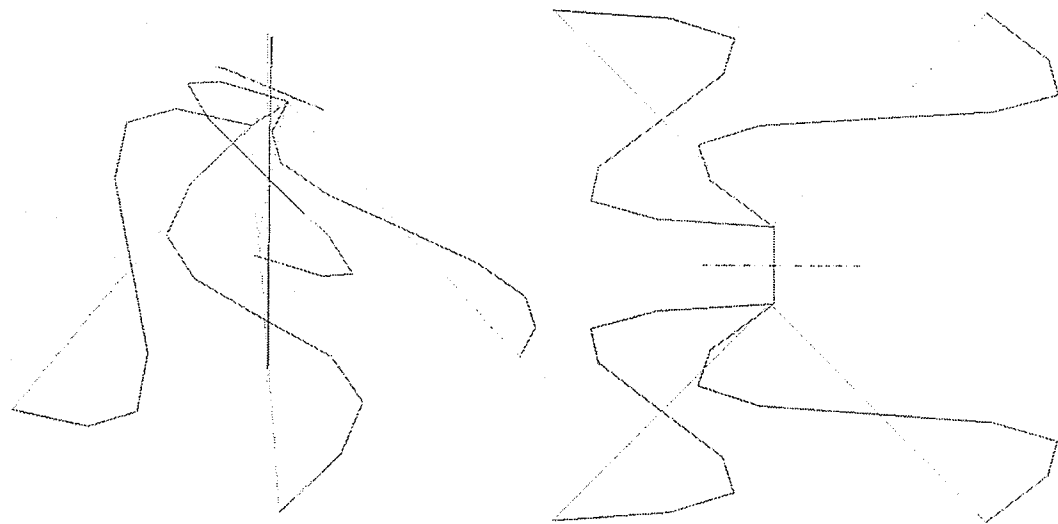


Lateral view



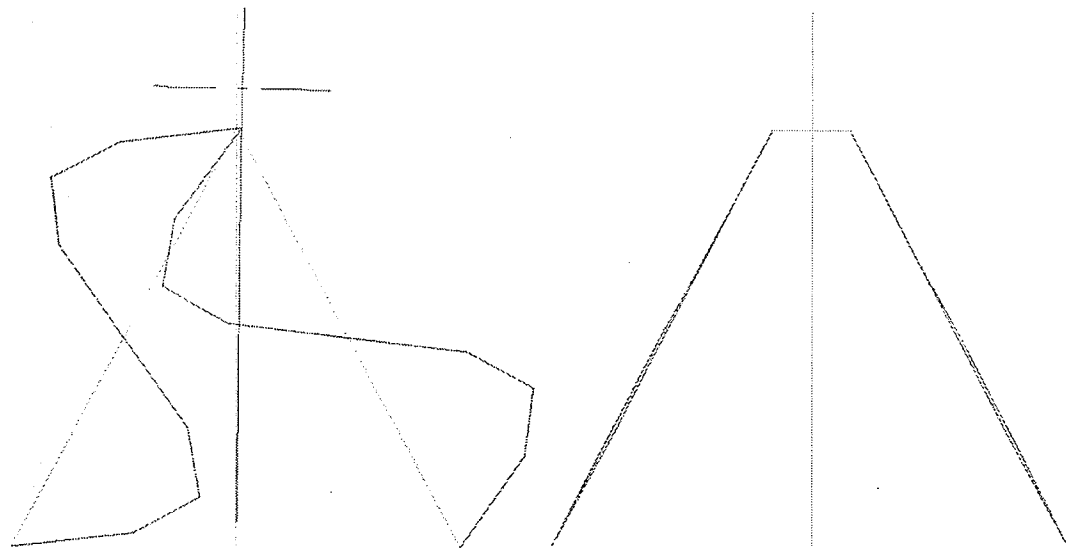
Transversal view

Figure A.21 - 18th Mode shape of Model 1 (frequency=3.09 Hz) (magnification: $\times 10$).



Three dimensional view

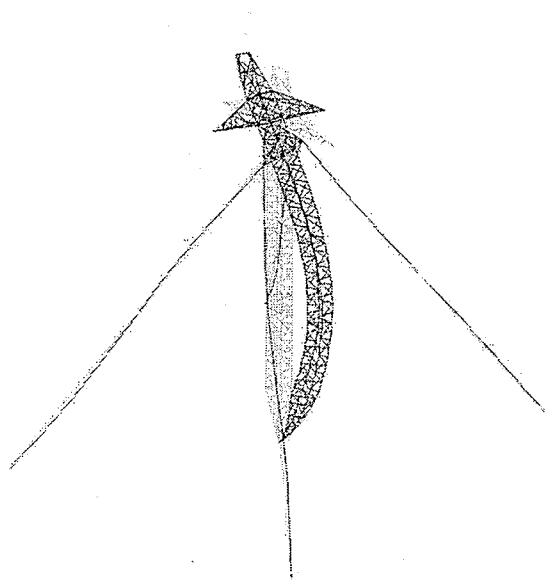
Top view



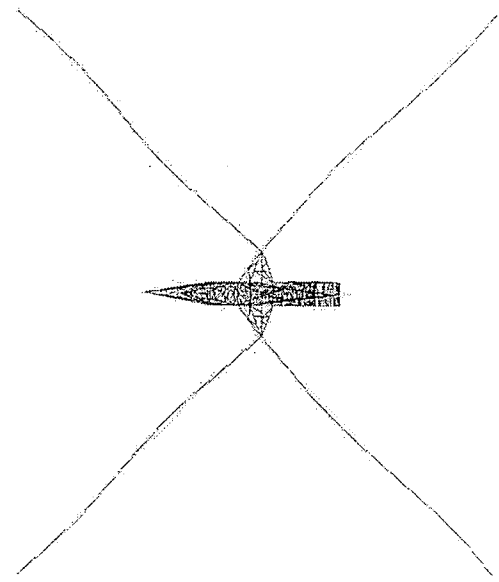
Lateral view

Transversal view

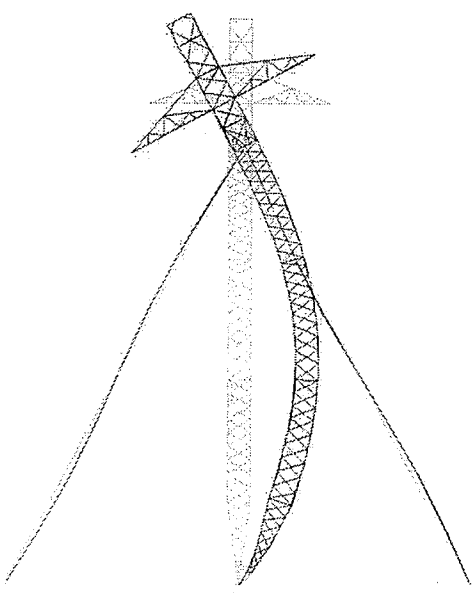
Figure A.22 - 18th Mode shape of Model 2 (frequency=3.12 Hz) (magnification: ×10).



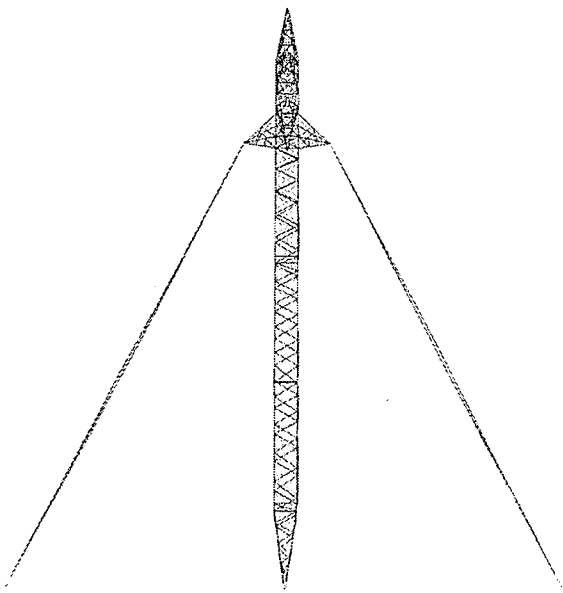
Three dimensional view



Top view

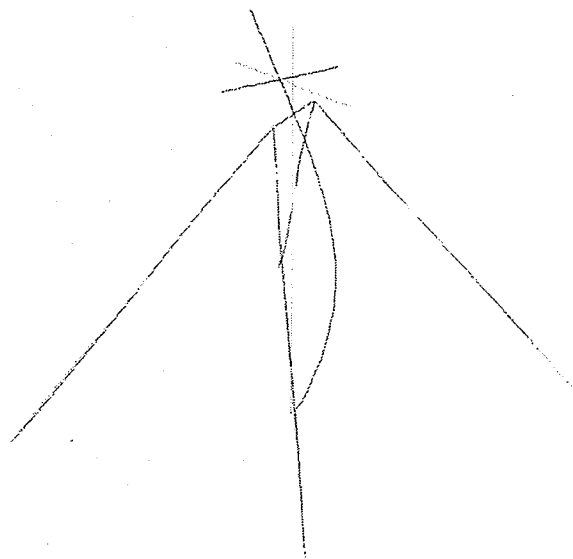


Lateral view

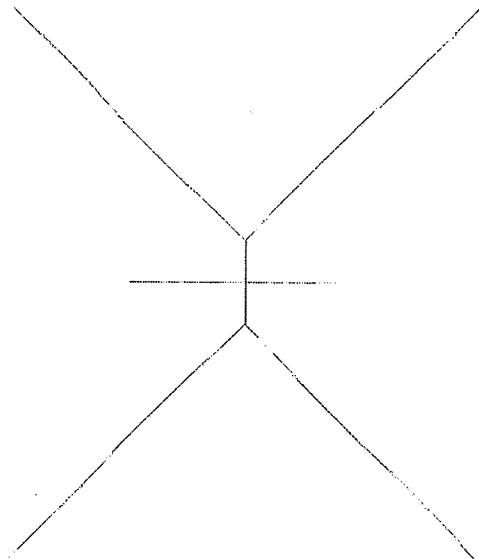


Transversal view

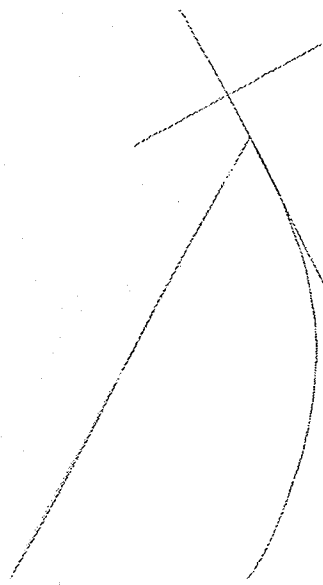
Figure A.23 - 19th Mode shape of Model 1 (frequency=3.55 Hz) (magnification: $\times 5$).



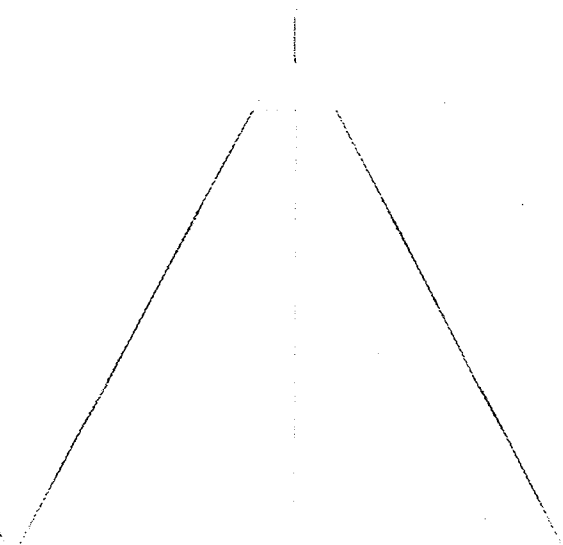
Three dimensional view



Top view

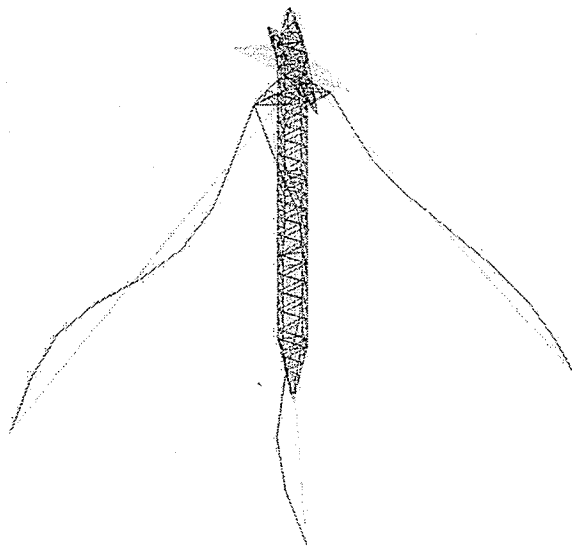


Lateral view

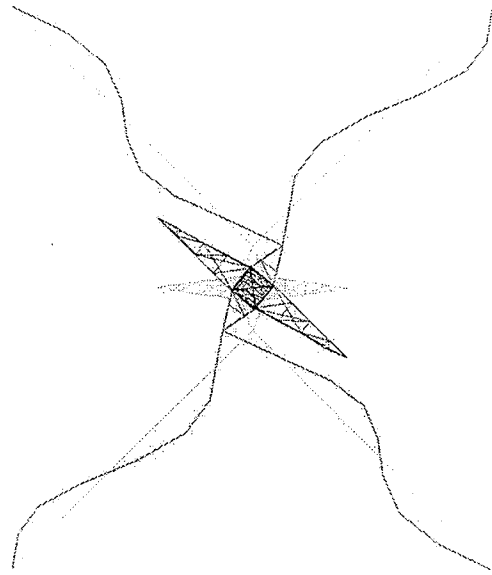


Transversal view

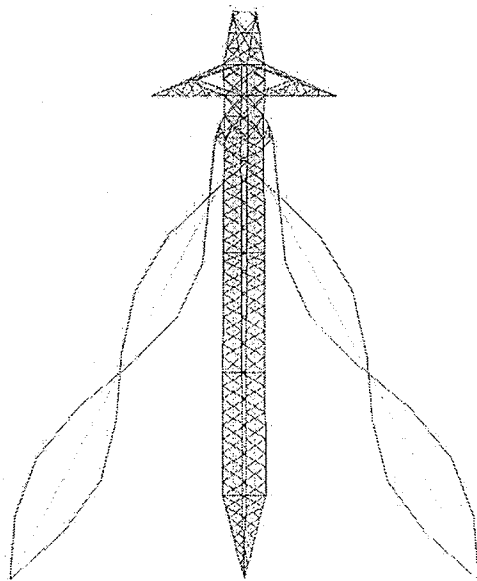
Figure A.24 - 20th Mode shape of Model 2 (frequency=3.66 Hz) (magnification: $\times 5$).



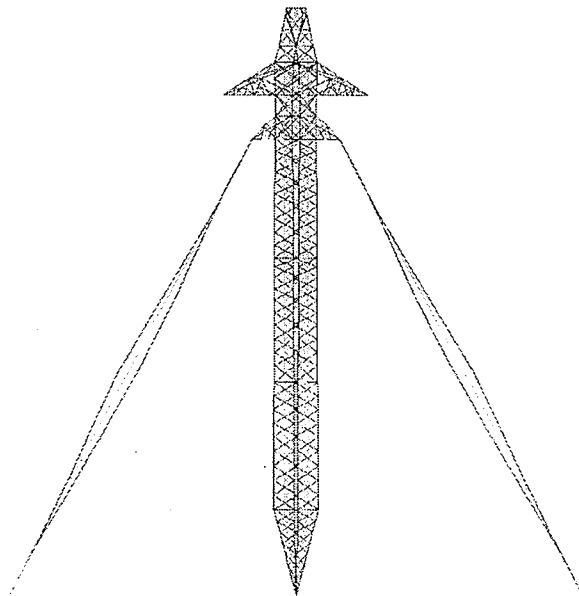
Three dimensional view



Top view

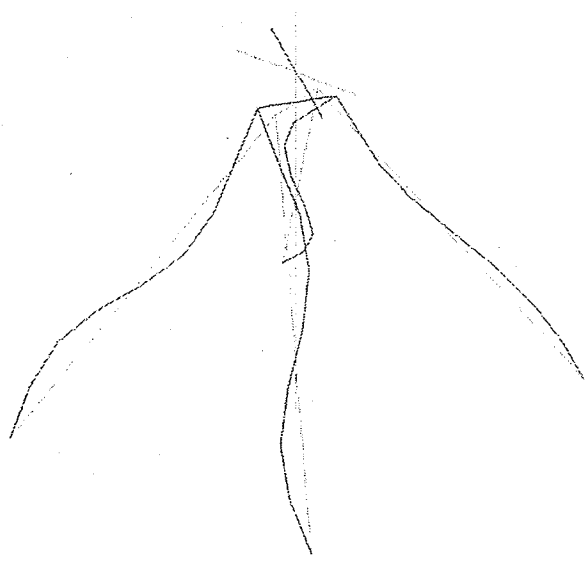


Lateral view

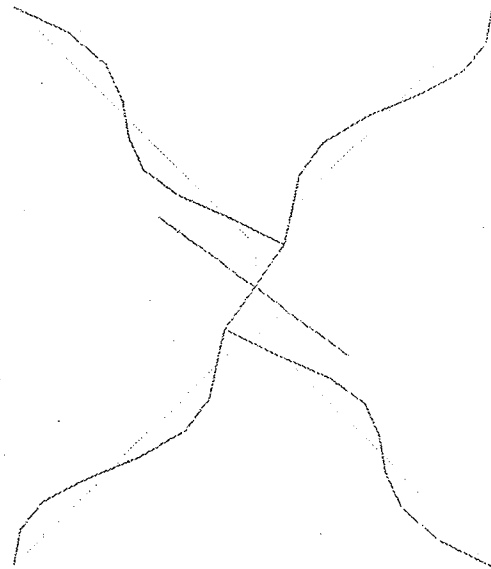


Transversal view

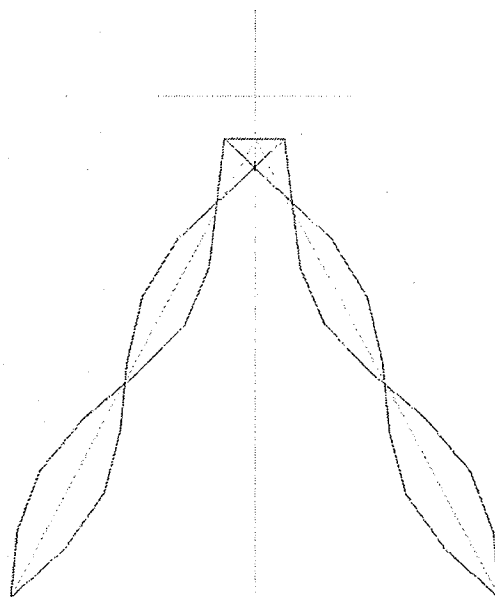
Figure A.25 - 20th Mode shape of Model 1 (frequency=3.57 Hz) (magnification: ×5).



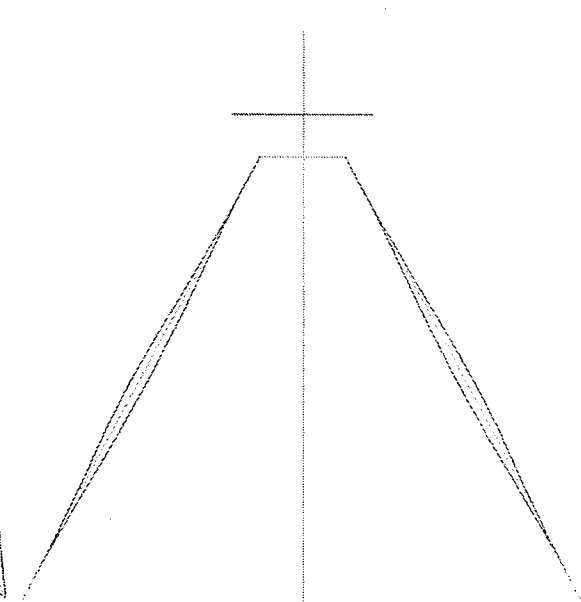
Three dimensional view



Top view

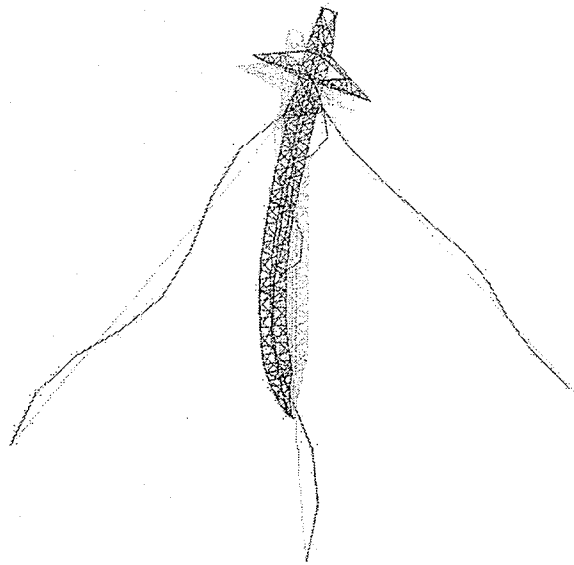


Lateral view

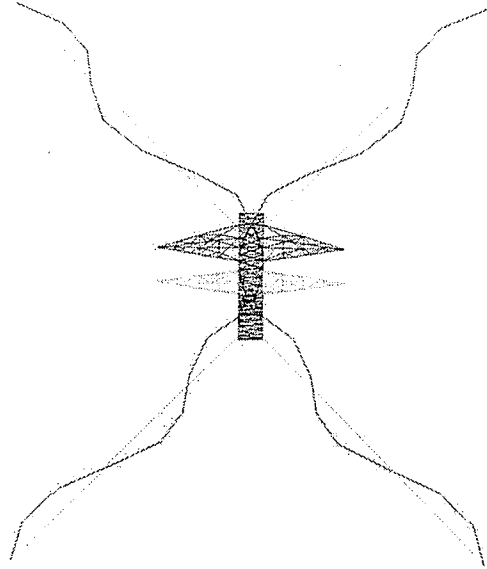


Transversal view

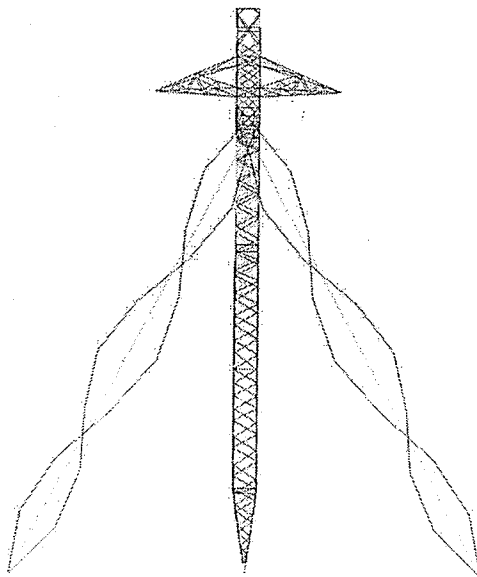
Figure A.26 - 19th Mode shape of Model 2 (frequency=3.63 Hz) (magnification: $\times 5$).



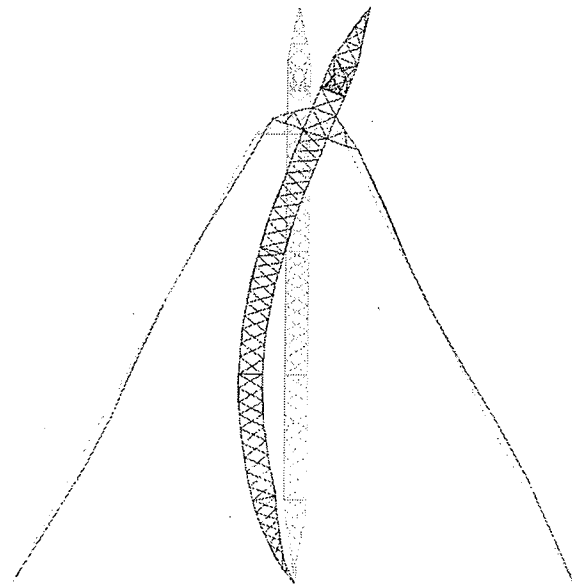
Three dimensional view



Top view

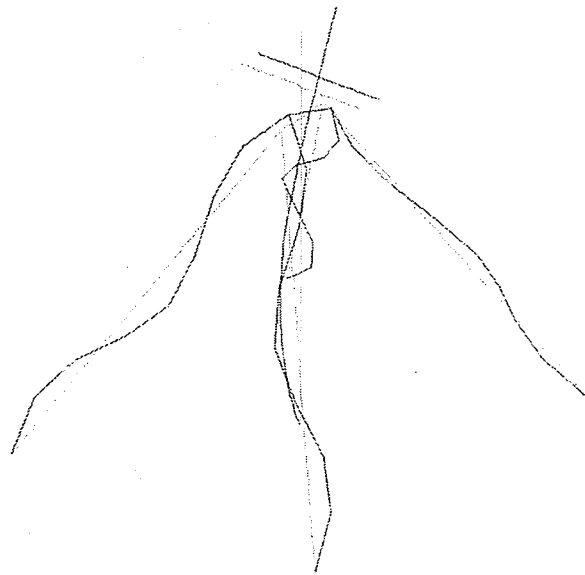


Lateral view

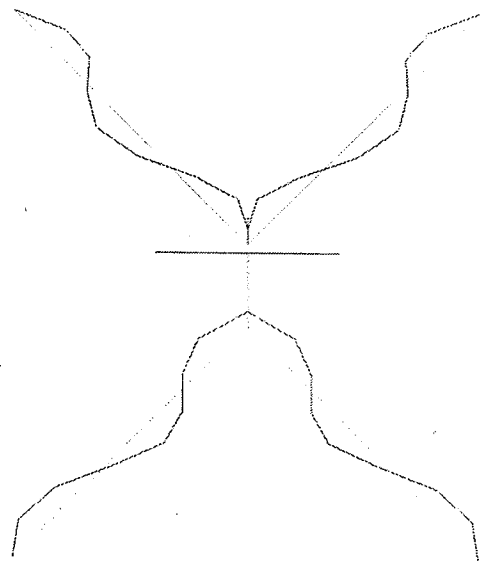


Transversal view

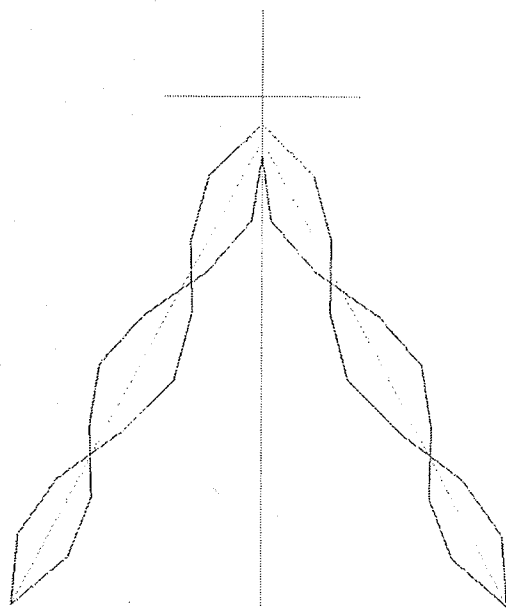
Figure A.27 - 21st Mode shape of Model 1 (frequency=4.44 Hz) (magnification: $\times 5$).



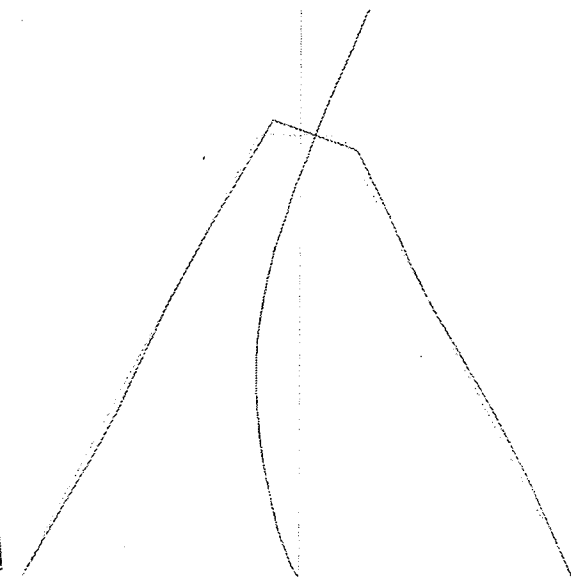
Three dimensional view



Top view



Lateral view



Transversal view

Figure A.28 - 21st Mode shape of Model 2 (frequency=4.56 Hz) (magnification: $\times 5$).

APPENDIX - B

Extra examples in the validation of the elements and verification of the program
procedures

Table B.1 – Summary of examples

Beam-column				
Example No.	Example name	Features tested	Analysis type	Method of Verification
1	General load 1	Automatic self weight	Linear static	Ansys version 11
		Concentrated load		Weaver and Gere, 1980 pages 344 to 357
2	Local axis	Rotation of the local axis	Linear static	Weaver and Gere, 1980 pages 344 to 357
3	Buckling of column	Nonlinear analysis	Nonlinear static	Theoretical results
4	Eigenvalue problem 1	Eigenvalue analysis	Eigenvalue	Militano, 2000 pages 32 to 35
5	Eigenvalue problem 2	Eigenvalue analysis with axial force	Eigenvalue	Przemieniecki, 1985 pages 403 to 406
6	Vibration 1	Dynamic solver	Linear dynamic	Battista, 2007-C page 138
Truss				
Example No.	Example name	Features tested	Analysis type	Method of Verification
7	General load 2	Automatic self weight	Linear static	Ansys version 11
		Concentrated load		Weaver and Gere, 1980 pages 343 to 345
8	Buckling	Nonlinear analysis	Nonlinear static	Theoretical results
9	Eigenvalue problem 3	Eigenvalue analysis	Eigenvalue	Mario Paz, 2004 page 434 to 437
Spring				
Example No.	Example name	Features tested	Analysis type	Method of Verification
10	General load 3	Automatic self weight	Linear static	Theoretical results
		Concentrated load		
11	Eigenvalue problem 4	Eigenvalue analysis	Eigenvalue	Theoretical results
12	Vibration 2	Dynamic solver	Linear dynamic	Theoretical results
Cable				
Example No.	Example name	Features tested	Analysis type	Method of Verification
13	General load 4	Automatic self weight	Nonlinear static	Theoretical results
		Concentrated load		
14	Eigenvalue problem 5	Eigenvalue analysis	Eigenvalue	Irvine, 1992 page 192
Tapered tower				
Example No.	Example name	Features tested	Analysis type	Method of Verification
15	General load 5	Automatic self weight	Nonlinear static	Frame and Truss element comparison
		Concentrated load		
16	Eigenvalue problem 6	Eigenvalue analysis	Eigenvalue	Frame and Truss element comparison
Beam-column (stability functions)				
Example No.	Example name	Features tested	Analysis type	Method of Verification
17	General load 6	Automatic self weight	Linear static	Ansys version 11
		Uniform distributed load		Weaver and Gere, 1980 pages 344 to 357
		Concentrated load		
18	Local axis	Rotation of the local axis	Linear static	Ansys version 11
19	Buckling of column	Nonlinear analysis	Nonlinear static	Theoretical results
20	Eigenvalue problem 7	Eigenvalue analysis	Eigenvalue	Militano, 2000 pages 32 to 35
21	Eigenvalue problem 8	Eigenvalue analysis with axial force	Eigenvalue	Przemieniecki, 1985 pages 403 to 406
22	Vibration 3	Dynamic solver	Linear dynamic	Battista, 2007-C page 138
Insulator string				
Example No.	Example name	Features tested	Analysis type	Method of Verification
23	General load 7	Automatic self weight	Nonlinear static	Theoretical results
		Concentrated load		
24	Eigenvalue problem 9	Eigenvalue analysis	Eigenvalue	Theoretical results
25	Vibration 4	Dynamic solver	Linear dynamic	Theoretical results
Straigh tower				
Example No.	Example name	Features tested	Analysis type	Method of Verification
26	General load 8	Automatic self weight	Nonlinear static	Frame and Truss element comparison
		Concentrated load		
27	Eigenvalue problem 8	Eigenvalue analysis	Eigenvalue	Frame and Truss element comparison

Example No. 1:

This 3D beam-column example (Figure B.1) is presented to verify the frame element behavior under self weight and also response under only external load (not including the self weight) through a linear static analysis. The Finite Element program ANSYS is used to verify the automatic self-weight analysis, and Weaver and Gere (1980) to verify the external load. The model properties are

$$\begin{aligned}
 E &= 2.00 \times 10^{10} \text{ kN/m} & I_x &= 2.00 \times 10^{-03} \text{ m}^4 & \rho &= 7.86 \text{ ton/m}^3 \\
 \nu &= 0.25 & I_y &= 1.00 \times 10^{-03} \text{ m}^4 & g_y &= -9.81 \text{ m/s}^2 \\
 A &= 0.01 \text{ m}^2 & I_z &= 1.00 \times 10^{-03} \text{ m}^4 & &
 \end{aligned}$$

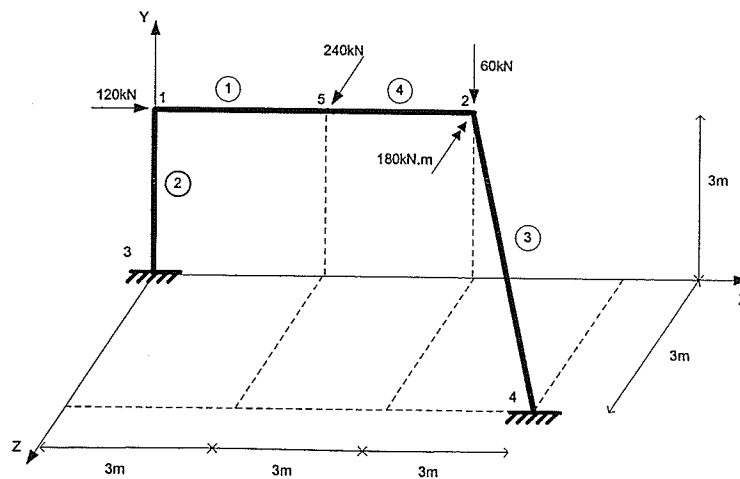


Figure B.1 - Beam-column element (example 1).

Results from ANSYS (self weight linear static analysis only):

PRINT ELEMENT TABLE ITEMS PER ELEMENT

***** POST1 ELEMENT TABLE LISTING *****

STAT	CURRENT
ELEM	SAXL
1	-197.37
2	-556.46
3	-224.23
4	-197.37

PRINT U NODAL SOLUTION PER NODE

***** POST1 NODAL DEGREE OF FREEDOM LISTING *****

LOAD STEP= 1 SUBSTEP= 1
TIME= 1.0000 LOAD CASE= 0

THE FOLLOWING DEGREE OF FREEDOM RESULTS ARE IN THE GLOBAL COORDINATE SYSTEM

NODE	UX	UY	UZ	USUM
1	0.12826E-04	-0.66119E-05	-0.46335E-04	0.48530E-04
2	0.69051E-05	-0.17625E-03	-0.16786E-03	0.24349E-03
3	0.0000	0.0000	0.0000	0.0000
4	0.0000	0.0000	0.0000	0.0000
5	0.98657E-05	-0.11817E-03	-0.11901E-03	0.16801E-03

PRINT ROT NODAL SOLUTION PER NODE

***** POST1 NODAL DEGREE OF FREEDOM LISTING *****

LOAD STEP= 1 SUBSTEP= 1
TIME= 1.0000 LOAD CASE= 0

THE FOLLOWING DEGREE OF FREEDOM RESULTS ARE IN THE GLOBAL COORDINATE SYSTEM

NODE	ROTX	ROTY	ROTZ	RSUM
1	-0.26877E-04	0.20171E-04	-0.23354E-04	0.40922E-04
2	-0.63969E-04	0.42854E-05	-0.50480E-05	0.64311E-04
3	0.0000	0.0000	0.0000	0.0000
4	0.0000	0.0000	0.0000	0.0000
5	-0.45423E-04	0.24268E-04	-0.35309E-04	0.62441E-04

PRINT F REACTION SOLUTIONS PER NODE

***** POST1 TOTAL REACTION SOLUTION LISTING *****

LOAD STEP= 1 SUBSTEP= 1
TIME= 1.0000 LOAD CASE= 0

THE FOLLOWING X,Y,Z SOLUTIONS ARE IN THE GLOBAL COORDINATE SYSTEM

NODE	FX	FY	FZ
3	1.9737	5.5646	0.53509
4	-1.9737	5.3816	-0.53509

PRINT M SUMMED NODAL LOADS

***** POST1 SUMMED TOTAL NODAL LOADS LISTING *****

LOAD STEP= 1 SUBSTEP= 1
TIME= 1.0000 LOAD CASE= 0

THE FOLLOWING X,Y,Z SOLUTIONS ARE IN THE GLOBAL COORDINATE SYSTEM

NODE	MX	MY	MZ
3	-2.5944	1.0758	1.4037
4	-7.5406	-2.1811	3.1024

SADAP results (automatic self weight analysis):

EXAMPLE_1_P.357-MATR
NONLINEAR STATIC AND DYNAMIC ANALYSIS OF STRUCTURES

NODAL POINTS:

NODE	X	Y	Z
1	0.0000	3.0000	0.0000
2	6.0000	3.0000	0.0000
3	0.0000	0.0000	0.0000
4	9.0000	0.0000	3.0000
5	3.0000	3.0000	0.0000

RESTRAINTS:

NODE	TRANS.X	TRANS.Y	TRANS.Z	ROT.X	ROT.Y	ROT.Z
3	1	1	1	1	1	1
4	1	1	1	1	1	1

AUTOMATIC SELF-WEIGHT ANALYSIS

FRAME ELEMENTS:

ELEM.	NODE1	NODE2	E	V	A	IX	IY	IZ	FP	QX	QY	QZ	ESP.MASS	FLANG
1	1	5	0.200E+09	0.25E+00	0.100E-01	0.200E-02	0.100E-02	0.100E-02	0.00	0.00	0.00	0.00	7.86	0.
2	3	1	0.200E+09	0.25E+00	0.100E-01	0.200E-02	0.100E-02	0.100E-02	0.00	0.00	0.00	0.00	7.86	0.
3	2	4	0.200E+09	0.25E+00	0.100E-01	0.200E-02	0.100E-02	0.100E-02	0.00	0.00	0.00	0.00	7.86	0.
4	5	2	0.200E+09	0.25E+00	0.100E-01	0.200E-02	0.100E-02	0.100E-02	0.00	0.00	0.00	0.00	7.86	0.

LOAD STEP= 1

FRAME ELEMENTS INTERNAL FORCES:

ELEM.	NODE	N	QY	QZ	T	MY	MZ
1	1	1.9737	3.2514	0.53509	0.98913	-1.0758	4.5175
	5	-1.9737	-0.93816	-0.53509	-0.98913	-0.52951	1.7668
2	3	5.5646	-1.9737	0.53509	-1.0758	-2.5944	-1.4037
	1	-3.2514	1.9737	-0.53509	1.0758	0.98913	-4.5175
3	2	2.2423	-0.98496E-01	-1.0173	-1.3032	1.6931	-1.4854
	4	-4.5555	3.3699	1.0173	1.3032	3.5927	-7.5257
4	5	1.9737	0.93816	0.53509	0.98913	0.52951	-1.7668
	2	-1.9737	1.3750	-0.53509	-0.98913	-2.1348	1.1115

SUPPORT REACTIONS:

NODE	RX	RY	RZ	MX	MY	MZ
3	1.9737	5.5646	0.53509	2.5944	-1.0758	-1.4037
4	-1.9737	5.3816	-0.53509	7.5406	2.1811	-3.1024

TOTAL DISPLACEMENTS:

NODE	TRANS.X	TRANS.Y	TRANS.Z	ROT.X	ROT.Y	ROT.Z
1	0.000012826	-0.000006612	-0.000046335	-0.000026877	0.000020171	-0.000023354
2	0.000006905	-0.000176252	-0.000167861	-0.000063969	0.000004285	-0.000005048
3	0.000000000	0.000000000	0.000000000	0.000000000	0.000000000	0.000000000
4	0.000000000	0.000000000	0.000000000	0.000000000	0.000000000	0.000000000
5	0.000009866	-0.000118173	-0.000119012	-0.000045423	0.000024268	-0.000035309

Results from Weaver and Gere, 1980 (only external load):

Join Displacement						
Join	Ux	Uy	Uz	Rx	Ry	Rz
1	-8.594E-04	5.776E-05	5.008E-03	2.393E-03	-1.623E-03	6.813E-04
2	-1.176E-03	3.253E-03	5.256E-03	1.288E-03	1.721E-03	-7.715E-04
3	0.000E+00	0.000E+00	0.000E+00	0.000E+00	0.000E+00	0.000E+00
4	0.000E+00	0.000E+00	0.000E+00	0.000E+00	0.000E+00	0.000E+00

Member End-Actions							
Member	Node	Fx	Fy	Fz	Mx	My	Mz
1	1	105.548	-38.509	-126.013	29.464	86.569	-67.100
	2	-105.548	38.509	-113.987	-29.464	-50.491	-163.954
2	3	-38.509	14.452	-126.013	86.569	348.575	-23.744
	1	38.509	-14.452	126.013	-86.569	29.464	67.100
3	2	183.623	9.192	5.967	-21.404	46.703	-32.181
	4	-183.623	-9.192	-5.967	21.404	-77.711	79.946

Support Reactions						
Node	Fx	Fy	Fz	Mx	My	Mz
3	-14.452	-38.509	-126.013	-348.575	86.569	-23.744
4	-105.548	98.509	-113.987	-75.898	-75.808	37.163

SADAP results (only external load):

LOAD STEP= 1

FRAME ELEMENTS INTERNAL FORCES:

ELEM.	NODE	N	QY	QZ	T	MY	MZ
1	1	105.55	-38.509	-126.01	29.464	86.569	-67.100
	5	-105.55	38.509	126.01	-29.464	291.47	-48.427
2	3	-38.509	14.452	-126.01	86.569	348.58	-23.744
	1	38.509	-14.452	126.01	-86.569	29.464	67.100
3	2	183.62	9.1924	5.9674	-21.404	46.703	-32.181
	4	-183.62	-9.1924	-5.9674	21.404	-77.711	79.946
4	5	105.55	-38.509	113.99	29.464	-291.47	48.427
	2	-105.55	38.509	-113.99	-29.464	-50.491	-163.95

SUPPORT REACTIONS:

NODE	RX	RY	RZ	MX	MY	MZ
3	-14.452	-38.509	-126.01	-348.58	86.569	-23.744
4	-105.55	98.509	-113.99	-75.898	-75.808	37.163

TOTAL DISPLACEMENTS:

NODE	TRANS.X	TRANS.Y	TRANS.Z	ROT.X	ROT.Y	ROT.Z
1	-0.000859410	0.000057764	0.005007645	0.002393332	-0.001623169	0.000681331
2	-0.001176053	0.003253162	0.005255517	0.001288428	0.001720936	-0.000771469
3	0.000000000	0.000000000	0.000000000	0.000000000	0.000000000	0.000000000
4	0.000000000	0.000000000	0.000000000	0.000000000	0.000000000	0.000000000
5	-0.001017731	0.002745063	0.008989659	0.001840880	-0.000086410	0.000821384

Verification:

P.D. = 0.00% for all the displacements, internal forces and support reactions.

Example No. 2:

The purpose of this example is to verify the local axis rotation of the 3D beam-column element. SADAP results were compared with Weaver and Gere (1980) and the commercial program ANSYS. The model properties are

$$\begin{aligned}
 E &= 10000 \text{ ksi} & I_x &= 64 \text{ in}^4 \\
 \nu &= 0.25 & I_y &= 28 \text{ in}^4 \\
 A &= 9 \text{ in}^2 & I_z &= 80 \text{ in}^4
 \end{aligned}$$

The third node of the element 2, 3 and 5 is located at: 128,96,0

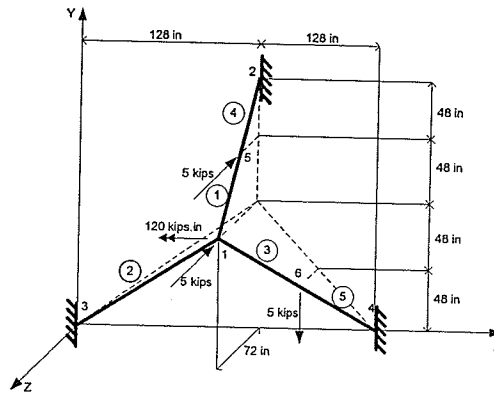


Figure B.2 - Beam-column element (example 2).

Results from Weaver and Gere (1980):

Join Displacement							
Join	Ux	Uy	Uz	Rx	Ry	Rz	
1	-2.176E-04	-4.062E-03	-1.674E-02	-5.202E-03	1.870E-04	-4.495E-03	
2	0.000E+00	0.000E+00	0.000E+00	0.000E+00	0.000E+00	0.000E+00	
3	0.000E+00	0.000E+00	0.000E+00	0.000E+00	0.000E+00	0.000E+00	
4	0.000E+00	0.000E+00	0.000E+00	0.000E+00	0.000E+00	0.000E+00	
Member End-Actions							
Member	Node	Fx	Fy	Fz	Mx	My	Mz
1	1	3.594	0.178	0.406	6.073	-32.492	-84.001
	2	-6.594	3.822	-0.406	-6.073	-16.233	-134.638
2	3	4.744	0.485	-0.131	8.080	7.610	27.616
	1	-4.744	-0.485	0.131	-8.080	15.390	57.444
3	1	3.214	0.178	1.678	-2.995	-50.178	-24.964
	4	-5.950	1.054	2.322	2.995	106.594	-51.865
Support Reactions							
Node	Fx	Fy	Fz	Mx	My	Mz	
2	-0.406	-2.982	7.014	-134.638	14.599	-9.343	
3	3.699	2.610	1.505	-8.177	28.387	-3.624	
4	-3.293	5.372	1.480	-63.927	-16.885	-98.434	

ANSYS results:

```

PRINT U      NODAL SOLUTION PER NODE

***** POST1 NODAL DEGREE OF FREEDOM LISTING *****

LOAD STEP=   1   SUBSTEP=   1
TIME=   1.0000   LOAD CASE=   0

THE FOLLOWING DEGREE OF FREEDOM RESULTS ARE IN THE GLOBAL COORDINATE SYSTEM

```

NODE	UX	UY	UZ	USUM
1	-0.21807E-03	-0.40618E-02	-0.16737E-01	0.17224E-01
2	0.0000	0.0000	0.0000	0.0000
3	0.0000	0.0000	0.0000	0.0000
4	0.0000	0.0000	0.0000	0.0000
5	0.52151E-01	-0.75051E-01	-0.10739	0.14102
6	-0.28168	-0.45366	0.89995E-01	0.54153

SADAP results:

```

LOAD STEP= 1

FRAME ELEMENTS INTERNAL FORCES:

```

ELEM.	NODE	N	QY	QZ	T	MY	MZ
1	1	3.5945	0.17801	0.40605	6.0732	-32.492	-84.001
	5	-3.5945	-0.17801	-0.40605	-6.0732	8.1294	94.681
2	3	4.7447	0.48480	-0.13109	8.0797	7.6099	27.616
	1	-4.7447	-0.48480	0.13109	-8.0797	15.390	57.444
3	1	3.2136	0.17766	1.6785	-2.9952	-50.178	-24.964
	6	-3.2136	-0.17766	-1.6785	2.9952	-97.068	40.550
4	5	6.5945	-3.8220	0.40605	6.0732	-8.1294	-94.681
	2	-6.5945	3.8220	-0.40605	-6.0732	-16.233	-134.64
5	6	5.9494	-1.0534	-2.3215	-2.9952	97.068	-40.550
	4	-5.9494	1.0534	2.3215	2.9952	106.59	-51.864

```

SUPPORT REACTIONS:

```

NODE	RX	RY	RZ	MX	MY	MZ
2	-0.40605	-2.9824	7.0143	-134.64	-14.599	-9.3428
3	3.6992	2.6106	1.5050	-8.1767	28.387	-3.6240
4	-3.2932	5.3718	1.4808	-63.927	-16.885	-98.434

```

TOTAL DISPLACEMENTS:

```

NODE	TRANS.X	TRANS.Y	TRANS.Z	ROT.X	ROT.Y	ROT.Z
1	-0.000218067	-0.004061807	-0.016736808	-0.005202205	0.000187037	-0.004495317
2	0.000000000	0.000000000	0.000000000	0.000000000	0.000000000	0.000000000
3	0.000000000	0.000000000	0.000000000	0.000000000	0.000000000	0.000000000
4	0.000000000	0.000000000	0.000000000	0.000000000	0.000000000	0.000000000
5	0.052151438	-0.075050749	-0.107394865	0.001498383	0.001659697	-0.000159420
6	-0.281675223	-0.453662190	0.089995388	0.000113304	0.000690493	0.001781987

Verification:

Even though there is a small difference on the x translation of node 1 when compared with Weaver and Gere (1980), the values were matching with ANSYS. This is due to a round off error in Weaver and Gere (1980). The *P.D.* = 0.00% for all the displacements, internal forces and support reactions.

Example No. 3:

The purpose of this example is to verify the critical buckling load of the 3D beam-column element; the program is expected to stop at the buckling load.

Theoretical values are used as comparison, the model properties are

$$\begin{aligned}
 E &= 2.00 \times 10^{10} \text{ kN/m}^2 & I_x &= 2.00 \times 10^{-03} \text{ m}^4 & P_{cr \text{ Linear}} &= \frac{\pi^2 EI}{(2L)^2} = 13707.784 \text{ kN} \\
 \nu &= 0.25 & I_y &= 1.00 \times 10^{-03} \text{ m}^4 & P_{cr \text{ Nonlinear}} &= \frac{\pi^2 EI}{\left[2 \left(L - \frac{P_{cr \text{ Nonlinear}} L}{EA} \right) \right]^2} = 13900.332 \text{ kN} \\
 A &= 0.01 \text{ m}^2 & I_z &= 1.00 \times 10^{-03} \text{ m}^4 & &
 \end{aligned}$$

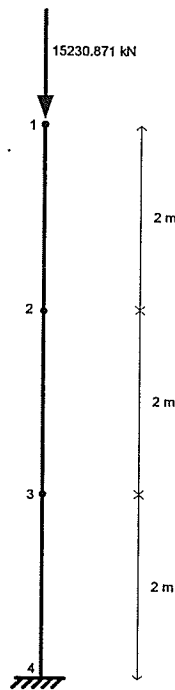


Figure B.3 - Beam-column element (example 3).

SADAP results:

LOAD STEP= 9128

FRAME ELEMENTS INTERNAL FORCES:

ELEM.	NODE	N	QY	QZ	T	MY	MZ
1	1	13901.	0.0000	0.0000	0.0000	0.0000	0.0000
	2	-13901.	0.0000	0.0000	0.0000	0.0000	0.0000
2	2	13901.	0.0000	0.0000	0.0000	0.0000	0.0000
	3	-13901.	0.0000	0.0000	0.0000	0.0000	0.0000
3	3	13901.	0.0000	0.0000	0.0000	0.0000	0.0000
	4	-13901.	0.0000	0.0000	0.0000	0.0000	0.0000

SUPPORT REACTIONS:

NODE	RX	RY	RZ	MX	MY	MZ
4	0.0000	13901.	0.0000	0.0000	0.0000	0.0000

Displacement of node 1:

0.0000000000 -0.0415590660 0.0000000000 0.0000000000 0.0000000000 0.0000000000

LOAD STEP= 9129

Verification:

$$P.D. = 4.808 \times 10^{-5} \%$$

Example No. 4:

The purpose of this example is to verify the torsion, bending and axial natural frequencies of a circular cantilever using 3D beam-column elements. The model properties are

$$\begin{aligned}
 E &= 2.00 \times 10^{+08} \text{ kN/m}^2 & I_x &= 4.97 \times 10^{-05} \text{ m}^4 & \rho &= 8 \text{ ton/m}^3 \\
 \nu &= 0.30 & I_y &= 2.485 \times 10^{-05} \text{ m}^4 & & \\
 A &= 0.01 \text{ m}^2 & I_z &= 2.485 \times 10^{-05} \text{ m}^4 & &
 \end{aligned}$$

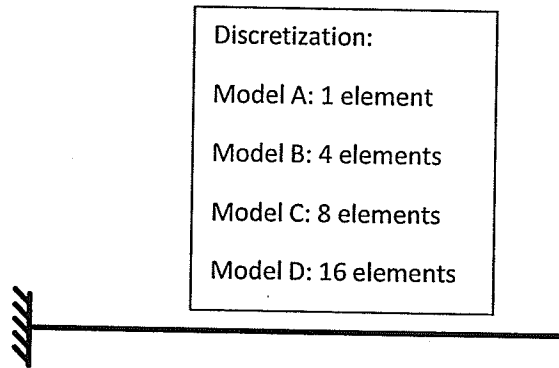


Figure B.4 - Beam-column element (example 4).

Theoretical results (Militano, 2000):

$$w_{n,bending} = (\beta_n L)^2 \sqrt{\frac{EI}{A\rho L^4}}$$

$$w_{n,torsion} = \frac{2n-1}{2L} \pi \sqrt{\frac{G}{\rho}}$$

$$w_{n,axial} = \frac{2n-1}{2L} \pi \sqrt{\frac{E}{\rho}}$$

$$\beta_n L = 1.875, 4.694, 7.854, 10.998$$

Militano (2000) results:

Natural circular frequency [rad/s]												
Mode Shape	Bending	Bending	Bending	Bending	Torsion	Axial	Torsion	Axial	Torsion	Torsion	Axial	Axial
Exact Solution	10.30	64.55	180.72	354.36	608.85	981.75	1826.56	2945.24	3044.27	4261.98	4908.74	6872.23
1 Element	10.35	-	-	-	671.00	1082.53	-	-	-	-	-	-
4 Elements	10.30	64.63	182.16	359.36	613.00	988.07	1933.00	3116.99	3511.00	5078.00	5662.13	8187.93
8 Elements	10.30	64.56	180.87	355.01	610.00	983.32	1853.00	2987.99	3167.00	4599.00	5107.44	7416.40
16 Elements	10.30	64.56	180.77	354.27	609.00	982.14	1833.00	2955.90	3075.00	4346.00	4958.16	7008.14

SADAP results and verification:

Natural circular frequency [rad/s]												
Mode Shape	Bending	P.D.	Bending	P.D.	Bending	P.D.	Bending	P.D.	Torsion	P.D.	Axial	P.D.
Exact Solution	10.30	-	64.55	-	180.72	-	354.36	-	608.85	-	981.75	-
1 Element	10.35	0.49%	-	-	-	-	-	-	671.36	10.27%	1082.53	10.27%
4 Elements	10.30	0.01%	64.63	0.12%	182.15	0.79%	359.35	1.41%	612.77	0.64%	988.07	0.64%
8 Elements	10.30	0.01%	64.56	0.01%	180.86	0.08%	355.00	0.18%	609.83	0.16%	983.33	0.16%
16 Elements	10.30	0.01%	64.55	0.00%	180.76	0.02%	354.26	-0.03%	609.10	0.04%	982.14	0.04%

Natural circular frequency [rad/s]												
Mode Shape	Torsion	P.D.	Axial	P.D.	Torsion	P.D.	Torsion	P.D.	Axial	P.D.	Axial	P.D.
Exact Solution	1826.56	-	2945.24	-	3044.27	-	4261.98	-	4908.74	-	6872.23	-
1 Element	-	-	-	-	-	-	-	-	-	-	-	-
4 Elements	1933.08	5.83%	3117.00	5.83%	3511.50	15.35%	5077.94	19.15%	5662.13	15.35%	8187.93	19.15%
8 Elements	1853.07	1.45%	2987.99	1.45%	3167.50	4.05%	4599.45	7.92%	5107.44	4.05%	7416.40	7.92%
16 Elements	1833.17	0.36%	2955.90	0.36%	3074.92	1.01%	4346.26	1.98%	4958.16	1.01%	7008.14	1.98%

Example No. 5:

The purpose of this example is to verify the variation of frequency with axial force in a column with both ends pinned (3D beam-column element).

The program results were compared with Przemieniecki (1985). A non-linear free vibration analysis was performed.

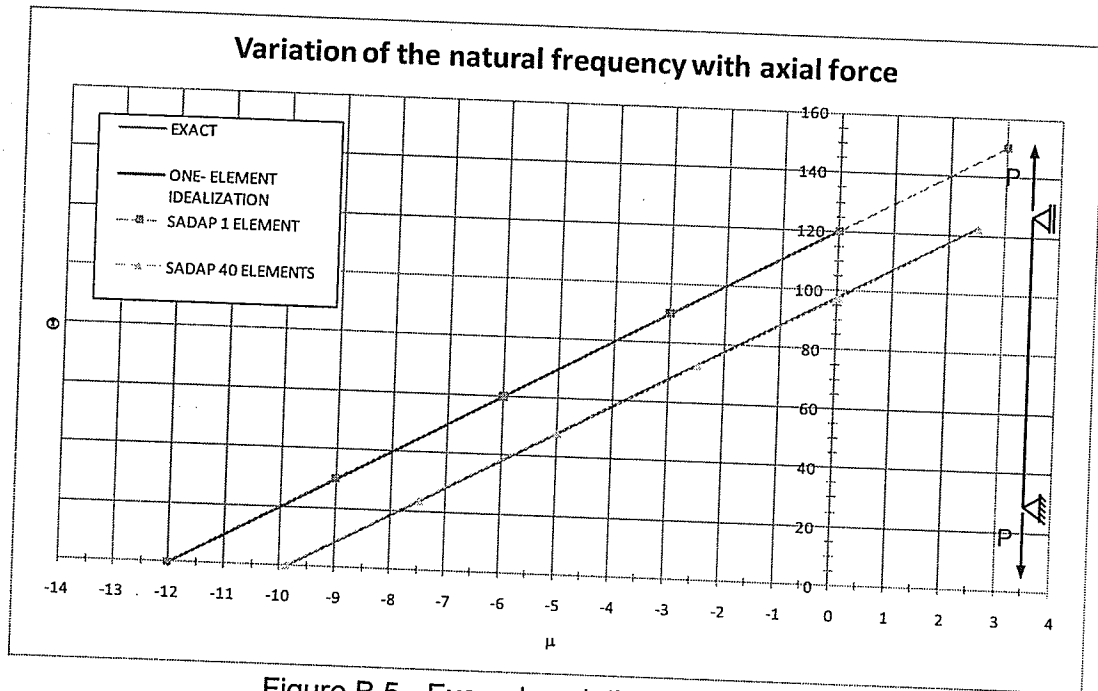


Figure B.5 - Example solution (example 5).

Where:

$$\Theta = w^2 \rho \frac{AL^4}{EI}$$

$$\mu = \frac{PL^2}{EI}$$

Verification:

$$P.D._{MAX} = -0.65\%$$

Example No. 6:

The purpose of this example is to verify the dynamic solver. Model properties, dynamic force, and displacement solution were taken from Battista (2007-C) and are given by

$$\begin{aligned}
 E &= 2.10 \times 10^{+08} \text{ kN/m}^2 & I_x &= 2.716 \times 10^{-04} \text{ m}^4 & \rho &= 7.85 \text{ ton/m}^3 \\
 \nu &= 0.30 & I_y &= 1.858 \times 10^{-04} \text{ m}^4 & \xi &= 0.01 \\
 A &= 8.06 \times 10^{-03} \text{ m}^2 & I_z &= 1.858 \times 10^{-04} \text{ m}^4 & &
 \end{aligned}$$

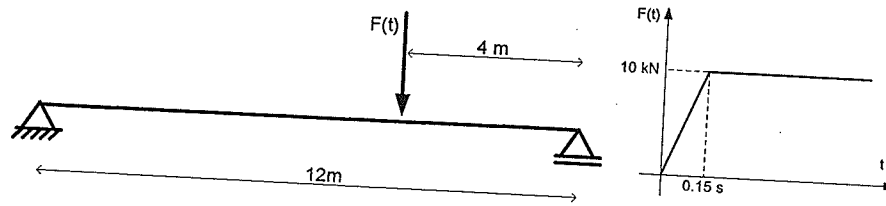


Figure A.6 - Beam-column element (example 6).

Theoretical solution:

$$w_n = n^2 \pi^2 \sqrt{\frac{EI}{\rho AL^4}} = 53.82 \text{ rad/s}, 215.29 \text{ rad/s}, 484.41 \text{ rad/s}$$

Battista (2007-C) solution (displacements where the load is applied):

$$u_y(0.15 \text{ s}) = 0.00643 \text{ m}$$

$$u_{y \text{ MAXIMUM}} = 0.00849 \text{ m}$$

SADAP solution and verification (using 30 elements):

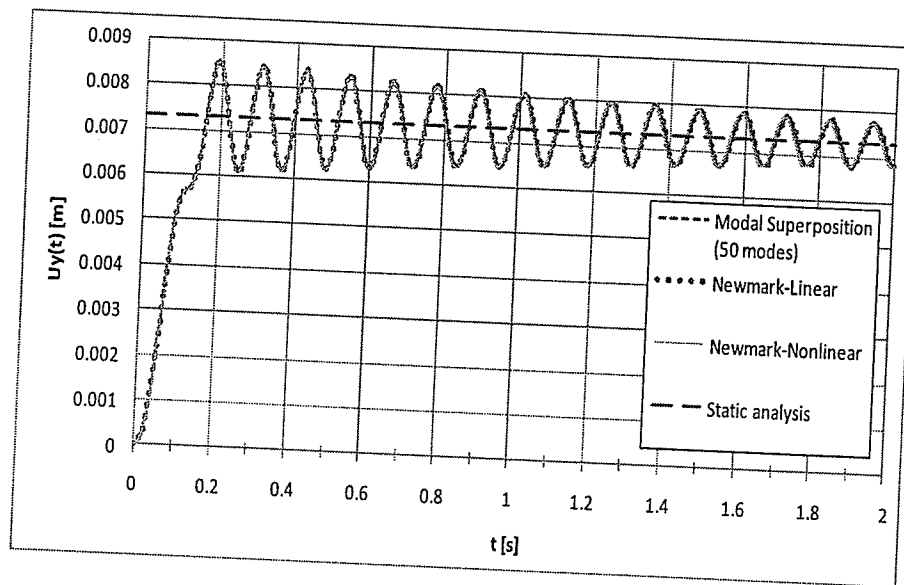


Figure B.7 - Example solution (example 6).

$$w_1 = 53.82 \text{ rad/s} \therefore P.D. = 0.00\%$$

$$w_2 = 215.29 \text{ rad/s} \therefore P.D. = 0.00\%$$

$$w_3 = 484.41 \text{ rad/s} \therefore P.D. = 0.00\%$$

Modal Superposition ($\Delta t = 0.0001$ s and 50 modes):

$$u_y(0.15 \text{ s}) = 0.00650 \text{ m} \therefore P.D. = 1.09\%$$

$$u_{y \text{ MAXIMUM}} = 0.00854 \text{ m} \therefore P.D. = 0.59\%$$

Newmark-Linear ($\Delta t = 0.0001$ s):

$$u_y(0.15 \text{ s}) = 0.00649 \text{ m} \therefore P.D. = 0.93\%$$

$$u_{y \text{ MAXIMUM}} = 0.00854 \text{ m} \therefore P.D. = 0.59\%$$

Newmark-Nonlinear ($\Delta t = 0.0001$ s):

$$u_y(0.15 \text{ s}) = 0.00648 \text{ m} \therefore P.D. = 0.78\%$$

$$u_{y \text{ MAXIMUM}} = 0.00852 \text{ m} \therefore P.D. = 0.35\%$$

Example No. 7:

This example is presented to verify the 3D truss element. Two analyses were performed: self-weight and only external loads. The results from the former were compared with the commercial Finite Element program ANSYS, while the results from the latter were compared with theoretical results from Weaver and Gere (1980). The model properties are

$$E = 8.00 \times 10^{+07} \text{ kN/m}^2$$

$$A = 0.01 \text{ m}^2$$

$$\rho = 25 \text{ ton/m}^3$$

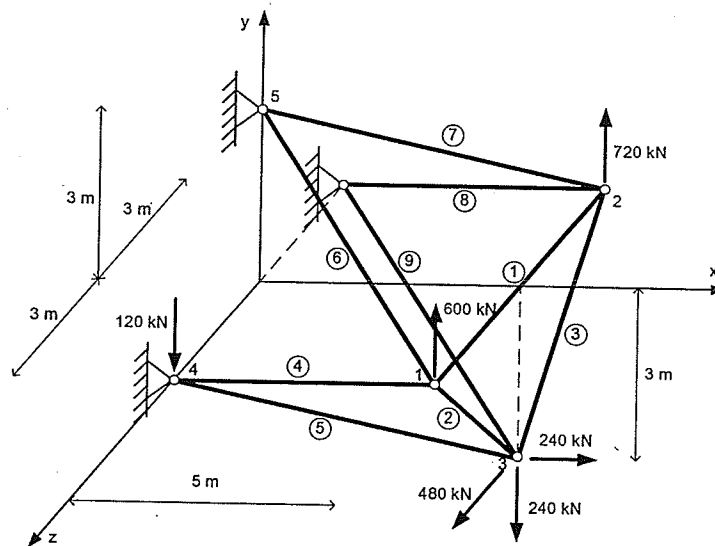


Figure B.8 - Truss element (example 7).

Results from ANSYS for self-weight:

PRINT U NODAL SOLUTION PER NODE

***** POST1 NODAL DEGREE OF FREEDOM LISTING *****

LOAD STEP= 1 SUBSTEP= 1
TIME= 1.0000 LOAD CASE= 0

THE FOLLOWING DEGREE OF FREEDOM RESULTS ARE IN THE GLOBAL COORDINATE SYSTEM

NODE	UX	UY	UZ	USUM
1	-0.32390E-03	-0.20706E-02	0.31303E-03	0.21190E-02
2	-0.32390E-03	-0.20706E-02	0.31303E-03	0.21190E-02
3	-0.15656E-02	-0.26094E-02	-0.32526E-18	0.30431E-02
4	0.0000	0.0000	0.0000	0.0000
5	0.0000	0.0000	0.0000	0.0000
6	0.0000	0.0000	0.0000	0.0000

PRINT ELEMENT TABLE ITEMS PER ELEMENT

***** POST1 ELEMENT TABLE LISTING *****

STAT	CURRENT	AREA	FORCE
ELEM	SAXL		
1	-8347.4	0.01	-83.474
2	3010.1	0.01	30.101
3	3010.1	0.01	30.101
4	-5182.4	0.02	-103.648
5	1.82E-12	0.02	3.6308E-14
6	6796.7	0.02	135.934
7	6796.7	0.02	135.934
8	-5182.4	0.02	-103.648
9	-1.82E-12	0.02	-3.6308E-14

PRINT F SUMMED NODAL LOADS

***** POST1 SUMMED TOTAL NODAL LOADS LISTING *****

LOAD STEP= 1 SUBSTEP= 1
TIME= 1.0000 LOAD CASE= 0

THE FOLLOWING X,Y,Z SOLUTIONS ARE IN THE GLOBAL COORDINATE SYSTEM

NODE	FX	FY	FZ
1		-0.28422E-13	
2		-0.28422E-13	
3		0.47433E-13	
4	-103.65	-28.345	-0.16611E-13
5	207.30	-156.54	0.42633E-13
6	-103.65	-28.345	-0.16611E-13

SADAP solution (automatic self-weight analysis):

TRUSS ELEMENTS INTERNAL FORCES: (TENSION +)

ELEM.	N NODE 1	N NODE 2
1	-83.474	-83.474
2	33.780	26.422
3	26.422	33.780
4	-103.65	-103.65
5	7.3575	-7.3575
6	143.29	128.58
7	143.29	128.58
8	-103.65	-103.65
9	7.3575	-7.3575

SUPPORT REACTIONS:

NODE	RX	RY	RZ	MX	MY	MZ
1	0.0000	0.0000	0.0000	0.0000	0.0000	0.0000
2	0.0000	0.0000	0.0000	0.0000	0.0000	0.0000
3	0.0000	0.0000	0.0000	0.0000	0.0000	0.0000
4	103.65	28.345	-0.29907E-13	0.0000	0.0000	0.0000
5	-207.30	156.54	-0.35527E-14	0.0000	0.0000	0.0000
6	103.65	28.345	0.26937E-13	0.0000	0.0000	0.0000

TOTAL DISPLACEMENTS:

NODE	TRANS.X	TRANS.Y	TRANS.Z	ROT.X	ROT.Y	ROT.Z
1	-0.000323903	-0.002070609	-0.000313027	0.000000000	0.000000000	0.000000000
2	-0.000323903	-0.002070609	0.000313027	0.000000000	0.000000000	0.000000000
3	-0.001565637	-0.002609394	0.000000000	0.000000000	0.000000000	0.000000000
4	0.000000000	0.000000000	0.000000000	0.000000000	0.000000000	0.000000000
5	0.000000000	0.000000000	0.000000000	0.000000000	0.000000000	0.000000000
6	0.000000000	0.000000000	0.000000000	0.000000000	0.000000000	0.000000000

Results from Weaver and Gere (1980) for external loads only:

Join Displacement			
Join	Ux	Uy	Uz
1	3.031E-01	2.088E-02	4.436E-03
2	3.344E-03	1.794E-02	2.059E-04
3	1.346E-02	2.102E-02	4.112E-03
4	0.000E+00	0.000E+00	0.000E+00
5	0.000E+00	0.000E+00	0.000E+00
6	0.000E+00	0.000E+00	0.000E+00
Member End-Actions			
Member	N1	N2	
1	-564.000	564.000	
2	-25.456	25.456	
3	-110.309	110.309	
4	-970.000	970.000	
5	301.642	-301.642	
6	1272.143	-1272.143	
7	1403.292	-1403.292	
8	-1070.000	1070.000	
9	-616.399	616.399	
Support Reactions			
Node	Fx	Fy	Fz
2	-740.000	-18.000	-138.000
3	2040.000	-1224.000	-60.000
4	-1540.000	282.000	-282.000

SADAP results for external loads only:

LOAD STEP= 1

TRUSS ELEMENTS INTERNAL FORCES: (TENSION +)

ELEM.	N NODE 1	N NODE 2
1	564.00	564.00
2	25.456	25.456
3	110.31	110.31
4	970.00	970.00
5	-301.64	-301.64
6	-1272.1	-1272.1
7	-1403.3	-1403.3
8	1070.0	1070.0
9	616.40	616.40

SUPPORT REACTIONS:

NODE	RX	RY	RZ	MX	MY	MZ
1	0.0000	0.0000	0.0000	0.0000	0.0000	0.0000
2	0.0000	0.0000	0.0000	0.0000	0.0000	0.0000
3	0.0000	0.0000	0.0000	0.0000	0.0000	0.0000
4	-740.00	-18.000	-138.00	0.0000	0.0000	0.0000
5	2040.0	-1224.0	-60.000	0.0000	0.0000	0.0000
6	-1540.0	282.00	-282.00	0.0000	0.0000	0.0000

TOTAL DISPLACEMENTS:

NODE	TRANS.X	TRANS.Y	TRANS.Z	ROT.X	ROT.Y	ROT.Z
1	0.003031250	0.020884223	0.004435858	0.000000000	0.000000000	0.000000000
2	0.003343750	0.017938215	0.000205858	0.000000000	0.000000000	0.000000000
3	0.013456171	0.021017102	0.004112060	0.000000000	0.000000000	0.000000000
4	0.000000000	0.000000000	0.000000000	0.000000000	0.000000000	0.000000000
5	0.000000000	0.000000000	0.000000000	0.000000000	0.000000000	0.000000000
6	0.000000000	0.000000000	0.000000000	0.000000000	0.000000000	0.000000000

Verification:

P.D. = 0.00% for all the displacements, internal forces and support reactions.

Example No. 8:

The purpose of this example is to verify the critical buckling load of the 3D truss element; a non-linear buckling analysis was performed. Results were compared with theoretical formulation from Timoshenko (Levy and Spillers, 2003) and the model properties are

$$\begin{aligned}
 E &= 2.00 \times 10^{10} \text{ kN/m}^2 & \alpha &= 45^\circ & F &\ll P_{cr} \\
 A &= 0.001 \text{ m}^2 & L &= 2 \text{ m} & F &= 100 \text{ kN} \\
 A_1 &= 0.0005 \text{ m}^2 & L_1 &= \sqrt{2} \text{ m} & P &= 20000 \text{ kN} \\
 P_{cr} &= \frac{EA}{\cot^2(\alpha) \left(3 + \frac{2L_1 A}{LA_1 \cos^2(\alpha)} \right)} = 16092.5768 \text{ kN}
 \end{aligned}$$

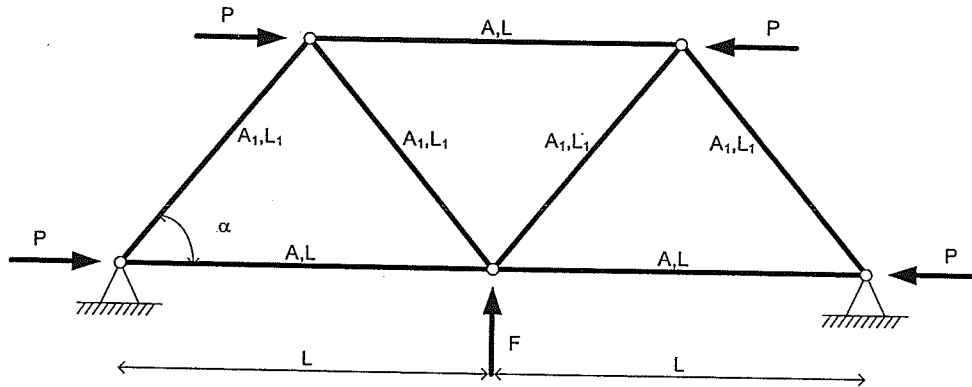


Figure B.9 - Truss element (example 8).

SADAP results:

LOAD STEP= 8080

TRUSS ELEMENTS INTERNAL FORCES: (TENSION +)

ELEM.	N NODE 1	N NODE 2
1	-16875.	-16875.
2	-16875.	-16875.
3	-14685.	-14685.
4	1107.5	1107.5
5	-1158.3	-1158.3
6	-1158.3	-1158.3
7	1107.5	1107.5

SUPPORT REACTIONS:

NODE	RX	RY	RZ	MX	MY	MZ
1	16158.	-40.395	0.0000	0.0000	0.0000	0.0000
2	0.0000	0.0000	0.0000	0.0000	0.0000	0.0000
3	0.0000	0.0000	0.0000	0.0000	0.0000	0.0000
4	0.0000	0.0000	0.0000	0.0000	0.0000	0.0000
5	0.0000	-40.395	0.0000	0.0000	0.0000	0.0000

LOAD STEP= 8081

Verification:

P.D. = 0.41%

Example No. 9:

The purpose of this example is to verify the natural frequencies of the 3D truss element. A free vibration analysis was carried out; model properties and theoretical results were taken from (Paz and Leigh, 2003) and are given by

$$E = 3.00 \times 10^{10} \text{ lb/in}^2 \quad A = 0.001 \text{ in}^2 \quad L = 60 \text{ in} \quad m = 0.1 \text{ lb} \times \text{s}^2/\text{in}^2$$

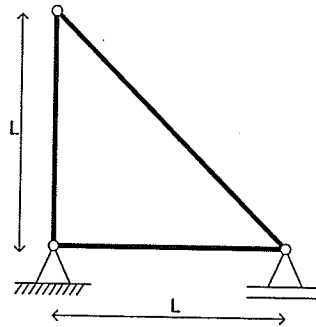


Figure B.10 - Truss element (example 9).

Results from Paz and Leigh (2003):

$$\omega = \begin{pmatrix} 415 \\ 1034 \\ 1526 \end{pmatrix} \text{ rad/s}$$

$$\phi_{\text{normalized}} = \begin{bmatrix} 1.000 & 0.182 & -0.656 \\ 0.216 & 1.000 & 0.656 \\ 0.274 & -0.729 & 1.000 \end{bmatrix}$$

SADAP results:

MODE	MODAL MASS	FREQ[RAD]	FREQ[HZ]
1	6.19486	415.42320	66.11665
2	7.17003	1033.70420	164.51913
3	7.11610	1526.03014	242.87523

MODAL SHAPES

MODAL SHAPE: 1

NODE	DX	DY	DZ	RX	RY	RZ
1	0.00000	0.00000	0.00000	0.00000	0.00000	0.00000
2	1.00000	0.21607	0.00000	0.00000	0.00000	0.00000
3	0.27464	0.00000	0.00000	0.00000	0.00000	0.00000

MODAL SHAPE: 2

NODE	DX	DY	DZ	RX	RY	RZ
1	0.00000	0.00000	0.00000	0.00000	0.00000	0.00000
2	0.18222	1.00000	0.00000	0.00000	0.00000	0.00000
3	-0.72762	0.00000	0.00000	0.00000	0.00000	0.00000

MODAL SHAPE: 3

NODE	DX	DY	DZ	RX	RY	RZ
1	0.00000	0.00000	0.00000	0.00000	0.00000	0.00000
2	-0.65607	0.65398	0.00000	0.00000	0.00000	0.00000
3	1.00000	0.00000	0.00000	0.00000	0.00000	0.00000

Verification:

$$P.D._{MAX} = 0.30\%$$

Example No. 10:

This example was chosen to verify the static analysis of the spring element. The model properties are

$$\begin{aligned}
 KUX &= 30 \text{ kN/m} & KRX &= 100 \text{ kNm} & m &= 5 \text{ ton} \\
 KUY &= 20 \text{ kN/m} & KRY &= 120 \text{ kNm} \\
 KUZ &= 35 \text{ kN/m} & KRZ &= 80 \text{ kNm}
 \end{aligned}$$

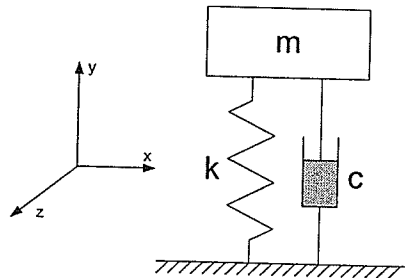


Figure B.11 - Spring element (example 10).

Automatic self-weight (always loaded at node 2): $U_y = \frac{5 \times 9.81}{20} = 2.4525 \text{ m}$

SADAP self weight results:

LOAD STEP= 1

SUPPORT REACTIONS:

NODE	RX	RY	RZ	MX	MY	MZ
1	0.0000	49.050	0.0000	0.0000	0.0000	0.0000

TOTAL DISPLACEMENTS:

NODE	TRANS.X	TRANS.Y	TRANS.Z	ROT.X	ROT.Y	ROT.Z
1	0.000000000	0.000000000	0.000000000	0.000000000	0.000000000	0.000000000
2	0.000000000	-2.452500000	0.000000000	0.000000000	0.000000000	0.000000000

The external load vector was chosen to produce a unit displacement in all degrees of freedom (DOF) of the element.

$$F = \begin{Bmatrix} 30 \text{ kN} \\ 20 \text{ kN} \\ 35 \text{ kN} \\ 100 \text{ kN.m} \\ 120 \text{ kN.m} \\ 80 \text{ kN.m} \end{Bmatrix}$$

SADAP external load results:

LOAD STEP= 1

SUPPORT REACTIONS:

NODE	RX	RY	RZ	MX	MY	MZ
1	-30.000	-20.000	-35.000	-100.00	-120.00	-80.000

TOTAL DISPLACEMENTS:

NODE	TRANS.X	TRANS.Y	TRANS.Z	ROT.X	ROT.Y	ROT.Z
1	0.000000000	0.000000000	0.000000000	0.000000000	0.000000000	0.000000000
2	1.000000000	1.000000000	1.000000000	1.000000000	1.000000000	1.000000000

Verification:

$P.D. = 0.00\%$ for both types of loading.

The examples 11 to 16 are described in the chapter 4 (item 4.2).

Example No. 17:

This 3D beam-column example (Figure B.12) is presented to verify the frame element behavior using stability functions under self weight and also response under only external load (not including the self weight) through a linear static analysis. ANSYS is used to verify the automatic self-weight analysis, and Weaver and Gere (1980) to verify the external load. The model properties are

$$\begin{aligned}
 E &= 2.00 \times 10^{10} \text{ kN/m} & I_x &= 2.00 \times 10^{-3} \text{ m}^4 & \rho &= 7.86 \text{ ton/m}^3 \\
 \nu &= 0.25 & I_y &= 1.00 \times 10^{-3} \text{ m}^4 & g_y &= -9.81 \text{ m/s}^2 \\
 A &= 0.01 \text{ m}^2 & I_z &= 1.00 \times 10^{-3} \text{ m}^4 & &
 \end{aligned}$$

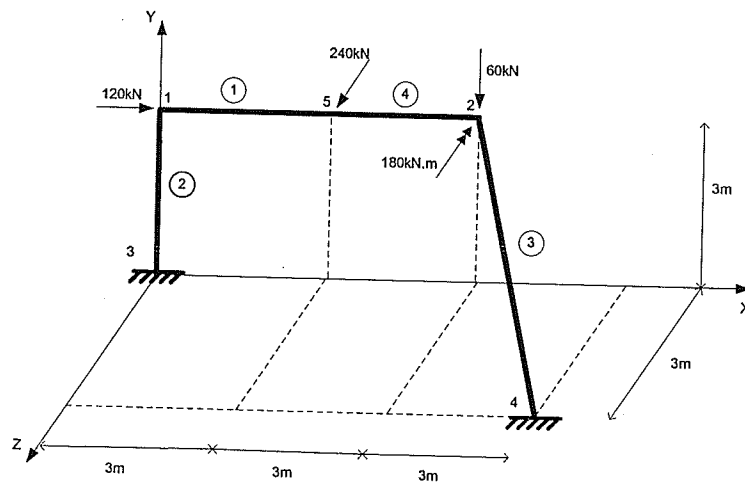


Figure B.12 - Beam-column element (example 17).

Results from ANSYS (self weight linear static analysis only):

PRINT ELEMENT TABLE ITEMS PER ELEMENT

***** POST1 ELEMENT TABLE LISTING *****

STAT	CURRENT
ELEM	SAXL
1	-197.37
2	-556.46
3	-224.23
4	-197.37

PRINT U NODAL SOLUTION PER NODE

***** POST1 NODAL DEGREE OF FREEDOM LISTING *****

LOAD STEP= 1 SUBSTEP= 1
TIME= 1.0000 LOAD CASE= 0

THE FOLLOWING DEGREE OF FREEDOM RESULTS ARE IN THE GLOBAL COORDINATE SYSTEM

NODE	UX	UY	UZ	USUM
1	0.12826E-04	-0.66119E-05	-0.46335E-04	0.48530E-04
2	0.69051E-05	-0.17625E-03	-0.16786E-03	0.24349E-03
3	0.0000	0.0000	0.0000	0.0000
4	0.0000	0.0000	0.0000	0.0000
5	0.98657E-05	-0.11817E-03	-0.11901E-03	0.16801E-03

PRINT ROT NODAL SOLUTION PER NODE

***** POST1 NODAL DEGREE OF FREEDOM LISTING *****

LOAD STEP= 1 SUBSTEP= 1
TIME= 1.0000 LOAD CASE= 0

THE FOLLOWING DEGREE OF FREEDOM RESULTS ARE IN THE GLOBAL COORDINATE SYSTEM

NODE	ROTX	ROTY	ROTZ	RSUM
1	-0.26877E-04	0.20171E-04	-0.23354E-04	0.40922E-04
2	-0.63969E-04	0.42854E-05	-0.50480E-05	0.64311E-04
3	0.0000	0.0000	0.0000	0.0000
4	0.0000	0.0000	0.0000	0.0000
5	-0.45423E-04	0.24268E-04	-0.35309E-04	0.62441E-04

PRINT F REACTION SOLUTIONS PER NODE

***** POST1 TOTAL REACTION SOLUTION LISTING *****

LOAD STEP= 1 SUBSTEP= 1
TIME= 1.0000 LOAD CASE= 0

THE FOLLOWING X,Y,Z SOLUTIONS ARE IN THE GLOBAL COORDINATE SYSTEM

NODE	FX	FY	FZ
3	1.9737	5.5646	0.53509
4	-1.9737	5.3816	-0.53509

PRINT M SUMMED NODAL LOADS

***** POST1 SUMMED TOTAL NODAL LOADS LISTING *****

LOAD STEP= 1 SUBSTEP= 1
TIME= 1.0000 LOAD CASE= 0

THE FOLLOWING X,Y,Z SOLUTIONS ARE IN THE GLOBAL COORDINATE SYSTEM

NODE	MX	MY	MZ
3	-2.5944	1.0758	1.4037
4	-7.5406	-2.1811	3.1024

SADAP results (only self-weight):

EXAMPLE_17_P.357-MATR
NONLINEAR STATIC AND DYNAMIC ANALYSIS OF STRUCTURES

NODAL POINTS:

NODE	X	Y	Z
1	0.0000	3.0000	0.0000
2	6.0000	3.0000	0.0000
3	0.0000	0.0000	0.0000
4	9.0000	0.0000	3.0000
5	3.0000	3.0000	0.0000

RESTRAINTS:

NODE	TRANS.X	TRANS.Y	TRANS.Z	ROT.X	ROT.Y	ROT.Z
3	1	1	1	1	1	1
4	1	1	1	1	1	1

AUTOMATIC SELF-WEIGHT ANALYSIS

FRAME ELEMENTS (STABILITY FUNCTIONS):

ELEM.	NODE1	NODE2	E	V	A	IX	IY	IZ	FP	QX	QY	QZ	ESP.MASS	FLANG
1	1	5	0.200E+09	0.25E+00	0.100E-01	0.200E-02	0.100E-02	0.100E-02	0.00	0.00	0.00	0.00	7.86	0.
2	3	1	0.200E+09	0.25E+00	0.100E-01	0.200E-02	0.100E-02	0.100E-02	0.00	0.00	0.00	0.00	7.86	0.
3	2	4	0.200E+09	0.25E+00	0.100E-01	0.200E-02	0.100E-02	0.100E-02	0.00	0.00	0.00	0.00	7.86	0.
4	5	2	0.200E+09	0.25E+00	0.100E-01	0.200E-02	0.100E-02	0.100E-02	0.00	0.00	0.00	0.00	7.86	0.

LOAD STEP= 1

FRAME ELEMENTS (STABILITY FUNCTIONS) INTERNAL FORCES:

ELEM.	NODE	N	QY	QZ	T	MY	MZ
1	1	1.9737	3.2514	0.53509	0.98913	-1.0758	4.5175
	5	-1.9737	-0.93816	-0.53509	-0.98913	-0.52951	1.7668
2	3	5.5646	-1.9737	0.53509	-1.0758	-2.5944	-1.4037
	1	-3.2514	1.9737	-0.53509	1.0758	0.98913	-4.5175
3	2	2.2423	-0.98496E-01	-1.0173	-1.3032	1.6931	-1.4854
	4	-4.5555	3.3699	1.0173	1.3032	3.5927	-7.5257
4	5	1.9737	0.93816	0.53509	0.98913	0.52951	-1.7668
	2	-1.9737	1.3750	-0.53509	-0.98913	-2.1348	1.1115

SUPPORT REACTIONS:

NODE	RX	RY	RZ	MX	MY	MZ
3	1.9737	5.5646	0.53509	2.5944	-1.0758	-1.4037
4	-1.9737	5.3816	-0.53509	7.5406	2.1811	-3.1024

TOTAL DISPLACEMENTS:

NODE	TRANS.X	TRANS.Y	TRANS.Z	ROT.X	ROT.Y	ROT.Z
1	0.000012826	-0.000006612	-0.000046335	-0.000026877	0.000020171	-0.000023354
2	0.000006905	-0.000176252	-0.000167861	-0.000063969	0.000004285	-0.000005048
3	0.000000000	0.000000000	0.000000000	0.000000000	0.000000000	0.000000000
4	0.000000000	0.000000000	0.000000000	0.000000000	0.000000000	0.000000000
5	0.000009866	-0.000118173	-0.000119012	-0.000045423	0.000024268	-0.000035309

Results from Weaver and Gere (1980), only external loads:

Join Displacement							
Join	Ux	Uy	Uz	Rx	Ry	Rz	
1	-8.594E-04	5.776E-05	5.008E-03	2.393E-03	-1.623E-03	6.813E-04	
2	-1.176E-03	3.253E-03	5.256E-03	1.288E-03	1.721E-03	-7.715E-04	
3	0.000E+00	0.000E+00	0.000E+00	0.000E+00	0.000E+00	0.000E+00	
4	0.000E+00	0.000E+00	0.000E+00	0.000E+00	0.000E+00	0.000E+00	

Member End-Actions							
Member	Node	Fx	Fy	Fz	Mx	My	Mz
1	1	105.548	-38.509	-126.013	29.464	86.569	-67.100
	2	-105.548	38.509	-113.987	-29.464	-50.491	-163.954
2	3	-38.509	14.452	-126.013	86.569	348.575	-23.744
	1	38.509	-14.452	126.013	-86.569	29.464	67.100
3	2	183.623	9.192	5.967	-21.404	46.703	-32.181
	4	-183.623	-9.192	-5.967	21.404	-77.711	79.946

Support Reactions							
Node	Fx	Fy	Fz	Mx	My	Mz	
3	-14.452	-38.509	-126.013	-348.575	86.569	-23.744	
4	-105.548	98.509	-113.987	-75.898	-75.808	37.163	

SADAP results (only external loads):

LOAD STEP= 1

FRAME ELEMENTS (STABILITY FUNCTIONS) INTERNAL FORCES:

ELEM.	NODE	N	QY	QZ	T	MY	MZ
1	1	105.55	-38.509	-126.01	29.464	86.569	-67.100
	5	-105.55	38.509	126.01	-29.464	291.47	-48.427
2	3	-38.509	14.452	-126.01	86.569	348.58	-23.744
	1	38.509	-14.452	126.01	-86.569	29.464	67.100
3	2	183.62	9.1924	5.9674	-21.404	46.703	-32.181
	4	-183.62	-9.1924	-5.9674	21.404	-77.711	79.946
4	5	105.55	-38.509	113.99	29.464	-291.47	48.427
	2	-105.55	38.509	-113.99	-29.464	-50.491	-163.95

SUPPORT REACTIONS:

NODE	RX	RY	RZ	MX	MY	MZ
3	-14.452	-38.509	-126.01	-348.58	86.569	-23.744
4	-105.55	98.509	-113.99	-75.898	-75.808	37.163

TOTAL DISPLACEMENTS:

NODE	TRANS.X	TRANS.Y	TRANS.Z	ROT.X	ROT.Y	ROT.Z
1	-0.000859410	0.000057764	0.005007645	0.002393332	-0.001623169	0.000681331
2	-0.001176053	0.003253182	0.005255517	0.001288428	0.001720936	-0.000771469
3	0.000000000	0.000000000	0.000000000	0.000000000	0.000000000	0.000000000
4	0.000000000	0.000000000	0.000000000	0.000000000	0.000000000	0.000000000
5	-0.001017731	0.002745063	0.008989659	0.001840880	-0.000086410	0.000821384

Verification:

P.D. = 0.00% for all the displacements, internal forces and support reactions.

Example No. 18:

The purpose of this example is to verify the local axis rotation of the 3D beam-column element using stability functions. SADAP results were compared with Weaver and Gere (1980) and the commercial program ANSYS. The model properties are

$$\begin{aligned} E &= 10000 \text{ ksi} & I_x &= 64 \text{ in}^4 \\ \nu &= 0.25 & I_y &= 28 \text{ in}^4 \\ A &= 9 \text{ in}^2 & I_z &= 80 \text{ in}^4 \end{aligned}$$

The third node of the element 2, 3 and 5 is located at: 128,96,0

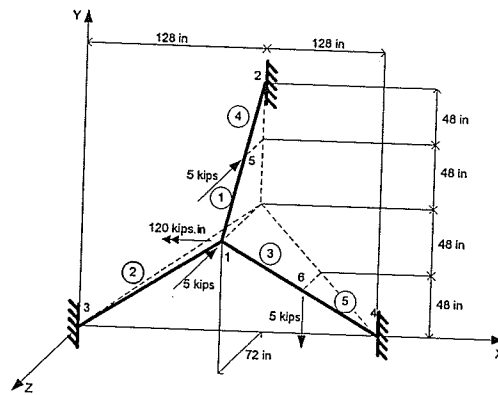


Figure B.13 - Beam-column element (example 18).

Results from Weaver and Gere (1980):

Join Displacement							
Join	Ux	Uy	Uz	Rx	Ry	Rz	
1	-2.176E-04	-4.062E-03	-1.674E-02	-5.202E-03	1.870E-04	-4.495E-03	
2	0.000E+00	0.000E+00	0.000E+00	0.000E+00	0.000E+00	0.000E+00	
3	0.000E+00	0.000E+00	0.000E+00	0.000E+00	0.000E+00	0.000E+00	
4	0.000E+00	0.000E+00	0.000E+00	0.000E+00	0.000E+00	0.000E+00	
Member End-Actions							
Member	Node	Fx	Fy	Fz	Mx	My	Mz
1	1	3.594	0.178	0.406	6.073	-32.492	-84.001
	2	-6.594	3.822	-0.406	-6.073	-16.233	-134.638
2	3	4.744	0.485	-0.131	8.080	7.610	27.616
	1	-4.744	-0.485	0.131	-8.080	15.390	57.444
3	1	3.214	0.178	1.678	-2.995	-50.178	-24.964
	4	-5.950	1.054	2.322	2.995	106.594	-51.865
Support Reactions							
Node	Fx	Fy	Fz	Mx	My	Mz	
2	-0.406	-2.982	7.014	-134.638	14.599	-9.343	
3	3.699	2.610	1.505	-8.177	28.387	-3.624	
4	-3.293	5.372	1.480	-63.927	-16.885	-98.434	

ANSYS results:

PRINT U NODAL SOLUTION PER NODE

***** POST1 NODAL DEGREE OF FREEDOM LISTING *****

LOAD STEP= 1 SUBSTEP= 1
TIME= 1.0000 LOAD CASE= 0

THE FOLLOWING DEGREE OF FREEDOM RESULTS ARE IN THE GLOBAL COORDINATE SYSTEM

NODE	UX	UY	UZ	USUM
1	-0.21807E-03	-0.40618E-02	-0.16737E-01	0.17224E-01
2	0.0000	0.0000	0.0000	0.0000
3	0.0000	0.0000	0.0000	0.0000
4	0.0000	0.0000	0.0000	0.0000
5	0.52151E-01	-0.75051E-01	-0.10739	0.14102
6	-0.28168	-0.45366	0.89995E-01	0.54153

SADAP results:

LOAD STEP= 1

FRAME ELEMENTS (STABILITY FUNCTIONS) INTERNAL FORCES:

ELEM.	NODE	N	QY	QZ	T	MY	MZ
1	1	3.5945	0.17801	0.40605	6.0732	-32.492	-84.001
	5	-3.5945	-0.17801	-0.40605	-6.0732	8.1294	94.681
2	3	4.7447	0.48480	-0.13109	8.0797	7.6099	27.616
	1	-4.7447	-0.48480	0.13109	-8.0797	15.390	57.444
3	1	3.2136	0.17766	1.6785	-2.9952	-50.178	-24.964
	6	-3.2136	-0.17766	-1.6785	2.9952	-97.068	40.550
4	5	6.5945	-3.8220	0.40605	6.0732	-8.1294	-94.681
	2	-6.5945	3.8220	-0.40605	-6.0732	-16.233	-134.64
5	6	5.9494	-1.0534	-2.3215	-2.9952	97.068	-40.550
	4	-5.9494	1.0534	2.3215	2.9952	106.59	-51.864

SUPPORT REACTIONS:

NODE	RX	RY	RZ	MX	MY	MZ
2	-0.40605	-2.9924	7.0143	-134.64	-14.599	-9.3428
3	3.6992	2.6106	1.5050	-8.1767	28.387	-3.6240
4	-3.2932	5.3718	1.4808	-63.927	-16.885	-98.434

TOTAL DISPLACEMENTS:

NODE	TRANS.X	TRANS.Y	TRANS.Z	ROT.X	ROT.Y	ROT.Z
1	-0.000218067	-0.004061807	-0.016736808	-0.005202205	0.000187037	-0.004495317
2	0.000000000	0.000000000	0.000000000	0.000000000	0.000000000	0.000000000
3	0.000000000	0.000000000	0.000000000	0.000000000	0.000000000	0.000000000
4	0.000000000	0.000000000	0.000000000	0.000000000	0.000000000	0.000000000
5	0.052151438	-0.075050749	-0.107394865	0.001498383	0.001659697	-0.000159420
6	-0.281675223	-0.453662190	0.089995388	0.000113304	0.000690493	0.001781987

Verification:

Even though there is a small difference on the x translation of node 1 when compared with Weaver and Gere (1980), the values were matching with ANSYS. This is due to a round off error in Weaver and Gere (1980). The $P.D. = 0.00\%$ for all the displacements, internal forces and support reactions.

Example No. 19:

The purpose of this example is to verify the critical buckling load of the 3D beam-column element using stability functions; the program is expected to stop at the buckling load. Theoretical values are used as comparison, the model properties are

$$\begin{aligned}
 E &= 2.00 \times 10^{+08} \text{ kN/m}^2 & I_x &= 2.00 \times 10^{-03} \text{ m}^4 & P_{cr \text{ Linear}} &= \frac{\pi^2 EI}{(2L)^2} = 13707.784 \text{ kN} \\
 \nu &= 0.25 & I_y &= 1.00 \times 10^{-03} \text{ m}^4 & P_{cr \text{ Nonlinear}} &= \frac{\pi^2 EI}{\left[2 \left(L - \frac{P_{cr \text{ Nonlinear}} L}{EA} \right) \right]^2} = 13900.332 \text{ kN} \\
 A &= 0.01 \text{ m}^2 & I_z &= 1.00 \times 10^{-03} \text{ m}^4 & &
 \end{aligned}$$

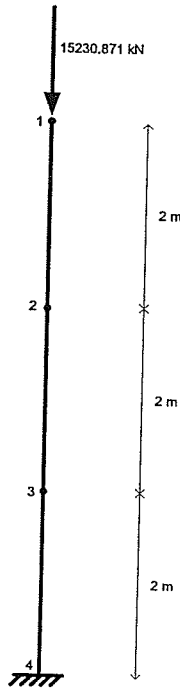


Figure B.14 - Beam-column element (example 19).

SADAP results:

LOAD STEP= 9127

FRAME ELEMENTS (STABILITY FUNCTIONS) INTERNAL FORCES:

ELEM.	NODE	N	QY	QZ	T	MY	MZ
1	1	13900.	0.0000	0.0000	0.0000	0.0000	0.0000
	2	-13900.	0.0000	0.0000	0.0000	0.0000	0.0000
2	2	13900.	0.0000	0.0000	0.0000	0.0000	0.0000
	3	-13900.	0.0000	0.0000	0.0000	0.0000	0.0000
3	3	13900.	0.0000	0.0000	0.0000	0.0000	0.0000
	4	-13900.	0.0000	0.0000	0.0000	0.0000	0.0000

Displacement of node 1:

0.0000000000 -0.0415545284 0.0000000000 0.0000000000 0.0000000000 0.0000000000

SUPPORT REACTIONS:

NODE	RX	RY	RZ	MX	MY	MZ
4	0.0000	13900.	0.0000	0.0000	0.0000	0.0000

LOAD STEP= 9128

Verification:

P.D. = 0.00%

Example No. 20:

The purpose of this example is to verify the torsion, bending and axial natural frequencies of a circular cantilever using 3D beam-column elements using stability functions. The model properties are

$$\begin{aligned}
 E &= 2.00 \times 10^{+08} \text{ kN/m}^2 & I_x &= 4.97 \times 10^{-05} \text{ m}^4 & \rho &= 8 \text{ ton/m}^3 \\
 \nu &= 0.30 & I_y &= 2.485 \times 10^{-05} \text{ m}^4 & & \\
 A &= 0.01 \text{ m}^2 & I_z &= 2.485 \times 10^{-05} \text{ m}^4 & &
 \end{aligned}$$

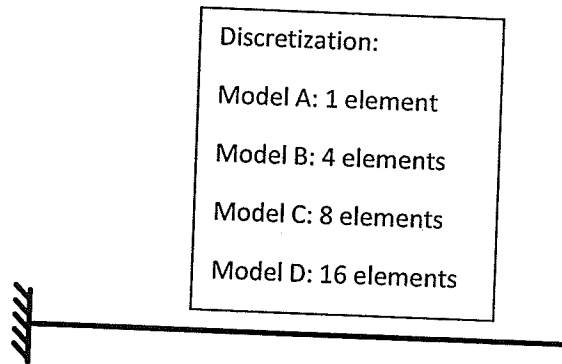


Figure B.15 - Beam-column element (example 20).

Theoretical results (Militano, 2000):

$$w_{n,bending} = (\beta_n \cdot L)^2 \cdot \sqrt{\frac{E \cdot I}{A \cdot \rho \cdot L^4}}$$

$$w_{n,torsion} = \frac{2 \cdot n - 1}{2 \cdot L} \cdot \pi \cdot \sqrt{\frac{G}{\rho}}$$

$$w_{n,axial} = \frac{2 \cdot n - 1}{2 \cdot L} \cdot \pi \cdot \sqrt{\frac{E}{\rho}}$$

$$\beta_n \cdot L = 1.875, 4.694, 7.854, 10.998$$

Militano (2000) results:

Natural circular frequency [rad/s]												
Mode Shape	Bending	Bending	Bending	Bending	Torsion	Axial	Torsion	Axial	Torsion	Torsion	Axial	Axial
Exact Solution	10.30	64.55	180.72	354.36	608.85	981.75	1826.56	2945.24	3044.27	4261.98	4908.74	6872.23
1 Element	10.35	-	-	-	671.00	1082.53	-	-	-	-	-	-
4 Elements	10.30	64.63	182.16	359.36	613.00	988.07	1933.00	3116.99	3511.00	5078.00	5662.13	8187.93
8 Elements	10.30	64.56	180.87	355.01	610.00	983.32	1853.00	2987.99	3167.00	4599.00	5107.44	7416.40
16 Elements	10.30	64.56	180.77	354.27	609.00	982.14	1833.00	2955.90	3075.00	4346.00	4958.16	7008.14

SADAP results and verifications:

Natural circular frequency [rad/s]												
Mode Shape	Bending	P.D.	Bending	P.D.	Bending	P.D.	Bending	P.D.	Torsion	P.D.	Axial	P.D.
Exact Solution	10.30	-	64.55	-	180.72	-	354.36	-	608.85	-	981.75	-
1 Element	10.35	0.49%	-	-	-	-	-	-	671.36	10.27%	1082.53	10.27%
4 Elements	10.30	0.01%	64.63	0.12%	182.15	0.79%	359.35	1.41%	612.77	0.64%	988.07	0.64%
8 Elements	10.30	0.01%	64.56	0.01%	180.86	0.08%	355.00	0.18%	609.83	0.16%	983.33	0.16%
16 Elements	10.30	0.01%	64.55	0.00%	180.76	0.02%	354.26	-0.03%	609.10	0.04%	982.14	0.04%

Natural circular frequency [rad/s]												
Mode Shape	Torsion	P.D.	Axial	P.D.	Torsion	P.D.	Torsion	P.D.	Axial	P.D.	Axial	P.D.
Exact Solution	1826.56	-	2945.24	-	3044.27	-	4261.98	-	4908.74	-	6872.23	-
1 Element	-	-	-	-	-	-	-	-	-	-	-	-
4 Elements	1933.08	5.83%	3117.00	5.83%	3511.50	15.35%	5077.94	19.15%	5662.13	15.35%	8187.93	19.15%
8 Elements	1853.07	1.45%	2987.99	1.45%	3167.50	4.05%	4599.45	7.92%	5107.44	4.05%	7416.40	7.92%
16 Elements	1833.17	0.36%	2955.90	0.36%	3074.92	1.01%	4346.26	1.98%	4958.16	1.01%	7008.14	1.98%

Example No. 21:

The purpose of this example is to verify the variation of frequency with axial force in a column with both ends pinned (3D beam-column element using stability functions).

The program results were compared with the results from Przemieniecki (1985). A non-linear free vibration analysis was performed.

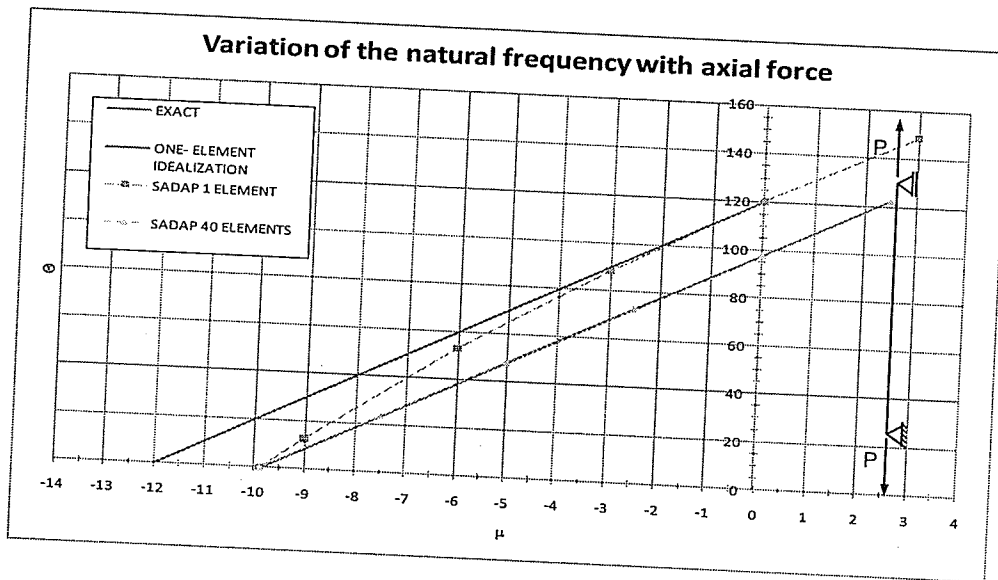


Figure B.16 - Example solution (example 21).

Where:

$$\Theta = w^2 \rho \frac{AL^4}{EI}$$

$$\mu = \frac{PL^2}{EI}$$

Verification:

$$P.D._{MAX} = -0.65\%$$

Example No. 22:

The purpose of this example is to verify the dynamic solver using the 3D beam-column element (using stability functions). Model properties, dynamic force, and displacement solution were taken from Battista (2007-C) and are given by

$$\begin{aligned}
 E &= 2.10 \times 10^{+08} \text{ kN/m}^2 & I_x &= 2.716 \times 10^{-04} \text{ m}^4 & \rho &= 7.85 \text{ ton/m}^3 \\
 \nu &= 0.30 & I_y &= 1.858 \times 10^{-04} \text{ m}^4 & \xi &= 0.01 \\
 A &= 8.06 \times 10^{-03} \text{ m}^2 & I_z &= 1.858 \times 10^{-04} \text{ m}^4 & &
 \end{aligned}$$

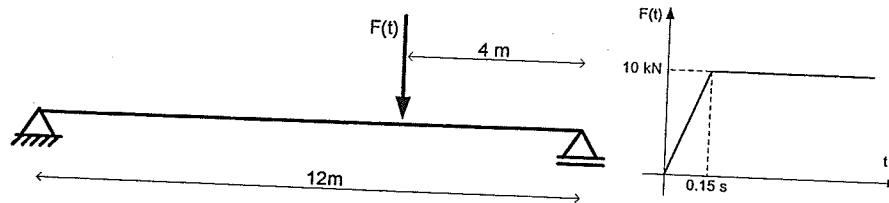


Figure B.17 - Beam-column element (example 22).

Theoretical solution:

$$w_n = n^2 \pi^2 \sqrt{\frac{EI}{\rho AL^4}} = 53.82 \text{ rad/s}, 215.29 \text{ rad/s}, 484.41 \text{ rad/s}$$

Battista (2007-C) solution (displacements where the load is applied):

$$u_y(0.15 \text{ s}) = 0.00643 \text{ m}$$

$$u_{y, \text{MAXIMUM}} = 0.00849 \text{ m}$$

SADAP solution and verification (using 30 elements):

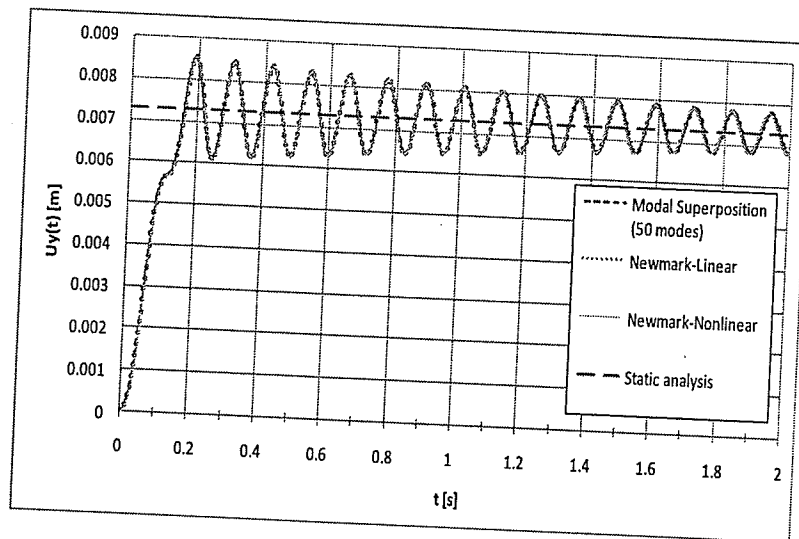


Figure B.18 - Example solution (example 22).

$w_1 = 53.82 \text{ rad/s} \therefore P.D. = 0.00\%$
 $w_2 = 215.29 \text{ rad/s} \therefore P.D. = 0.00\%$
 $w_3 = 484.41 \text{ rad/s} \therefore P.D. = 0.00\%$

Modal Superposition ($\Delta t = 0.0001 \text{ s}$ and 50 modes):

$u_y(0.15 \text{ s}) = 0.00650 \text{ m} \therefore P.D. = 1.09\%$
 $u_{y \text{ MAXIMUM}} = 0.00854 \text{ m} \therefore P.D. = 0.59\%$

Newmark-Linear ($\Delta t = 0.0001 \text{ s}$):

$u_y(0.15 \text{ s}) = 0.00649 \text{ m} \therefore P.D. = 0.93\%$
 $u_{y \text{ MAXIMUM}} = 0.00854 \text{ m} \therefore P.D. = 0.59\%$

Newmark-Nonlinear ($\Delta t = 0.0001 \text{ s}$):

$u_y(0.15 \text{ s}) = 0.00649 \text{ m} \therefore P.D. = 0.93\%$
 $u_{y \text{ MAXIMUM}} = 0.00851 \text{ m} \therefore P.D. = 0.24\%$

Example No. 23:

The purpose of this example is to verify the nonlinear static analysis of the insulator string elements. The results were compared with theoretical analyses. Model properties are (the insulator string element is mass less)

$$L = 1.50 \text{ m} \quad A = 1.00 \times 10^{-03} \text{ m}^2 \quad F_x = 9.81 \text{ kN}$$

$$E = 2.00 \times 10^{+08} \text{ kN/m}^2 \quad \text{Conductor weight} = 9.81 \text{ kN}$$

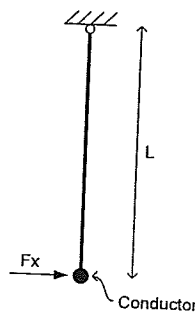


Figure B.19 - Insulator string element (example 23).

Theoretical results

$$u_y = -\frac{L}{EA} \text{ conductor weight} = 0.00007358 \text{ m}$$

Self weight analysis:

$$\text{Tension } i = 9.81 \text{ kN}$$

$$\text{Tension } j = 9.81 \text{ kN}$$

$$u_x \approx \frac{L}{\sqrt{2}} = 1.06066 \text{ m}$$

External load and self weight analysis: $u_y \approx L \left(1 - \frac{1}{\sqrt{2}} \right) = 0.43934 \text{ m}$

$$\text{Tension } i = 13.8734 \text{ kN}$$

$$\text{Tension } j = 13.8734 \text{ kN}$$

SADAP results:

NODAL POINTS:

NODE	X	Y	Z
1	0.0000	0.0000	0.0000
2	0.0000	-1.5000	0.0000
3	0.0000	-1.5000	0.0000

RESTRAINTS:

NODE	TRANS.X	TRANS.Y	TRANS.Z	ROT.X	ROT.Y	ROT.Z
1	1	1	1	1	1	1

NODAL FORCES:

NODE	FX	FY	FZ	MX	MY	MZ
2	9.81000	0.00000	0.00000	0.00000	0.00000	0.00000

AUTOMATIC SELF-WEIGHT ANALYSIS

SPRING ELEMENTS:

ELEM.	NODE1	NODE2	KUX	KUY	KUZ	KRX	KRY	KRZ	MASS	ALFA	BETA	
2	3	2	0.10000E+07	1.0000	0.0000	0.0000						

INSULATOR ELEMENTS:

ELEM.	NODE 1	NODE 2	E	A	WC	TOTAL MASS
1	1	2	0.20000E+09	0.10000E-02	0.10000E-01	0.0000

LOAD STEP= 1

INSULATOR ELEMENTS INTERNAL FORCES: (TENSION +)

ELEM.	N NODE1	N NODE2
1	9.8100	9.8100

Displacement of node 2:
 0.0000000000 -0.0000735750 0.0000000000 0.0000000000 0.0000000000 0.0000000000

SUPPORT REACTIONS:

NODE	RX	RY	RZ	MX	MY	MZ
1	0.0000	9.8100	0.0000	0.0000	0.0000	0.0000

LOAD STEP= 101

INSULATOR ELEMENTS INTERNAL FORCES: (TENSION +)

ELEM.	N NODE1	N NODE2
1	13.881	13.881

SUPPORT REACTIONS:

NODE	RX	RY	RZ	MX	MY	MZ
1	-9.8100	9.8100	0.0000	0.0000	0.0000	0.0000

TOTAL DISPLACEMENTS:

NODE	TRANS.X	TRANS.Y	TRANS.Z	ROT.X	ROT.Y	ROT.Z
1	0.0000000000	0.0000000000	0.0000000000	0.0000000000	0.0000000000	0.0000000000
2	1.066243283	0.437919529	0.0000000000	0.0000000000	0.0000000000	0.0000000000
3	1.066243283	0.437919529	0.0000000000	0.0000000000	0.0000000000	0.0000000000

Self weight

Self weight and external load

Verification:

$$P.D._{MAX} = 0.06\%$$

Example No. 24:

The purpose of this example is to verify the Free Vibration analysis of the insulator string element. The results were compared with a theoretical analysis. Model properties are (the insulator string element is mass less)

$$L = 1.50 \text{ m} \quad A = 1.00 \times 10^{-03} \text{ m}^2$$
$$E = 2.00 \times 10^{+08} \text{ kN/m}^2 \quad \text{Conductor weight} = 9.81 \text{ kN}$$

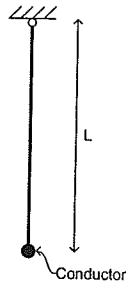


Figure B.20 - Insulator string element (example 24).

Theoretical results:

$$w = \sqrt{\frac{g}{L}} = \sqrt{\frac{9.81}{1.5}} = 2.55734 \text{ rad/s}$$

SADAP results:

MODE	MODAL MASS	FREQ[RAD]	FREQ[HZ]
1	1.00000	2.55728	0.40700

Verification:

$$P.D. = 0.00\%$$

Example No. 25:

The purpose of this example is to verify the linear dynamic solver using the insulator string element. Model properties are (the insulator string element is mass less)

$$L = 1.50 \text{ m} \quad A = 1.00 \times 10^{-3} \text{ m}^2 \quad F_x = 9.81 \text{ kN}$$

$$E = 2.00 \times 10^8 \text{ kN/m}^2 \quad \text{Conductor weight} = 29.43 \text{ kN} \quad C = 4.00 \text{ kN} \times \text{s/m}$$

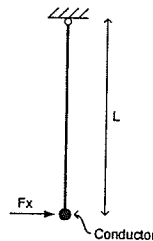


Figure B.21 - Insulator string element (example 25).

Theoretical results:

$$\text{Static displacement} = \frac{F_x L}{\text{Conductor weight}} = 0.5 \text{ m}$$

SADAP results:

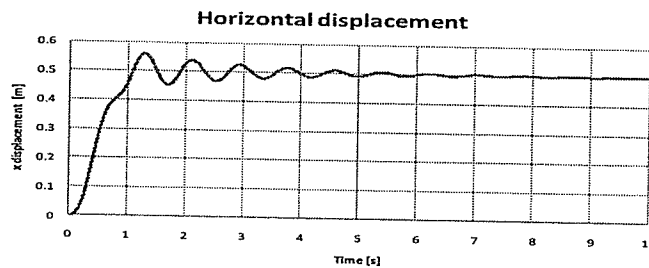


Figure B.22 - Example results (example 25).

Verification:

$$P.D. = -0.10\%$$

Example No. 26:

The purpose of this example is to verify the non-linear static analysis of the straight tower element. The results of the model with straight tower elements were compared with a model using the 3D beam-column (vertical bars) and truss (diagonal and horizontal bars) elements. The model properties are

Longitudinal bars		Diagonals and Horizontal bars
$E = 2.10 \times 10^{+08} \text{ kN/m}^2$	$I_x = 2.45 \times 10^{-06} \text{ m}^4$	$E = 2.10 \times 10^{+08} \text{ kN/m}^2$
$\nu = 0.3$	$I_y = 1.23 \times 10^{-06} \text{ m}^4$	$A = 5.00 \times 10^{-04} \text{ m}^2$
$A = 1.00 \times 10^{-03} \text{ m}^2$	$I_z = 1.23 \times 10^{-06} \text{ m}^4$	$\rho = 7.86 \text{ ton/m}^3$
$\rho = 7.86 \text{ ton/m}^3$		

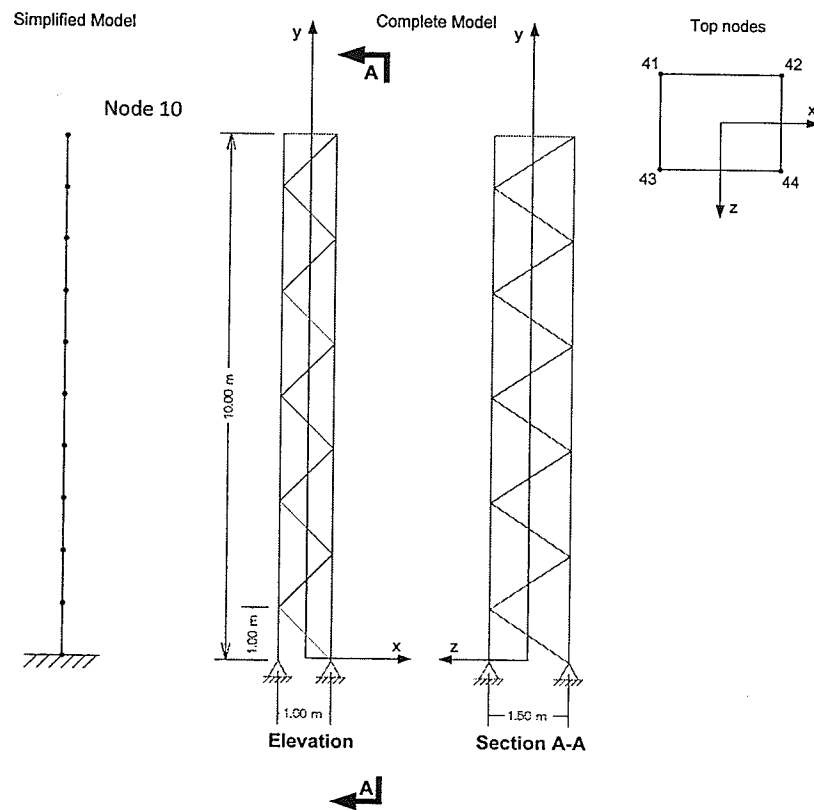


Figure B.23 - Straight tower element (example 26).

The applied force in the following table was chosen to be close to the critical buckling load of the tower (calculated based on a non-linear stability analysis) to verify the behavior of the simplified element.

Model	Node	Fx	Fy	Fz	Mx	My	Mz
		kN	kN	kN	kNm	kNm	kNm
Complete Model	41	10	-350	10	0	0	0
	42	10	-350	10	0	0	0
	43	10	-350	10	0	0	0
	44	10	-350	10	0	0	0
Simpl. Model	10	40	-1400	40	0	0	0

The effect on the non-linear static analysis result in considering the diagonal bars to resist shear deformation was also investigated.

SADAP results:

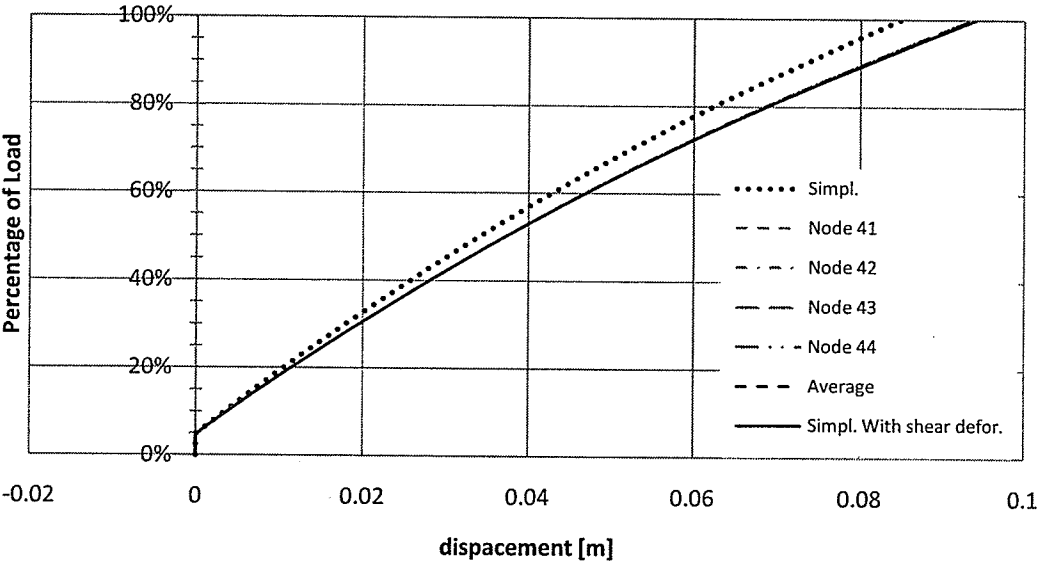


Figure B.24 - Example results for x displacement (example 26).

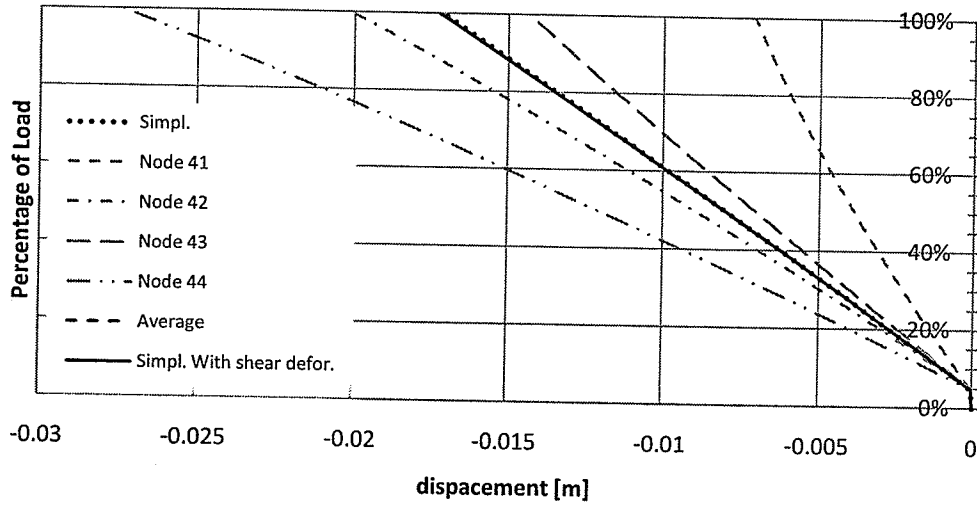


Figure B.25 - Example results for y displacement (example 26).

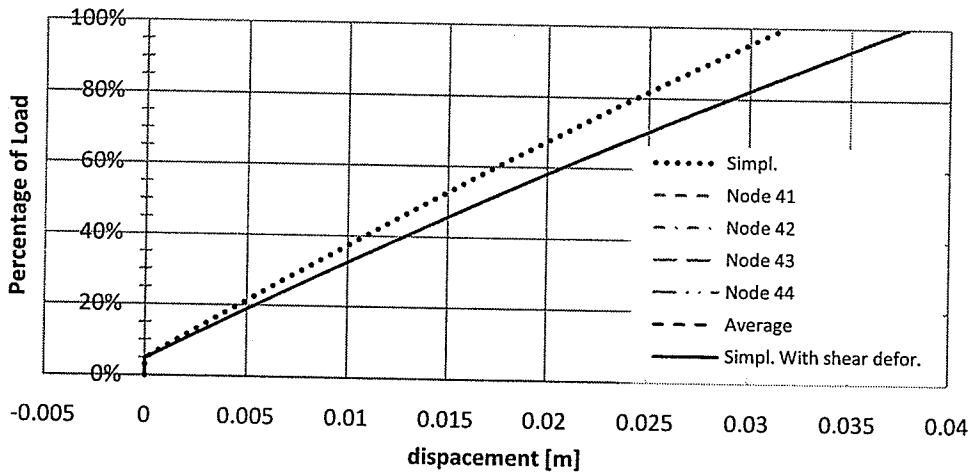


Figure B.26 - Example results for z displacement (example 26).

Verification:

$$P.D._{MAX, without shear deformation} = 16.33\%$$

$$P.D._{MAX, with shear deformation} = 0.52\%$$

Example No. 27:

The purpose of this example is to verify the Free Vibration analysis of the straight tower element. The results of the model with straight tower elements were compared with a model using the 3D beam-column (vertical bars) and truss (diagonal and horizontal bars) elements. The model properties are

Longitudinal bars		Diagonals and Horizontal bars
$E = 2.10 \times 10^{+08} \text{ kN/m}^2$	$I_x = 2.45 \times 10^{-06} \text{ m}^4$	$E = 2.10 \times 10^{+08} \text{ kN/m}^2$
$\nu = 0.3$	$I_y = 1.23 \times 10^{-06} \text{ m}^4$	$A = 5.00 \times 10^{-04} \text{ m}^2$
$A = 1.00 \times 10^{-03} \text{ m}^2$	$I_z = 1.23 \times 10^{-06} \text{ m}^4$	$\rho = 7.86 \text{ ton/m}^3$
$\rho = 7.86 \text{ ton/m}^3$		

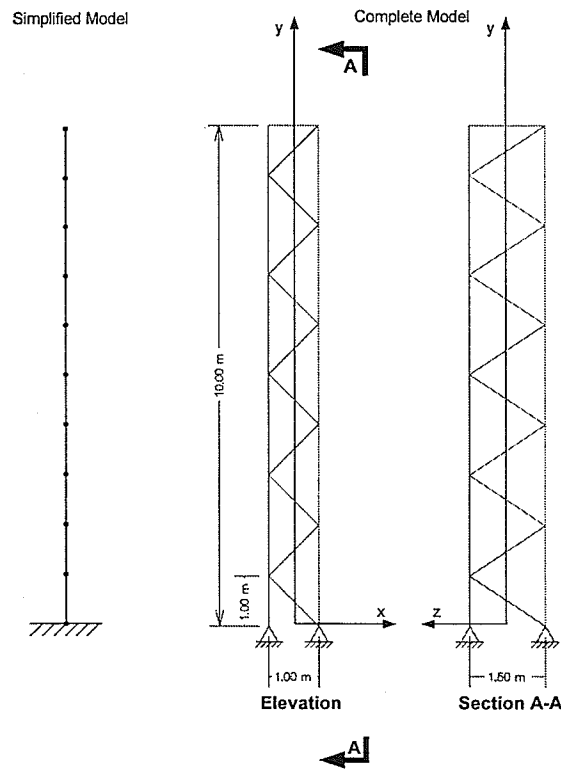


Figure B.27 - Straight tower element (example 27).

SADAP results:

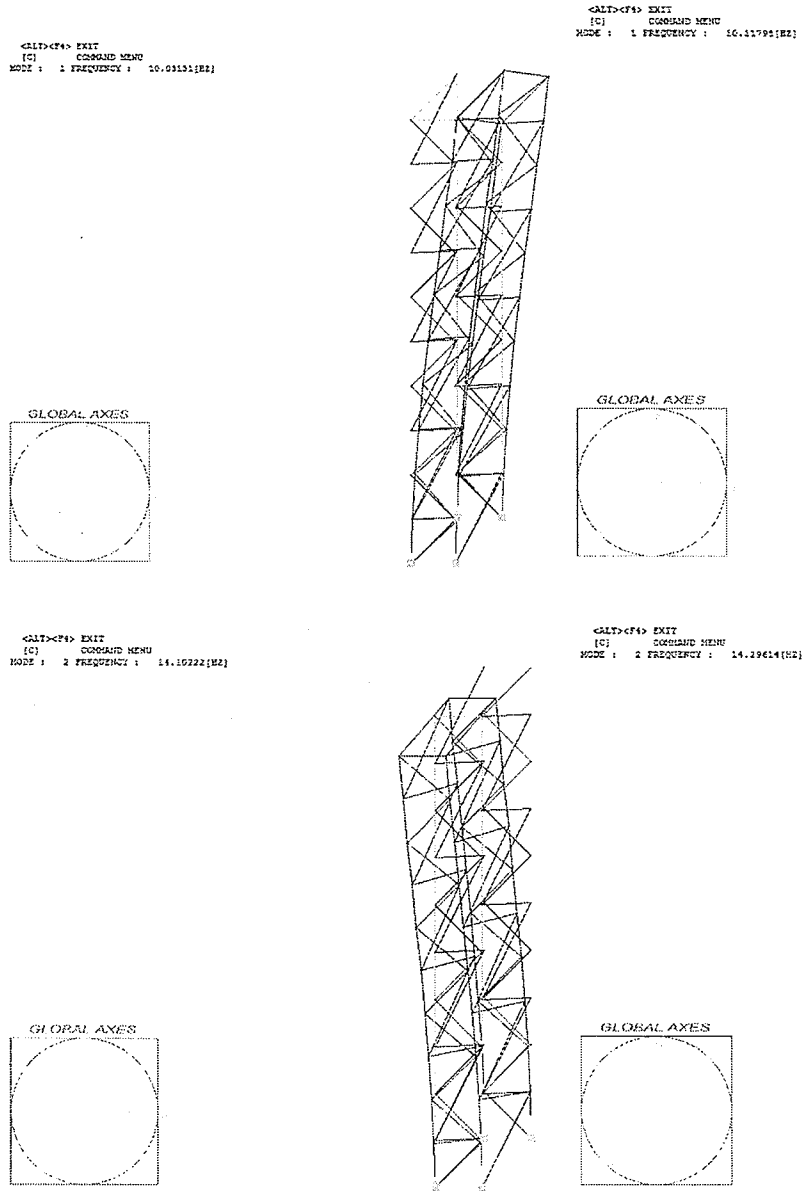
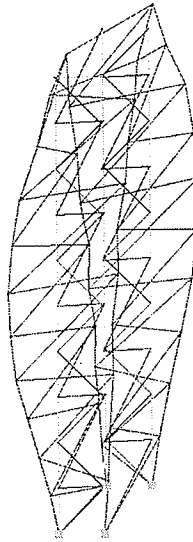


Figure B.28 - Mode shapes and frequencies results (example 27).

<ALT><F4> EXIT
[C] COMMAND MENU
MODE : 4 FREQUENCY : 33.57542[Hz]

<ALT><F4> EXIT
[C] COMMAND MENU
MODE : 5 FREQUENCY : 34.57651[Hz]



<ALT><F4> EXIT
[C] COMMAND MENU
MODE : 5 FREQUENCY : 44.59701[Hz]

<ALT><F4> EXIT
[C] COMMAND MENU
MODE : 4 FREQUENCY : 45.62752[Hz]

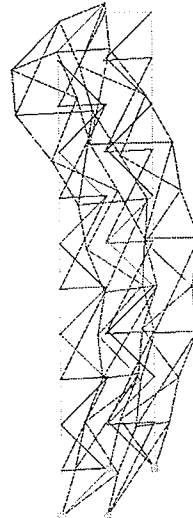


Figure B.28 (cont'd) - Mode shapes and frequencies results (example 27).

Verification:

$$P.D._{w1} = 0.86\%, \quad P.D._{w2} = 1.38\% \quad P.D._{w3} = 2.07\%, \quad P.D._{w4} = -8.85\%$$